



PHD THESIS

A tale of two studies:
threshold radiation in QCD,
and
the classical double copy

NADIA BAHJAT-ABBAS

Supervisor

DR. CHRISTOPHER WHITE

2021

Centre for Research in String Theory
School of Physics and Astronomy
Queen Mary University of London

Abstract

When calculating a fixed order differential cross section in QCD, one must take into account the contribution of threshold radiation, i.e., soft or collinear radiation produced in the threshold limit of the kinematic invariants of a given process. However, large logarithmic terms associated with threshold radiation threaten the stability of the fixed order theory prediction. A possible antidote to this problem is the resummation of such terms. Part one of this thesis is concerned with the resummation of a particular class of large log, the next-to-leading-power (NLP) logs. We investigate the structure and sources of NLP logs by using the Drell-Yan process as a probe. More specifically, we consider the case of two real emissions and 1 virtual emission, as well as the case of any number of real emissions.

The second half of this thesis changes course towards the double copy - a duality relating gravity and gauge theories. The double copy operates perturbatively, linking the amplitudes of these theories, as well as the exact solutions of the equations of motion when considering the classical limit. The double copy package includes biadjoint scalar theory - a scalar theory that encapsulates much of the information encoded in the propagators of gravity and gauge theories, but with the benefit of relative simplicity. We pose the question of whether the double copy operates at a non-perturbative level, and use biadjoint scalar theory as a probe. We explore monopole solutions in biadjoint scalar theory, and attempt to match these to monopoles in Yang-Mills theory, using the Aichelburg-Sexl ultraboost procedure to generate shockwave solutions in aid of this inquiry. Although the monopoles do not seem to match up, we attain new insights regarding how Abelian and non-Abelian monopoles can double copy to the same gravity object.

Acknowledgements

I would like to thank my loved ones for their immense support, as well as colleagues and staff at QMUL and beyond for all of the priceless things I've learned over the past few years.

I am grateful to my supervisor, Chris White, for generously giving me copious amounts of his time, as well as patience! I especially appreciate his great enthusiasm toward our work. Above all, he encouraged me.

My second supervisor, Andi Brandhuber, has given me helpful feedback on my thesis, and somehow created a calming atmosphere whenever he was in the room. After a conversation with him, I always walked away feeling better than I had before.

I thank my collaborators in the phenomenology portion of my research, Domenico Bonocore, Jort Sinninghe Damsté, Eric Laenen, Lorenzo Magnea, and Leonardo Vernazza. I also thank Andrés Luna Godoy, my collaborator in the months preceding the start of my PhD, and from whom I learned many important aspects of the double copy.

I owe a great debt to my dearest friend and partner in research, Ricardo Stark-Muchão. He is a fantastic teacher, and an empathetic soul. I cannot and do not want to imagine how the PhD experience would have been without him by my side.

There are no words that can do justice to the love, support, and understanding my husband Maruro Okamoto lavished on me during this period. His wisdom and advice stood out from the crowd every day, seeing me to the end of this degree with all of my faculties intact.

Finally, I thank the STFC for the funding I received to carry out this work.

Declaration

I, Nadia Bahjat-Abbas, confirm that the research included within this thesis is my own work or that where it has been carried out in collaboration with, or supported by others, that this is duly acknowledged below and my contribution indicated. Previously published material is also acknowledged below.

I attest that I have exercised reasonable care to ensure that the work is original, and does not to the best of my knowledge break any UK law, infringe any third party's copyright or other Intellectual Property Right, or contain any confidential material. I accept that the College has the right to use plagiarism detection software to check the electronic version of the thesis.

I confirm that this thesis has not been previously submitted for the award of a degree by this or any other university. The copyright of this thesis rests with the author and no quotation from it or information derived from it may be published without the prior written consent of the author.

Signature:

Date: May 21, 2021

This thesis describes research carried out with my supervisor Christopher White which was published in [1–4]. It also contains some unpublished material. We collaborated with Ricardo Stark-Muchão on [1,2]. We collaborated with Jort Sinninghe Damsté and Leonardo Vernazza on [3,4], and with Domenico Bonocore, Eric Laenen, and Lorenzo Magnea on [4]. Where other sources have been used, they are cited in the bibliography.

Contents

1	Introduction	10
I	Threshold Radiation	12
2	The QCD Differential Cross Section - an Overview	13
2.1	QCD - A brief introduction	15
2.1.1	The running coupling and asymptotic freedom	16
2.2	Hadronic vs. partonic cross sections	18
2.3	Our probe: Drell-Yan production	19
2.3.1	Leading order	20
2.3.2	Next-to-leading order	22
2.4	The general differential cross section for heavy particle production	24
2.4.1	Classification of logs	25
2.4.2	The K -factor	26
2.5	Summary	26
3	Resummation	27
3.1	Factorisation at the amplitude level	28
3.1.1	Feynman rules for soft emissions	28
3.1.2	The soft function: exponentiation and Wilson lines	31
3.2	Resummation of LP terms in the Drell-Yan cross section	33
3.2.1	Factorisation and the soft function	34
3.2.2	The soft function: exponentiation and Wilson lines	36
3.2.3	The eikonal cross section at NLO	38
3.3	The prospect of resummation beyond LP terms	43
4	Next-to-Leading Power Leading Logs at N³LO	45
4.1	Squared matrix element for 2-real, 1-virtual emissions	46
4.1.1	Method of regions	46
4.1.2	Squared matrix element terms	49

4.2	Phase space integrals	50
4.2.1	Master integral 1	54
4.2.2	Master integral 2	58
4.2.3	Results for the K -factor from each region	59
4.3	Conclusions and learnings for resummation	61
5	Next-to-Leading Power Leading Logs at N^nLO	62
5.1	Leading soft term for the squared matrix element	63
5.2	Phase space integral	63
5.2.1	Integral A	67
5.2.2	Integrals $B1$ and $B2$	68
5.2.3	Finale	69
5.2.4	NLP phase space integral	69
5.3	Resummation of NLP leading logs	71
5.4	Conclusions	73
6	Threshold Radiation Conclusion	74
6.1	Recap	74
6.2	Learnings and achievements	74
6.3	Impact	75
6.4	Further work	75
6.5	A bridge to gravity and other theories	75
II	The Double Copy	76
7	Introduction to the Double Copy	77
7.1	Yang-Mills theory	77
7.1.1	Feynman rules	80
7.1.2	Amplitude for four-point scattering ($gg \rightarrow gg$)	80
7.1.3	Amplitude for m -point scattering	84
7.2	Perturbative gravity	85
7.3	Colour-kinematics duality	88
7.4	BCJ double copy	89
7.4.1	Biadjoint scalar theory	91
7.5	Conclusion	92
8	The Classical Double Copy	93
8.1	Classical gauge theory	94
8.2	General relativity	97
8.2.1	Kerr-Schild metrics	97

8.3	The Kerr-Schild double copy	98
8.3.1	Black hole and point charge examples	99
8.3.2	Beyond weak coupling and Abelian-like solutions	106
8.3.3	Comparison with the BCJ double copy	106
8.4	Conclusion	107
9	The Biadjoint Monopole Zoo	109
9.1	Biadjoint monopoles involving spherical symmetry	110
9.2	Biadjoint monopoles involving cylindrical symmetry	113
9.2.1	Solutions with a common gauge group	113
9.2.2	Solutions for $SU(2) \times SU(2)$	116
9.2.3	Extended solutions	120
9.3	Conclusion	124
10	Making Shockwaves - the Ultraboost	126
10.1	Ultraboosting the linear solutions	127
10.1.1	Linear solutions of the double copy	127
10.1.2	Abelian-like biadjoint scalar theory	128
10.1.3	Coulomb potential in Kerr-Schild coordinates	132
10.1.4	Schwarzschild black hole in Kerr-Schild coordinates	136
10.1.5	Comparison of shockwaves across theories	138
10.2	Ultraboosting the biadjoint monopole	139
10.3	The Wu-Yang and Dirac monopoles	140
10.3.1	New insights to the double copy	142
10.4	Conclusion	142
11	Double Copy Conclusion	144
11.1	Recap	144
11.2	Learnings and achievements	144
11.3	Impact	145
11.4	Further work	145
A	Feynman Rules	146
B	Special Functions	148
B.1	Gamma	148
B.2	Polygamma	149
B.3	The Beta Function	149
B.4	The Zeta Function	150

C Distributions and Transformations	151
C.1 Delta Plus	151
C.2 The Plus Distribution	151
C.3 The Mellin Transform	152
C.4 The Laplace Transform	156
D Sudakov Decomposition	158
D.1 Jacobian	159
D.2 Integration bounds for k_+ and k_-	160
E Integrals	161
F N³LO Data	162
G The Schwarzschild Metric in Kerr-Schild coordinates	164
G.0.1 Mostly + signature	164
G.0.2 Mostly - signature	165
H Ultraboosting the general SU(2)×SU(2) Monopole	166
I Gauge Transforming the Dirac Monopole to the Wu-Yang Monopole	167
J Ultraboosting the Wu-Yang Monopole	170
Bibliography	171

List of Figures

1	Schematic depiction of an all order amplitude on the left as a perturbative expansion where each correction on the right corresponds to the addition of a virtual particle.	14
2	Infrared radiation: zoom in on gluon radiation too soft or too close to quark leg (collinear) to resolve	15
3	LO: $q\bar{q} \rightarrow \gamma^*$	20
4	NLO: $q\bar{q} \rightarrow \gamma^*g$, 1 real emission from the quark leg only	20
5	Cut diagrams for Drell-Yan NLO 1 real emission	22
6	fermion with n soft emissions	29
7	(a) An example of connected diagrams G_c of soft virtual photon exchange between incoming hard fermionic legs; (b) An example of webs W of soft virtual gluon exchange between incoming hard fermionic legs.	31
8	Drell-Yan 2 real, 1 virtual emission - 1 example scalar Feynman diagram	47
9	Integrated hard region coefficients at N ³ LO, 2R1V	60
10	Integrated collinear region coefficients at N ³ LO, 2R1V	60
11	$gg \rightarrow gg$ at tree-level	81
12	s - channel for $gg \rightarrow gg$ at tree-level	81
13	The Jacobi identity $c_s = c_t - c_u$ in terms of tree-level diagrams.	83
14	The Jacobi identity $c_s = c_t - c_u$ embedded in a 1-loop diagram.	84
15	Feynman diagrams for gravity interactions	86
16	The double copy mappings for perturbative amplitudes	91
17	The double copy mappings for exact solutions	100
18	Integral curves of the vector field defined by (9.73), with critical points in red.	122
19	Numerical solution to (9.73) using a built-in Mathematica solver, with boundary conditions set by (9.82).	123
20	Numerical solution in terms of ρ	123

21	Generalisation of the Kerr-Schild double copy, in which one may identify Abelian or non-Abelian exact solutions of a gauge theory with the same gravity solution	143
----	--	-----

Chapter 1

Introduction

Bridging the gap between gauge theories and gravity is one of the most important and notorious open problems in theoretical physics today. Although these theories boast great success in describing an impressive array of physical phenomena, they do so independently of each other. This is problematic as some phenomena, such as black holes, require a dual description. There are a number of proposals to unify or bridge these seemingly disparate theories - one of which is the *double copy*, which constitutes a significant part of the research underpinning this thesis.

As important as it is to find a correspondence between theories of nature, it is of equal importance to improve the precision of a theory prediction, i.e., an *observable*. Gaining greater insight into the theories governing the experiments carried out at the LHC could enable us to see exciting new physics beyond the Standard Model, such as the detection of previously unseen heavy particles. One contribution to this endeavour comes in the form of calculating quantities related to the differential cross section in Quantum Chromodynamics (QCD). A QCD prediction can be enhanced by accounting for the phenomenon of *threshold radiation* associated with the scattering process.

I have had the rare privilege of studying these two different avenues throughout my PhD research. As such, this thesis is organised in two parts.

Part I of the thesis covers the topic of threshold radiation. Chapter 2 introduces the key foundations of QCD underpinning the calculation and structure of the differential cross section (our observable) via our probe, the Drell-Yan process. Having been acquainted with problematic large logarithmic terms in differential cross section calculations, in chapter 3 we will review a technique to tackle them, i.e. resummation. We break new ground in chapter 4 with a fixed order calculation (next-to next-to next-to leading order, or N^3LO), where we discover some important features about the substructure and

sources of a class of large logs. Spurred by our findings, we embark on investigating this same class of large logs for a key part of the differential cross section at *any* order in chapter 5. We recap and conclude our findings in chapter 6, and build a small bridge to the next half of the thesis.

Part II of the thesis covers the topic of the double copy. Chapter 7 introduces the BCJ double copy, which draws a relationship between scattering amplitudes of gauge theory and gravity, as well as a third theory - biadjoint scalar theory. This paves the way for the Kerr-Schild double copy reviewed in chapter 8, where we explain our claim that although this double copy relates exact classical solutions, it nonetheless relates their respective theories in an approximate way. This raises the question of whether the double copy operates at an arguably deeper *non-perturbative* level. We explore this idea by expanding the catalogue of non-Abelian strongly coupled exact solutions of biadjoint scalar theory in chapter 9. We rule out a prospective link between one of those solutions and its proposed gauge theory counterpart in chapter 10. Although this leaves the question of the existence of a non-perturbative double copy unresolved, we do discover some novelties regarding shockwaves, as well as the nature of many-to-one mappings in the double copy.

Part I

Threshold Radiation

Chapter 2

The QCD Differential Cross Section - an Overview

Comparing a theory prediction against LHC data requires developing some expectation of what is possible according to the Standard Model. If this is done accurately, then a mismatch between observed data and the expectation could signal new physics, such as that associated with the production of heavy particles. Such a theoretical prediction is the differential cross section.

We calculate the differential cross section by using perturbation theory, which approximates the physical observable by a power series expansion in the theory's coupling constant, $\alpha_s = \frac{g_s^2}{4\pi}$ in QCD. We can interpret each order in the series as accounting for the effect of adding a parton (i.e. a gluon or quark) emission to the underlying process, including all possibilities of this additional parton being virtual, or a real emission. Figure 1 schematically illustrates this idea. Calculating the differential cross section typically proceeds order by order, that is, by starting with the leading order term, and correcting it by successively adding a particle (real and virtual configurations) to arrive at a *fixed order* (i.e. a truncated) expansion. In this thesis, we will focus on corrections associated with gluon emissions.

The series expansion of the physical observable (i.e. the differential cross section) depends on the kinematic invariants of the underlying process. In QCD, the coefficients of the perturbation expansion can take the form of a function of a dimensionless variable, e.g. for the production of a heavy particle,

$$z \equiv \frac{Q^2}{\sqrt{\hat{s}}}, \tag{2.1}$$

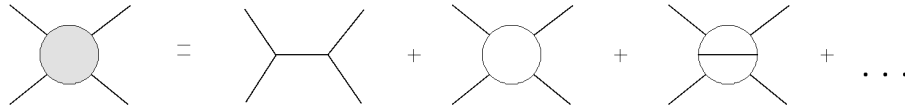


Figure 1: Schematic depiction of an all order amplitude on the left as a perturbative expansion where each correction on the right corresponds to the addition of a virtual particle.

where Q is the energy of the outgoing virtual boson or heavy particle, and \sqrt{s} is the partonic centre of mass energy of the process producing such a particle. This ratio of kinematic invariants can effectively track the proportion of initial state energy going toward producing heavy particles and therefore also that lost to radiative emissions.

The differential cross section is particularly interesting and notoriously challenging to calculate in the *threshold limit* $z \rightarrow 1$. In this limit, nearly all available incoming energy goes toward heavy particle production, and so any residual or accompanying radiation must be *infrared*. Infrared radiation (IR) can take the form of *soft* gluons, i.e. gluons with four-momentum $k^\mu \rightarrow 0$, or *collinear* gluons, i.e. gluons with nearly vanishing transverse momentum with respect to the hard particles of the process, or indeed both soft and collinear gluons. Physically, a detector can not resolve this type of emission, because the emissions are either too weak to resolve, or can not be distinguished from the hard particles, as illustrated by figure 2. However, their inclusion in a differential cross section calculation is necessary for improving the accuracy of the prediction. References [5,6] offer a few pedagogical examples of the impact of including information from threshold contributions for predictions at fixed order.

Crucially, near the threshold limit, the coefficient of the coupling becomes large enough to override the smallness of the coupling. The perturbative expansion is populated by large logarithms, and exactly at threshold, divergent terms. The divergent terms do not pose any real threat to producing a finite physical observable, as the Kinoshita-Lee-Nauenberg theorem guarantees that at all orders real and virtual emissions associated with IR divergences will cancel [7–9]. On the other hand, the large logarithms near threshold offer, at each order, large corrections to the first term of the series. This means that order by order, the fixed order differential cross section may vary wildly, and therefore the use of these logs as corrections requires care.

Although the fixed order logarithmic terms in the perturbative expansion are large near threshold, they do contain useful information for improving predictions, which motivates their study. By examining these large logs, it is possible to construct a stable correction to the fixed order prediction that captures some *all-order* information. This construction is typically achieved via *resummation*, which will be explored in the

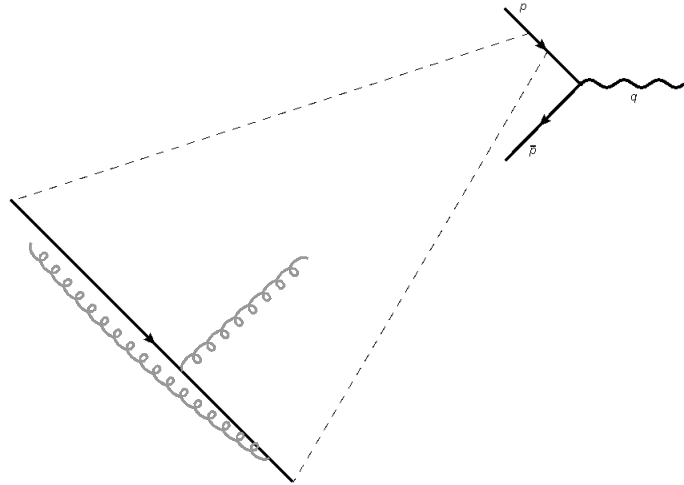


Figure 2: Infrared radiation: zoom in on gluon radiation too soft or too close to quark leg (collinear) to resolve

subsequent chapter.

In this chapter, we will briefly familiarise the reader with differential cross sections in QCD, and classify the large logarithmic terms in fixed order differential cross sections associated with near threshold radiation.

As a precursor, we will review some key aspects of QCD that underpin the calculations associated with the differential cross section.

2.1 QCD - A brief introduction

QCD is a quantum field theory describing how the constituents of a hadron bind together via the strong nuclear force. The constituents, also referred to as *partons*, are the 6 flavours of quark, and the force-carrying gluons, all of which carry the “colour” charge. Quarks and gluons exchange colour charges in accordance with the symmetry set out by the non-abelian gauge group $SU(3)$. In this context, the gauge transformations acting on gluons contain the 8 generators of group, typically represented by the Gell-Mann matrices. These matrices can act on each other and on quarks, which are represented by 3-vectors in colour space.

An important feature of QCD is that the gluon carries the charge of the gauge group (i.e. the colour charge), unlike the chargeless photon in QED. This allows for gluon self interactions, greatly complicating the number of Feynman diagrams possible, and thus realistically impairing the calculation of full fixed order differential cross sections at higher orders. This motivates a whole host of research into methods that can reduce

or streamline calculations. Some of these involve looking for patterns or substructure inside fixed order partonic cross section expressions.

A further complication to calculating partonic cross sections is the phenomenon of confinement. Non-neutral colour charged particles, or free quarks or gluons have not been observed in nature. Rather, we have observed hadrons and other bound states of quarks and gluons where the net colour charge is neutral. This begs the question, under what conditions can we meaningfully calculate partonic processes where partons are treated as free particles?

2.1.1 The running coupling and asymptotic freedom

So far, we have described some features of the colour charge in quarks and gluons, but we have not yet touched on the strength with which these partons are bound to each other. It is slightly misleading to call the QCD coupling α_s a “constant” as it varies with the energy scale of the process, a phenomenon known as *running coupling*. The running coupling has serious implications for how we can use perturbation theory. Firstly, at a particular energy scale, the coupling should be sufficiently weak to justify treating partons as free particles, rather than particles confined in bound states. Secondly, the validity of the perturbative expansion depends on its expansion parameter and coefficients being sufficiently small. In other words, perturbation theory will hold only for certain energy scales.

The running of the coupling becomes visible in perturbation theory when calculating higher order diagrams. When performing integrals over infinite loop momenta, *ultraviolet* (UV) divergences (i.e. divergences associated with high energy scales) appear. These expressions form physical observables representing probabilities, which can not be infinite. UV divergences may indicate that at very high energies, well beyond the operating level of any collider, QCD could break down as a theory. Typically, this challenge is dealt with via renormalisation, in which divergences above a mass or energy scale cut-off are removed from amplitude calculations by absorbing them in the parameters of the theory. More specifically, each *bare* parameter can be decomposed into a finite term and a *counterterm* absorbing divergent behaviour. There is some choice in how this is done, the most common being the *modified minimal subtraction* scheme, \overline{MS} . This is a modification of the *minimal subtraction* scheme, in which the counterterms are chosen to have no finite parts at all. In the modified version, some constants arising from dimensional regularisation are also subtracted off the finite terms.

In performing renormalisation, the bare coupling takes on a dependence on the ar-

bitrary mass scale parameter μ according to the Callan-Symanzik equation

$$\mu^2 \frac{d\alpha_s}{d\mu^2} = \beta(\alpha_s) \quad (2.2)$$

where the beta function is a power series in α_s . The coefficients are determined by calculating higher order diagrams:

$$\beta(\alpha_s) = -\alpha_s^2 (b_0 + b_1 \alpha_s + b_2 \alpha_s^2 + \dots). \quad (2.3)$$

For example, at the first order in QCD which is governed by the SU(3) group, we have

$$b_0 = \frac{33 - 2n_f}{12\pi} \quad (2.4)$$

where n_f is the number of quark flavours. At most, n_f can be 6, which ensures that b_0 is positive. At the subsequent order we have

$$b_1 = \frac{153 - 19n_f}{24\pi}. \quad (2.5)$$

Consider the Callan-Symanzik equation (2.2) up to first order. This can be analytically solved between two energy scales, where

$$\int_{\alpha_s(Q_0)}^{\alpha_s(Q_1)} \frac{1}{\beta(\alpha_s)} d\alpha_s = \int_{Q_0^2}^{Q_1^2} \frac{1}{\mu^2} d\mu^2 \quad (2.6)$$

is solved by

$$\alpha_s(Q_1) = \frac{\alpha_s(Q_0)}{1 + \alpha_s(Q_0) b_0 \ln \left(\frac{Q_1^2}{Q_0^2} \right)}. \quad (2.7)$$

There are several important features to note about this expression. Firstly, we only know the value of the coupling constant α_s at an energy level relative to its value at another energy level, i.e. we can not read off an absolute value of the coupling. Secondly, the phenomenon of running coupling is explicit given that the value of α_s varies with energy. Thirdly, we can see that if we fix Q_0 , then as Q_1 increases, α_s decreases as we are guaranteed that b_0 is positive. This last feature is especially pertinent in the context of perturbation theory, where the coupling needs to be sufficiently small to serve as a suitable expansion parameter. At very high energies, the partons behave as free particles - a property known as *asymptotic freedom*. At very low energies, typically at scales less than 1 GeV, the coupling will be too strong to allow for a perturbative expansion. The coupling diverges to infinity at a reference energy scale $Q_0 = \Lambda$, where (2.7) can be rewritten as:

$$\alpha_s(Q_1) = \frac{1}{b_0 \ln \left(\frac{Q_1^2}{\Lambda^2} \right)} \quad (2.8)$$

As $Q_1 \rightarrow \Lambda \sim 200$ MeV, i.e. roughly approaching the scale of a pion's mass, the coupling becomes infinite. This is known as the Landau pole, which can be viewed as an energy scale cut-off effectively separating perturbative from non-perturbative effects. This type of analysis suggests that it is possible to reason how and when partons can be treated as free particles, and when perturbation theory can be used meaningfully to calculate cross sections.

2.2 Hadronic vs. partonic cross sections

Asymptotic freedom allows us to treat partons as free particles, enabling calculations such as partonic cross sections. However, processes at the LHC require some prediction for hadronic processes. In order to offer an intuitive picture of how hadronic and partonic cross sections are related to each other, we will first state the relationship for the simplest case, leading order. In the next chapter, we will refine this and flesh it out for a specific process at a higher order. Hadronic and partonic cross sections at leading order can be related according to the formula

$$\sigma_{\text{hadronic}} = \sum_{i,j} \int_0^1 dx_1 \int_0^1 dx_2 f_i(x_1) f_j(x_2) \hat{\sigma}_{ij}, \quad (2.9)$$

where

- x_1 and x_2 are the *momentum fractions* representing the proportion of momentum carried off by two interacting partons from their parent hadrons. These variables run from 0, where the parton carries no momentum of the hadron, to 1, where the parton carries all of the momentum of the hadron.
- $f_i(x)$ is a *parton distribution function* (PDF), encapsulating the probability that a hadron will emit a parton of type i with momentum fraction x . Typically, we denote the f_i in literature by q, \bar{q}, g depending on whether the parton is a quark, antiquark, or gluon. At higher orders, PDFs can absorb collinear divergences, and as such, will be sensitive to the factorization scheme choice¹.
- The sum is over all possible parton types that can be emitted from a hadron, i.e. including all flavours of quark and antiquark. It is a necessary and intuitive condition that $\sum_i \int_0^1 dx f_i(x) = 1$.
- $\hat{\sigma}_{ij}$ is the partonic cross section. In general, the hat notation refers to partonic quantities rather than hadronic.

¹The factorization scale is a cut-off on transverse momenta, and can effectively serve as a separator of perturbative from non-perturbative physics.

The PDFs are sensitive to strongly interacting physics, and so we do not know how to derive these from first principles. These functions are treated as non-perturbative objects, determined by comparing against data. This area is an important and vast subject in its own right, as evidenced by references [10–12] to name only a few examples.

In contrast to the non-perturbative nature of PDFs, partonic cross sections can be calculated using perturbation theory. Note that the partonic cross section depends on the amount of energy transferred from the parent hadrons to the partons, which is variable. This means that in modelling parton interactions producing a particular heavy particle, the amount of incoming energy can exceed that needed for production. The “excess” energy can take the form of radiation, including the case where such radiation is soft. We begin the endeavour of studying soft radiation with a probe.

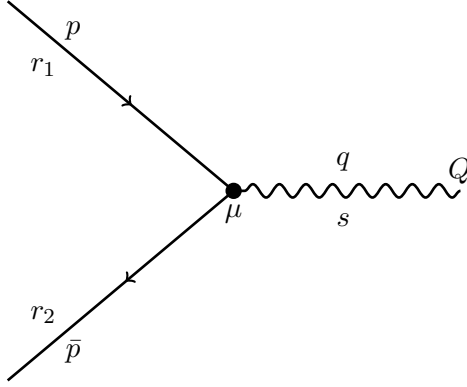
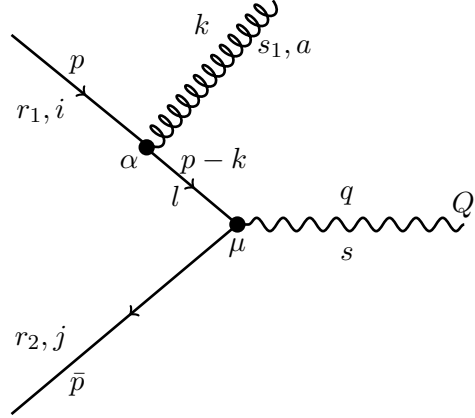
2.3 Our probe: Drell-Yan production

The Drell-Yan process is one of the most commonly studied processes for a number of reasons. Firstly, it is often the process directly producing heavy particles. Additionally, this process contributes to many of the background processes at the LHC, and thus can contribute to improving precision in data analysis. Drell-Yan is also a common probe in the search for signals of dark matter, with implications for cosmological research related to the anisotropy of the cosmic microwave background.

Although Drell-Yan can be used to directly model physical processes, it can also serve as a convenient testing ground for more abstract ventures such as resummation studies. This is partly thanks to the fact that particles produced via Drell-Yan are not enhanced by collinear final state radiation, only soft radiation, as a consequence of kinematics [13]. This simplifies greatly any resummation studies and so the process is often used as a probe in this domain.

In the standard model, Drell-Yan production is characterised by a quark-antiquark pair annihilation producing a virtual photon or Z boson, subsequently decaying into a pair of leptons. Higher orders are associated with real infrared gluon emissions as well as virtual gluons off the initial quark/antiquark legs. As our interest lies in threshold emissions associated with incoming particles, we do not need to be concerned with lepton production. That is, we only need to study a sub-process of Drell-Yan, as illustrated by figures 3 and 4 depicting this sub-process at leading order and next-to-leading order respectively, and defined by:

$$q(p) + \bar{q}(\bar{p}) \rightarrow \gamma^*(Q) + X \quad (2.10)$$


Figure 3: LO: $q\bar{q} \rightarrow \gamma^*$

Figure 4: NLO: $q\bar{q} \rightarrow \gamma^*g$, 1 real emission from the quark leg only

where the incoming quark and antiquark have d -dimensional momenta p and \bar{p} respectively, the energy of the outgoing virtual photon is fixed at Q , and X represents the total emitted radiation (although we will focus on gluon radiation only). The differential cross-section associated with this process at leading order and next-to-leading order is very well known and well-studied [14–20]. In light of this, we will very briefly review these results.

2.3.1 Leading order

At leading order, in d -dimensional spacetime, the amplitude corresponding to the process depicted in figure 3 according to the Feynman rules given in appendix A is

$$iM_{LO} = \bar{v}_{r_2}(\bar{p}) \times -ie\gamma^\mu \times u_{r_1}(p) \times \epsilon_{\mu,s}^*(q) \quad (2.11)$$

where e is the electromagnetic charge of the incoming quark, r_1 and r_2 are the spins of the incoming quark and antiquark respectively, and s is the spin of the virtual photon. We parametrise the d -dimensional momentum of the photon by q . The squared matrix element² is

$$|M|_{LO}^2 = \frac{e^2(d-2)s}{2N_c} \quad (2.12)$$

where $N_c = 3$ is the number of quark colours, and $s = 2p \cdot \bar{p}$ is the squared centre of mass energy³ in the limit where quark masses are negligible, which we will always assume. The differential cross section is simply this squared matrix element integrated over the phase space with one integral left undone. The leading order cross section is

²Unless otherwise stated, the “squared matrix element” reflects initial state spin and colour averaging, and summing over final state spins.

³Although this is a partonic quantity, we drop the hat notation as we are not at risk yet of confusing this with a hadronic quantity. Where we toggle between the partonic and hadronic quantities, we will reinstate the hat notation.

defined as

$$\hat{\sigma}^{(0)} = \frac{1}{F} \int d\Phi^{(1)} \overline{|M|}_{LO}^2 \quad (2.13)$$

where F is the flux factor associated with the initial state, i.e. $F = 2s$, and the $d\Phi^{(1)}$ signifies the phase space given by

$$\int d\Phi^{(1)} = (2\pi)^d \int \frac{d^d q}{(2\pi)^{d-1}} \delta_+(q^2 - Q^2) \delta^d(q - (p + \bar{p})). \quad (2.14)$$

The δ_+ distribution is defined in Appendix C.1.

Recall that earlier in this chapter, we defined the dimensionless threshold variable z in expression (2.1). This variable tracks how much of the initial state energy carried by the incoming quark and antiquark is transferred to the virtual photon and how much is lost to accompanying radiation. We are interested in how the cross section changes with respect to this variable, and so we will always leave one integral undone of the cross section.

At leading order, we do not model any radiation in the process, and so it must be the case that $z \rightarrow 1$. It is unsurprising then to see this reflected in the differential cross section at leading order in the threshold variable:

$$\frac{d\hat{\sigma}^{(0)}}{dz} = \frac{2\pi e^2(d-2)}{4sN_c} \delta(1-z). \quad (2.15)$$

There are no large logarithms, which is as expected since we have not yet encountered any gluon emissions. The delta function produces a distribution of the threshold variable z , effectively telling us that all incoming centre of mass energy \sqrt{s} must be transferred to the virtual photon.

For simplicity, we can rewrite the differential cross section as

$$\frac{d\hat{\sigma}^{(0)}}{dz} = \sigma_o \delta(1-z), \quad (2.16)$$

where σ_o is the Born level cross section:

$$\sigma_o = \frac{2\pi e^2(d-2)}{4sN_c}. \quad (2.17)$$

At higher orders, we will see the recurrence of this term.

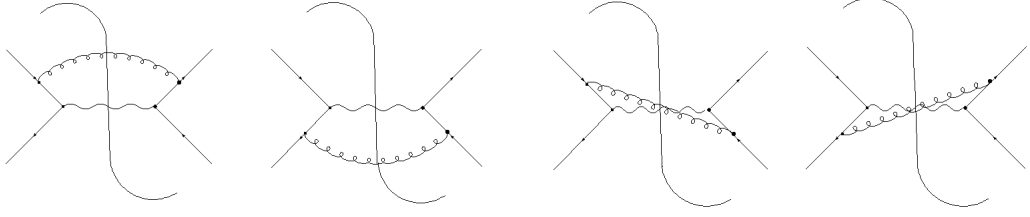


Figure 5: Cut diagrams for Drell-Yan NLO 1 real emission

2.3.2 Next-to-leading order

We will now consider the next-to-leading order case: 1 gluon emission with d -dimensional momenta k and spin s_1 from an incoming hard leg. We do not consider virtual gluons, as those diagrams will not yield any terms of interest for us, i.e. a particular class of large logarithm - to be discussed later on in this chapter. Consider diagram 4. The amplitude for this diagram (again using the Feynman rules in appendix A) is

$$iM = \bar{v}_{j,r_2}(\bar{p}) \times -ie\gamma^\mu \delta_{jl} \times \epsilon_{\mu,s}^*(q) \times \frac{i(\not{p} - \not{k})}{(p-k)^2} \times ig_s t_i^a \gamma^\alpha \times \epsilon_{\alpha,s_1}^*(k) \times u_{i,r_1}(p), \quad (2.18)$$

where we have included colour indices for all partons. Note that the gluon could have been emitted from the antiquark. Then the full squared matrix element corresponding to 1 real gluon emission is illustrated by the four diagrams of figure 5, with expression:

$$\overline{|M|^2}_{NLO} = \frac{e^2 g_s^2 C_F (d-2)}{2N_c} \left[(d-2) \left(\frac{p \cdot k}{\bar{p} \cdot k} + \frac{\bar{p} \cdot k}{p \cdot k} \right) + 2(d-4) + \left(\frac{s^2}{\bar{p} \cdot k p \cdot k} - \frac{2s}{\bar{p} \cdot k} - \frac{2s}{p \cdot k} \right) \right], \quad (2.19)$$

where $C_F = \frac{4}{3}$ is the quadratic Casimir associated with gluon emission. We can already identify some source of potentially divergent behaviour in the squared matrix element. If our gluon is soft, i.e. $k^\mu \rightarrow 0$, then the scalar products of the quark or antiquark with the gluon will vanish, i.e. $p \cdot k \rightarrow 0$, and $\bar{p} \cdot k \rightarrow 0$. Counting the occurrence of these terms in the denominator and adjusting for cancellation from the numerator would indicate some degree of divergence, with $\frac{s^2}{\bar{p} \cdot k p \cdot k}$ winning this race. However, the squared matrix element is not the only possible source of divergence when considering the cross section, defined as

$$\hat{\sigma}^{(1)} = \frac{1}{F} \int d\Phi^{(2)} \overline{|M|^2}_{NLO}. \quad (2.20)$$

The flux factor $F = 2s$ is the same at NLO as for LO as the incoming particles are the same at both orders. On the other hand, the phase space must now reflect the

additional outgoing gluon:

$$\int d\Phi^{(2)} = (2\pi)^d \int \frac{d^d q}{(2\pi)^{d-1}} \delta_+(q^2 - Q^2) \int \frac{d^d k}{(2\pi)^{d-1}} \delta_+(k^2) \delta^d(k + q - (p + \bar{p})). \quad (2.21)$$

Performing the integral as set out by (2.20), but leaving one integral undone in z gives us the differential cross section

$$\frac{d\hat{\sigma}^{(1)}}{dz} = \sigma_o \frac{\alpha_s}{4\pi} K^{(1)}(z). \quad (2.22)$$

where the K -factor⁴ is

$$K^{(1)}(z) = C_F 2^{6-d} \pi^{2-d/2} (1-z)^{d-3} s^{d/2-2} \times \left(\frac{-\Gamma(d/2-1)}{\Gamma(d-2)} + \left(\frac{d-2}{4} + \frac{z}{(1-z)^2} \right) \frac{\Gamma^2(d/2-2)}{\Gamma(d/2-1)\Gamma(d-4)} \right). \quad (2.23)$$

This is a common notation in the literature, representing a type of normalised differential cross section. We will generalise this notation further in this chapter. The dimensional regularisation convention is $d = 4 - 2\epsilon$, with a regularisation factor μ to keep the coupling dimensionless. We can see that there will be terms in (2.23) that are divergent as $z \rightarrow 1$ and $\epsilon \rightarrow 0$, warranting a Laurent expansion around $z \sim 1$ and $\epsilon \sim 0$:

$$K^{(1)}(z) = C_F \left(\frac{4\pi}{e^{\gamma_E}} \right)^{2\epsilon} \left[\frac{1}{\epsilon} \left(8 - \frac{8}{(1-z)} \right) + \frac{16 \log(1-z)}{1-z} - 16 \log(1-z) + 8 \right. \\ \left. + \epsilon \left(16 \log^2(1-z) - 16 \log(1-z) - 2\pi^2 + \frac{2\pi^2 - 16 \log^2(1-z)}{1-z} \right) \right] \quad (2.24)$$

where the prefactor $\frac{4\pi}{e^{\gamma_E}}$ containing the Euler-Mascheroni constant is a consequence of dimensional regularisation. We would like now to analyse this expression in the threshold limit $z \rightarrow 1$, close to 4 dimensions $\epsilon \rightarrow 1$. To begin, we can classify three sets of terms in (2.24), according to their order in ϵ :

- ϵ : The terms in the last set of brackets will vanish in the limit $\epsilon \rightarrow 0$.
- $\frac{1}{\epsilon}$: Virtual contributions are of this type, taking the form $\sim \delta(1-z)$ at this order, had we included them. The KLN theorem states that soft divergences (i.e. $z = 1$) cancel between virtual and real contributions. This implies that the terms in the first set of brackets dressed by the $\frac{1}{\epsilon}$ pole must be associated with collinear divergence. Collinear divergences arise in the limit where quarks are massless. This is an idealized picture - quarks are massive, and when cross sections are

⁴This is not exactly the complete K -factor, as it does not include virtual contributions.

calculated with non-zero mass, collinear divergences are not present. In this vein, collinear divergences do not pose any real threat to the stability of our prediction as they can be absorbed in the PDFs.

- ϵ^0 : There are two terms which are very large in the threshold limit $z \rightarrow 1$, threatening the stability of the correction to the fixed order differential cross section: $\frac{16 \log(1-z)}{1-z}$ which we call the *leading power* (LP) term, and $-16 \log(1-z)$, the *next-to-leading power* (NLP) term, as it is suppressed by a power of $(1-z)$ compared with the LP term. At higher orders, the LP terms of threshold processes are well catalogued and understood, while less is known about NLP terms and thus, this will be a focal point of this thesis.

In generalising beyond Drell-Yan at NLO, there is further substructure to LP and NLP terms in the threshold limit.

2.4 The general differential cross section for heavy particle production

In the previous section, we were introduced to the series of large log terms arising in the differential cross section at NLO for Drell-Yan production. In this section, we will generalise this picture to differential cross sections at all orders for any type of heavy particle production. Furthermore, we will classify the types of logarithmic terms that form the series, and identify the class of terms we will focus on in this thesis.

In the threshold limit, perturbation theory will give us the differential cross section of a process producing a heavy particle (including but not limited to Drell-Yan) to all orders as follows (see e.g. [21]):

$$\frac{d\hat{\sigma}}{d\xi} = \sigma_o \sum_{n=0}^{\infty} \left(\frac{\alpha_s}{\pi}\right)^n \sum_{m=0}^{2n-1} \left[c_{nm}^{(-1)} \left(\frac{\log^m \xi}{\xi}\right)_+ + c_{nm}^{(\delta)} \delta(\xi) + c_{nm}^{(0)} \log^m \xi + \mathcal{O}(\xi) \right] \quad (2.25)$$

where

- Generally, the precise definition of ξ is process-dependent. Our choice of process is Drell-Yan production, discussed earlier in this chapter, and $\xi = 1 - z$ where z is defined in (2.1).
- σ_o is the Born level cross section defined in (2.17).
- The index n counts each fixed order in an expansion set out by perturbation theory.

- The index m indicates some order to the size or impact of logarithmic terms - the logarithms raised to a higher value of m have a larger impact than those with a lower value of m .
- The coefficients $c_{nm}^{(r)}$ can be divergent (i.e., contain negative powers of ϵ) within a partonic cross section. At the level of the hadronic cross section, the divergent parts of these coefficients can be absorbed by parton distribution functions.
- The plus distribution $\left(\frac{\log^m \xi}{\xi}\right)_+$ is explained in appendix C.2.

In the threshold limit where $\xi \rightarrow 0$ (or in our case, $z \rightarrow 1$), the logarithmic terms dressed by the coefficients $c_{nm}^{(-1)}$ and $c_{nm}^{(0)}$ are large. Much is known about $c_{nm}^{(-1)}$, but less is known about $c_{nm}^{(0)}$. This will be our area of interest. Note that this coefficient concisely encapsulates a double sum - this means we will be scrutinizing many terms. It will be helpful then to assign names to the substructure of (2.25) in a manner consistent with supporting literature.

2.4.1 Classification of logs

The guide to the substructure is offered by the three indices of $c_{nm}^{(r)}$, each offering the following classification:

- The index n can effectively count virtual and real emissions. For example, $n = 0$ indicates a tree level process devoid of any emissions whether real or virtual, which we call *leading order* (LO). Adding one real or virtual emission ($n = 1$) is *next-to-leading order* (NLO). The perturbation expansion at a general n is N^n LO, a mnemonic containing n *next-to*'s.
- Lower r 's dress the largest terms, i.e. $c_{nm}^{(-1)}$, in (2.25) for a particular m . We call these terms *leading power* (LP). Much is known and written about LP terms, particularly in the context of *resummation* - a technique producing a stable, finite sum from a series of individually large terms [13, 22–26]. The terms dressed by $c_{nm}^{(0)}$ are the next largest, and so we refer to them as *next-to-leading power* (NLP). Our area of focus will be (the less well known) NLP terms.
- Expanding the sum in m gives a series of logarithms. The logarithms raised to the highest value of m are *leading logs* (LL), while those raised to the next highest value of m are referred to as *next-to-leading logs* (NLL). More generally, any log that is not leading can be referred to as *sub-leading*.

Each log term individually will be large, and with each order, the fixed order differential cross section may vary wildly. However, their combination, either by resummation or an alternative technique, can be finite and stable.

2.4.2 The K -factor

In literature associated with threshold radiation, fixed order differential cross sections are normalized to reveal pure radiative corrections. Such an expression is called a K -factor, which we saw in expression (2.23) for Drell-Yan at NLO. The K -factor can be generalised for higher orders:

$$\left(\frac{\alpha_s}{4\pi}\right)^n K^{(n)}(\xi) = \frac{1}{\sigma_o} \frac{d\hat{\sigma}^{(n)}}{d\xi} \quad (2.26)$$

where $\frac{d\hat{\sigma}^{(n)}}{d\xi}$ is the n^{th} order differential cross section.

Each K -factor will include a sum of large log terms as per (2.25). We will hunt for NLP logs either by calculating K -factors, or parts of K -factors contributing relevant terms at higher orders of Drell-Yan production.

2.5 Summary

Ultimately, our goal is to seek out new physics, such as those associated with processes at the LHC. Although these processes are hadronic, we have explained how, when, and why we can use partonic processes as a key ingredient to forming a physical observable to measure against experiment. The key observable we can calculate for a partonic process is the partonic differential cross section via perturbation theory. The partonic differential cross section will be a series of terms dependent on the kinematic invariants of the process. In a particular limit of these kinematics, i.e. the threshold limit where outgoing radiation is soft or collinear, this series will be populated by large logarithmic terms, challenging the stability of a fixed order theory prediction. A possible antidote comes in the form of resummation (the topic of the next chapter), however, to carry this out it is necessary to understand the substructure and sources of these large logs. We offered a gentle introduction via our probe, Drell-Yan production, where we reviewed the the differential cross section at LO and NLO (where we saw our first large logs). We then generalised this picture to an expression of a generic all-order differential cross section, with a bird's eye view of the log landscape and a classification of their interesting features. Our area of focus will be the NLP logs, for which we intend to perform a resummation. This is spurred by the success of past work to resum LP logs, which will be reviewed in the next chapter.

Chapter 3

Resummation

We finished the last chapter with a problem: when trying to correct differential cross sections, large NLP logs threaten the stability of fixed order predictions. We also suggested that the solution could take the form of resummation, where NLP log data is processed to simulate the effect of all-order information. The resummed quantity then offers a stable correction to the fixed order differential cross section.

Resummation is closely connected to *exponentiation*, the idea that an amplitude can be expressed as an exponential, where the terms in the exponent are determined by fixed order calculations. The act of placing a calculated fixed order result into an exponential to yield an all-order correction is resummation. Since the squared amplitude is an input to the cross section, the cross section can inherit some of this nice structure, provided that the phase space meets some requirements about how it factorizes.

Historically, we can date the resummation of LP logs in QCD to LL level back to 1980, when it was found that a resummed correction offered a well-behaved result in the threshold limit [27,28]. Since then, resummation was extended to include subleading logs at LP [22,23,29]. At present, NNLL is the state of the art for Drell-Yan. To get a sense of resummation in action, we will walk through the well-understood example of resummation of LP LL at NLO in this chapter.

The success of LP resummation gives us some confidence for investigating NLP resummation. We surmise that resummation may depend on factorisation of the amplitude (and by extension the differential cross section which should inherit the factorisation). This is a feature that LP terms have been demonstrated to have and studies so far suggest factorisation is a feature of NLP effects as well [21,30–38]. If factorisation is the bedrock of resummation, then we should begin by explaining what it is.

3.1 Factorisation at the amplitude level

Factorisation offers a complementary view of the differential cross section to that expressed in (2.25). Before launching into the arguably more complicated subject of factorisation at the level of the differential cross section, we will first become acquainted with the concept at the level of the amplitude. In the threshold limit, the amplitude for n external hard legs can be expressed as a product of independent factors

$$A_{(n)} = \mathcal{H}_{(n)} \cdot S_{(n)} \cdot \prod_i^n \frac{J_i}{\mathcal{J}_i}. \quad (3.1)$$

- The hard function $\mathcal{H}_{(n)}$ collects IR finite contributions to the amplitude at any order, and is free of infrared divergences.
- The jet function J_i accounts for emissions collinear to the hard leg i while \mathcal{J}_i corrects for any double counting of emissions that could be both soft and collinear.
- The soft function $S_{(n)}$ captures soft emission effects.

As the sole producer of leading logs, the soft function will be the primary focal point for the resummation discussion to come. Note that our interest in the soft function is highly dependent on what we are resumming. If we were to resum subleading logs, we would need to explore the jet functions encompassing the hard collinear effects that would start to contribute at NLL.

The soft function has properties inherently linked to resummation: universality and exponentiation. Universality is equivalent to the statement that soft gluons have their own Feynman rules independent of the underlying scattering process, as we shall see next.

3.1.1 Feynman rules for soft emissions

In this section, we will develop the Feynman rule for soft emissions. To do this, we will use the QED example of a fermion leg emitting n soft photons. The non-Abelian version, i.e. soft gluon emission, has a similar Feynman rule, but has a more complicated derivation due to the non-Abelian nature of QCD. Although it is not the original derivation, an easy to follow pedagogical treatment (in a context and notation similar to ours) can be found here: [39, 40].

Consider a variation of the Drell-Yan process that we were introduced to in the previous chapter, where the hard quark leg with momentum p^μ emits n soft photons (i.e. instead of gluons) with momentum k^μ as captured by figure 6. In the high energy limit,

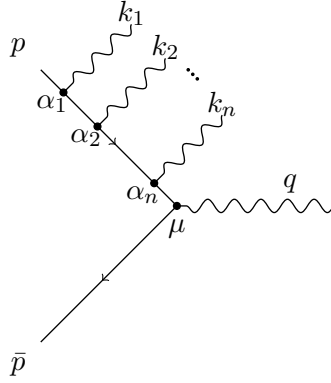


Figure 6: fermion with n soft emissions

stripping out emission polarisations, charges, and other such dressings, the amplitude associated with this picture will be

$$A_n^{\alpha_1 \alpha_2 \dots \alpha_n} = \bar{v}(\bar{p}) \gamma^\mu \frac{(\not{p} - \not{K}_n)}{(p - K_n)^2} \gamma^{\alpha_n} \dots \frac{(\not{p} - \not{K}_2)}{(p - K_2)^2} \gamma^{\alpha_2} \frac{(\not{p} - \not{K}_1)}{(p - K_1)^2} \gamma^{\alpha_1} u(p) \epsilon_\mu^*(q), \quad (3.2)$$

where $K_m = \sum_{i=1}^m k_i$ for $m = \{1, 2, \dots, n\}$.

In the soft limit $k_i \rightarrow 0$, the leading-power terms are

$$A_n^{\alpha_1 \alpha_2 \dots \alpha_n} = \bar{v}(\bar{p}) \gamma^\mu \frac{\not{p}}{(-2p \cdot K_n)} \gamma^{\alpha_n} \dots \frac{\not{p}}{(-2p \cdot K_2)} \gamma^{\alpha_2} \frac{\not{p}}{(-2p \cdot K_1)} \gamma^{\alpha_1} u(p) \epsilon_\mu^*(q). \quad (3.3)$$

A few words may be needed with regards to the denominator of the propagators. Examining one such denominator, we see three types of term:

$$(p - K_m)^2 = p^2 + K_m^2 - 2p \cdot K_m. \quad (3.4)$$

Given our assumption that the particles are massless, we have $p^2 = 0$. As for K_m^2 , the non-zero terms will be cross terms of the form $k_i \cdot k_j$. In the soft limit, these terms are dwarfed by the $p \cdot K_m$ terms, which is why we have discarded them.

Further simplifications can be made by using the anti-commutation properties of gamma matrices

$$\{\gamma^\mu, \gamma^\nu\} = 2\eta^{\mu\nu} \mathbb{1}_4, \quad (3.5)$$

as well as the Dirac equation for a massless fermion (in terms of spinors)

$$\not{p}u(p) = 0. \quad (3.6)$$

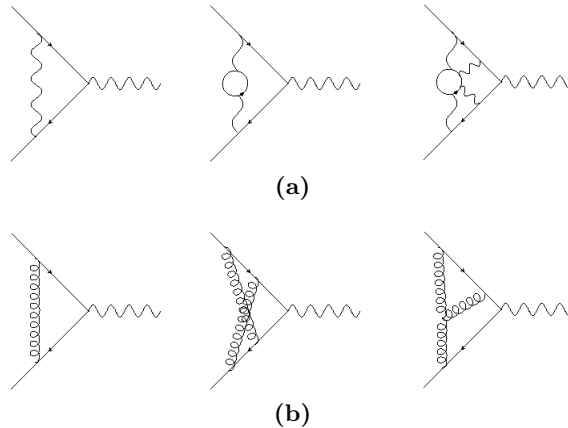


Figure 7: (a) An example of connected diagrams G_c of soft virtual photon exchange between incoming hard fermionic legs; (b) An example of webs W of soft virtual gluon exchange between incoming hard fermionic legs.

This result is so important and useful that it has earned its own box. In addition to the simplicity it lends to what could be quite complicated cross section calculations, the eikonal Feynman rule subtly suggests that the soft emission is independent of the underlying scattering process. This may appear surprising at first, but there is an intuitive explanation - a soft emission has a Compton wavelength too long to resolve the underlying hard scattering process. The property of universality is closely linked to factorisation, where all soft emission contributions can be neatly packaged into the soft function.

Considering the soft function contains its own Feynman rule, it can be considered to be an amplitude in its own right, or at least, have amplitude-like properties. One such property is exponentiation.

3.1.2 The soft function: exponentiation and Wilson lines

It is a well known result in QFT (using path integral methods) that Abelian amplitudes exponentiate, such that the exponential contains a series of connected diagrams. Disconnected diagrams are accounted for as they are expressed in terms of connected diagrams. This holds true for amplitudes involving soft virtual photon radiation, and thus the soft function will have the form (see e.g. [42])

$$S_{\text{Abelian}} \sim \exp \left[\sum G_c \right], \quad (3.14)$$

where G_c stands for connected diagrams, an example of which is captured in figure 7a. In this particular example, virtual soft photons are exchanged between the incoming hard fermionic legs of the Drell-Yan sub-process.

Exponentiation of the soft function at the level of the amplitude also holds for virtual soft gluon exchange, albeit complicated by the non-commutativity of the vertices (see [43–45] for the original proof, as well as [39, 42] for a more modern treatment). The series of diagrams in the exponent now reflects a non-trivial colour structure,

$$S_{\text{non-Abelian}} \sim \exp \left[\sum \bar{C}_W W \right] \quad (3.15)$$

where W are special diagrams called *webs*. These are connected diagrams, but furthermore, they are *two-eikonal irreducible*. Put simply, it is not possible to partition these diagrams into sub-diagrams by making cuts to the hard legs. This is reflected in the colour structure associated with the diagrams. An example is given by figure 7b, involving soft virtual gluon exchange. The colour factors \bar{C}_W are not the same as those normally dressing each graph, C_W , although the latter can be used to construct the former.

Equivalently, the effect of soft radiation can also be expressed in the language of Wilson lines. More precisely and formally, the soft function (at the level of the amplitude) is the vacuum expectation value of Wilson line operators, where the Wilson lines track the underlying hard colliding partons producing the soft radiation (see e.g. [46, 47]):

$$S_{\text{amp}} = \langle 0 | \Phi_{\bar{\beta}}(0, \infty) \Phi_{\beta}(-\infty, 0) | 0 \rangle. \quad (3.16)$$

The Wilson line operator related to the quark leg extends from the spacetime point $-\infty$ to 0 along the trajectory β^μ ,

$$\Phi_{\beta}(-\infty, 0) = \mathcal{P} \exp \left[ig_s T^a \int_{-\infty}^0 d\lambda \beta \cdot A(\lambda\beta) \right], \quad (3.17)$$

where \mathcal{P} indicates path ordering and T^a are the group generators. The dimensionless d -vectors β^μ and $\bar{\beta}^\mu$ are proportional to the momenta of the hard legs of the process,

$$p^\mu = \sqrt{\hat{s}} \beta^\mu \quad ; \quad \bar{p}^\mu = \sqrt{\hat{s}} \bar{\beta}^\mu. \quad (3.18)$$

A Wilson line operator $\Phi_{\bar{\beta}}$ for the antiquark leg can also be similarly defined. By this definition, gluon emission effects are captured within Wilson line operators. There is an intuitive connection between Wilson lines and soft gluons. A Wilson line connects a field at two spacetime points that may not be immediately comparable due to differences in phase choice. In this context, the soft gluon may be too weak to “kick” the hard quark’s momentum, but it can leave the hard leg changed by a phase factor, exactly as a Wilson line does. Additionally, Wilson lines are gauge covariant objects

which can be used to construct gauge invariant expressions.

To see how expression (3.16) really does capture soft effects, we will have a closer look at the exponent of the Wilson line operator where we will unearth the Feynman rule for soft gluon emissions. Consider the gauge field of (3.17), which can be expressed as the Fourier transform of its momentum space counterpart:

$$A(\lambda\beta) = \int \frac{d^d k}{(2\pi)^d} e^{i\lambda\beta \cdot k} \tilde{A}(k) \quad (3.19)$$

Then the exponent of (3.17) becomes

$$ig_s T^a \int_{-\infty}^0 d\lambda \beta \cdot A(\lambda\beta) = ig_s T^a \int \frac{d^d k}{(2\pi)^d} \beta \cdot \tilde{A}(k) \int_0^{\infty} d\lambda e^{-i\lambda(\beta \cdot k - i\epsilon)} \quad (3.20)$$

where we have switched the integration variable $\lambda \rightarrow -\lambda$. We have also manually included the Feynman prescription to preserve causality and ensure correct boundary conditions. The integral over λ is then straightforward to solve, with (3.20) resulting in

$$ig_s T^a \int_{-\infty}^0 d\lambda \beta \cdot A(\lambda\beta) = \int \frac{d^d k}{(2\pi)^d} \tilde{A}_\mu(k) \left[g_s T^a \frac{\beta^\mu}{\beta \cdot k - i\epsilon} \right] \quad (3.21)$$

Given that the dimensionless parameter β^μ is proportional to the momentum p^μ of the hard leg, we can recognise the term in square brackets as the Feynman rule for a soft gluon emission as per (3.13).

Although it is not strictly necessary to cast the soft function in the language of Wilson lines, doing so can ease the extension of exponentiation to the level of the differential cross section. So far, our discussion of factorisation and exponentiation has been confined to the level of the amplitude. In the next section, we will see how these principles should be interpreted for the differential cross section of the Drell-Yan process at NLO, laying the grounds for resummation.

3.2 Resummation of LP terms in the Drell-Yan cross section

This section reviews in detail the well-established resummation of leading logs of the leading power terms in the Drell-Yan cross section at NLO. By walking through this process slowly, we will gain a closer understanding of how resummation works, as well as the interdependence of resummation and factorisation. Further, it will establish confidence in approaching resummation of NLP terms to come in the subsequent chapters.

As a starting point, we isolate the part of the cross section where we will conduct the resummation exercise - the soft function.

3.2.1 Factorisation and the soft function

Here we will probe inside the hadronic cross section and fish out the soft function. We begin by relating the hadronic and partonic cross sections, building on the introduction given in section 2.2. As always, using Drell-Yan as the probe, the partonic process is that of (2.10). The hadronic differential cross section is then given by:

$$\frac{d\sigma}{d\tau} = \sigma_o(Q^2) \int_0^1 dz \int_0^1 dx_1 \int_0^1 dx_2 \delta(\tau - x_1 x_2 z) q(x_1, \mu_F^2) \bar{q}(x_2, \mu_F^2) \Delta \left(z, \alpha_s(\mu_R^2), \frac{\mu_F^2}{Q^2}, \frac{\mu_R^2}{Q^2} \right). \quad (3.22)$$

A few notes explaining the features and notation of the above:

- $z = \frac{Q^2}{\hat{s}}$ is the same familiar ratio defined in (2.1) tracking how much partonic centre of mass energy ($\sqrt{\hat{s}}$) is lost to radiation.
- $\tau = \frac{Q^2}{s}$ keeps track of how much hadronic centre of mass energy (\sqrt{s}) could be lost to radiation.
- x_1 and x_2 are the momentum fractions described in section 2.2, which also describes the PDFs q, \bar{q} (see (2.9) for the relation to f_i).
- the hadronic momenta (P, \bar{P}) are related to the partonic momenta (p, \bar{p}) according to $p = x_1 P$ and $\bar{p} = x_2 \bar{P}$, so that $\hat{s} = x_1 x_2 s$.
- The delta function $\delta(\tau - x_1 x_2 z)$ technically leads us to view (3.22) as a convolution of the PDFs and the partonic cross section Δ . It implements that the partonic and hadronic centre of mass energies are related to each other and not independent.
- μ_F and μ_R are the factorisation and renormalisation scales respectively. Given that scale choice effects contribute only to subleading logs, we can simplify (3.22) by setting $\mu_F = \mu_R = Q$ (see e.g. [23]).
- Δ is partonic, and closely related to the K -factor described in section 2.4.2. For example, at leading order, $\Delta^{(0)} = \delta(1 - z)$ which reconciles with the differential cross section of (2.16).

The interesting factorisation and exponentiation activity resides in Δ , however, many terms on the right hand side of (3.22) are interlinked by the delta function $\delta(\tau - x_1 x_2 z)$. It would be nice to decouple these terms in order to properly isolate Δ for further

exploration. This is easily done by taking Mellin moments with respect to τ , i.e.

$$\int_0^1 d\tau \tau^{N-1} \frac{d\sigma}{d\tau}. \quad (3.23)$$

The corresponding right hand side of this equation will be

$$\sigma_o(Q^2) \int_0^1 dz \int_0^1 dx_1 \int_0^1 dx_2 \int_0^1 d\tau \tau^{N-1} \delta(\tau - x_1 x_2 z) q(x_1, Q^2) \bar{q}(x_2, Q^2) \Delta(z, Q^2), \quad (3.24)$$

which simplifies and results in the relation

$$\int_0^1 d\tau \tau^{N-1} \frac{d\sigma}{d\tau} = \sigma_o(Q^2) q(N, Q^2) \bar{q}(N, Q^2) \Delta(N, Q^2) \quad (3.25)$$

where the partonic differential cross section in Mellin space is

$$\Delta(N, Q^2) = \int_0^1 dz z^{N-1} \Delta(z, Q^2), \quad (3.26)$$

and the transformed quark PDF is

$$q(N, Q^2) = \int_0^1 dx_1 x_1^{N-1} q(x_1, Q^2). \quad (3.27)$$

We described in the previous chapter how the partonic differential cross section will be populated by logs and we have described how to categorize these logs. In this section, we will resum the LP logs taken from calculations at NLO. In momentum space, these take the form of $\frac{\log(1-z)}{1-z}$. In Mellin space, this translates as (see appendix C.3):

$$\int_0^1 dz z^{N-1} \left(\frac{\log(1-z)}{1-z} \right)_+ \sim \frac{1}{2} \log^2(N) + \text{subleading terms}. \quad (3.28)$$

The threshold limit in Mellin space corresponds to $N \rightarrow \infty$. This is apparent when comparing the Mellin transforms of LP and NLP log terms, both of which can be found in appendix C.3. In comparison with the LP term, the NLP term is suppressed by a power in $(1-z)$ in z -space. In Mellin space, this suppression manifests itself by a power of $\frac{1}{N}$.

Finding the coefficients of these logs in this limit will enable the ultimate goal of resummation. To extract these logs, we need to pinpoint where to look for them in Δ . Factorisation helps us do this. Analogous to amplitude-level factorisation in section 3.1, the partonic differential cross section in Mellin space can be factorised into hard,

collinear, and soft contributions as follows:

$$\Delta(N, Q^2, \epsilon) = |\mathcal{H}(Q^2)|^2 \cdot \frac{\prod_i \psi_i(N, Q^2, \epsilon)}{\prod_i \psi_{\text{eik},i}(N, Q^2, \epsilon)} \cdot \mathcal{S}(N, Q^2, \epsilon). \quad (3.29)$$

A few notes about this:

- $\mathcal{H}(Q^2)$ is the familiar amplitude-level *hard function*, containing off-shell virtual contributions. This term is finite.
- $\psi_i(N, Q^2, \epsilon)$ is a *perturbative quark distribution function* collecting collinear singularities associated with line i , while $\psi_{\text{eik},i}(N, Q^2, \epsilon)$ accounts for any possible double counting of contributions that could be both soft and collinear.
- $\mathcal{S}(N, Q^2, \epsilon)$ is the *soft function*, containing all real and virtual contributions associated with soft radiation.

The hard collinear contributions do not produce any leading logs at leading power. This is because at any fixed order in α_s , leading logs at leading power only arise when the maximum number of singular integrations is performed - yielding the highest inverse power of ϵ . In this context, we can set the hard collinear contributing terms collectively to unity as per

$$\frac{\prod_i \psi_i(N, Q^2, \epsilon)}{\prod_i \psi_{\text{eik},i}(N, Q^2, \epsilon)} \equiv 1. \quad (3.30)$$

This leaves us with a simplified factorized form of Δ producing leading logs,

$$\Delta(N, Q^2, \epsilon) = |\mathcal{H}(Q^2)|^2 \cdot \mathcal{S}(N, Q^2, \epsilon). \quad (3.31)$$

As desired, we have isolated the soft function \mathcal{S} in the partonic differential cross section, which governs the landscape of leading logs in Drell-Yan. A resummation of these logs requires some confidence that this function exponentiates. We already been introduced to exponentiation at the level of the amplitude in section 3.1.2, but now we will explore this concept at the level of the differential cross section.

3.2.2 The soft function: exponentiation and Wilson lines

The soft function at the level of the amplitude was defined as the expectation value of Wilson line operators (3.16). At the level of the differential cross section, the soft function must reflect the integration of a “square” over an appropriate phase space, all of which is formally given by

$$\mathcal{S}(z, Q^2, \epsilon) = \frac{1}{N_c} \sum_n \text{Tr} \left[\langle 0 | \Phi_\beta^\dagger \Phi_{\bar{\beta}} | n \rangle \langle n | \Phi_{\bar{\beta}}^\dagger \Phi_\beta | 0 \rangle \right] \delta \left(z - \frac{Q^2}{\hat{s}} \right). \quad (3.32)$$

	L	L^2	L^3	L^4	L^5	\dots
α_s	$c_{11}^{(-1)}$					
α_s^2	$c_{21}^{(-1)}$	$c_{22}^{(-1)}$	$c_{23}^{(-1)}$			
α_s^3	$c_{31}^{(-1)}$	$c_{32}^{(-1)}$	$c_{33}^{(-1)}$	$c_{34}^{(-1)}$	$c_{35}^{(-1)}$	
\vdots						

Table 1: LP coefficients of (2.25), with LL terms in red, NLL in green, and subleading logs in blue. Here we use the shorthand $L \equiv \frac{\log \xi}{\xi}$.

The sum over final states containing n partons generated by Wilson lines includes the integration over the phase space. This is subject to constraint on the total final state energy imposed by the the delta function. The trace is over the colour indices. The soft function can then be shown to have a manifestly exponential form at the level of the differential cross section provided two conditions are met:

- The vacuum expectation value of Wilson lines exponentiates prior to phase space integration (shown diagrammatically in [43–45], or by using renormalisation group arguments in [48–53]).
- The phase space for n soft gluons factorizes into n decoupled 1-parton phase space integrals, which is a necessary condition for factorisation at the level of the cross section.

Proof of exponentiation has also more recently been reinterpreted by a path integral approach that uses the “replica trick” [42], a method borrowed from statistical physics. The bottom line is that the soft function will indeed have an exponential form, with a series of webs populating the exponent. In other words, the exponent will contain an expansion in the coupling constant of the theory, i.e.,

$$S \sim \exp [\alpha_s c_1 + \alpha_s^2 c_2 + \alpha_s^3 c_3 + \dots]. \quad (3.33)$$

We can relate this picture back to the differential cross section of (2.25). Consider for example, the LP terms only, i.e. those dressed by the coefficients $c_{nm}^{(-1)}$. These terms are neatly packaged into a double sum. In table 1, we have unpacked the first few orders of these terms, and colour coded them by the leading power of the log. The LL terms begin at order α_s , while the NLL terms begin at order α_s^2 . Therefore, if we are interested in collecting some leading log information for LP terms, we can calculate the NLO diagrams, isolate the LP LL terms, and place them in an exponential. This process is resummation. Alternatively, should we wish to resum subleading log data, we would need to calculate diagrams at higher orders, and exponentiate the appropriate terms.

Now that we have seen in principle how resummation works, we will flesh out a well-understood example that we have already briefly started to discuss - the resummation of the LP LL terms at NLO for the Drell-Yan process.

3.2.3 The eikonal cross section at NLO

The soft function, or eikonal cross-section (i.e. the cross section involving the leading soft term with Feynman rule established in section 3.1.1) up to NLO in momentum space is

$$S(z, Q^2, \epsilon) = (1 + S_{\text{virtual}}^{(1)})\delta(1 - z) + S_{\text{real}}^{(1)}(z) + \mathcal{O}(\alpha_s^2) \quad (3.34)$$

where the contribution attributed to real emissions $S_{\text{real}}^{(1)}(z)$ is illustrated in figure 5. This part of the cross-section is (using the soft Feynman rule (3.13), and corresponding to the third last term of (2.19))

$$S_{\text{real}}^{(1)}(z) = \frac{\hat{s}}{2\pi} \mu^{2\epsilon} g_s^2 C_F \int d\Phi^{(2)} \frac{\hat{s}}{p \cdot k \bar{p} \cdot k} \quad (3.35)$$

where the two-body phase space is given by (2.21), but reproduced here for the reader's convenience:

$$\int d\Phi^{(2)} = (2\pi)^d \int \frac{d^d k}{(2\pi)^{d-1}} \delta_+(k^2) \int \frac{d^d q}{(2\pi)^{d-1}} \delta_+(q^2 - Q^2) \delta^{(d)}(q + k - p - \bar{p}). \quad (3.36)$$

Note that in (3.35), some dressing factors (e.g. flux factor, electric charge etc.) have already been absorbed in the hard factor seen in (3.31). Also note the absence of the outgoing virtual photon momentum in the integrand, as expected since this is not present in the Feynman rule for the soft gluon. We can then carry out the integral over the photon momentum in the phase space integral by applying one of the delta functions:

$$\int d\Phi^{(2)} = \frac{(2\pi)}{\hat{s}} \int \frac{d^d k}{(2\pi)^{d-1}} \delta_+(k^2) \delta \left(1 - z - \frac{2k \cdot (p + \bar{p})}{\hat{s}} \right). \quad (3.37)$$

In applying the delta function, we made use of the definition of z as per (2.1) as well as the property $\delta(ax) = \frac{1}{|a|} \delta(x)$. This brings us to

$$S_{\text{real}}^{(1)}(z) = \mu^{2\epsilon} g_s^2 C_F \int \frac{d^d k}{(2\pi)^{d-1}} \delta_+(k^2) \delta \left(1 - z - \frac{2k \cdot (p + \bar{p})}{\hat{s}} \right) \frac{\hat{s}}{p \cdot k \bar{p} \cdot k}. \quad (3.38)$$

As for the virtual contribution, we can calculate this directly or use the soft gluon unitarity requirement

$$\int_0^1 dz S(z, Q^2, \epsilon) = 1, \quad (3.39)$$

which when combined with (3.34) offers the simple relationship linking virtual to real corrections

$$S_{\text{virtual}}^{(1)} = - \int_0^1 d\tilde{z} S_{\text{real}}^{(1)}(\tilde{z}). \quad (3.40)$$

The full NLO eikonal contribution is then composed of building blocks of real contributions:

$$S^{(1)}(z) = S_{\text{real}}^{(1)}(z) - \int_0^1 d\tilde{z} S_{\text{real}}^{(1)}(\tilde{z}) \delta(1 - z), \quad (3.41)$$

which reduces nicely to the integral

$$S^{(1)}(z) = \mu^{2\epsilon} g_s^2 C_F \int \frac{d^d k}{(2\pi)^{d-1}} \delta_+(k^2) \left[\delta \left(1 - z - \frac{2k \cdot (p + \bar{p})}{\hat{s}} \right) - \delta(1 - z) \right] \frac{2p \cdot \bar{p}}{p \cdot k \bar{p} \cdot k}. \quad (3.42)$$

This integral is easily solvable using a Sudakov decomposition, such as

$$k^\mu = k_+ \beta^\mu + k_- \bar{\beta}^\mu + k_T^\mu, \quad (3.43)$$

where k_T is a d -vector transverse to the dimensionless vectors β^μ and $\bar{\beta}^\mu$ defined in (3.18),

$$k_T \cdot \beta = k_T \cdot \bar{\beta} = 0. \quad (3.44)$$

The k_+ and k_- terms can be arrived at by contracting (3.43) with \bar{p} and p respectively:

$$k_+ = \frac{2\bar{p} \cdot k}{\sqrt{\hat{s}}} \quad ; \quad k_- = \frac{2p \cdot k}{\sqrt{\hat{s}}}. \quad (3.45)$$

In the Sudakov decomposition, the integration measure becomes

$$\int d^d k = \frac{1}{2} \int dk_+ dk_- d^{d-2} \mathbf{k}_T \quad (3.46)$$

where \mathbf{k}_T is the $d - 2$ dimensional vector contained in k_T^μ , and the factor of $1/2$ is the Jacobian associated with the change to Sudakov coordinates (see appendix D.1 for more details). Moving to spherical polar coordinates yields the integration measure

$$\int d^d k = \frac{1}{4} \int dk_+ dk_- d\mathbf{k}_T^2 d\Omega_{d-2}(\mathbf{k}_T^2)^{\frac{d-4}{2}}, \quad (3.47)$$

where $d\Omega_m$ is the element of solid angle in m spatial dimensions. Having taken care of the integration measure, we now express the integrand in Sudakov coordinates, made of the following terms:

$$\delta_+(k^2) = \delta_+(k_+ k_- - \mathbf{k}_T^2) \quad (3.48)$$

$$\frac{2p \cdot \bar{p}}{p \cdot k \bar{p} \cdot k} = \frac{4}{k_+ k_-} \quad (3.49)$$

$$\delta\left(1-z-\frac{2k\cdot(p+\bar{p})}{\sqrt{\hat{s}}}\right)=\delta\left(1-z-\frac{1}{\sqrt{\hat{s}}}(k_++k_-)\right). \quad (3.50)$$

Altogether, the integral in Sudakov coordinates is now

$$\begin{aligned} S^{(1)}(z) &= \frac{\mu^{2\epsilon}g_s^2\Omega_{d-2}C_F}{(2\pi)^{d-1}} \int dk_+dk_-d\mathbf{k}_T^2 (\mathbf{k}_T^2)^{\frac{d-4}{2}} \delta_+(k_+k_- - \mathbf{k}_T^2) \\ &\quad \times \left[\delta\left(1-z-\frac{1}{\sqrt{\hat{s}}}(k_++k_-)\right) - \delta(1-z) \right] \frac{1}{k_+k_-}. \end{aligned} \quad (3.51)$$

Applying the δ_+ will act to change the integration bounds (see appendix D.2):

$$S^{(1)}(z) = \frac{\mu^{2\epsilon}g_s^2\Omega_{d-2}C_F}{(2\pi)^{d-1}} \int_0^\infty dk_+dk_- (k_+k_-)^{\frac{d-6}{2}} \left[\delta\left(1-z-\frac{1}{\sqrt{\hat{s}}}(k_++k_-)\right) - \delta(1-z) \right]. \quad (3.52)$$

This is easily solved with a variable change

$$k_+ = \sqrt{\hat{s}}(1-\tilde{z})y \quad ; \quad k_- = \sqrt{\hat{s}}(1-\tilde{z})(1-y), \quad (3.53)$$

which has the corresponding integration measure:

$$\int_0^\infty dk_+dk_- = \int_0^1 \hat{s}(1-\tilde{z})d\tilde{z}dy. \quad (3.54)$$

The transformed integral becomes

$$\begin{aligned} S^{(1)}(z) &= \frac{\mu^{2\epsilon}g_s^2\Omega_{d-2}C_F}{(2\pi)^{d-1}} \hat{s}^{\frac{d-4}{2}} \int_0^1 d\tilde{z} dy (1-\tilde{z})^{d-5} y^{\frac{d-6}{2}} (1-y)^{\frac{d-6}{2}} \\ &\quad \times \left[\underbrace{\delta(\tilde{z}-z)}_A - \underbrace{\delta(1-z)}_B \right]. \end{aligned} \quad (3.55)$$

The integral has been broken into two integrals. The first, integral A , is a beta function (see appendix B.3):

$$\begin{aligned} &\int_0^1 d\tilde{z} dy (1-\tilde{z})^{d-5} y^{\frac{d-6}{2}} (1-y)^{\frac{d-6}{2}} \delta(\tilde{z}-z) \\ &= (1-z)^{d-5} \int_0^1 dy y^{\frac{d-6}{2}} (1-y)^{\frac{d-6}{2}} \\ &= (1-z)^{-1-2\epsilon} \frac{\Gamma^2(-\epsilon)}{\Gamma(-2\epsilon)}, \end{aligned} \quad (3.56)$$

where, in the last step, we replaced d by our dimensional regularisation convention $d = 4 - 2\epsilon$. Integral B is actually the product of two beta functions if recast in the

format:

$$\begin{aligned}
 & - \int_0^1 d\tilde{z} dy (1 - \tilde{z})^{d-5} y^{\frac{d-6}{2}} (1 - y)^{\frac{d-6}{2}} \delta(1 - z) \\
 & = -\delta(1 - z) \int_0^1 d\tilde{z} \tilde{z}^0 (1 - \tilde{z})^{d-5} \int_0^1 dy y^{\frac{d-6}{2}} (1 - y)^{\frac{d-6}{2}} \\
 & = \delta(1 - z) \frac{\Gamma^2(-\epsilon)}{2\epsilon\Gamma(-2\epsilon)}. \tag{3.57}
 \end{aligned}$$

In the last step, we used the property $\Gamma(n + 1) = n\Gamma(n)$. Now that all integrals have been carried out, we only have to tidy up the prefactor of (3.55). The solid angle in our dimensional regularisation convention is

$$\Omega_{d-2} = \frac{2\pi^{\frac{d-2}{2}}}{\Gamma(\frac{d-2}{2})} \longrightarrow \Omega_{2-2\epsilon} = \frac{2\pi^{1-\epsilon}}{\Gamma(1-\epsilon)}. \tag{3.58}$$

Further, we can rewrite (3.55) using the \overline{MS} renormalisation scale $\bar{\mu}^2 = 4\pi e^{-\gamma_E} \mu^2$ as well as $\alpha_s = \frac{g_s^2}{4\pi}$. Altogether, (3.55) becomes

$$S^{(1)}(z) = \frac{\bar{\mu}^{2\epsilon} e^{\epsilon\gamma_E} \alpha_s}{\pi} \frac{C_F}{\Gamma(1-\epsilon)} \left(\frac{1}{\hat{s}}\right)^\epsilon \frac{\Gamma^2(-\epsilon)}{\Gamma(-2\epsilon)} \left[(1-z)^{-1-2\epsilon} + \frac{1}{2\epsilon} \delta(1-z) \right]. \tag{3.59}$$

Clearly this expression is divergent close to 4 dimensions, i.e. as $\epsilon \rightarrow 0$, and in the threshold limit $z \rightarrow 1$. If we want to understand this expression in these limits, then we must perform the appropriate Laurent expansions which will produce the threshold logs of interest to us. Prior to doing so however, we should recognise that there are extra factors of z hiding in the $(\frac{1}{\hat{s}})^\epsilon$ dressing since $z = \frac{Q^2}{\hat{s}}$. More precisely, we incur an extra factor of z^ϵ , which, when expanded is

$$z^\epsilon = 1 - \epsilon(1 - z) + \dots \tag{3.60}$$

where the ellipses denote quadratic and higher order terms in ϵ and $(1 - z)$. In light of this, with dependence on the energy of the virtual momentum now made explicit, (3.59) becomes

$$S^{(1)}(z, Q^2) = \frac{\alpha_s C_F}{\pi} \left(\frac{\bar{\mu}^2}{Q^2}\right)^\epsilon \frac{e^{\epsilon\gamma_E} \Gamma^2(-\epsilon)}{\Gamma(1-\epsilon)\Gamma(-2\epsilon)} (1 - \epsilon(1 - z) + \dots) \left[(1 - z)^{-1-2\epsilon} + \frac{1}{2\epsilon} \delta(1 - z) \right]. \tag{3.61}$$

It is evident that the factor of $\epsilon(1 - z)$ will only act to suppress divergences and powers of $(1 - z)$, resulting in power-suppressed log behaviour. As we are interested in leading power behaviour, we can ignore these terms and instead simply consider only the leading

term, i.e. truncate at $z^\epsilon = 1$. Then (3.61) becomes

$$S^{(1)}(z, Q^2) = \frac{\alpha_s C_F}{\pi} \left(\frac{\bar{\mu}^2}{Q^2} \right)^\epsilon \frac{e^{\epsilon\gamma_E} \Gamma^2(-\epsilon)}{\Gamma(1-\epsilon)\Gamma(-2\epsilon)} \left[(1-z)^{-1-2\epsilon} + \frac{1}{2\epsilon} \delta(1-z) \right]. \quad (3.62)$$

Ultimately, we are interested in resumming the leading logs of the leading power terms. The prerequisites to resummation are exponentiation and factorisation, which are apparent in Mellin space. Our expression for the NLO eikonal cross section is in terms of z in momentum space. To move from momentum space to Mellin space, we perform a Mellin transform as set out below:

$$S^{(1)}(N, Q^2) = \int_0^1 dz z^{N-1} S^{(1)}(z, Q^2). \quad (3.63)$$

Applying this transform to (3.62) is straightforward, and the resulting integral is similar to those of past steps in this section. In Mellin space, we have

$$S^{(1)}(N, Q^2) = \frac{\alpha_s C_F}{\pi} \left(\frac{\bar{\mu}^2}{Q^2} \right)^\epsilon \frac{e^{\epsilon\gamma_E} \Gamma^2(-\epsilon)}{\Gamma(1-\epsilon)\Gamma(-2\epsilon)} \left[\frac{\Gamma(N)\Gamma(-2\epsilon)}{\Gamma(-2\epsilon+N)} + \frac{1}{2\epsilon} \right]. \quad (3.64)$$

Expanding this in $\epsilon \sim 0$, keeping only terms of order $\frac{1}{\epsilon}$ and ϵ^0 (as terms of higher order will vanish in this limit), we have

$$S^{(1)}(N, Q^2, \epsilon) = \frac{\alpha_s C_F}{\pi} \left(\frac{\bar{\mu}^2}{Q^2} \right)^\epsilon \left[\frac{2}{\epsilon} \left(\psi^{(0)}(N) + \gamma_E \right) + 2 \left((\psi^{(0)}(N))^2 + 2\gamma_E \psi^{(0)}(N) - \psi^{(1)}(N) + \gamma_E^2 + \frac{\pi^2}{6} \right) \right], \quad (3.65)$$

where the polygamma functions $\psi^{(m)}(N)$ are defined in appendix. In the limit $N \rightarrow \infty$, if we truncate any subleading log behaviour, then (3.65) reduces to

$$S^{(1)}(N, Q^2, \epsilon)|_{\text{LL}} = \left(\frac{\bar{\mu}^2}{Q^2} \right)^\epsilon \frac{2\alpha_s}{\pi} C_F \left[\frac{\log N}{\epsilon} + \log^2 N \right], \quad (3.66)$$

where the first term accounts for the (anti-)collinear contributions (to be absorbed in PDFs) and the second is the dominant log of the soft contribution. We know \mathcal{S} exponentiates, and so, the resummed soft function will contain the term:

$$S_{\text{resummed}} \sim \exp \left[\frac{2\alpha_s}{\pi} C_F \left(\frac{\log N}{\epsilon} + \log^2 N \right) \right]. \quad (3.67)$$

We relate this back now to our original cross section defined in (3.25), although here we truncate this expression strictly to the leading logs at leading power, i.e.

$$\int_0^1 d\tau \tau^{N-1} \frac{d\sigma}{d\tau} |_{\text{LL}} = \sigma_o(Q^2) q_{\text{LL}}(N, Q^2) \bar{q}_{\text{LL}}(N, Q^2) \Delta(N, Q^2) |_{\text{LL}}. \quad (3.68)$$

Firstly, we can allow the PDFs to absorb the collinear and anti-collinear divergent leading log contributions. The quark PDF thus becomes

$$q_{\text{LL}}(N, Q^2) = q(N, Q^2) \exp \left[\frac{\alpha_s}{\pi} C_F \frac{\log N}{\epsilon} \right] \quad (3.69)$$

and the antiquark PDF is similarly modified. This leaves us with a resummed expression for the leading logs of the leading power terms of the cross section (or K -factor):

$$\Delta(N, Q^2) |_{\text{LP,LL}} = \exp \left[\frac{2\alpha_s}{\pi} C_F \log^2 N \right], \quad (3.70)$$

where the hard function here is unity since the Born-level cross section is factored out. This expression resums the leading logs at leading power based on information gleaned at NLO, simulating the effect of an all order correction.⁵ It is easily verified by earlier publications (see e.g. [15, 28]).

Lastly, if we want to recover our expression for the leading power part of the differential cross section in z -space, we would need to expand (3.70) in powers of α_s , and include all of the terms in the second line of (3.65) (rather than truncating at the leading log) before performing an inverse Mellin transform. Comparing this second line with that of (C.31), it is evident that our NLO LP differential cross section in z -space is

$$\Delta(N, Q^2) |_{\text{LP}} = \frac{2\alpha_s}{\pi} C_F \left(2 \left(\frac{\log(1-z)}{1-z} \right)_+ \right) \quad (3.71)$$

which is consistent with the expression (2.24). In a later chapter, we will combine the LP result with that pertaining to NLP terms.

3.3 The prospect of resummation beyond LP terms

To recap, we are motivated to improve the accuracy of the differential cross section by including threshold radiation, but this leads to large logs at fixed order. The cure for this is resummation, where large logs can be used to simulate an all-order correction to the differential cross section. We have reproduced the resummation of a particular class of logs - the leading logs at leading power for a differential cross section at NLO, which is

⁵Note that in practice, this exponential would need to be inverse Mellin transformed as part of the hadronic cross section to be useful.

a well-known piece of analysis. We now pose the question of whether a similar treatment can be carried out for the NLP leading logs. We have a reasonable understanding of what kind of data we need to perform such an exercise - i.e. the coefficients dressing the large logs associated with differential cross section calculations. However, performing such calculations is a considerable task. It may be worth probing first what part of the differential cross section could be a source of leading behaviour, and which parts produce subleading logs at NLP and therefore can be disregarded. The next two chapters explore the sources of leading and subleading logs at NLP, for a process involving 3 gluons (2 real 1 virtual) and for a process involving any number of real emissions.

Chapter 4

Next-to-Leading Power Leading Logs at N³LO

We would like to improve the accuracy of cross section or K -factor expressions by including threshold corrections given by the resummation of NLP LL terms. This involves calculating fixed order cross sections to gather data useful for resummation. However, calculating entire cross sections or random pieces of cross sections blindly is computationally expensive. This is one of many motivations to investigate whether there are some substructures within cross sections that are sources of leading terms, and other substructures which are consistently producing subleading terms and can therefore be disregarded from further calculations.

A natural question arises of what has been done to date to answer such a question. So far, NNLO is the state of the art for Drell-Yan cross section predictions, supplemented by resummed logs [14–16, 18, 19, 54, 55]. A convenient method for calculating contributions to NNLO involving virtual corrections is the *method of regions* in which the loop momentum can be separated out into non-overlapping hard, soft, and (anti-)collinear modes or *regions* [56–58]. When using this classification for calculating the cross section for the 1-real, 1-virtual contribution to NNLO, it was found that certain types of log term had clear links to particular regions [59].

How persistent are the method of regions/NLP LL relationships beyond NNLO? We explore a subset of N³LO contributions to the K -factor via the method of regions. More specifically, we will focus on the “easiest” possible starting point - 2-real, 1-virtual *Abelian* diagrams, i.e., diagrams associated with colour structure C_F^3 at $\mathcal{O}(\alpha_s^3)$. Any learnings in this arena can be carried forward toward a more general case (e.g. non-Abelian diagrams) down the line. To understand how NLP LL are connected to the region substructures of the differential cross section, we will need to set up the right

machinery which will be a combination of method of regions and Sudakov parametrisations, coming right up.

4.1 Squared matrix element for 2-real, 1-virtual emissions

Consider the subset of Abelian diagrams of the Drell-Yan process in which the higher order emissions are of the form of 2 real gluon emissions and 1 virtual gluon. These diagrams can be reduced to a set of scalar diagrams via methods such as the Passarino-Veltman reduction, or Integration by Parts. An example of such a scalar diagram is illustrated in figure 8, although it must be said that this is only one of the many Abelian diagrams of this order (see [3] for full details).

One could use the method of regions to calculate 4 “region-specific” squared matrix elements associated with this process, such that the sum of all 4 expressions is the total squared matrix element. The regions are determined by a book-keeping parameter λ related to our threshold parameter z according to $\lambda \sim \sqrt{1-z}$. Further to this classification, each region-specific squared matrix element can be expressed as a series of terms organised by degree in λ . Once integrated over the full phase space (to be shown in detail in the next section), clear relationships between the region substructures and the LP, NLP etc. log structures of the K -factor will become apparent.

This section is intended help the reader understand what is meant by a “region-specific” squared matrix element, and what its substructures are in terms of leading and sub-leading behaviour in λ . To shine light on this, we will briefly explore some features of the sample amplitude of figure 8 in the context of the method of regions. Familiarity with the language around method of regions will allow us to state (but we will not derive ⁶) the “region-specific” squared matrix elements.

4.1.1 Method of regions

Working with figure 8, we make use of a Sudakov decomposition to separate out collinear from transverse momenta etc for the virtual gluon momentum,

$$k^\mu = \underbrace{\frac{1}{2}(n_- \cdot k) n_+^\mu}_{\equiv k_+} + \underbrace{\frac{1}{2}(n_+ \cdot k) n_-^\mu}_{\equiv k_-} + k_T^\mu, \quad (4.1)$$

⁶Although the derivation of the squared matrix elements does not form part of this thesis, the reader may find further information about this in [3].

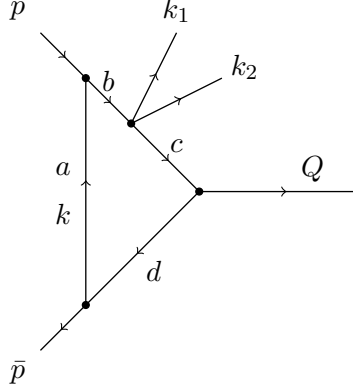


Figure 8: Drell-Yan 2 real, 1 virtual emission - 1 example scalar Feynman diagram

where we have defined dimensionless null vectors

$$n_+^\mu = \frac{2}{\sqrt{\hat{s}}} p^\mu, \quad n_-^\mu = \frac{2}{\sqrt{\hat{s}}} \bar{p}^\mu, \quad n_+ \cdot n_- = 2, \quad (4.2)$$

and we can treat transverse momentum as one component

$$k^\mu = (k_+, \mathbf{k}_T, k_-). \quad (4.3)$$

We now attempt to account for “thresholdness”, i.e. degrees of threshold behaviour, in the hope of decomposing our amplitude into non-overlapping soft, hard, (anti-)collinear contributions led by the virtual gluon. We use the scaling parameter $\lambda \sim \sqrt{1-z}$ to divide the virtual gluon momentum into the four regions:

$$\begin{aligned} \text{Hard: } k &\sim \sqrt{\hat{s}}(1, 1, 1); & \text{Soft: } k &\sim \sqrt{\hat{s}}(\lambda^2, \lambda^2, \lambda^2); \\ \text{Collinear: } k &\sim \sqrt{\hat{s}}(1, \lambda, \lambda^2); & \text{Anticollinear: } k &\sim \sqrt{\hat{s}}(\lambda^2, \lambda, 1). \end{aligned} \quad (4.4)$$

This is not the only possible scaling, however, it can be shown that these regions are the only ones relevant for threshold expansion [3].

Using the region scaling and the Sudakov parametrisation, it is possible then to derive 4 region-specific amplitudes, each of which can be organised in powers of λ - the threshold accountancy parameter. We can explore this principle in the amplitude associated with diagram 8.

The contribution specific to figure 8 will roughly be a loop integral with integrand being a product of propagators

$$I = \int [dK] \frac{1}{D_a D_b D_c D_d} \quad (4.5)$$

where the propagator denominators D_i are

$$\begin{aligned}
 D_a &= k^2 \\
 D_b &= (k+p)^2 = k^2 + 2p \cdot k \\
 D_c &= (k+p - (k_1+k_2))^2 = k^2 + 2k \cdot p - 2k \cdot (k_1+k_2) - 2p \cdot (k_1+k_2) + 2k_1 \cdot k_2 \\
 D_d &= (\bar{p}-k)^2 = k^2 - 2\bar{p} \cdot k.
 \end{aligned} \tag{4.6}$$

We express this in the Sudakov decomposition, which we can connect back to the region scaling.

$$\begin{aligned}
 D_a &= k^2 \\
 D_b &= k^2 + \sqrt{\hat{s}} n_+ \cdot k \\
 D_c &= k^2 + \sqrt{\hat{s}} n_+ \cdot k - (n_- \cdot k) n_+ \cdot (k_1+k_2) - (n_+ \cdot k) n_- \cdot (k_1+k_2) \\
 &\quad - \sqrt{\hat{s}} n_+ \cdot (k_1+k_2) - 2k_T \cdot (k_1+k_2) + 2k_1 \cdot k_2 \\
 D_d &= k^2 - \sqrt{\hat{s}} n_- \cdot k.
 \end{aligned} \tag{4.7}$$

Each of the 4 D_i can be split into 4 regions according to the scaling set out in (4.4). For illustrative purposes, this has been for the propagator D_b (where we use the Minkowski metric in lightcone coordinates):

region for D_b	k_+	\mathbf{k}_T	k_-	$k^2 = 4k_-k_+ - \mathbf{k}_T^2$	$\sqrt{\hat{s}} n_+ \cdot k = \sqrt{\hat{s}} k_-$
hard (h)	1	1	1	1	1
collinear (c)	1	λ	λ^2	λ^2	λ^2
anti-collinear (\bar{c})	λ^2	λ	1	λ^2	1
soft(s)	λ^2	λ^2	λ^2	λ^4	λ^2

Leading terms in λ are highlighted grey in the table. Similar tables can also be arranged for each propagator, providing all of the ingredients needed to build region-specific amplitudes organised by leading behaviour in λ . However, there are a few crucial points to be mindful of when using this approach:

- There are some subtleties regarding shifting the loop momentum, as the decomposition of k into regions breaks Lorentz invariance, leading to a violation in shift symmetry⁷. The consequence is then that certain regions may be missed if the loop momentum is chosen naïvely and propagators are truncated to leading terms in λ prior to loop integration. This is not a serious problem, however, as it can be cured by a careful choice of loop momentum parametrisation and/or conducting

⁷For a given master integral, shifting the loop momentum should not affect the final calculations. Region expansion changes this.

sensitivity analysis of propagator expansion before and after loop integration. A full treatment of this phenomenon is explored in [3].

- There is some interplay between UV and IR divergences between the hard and soft regions, which leads to some counterintuitive or surprising results such as spurious infrared singularities seen in the hard region. This is because the method of regions can alter the propagators, hence producing spurious divergences.
- Adding another gluon to the process could introduce new regional effects not seen before. For example, at N³LO, the soft region contributes NLP terms in contrast to NNLO where the soft region contributes nothing [59].

4.1.2 Squared matrix element terms

We have some idea of how amplitudes can be organised using the method of regions. These amplitudes are the building blocks of squared matrix elements. The derivation of these squared matrix elements and their building block amplitudes does not form part of this thesis, however, we can state what the squared matrix elements are split by region as well as identify whether they are LP or NLP .

For the squared matrix elements, it is convenient to adopt a notation of invariants:

$$\begin{aligned}
 t_2 &= (p - k_1)^2 = -2p \cdot k_1, \\
 t_3 &= (p - k_2)^2 = -2p \cdot k_2, \\
 u_2 &= (\bar{p} - k_1)^2 = -2\bar{p} \cdot k_1, \\
 u_3 &= (\bar{p} - k_2)^2 = -2\bar{p} \cdot k_2, \\
 s_{12} &= (k_1 + k_2)^2 = 2k_1 \cdot k_2.
 \end{aligned} \tag{4.8}$$

In addition to this notation, we will capture the dressing of the squared matrix elements by the factor

$$\mathcal{N} = 128\pi\alpha_s^3(1 - \epsilon)C_F^3e^2N_c(\mu^2)^{2\epsilon}. \tag{4.9}$$

Finally, we also define functions $\{f_i^X\}$ in appendix F.

The squared matrix elements per region are as follows:

Hard Region

$$\mathcal{M}_{\text{hard}}^{\text{LP}} = \mathcal{N} \left(\frac{\mu_{\overline{\text{MS}}}^2}{-\hat{s}} \right)^\epsilon f_1^{\text{H}} \frac{\hat{s}^3}{t_2 t_3 u_2 u_3};$$

$$\mathcal{M}_{\text{hard}}^{\text{NLP}} = \mathcal{N} \left(\frac{\mu_{\overline{\text{MS}}}^2}{-\hat{s}} \right)^\epsilon \frac{\hat{s}^2(t_2 + t_3 + u_2 + u_3)}{t_2 t_3 u_2 u_3} \left[f_2^{\text{H}} + \frac{1}{2} \frac{t_2 u_3 + t_3 u_2 - s_{12} \hat{s}}{(t_2 + t_3)(u_2 + u_3)} f_1^{\text{H}} \right]; \quad (4.10)$$

Collinear Region

$$\begin{aligned} \mathcal{M}_{\text{col.}}^{\text{LP}} &= 0; \\ \mathcal{M}_{\text{col.}}^{\text{NLP}} &= \mathcal{N} \left(\mu_{\overline{\text{MS}}}^2 \right)^\epsilon \frac{\hat{s}^2}{t_2 t_3 u_2 u_3} \left\{ [u_2(-t_2)^{-\epsilon} + u_3(-t_3)^{-\epsilon}] f_1^{\text{C}} \right. \\ &\quad + \frac{t_3 u_2 + t_2 u_3 - s_{12} \hat{s}}{t_2 + t_3} \left[((-t_2)^{-\epsilon} - 2(-t_2 - t_3)^{-\epsilon} + (-t_3)^{-\epsilon}) f_2^{\text{C}} \right. \\ &\quad \left. \left. - \left(\frac{t_2}{t_3} (-t_2)^{-\epsilon} - \frac{(t_2^2 + t_3^2)}{t_2 t_3} (-t_2 - t_3)^{-\epsilon} + \frac{t_3}{t_2} (-t_3)^{-\epsilon} \right) f_3^{\text{C}} \right] \right\}. \quad (4.11) \end{aligned}$$

The anticollinear region expressions are obtained through the simple exchange of $p \leftrightarrow \bar{p}$.

Soft Region

$$\begin{aligned} \mathcal{M}_{\text{soft}}^{\text{LP}} &= 0; \\ \mathcal{M}_{\text{soft}}^{\text{NLP}} &= \mathcal{N} \left(\frac{\mu_{\overline{\text{MS}}}^2}{-s_{12}} \right)^\epsilon \frac{\hat{s}^2}{t_2 t_3 u_2 u_3} \\ &\quad \times \left\{ \frac{t_3 f_1^{\text{S}}}{t_2(t_2 + t_3)^2} \left[(s_{12} \hat{s} - t_2 u_3 - t_3 u_2) \left(t_2 + t_3 - t_3 {}_2F_1 \left(1, 1, 1 - \epsilon, \frac{t_2}{t_2 + t_3} \right) \right) \right] \right. \\ &\quad + \frac{f_2^{\text{S}}}{\hat{s} s_{12}(t_2 + t_3)} [(t_2 u_3 - t_3 u_2)^2 - s_{12} \hat{s}(t_2 u_3 + t_3 u_2)] \\ &\quad + \frac{f_3^{\text{S}}}{\hat{s} s_{12} t_2 (t_2 + t_3)^2} \left[s_{12}^2 \hat{s}^2 t_3 (t_2 - t_3) + t_3 (t_2 + t_3) (t_2 u_3 - t_3 u_2)^2 \right. \\ &\quad + s_{12} \hat{s} t_2 (t_2 + t_3) (t_2 u_3 - t_3 u_2) - t_3 (s_{12}^2 \hat{s}^2 (t_2 - t_3) + (t_2 + t_3) (t_2 u_3 - t_3 u_2)^2 \\ &\quad \left. \left. - 2s_{12} \hat{s} t_2 (t_2 u_3 + t_3 u_2) \right) {}_2F_1 \left(1, 1, 1 - \epsilon, \frac{t_2}{t_2 + t_3} \right) \right] \\ &\quad \left. + \{t_2, t_3 \leftrightarrow u_2, u_3\} + \{t_2, t_3 \leftrightarrow u_3, u_2\} + \{t_2, u_2 \leftrightarrow t_3, u_3\} \right\}. \quad (4.12) \end{aligned}$$

Note that ${}_2F_1 \left(1, 1, 1 - \epsilon, \frac{t_2}{t_2 + t_3} \right)$ is a hypergeometric function.

4.2 Phase space integrals

All of the terms present in the region-specific squared matrix elements given by (4.10),(4.11), (4.12) can be distilled into 4 master expressions. When integrating over the phase space,

this translates to four master integrals:⁸

$$\text{Integral 1 : } I_1(\alpha_1, \alpha_2, \beta_1, \beta_2, \gamma_1, \gamma_2) = \int d\Phi^{(3)} \prod_{i=1}^2 \left(\frac{1}{p \cdot k_i} \right)^{\alpha_i} \left(\frac{1}{\bar{p} \cdot k_i} \right)^{\beta_i} \left(\frac{1}{p \cdot k_1 + p \cdot k_2} \right)^{\gamma_1} \left(\frac{1}{\bar{p} \cdot k_1 + \bar{p} \cdot k_2} \right)^{\gamma_2} \quad (4.13)$$

$$\text{Integral 2 : } I_2(\alpha_1, \alpha_2, \beta_1, \beta_2, \gamma_1, \gamma_2) = \int d\Phi^{(3)} \prod_{i=1}^2 \left(\frac{1}{p \cdot k_i} \right)^{\alpha_i} \left(\frac{1}{\bar{p} \cdot k_i} \right)^{\beta_i} \left(\frac{1}{p \cdot k_1 + p \cdot k_2} \right)^{\gamma_1} \left(\frac{1}{\bar{p} \cdot k_1 + \bar{p} \cdot k_2} \right)^{\gamma_2} 2k_1 \cdot k_2 \quad (4.14)$$

Integral 3 :

$$\int d\Phi^{(3)} \prod_{i=1}^2 \left(\frac{1}{p \cdot k_i} \right)^{\alpha_i} \left(\frac{1}{\bar{p} \cdot k_i} \right)^{\beta_i} \left(\frac{1}{p \cdot k_1 + p \cdot k_2} \right)^{\gamma_1} \left(\frac{1}{\bar{p} \cdot k_1 + \bar{p} \cdot k_2} \right)^{\gamma_2} (2k_1 \cdot k_2)^\delta \quad (4.15)$$

Integral 4 :

$$\int d\Phi^{(3)} \prod_{i=1}^2 \left(\frac{1}{p \cdot k_i} \right)^{\alpha_i} \left(\frac{1}{\bar{p} \cdot k_i} \right)^{\beta_i} \left(\frac{1}{p \cdot k_1 + p \cdot k_2} \right)^{\gamma_1} \left(\frac{1}{\bar{p} \cdot k_1 + \bar{p} \cdot k_2} \right)^{\gamma_2} (2k_1 \cdot k_2)^\delta \times {}_2F_1 \left(1, 1; a+1; \frac{p \cdot k_1}{p \cdot k_1 + p \cdot k_2} \right) \quad (4.16)$$

The parameters $\alpha_i, \beta_i, \gamma_i, \delta$ can be (but are not necessarily) fractional powers, or can be also set to 0. The hard and (anti)collinear regions can be constructed strictly out of Integrals 1 (4.13) and 2 (4.14) while Integrals 3 (4.15) and 4 (4.16) are specific to the soft region only. The former integrations make up the bulk of this chapter. The integration associated with the soft region does not form part of this thesis.

The 3-body phase space in d dimensions is given by

$$\int d\Phi^{(3)} = (2\pi)^d \int \frac{d^d q}{(2\pi)^{d-1}} \left(\prod_{i=1}^2 \int \frac{d^d k_i}{(2\pi)^{d-1}} \delta_+(k_i^2) \right) \delta_+(q^2 - Q^2) \times \delta^{(d)}(q + k_1 + k_2 - (p + \bar{p})), \quad (4.17)$$

where the δ_+ distributions are defined in appendix C.1. We can immediately carry out the integral over the photon momentum q using the delta function, simplifying the

⁸Note that there are small differences in the naming convention of the master integrals presented here and those in [3].

phase space to

$$\int d\Phi^{(3)} = (2\pi)^{(3-2d)} \left(\prod_{i=1}^2 \int d^d k_i \delta_+(k_i^2) \right) \delta(((p + \bar{p}) - (k_1 + k_2))^2 - Q^2), \quad (4.18)$$

where we were able to drop the “+” from the delta function, as we are guaranteed that the centre of mass energy will never be less than the total gluon energy. Throughout the integration, we will use a slightly different convention of the Sudakov decomposition to that laid out in section 4.1.1. Here we define

$$k_{i+} = n_- \cdot k_i ; \quad k_{i-} = n_+ \cdot k_i. \quad (4.19)$$

For the reader’s convenience, table 2 offers a Rosetta stone of some popular terms.

Description	Expression	Sudakov Coordinates
\hat{s}	$2p \cdot \bar{p}$	\hat{s}
$-t_i$	$2p \cdot k_i$	$\sqrt{\hat{s}} k_{i-}$
$-u_i$	$2\bar{p} \cdot k_i$	$\sqrt{\hat{s}} k_{i+}$
gluon correlation	$2k_i \cdot k_j$	$k_{i+} k_{j-} + k_{i-} k_{j+} - 2\mathbf{k}_{iT} \cdot \mathbf{k}_{jT}$
on shell condition	$k_i^2 = 0$	$k_{i+} k_{i-} - \mathbf{k}_{iT} ^2 = 0$

Table 2: Notation Key

We can translate the phase space integration measure into the Sudakov decomposition as we did in (3.46),

$$\int d^d k_i = \frac{1}{2} \int dk_{i+} dk_{i-} d^{d-2} \mathbf{k}_{iT}. \quad (4.20)$$

The on shell condition is enforced by the delta plus,

$$\delta_+(k_i^2) = \delta_+(k_{i+} k_{i-} - |\mathbf{k}_{iT}|^2), \quad (4.21)$$

where the “+” will work toward changing the integration bounds on the k_{i+}, k_{i-} integrals to coincide with positive energy requirements while leaving the transverse momentum integral bounds stretching from negative to positive infinity (see appendix D.2).

Finally we have the the last delta function,

$$\delta(((p+\bar{p})-(k_1+k_2))^2-Q^2) = \frac{1}{\hat{s}} \delta \left((1-z) - \frac{1}{\sqrt{\hat{s}}} (k_{1+} + k_{1-} + k_{2+} + k_{2-}) + \frac{2}{\hat{s}} k_1 \cdot k_2 \right) \quad (4.22)$$

where we have used the definition of $z = \frac{Q^2}{\hat{s}}$ as per (2.1), as well as the property $\delta(ax) = \frac{1}{|a|} \delta(x)$. The cross term $k_1 \cdot k_2$ at first glance looks like a fly in the ointment for integration, however, we will soon see it is really not a problem. We will deal with this first by expressing the delta function as a Fourier transform,

$$\begin{aligned} \delta \left((1-z) - \frac{1}{\sqrt{\hat{s}}} (k_{1+} + k_{1-} + k_{2+} + k_{2-}) + \frac{2}{\hat{s}} k_1 \cdot k_2 \right) \\ = \int_{-\infty}^{\infty} \frac{d\omega}{2\pi} e^{i\omega(1-z)} e^{\frac{-i\omega}{\sqrt{\hat{s}}} (k_{1+} + k_{1-} + k_{2+} + k_{2-})} e^{\frac{2i\omega}{\hat{s}} k_1 \cdot k_2}. \end{aligned} \quad (4.23)$$

We can Taylor expand the exponential in $k_1 \cdot k_2$, given that higher order terms will be suppressed by powers of $1-z$:

$$\begin{aligned} e^{\frac{2i\omega}{\hat{s}} k_1 \cdot k_2} &= 1 + \frac{2i\omega}{\hat{s}} k_1 \cdot k_2 + \mathcal{O}(k_i^4) \\ &= 1 + \frac{i\omega}{\hat{s}} (k_{1+}k_{2-} + k_{1-}k_{2+} - 2\mathbf{k}_{1T} \cdot \mathbf{k}_{2T}) \\ &\quad + \text{terms suppressed by powers of } (1-z). \end{aligned} \quad (4.24)$$

So far, our phase space has the form

$$\begin{aligned} \int d\Phi^{(3)} &= \frac{(2\pi)^{(3-2d)}}{2^2 \hat{s}} \prod_{i=1}^2 \int_0^\infty dk_{i+} \int_0^\infty dk_{i-} \int_{-\infty}^\infty d^{d-2} \mathbf{k}_{iT} \delta(k_{i+}k_{i-} - |\mathbf{k}_{iT}|^2) \\ &\quad \times \int_{-i\infty}^{i\infty} \frac{d\tilde{\omega}}{2\pi i} e^{\tilde{\omega}(1-z)} e^{\frac{-\tilde{\omega}}{\sqrt{\hat{s}}} (k_{1+} + k_{1-} + k_{2+} + k_{2-})} \\ &\quad \times \left[1 + \frac{\tilde{\omega}}{\hat{s}} (k_{1+}k_{2-} + k_{1-}k_{2+} - 2\mathbf{k}_{1T} \cdot \mathbf{k}_{2T}) \right], \end{aligned} \quad (4.25)$$

where we have transformed $\tilde{\omega} = i\omega$.

At this point, we will need to bring the integrand (i.e. squared matrix element) into the picture as the second master integral (4.14) has a cross term, unlike the first master integral (4.13). The implication of this of course is that the cross term will need careful handling within each master integral. We will begin with the easier of the two, the first master integral.

4.2.1 Master integral 1

Consulting table 2, the squared matrix element of the first master integral (4.13) in the Sudakov decomposition has the form:

$$\begin{aligned}
 M &\equiv \prod_{i=1}^2 \left(\frac{1}{p \cdot k_i} \right)^{\alpha_i} \left(\frac{1}{\bar{p} \cdot k_i} \right)^{\beta_i} \left(\frac{1}{p \cdot k_1 + p \cdot k_2} \right)^{\gamma_1} \left(\frac{1}{\bar{p} \cdot k_1 + \bar{p} \cdot k_2} \right)^{\gamma_2} \\
 &= \left(\frac{2}{\sqrt{\hat{s}}} \right)^C \prod_{i=1}^2 \left(\frac{1}{k_{i-}} \right)^{\alpha_i} \left(\frac{1}{k_{i-}} \right)^{\beta_i} \left(\frac{1}{k_{1-} + k_{2-}} \right)^{\gamma_1} \left(\frac{1}{k_{1+} + k_{2+}} \right)^{\gamma_2}
 \end{aligned} \tag{4.26}$$

where

$$C = \alpha_1 + \alpha_2 + \beta_1 + \beta_2 + \gamma_1 + \gamma_2. \tag{4.27}$$

We notice two nice properties in the above, namely the independence of the squared matrix element from cross terms in gluon momentum $k_1 \cdot k_2$, and transverse momentum. The lack of cross terms means that we can make short work of the cross term present in the phase space given by (4.25). Consider the gluon transverse momentum cross term $\mathbf{k}_{1T} \cdot \mathbf{k}_{2T}$ in the context of one of the transverse momentum integrals. When this odd function (i.e. linear in \mathbf{k}_{1T}) is coupled with the inherently even delta function, the integral will vanish, i.e.

$$\int_{-\infty}^{\infty} d^{d-2} \mathbf{k}_{1T} \delta(k_{1+} k_{1-} - |\mathbf{k}_{1T}|^2) \mathbf{k}_{1T} \cdot \mathbf{k}_{2T} = 0. \tag{4.28}$$

This leaves us with the phase space,

$$\begin{aligned}
 \int d\Phi^{(3)} &= \frac{(2\pi)^{(3-2d)}}{2^4 \hat{s}} \prod_{i=1}^2 \int_0^{\infty} dk_{i+} \int_0^{\infty} dk_{i-} \int_0^{\infty} d^{d-2} \mathbf{k}_{iT} \delta(k_{i+} k_{i-} - |\mathbf{k}_{iT}|^2) \\
 &\times \int_{-i\infty}^{i\infty} \frac{d\tilde{\omega}}{2\pi i} e^{\tilde{\omega}(1-z)} e^{\frac{-\tilde{\omega}}{\sqrt{\hat{s}}}(k_{1+} + k_{1-} + k_{2+} + k_{2-})} \\
 &\times \left[1 + \frac{\tilde{\omega}}{\hat{s}} (k_{1+} k_{2-} + k_{1-} k_{2+}) \right].
 \end{aligned} \tag{4.29}$$

The transverse momentum integrals can further be transformed into spherical polar coordinates, much as we did in (3.47). This will yield the phase space

$$\begin{aligned}
 \int d\Phi^{(3)} &= \frac{(2\pi)^{(3-2d)}}{2^4 \hat{s}} \Omega_{d-2}^2 \prod_{i=1}^2 \int_0^{\infty} dk_{i+} \int_0^{\infty} dk_{i-} \int_0^{\infty} d|\mathbf{k}_{iT}|^2 (|\mathbf{k}_{iT}|^2)^{\frac{d-4}{2}} \\
 &\times \delta(k_{i+} k_{i-} - |\mathbf{k}_{iT}|^2) \\
 &\times \int_{-i\infty}^{i\infty} \frac{d\tilde{\omega}}{2\pi i} e^{\tilde{\omega}(1-z)} e^{\frac{-\tilde{\omega}}{\sqrt{\hat{s}}}(k_{1+} + k_{1-} + k_{2+} + k_{2-})}
 \end{aligned}$$

$$\times \left[1 + \frac{\tilde{\omega}}{\hat{s}} (k_{1+}k_{2-} + k_{1-}k_{2+}) \right]. \quad (4.30)$$

Note that we were able to carry out our solid angle integration directly as there is no angular dependence at all (in any of our master integrals), and that each real gluon emission incurred its own solid angle factor. As the squared matrix element has no dependence on transverse momentum, we can perform our transverse momentum phase space integrals in (4.30) immediately, i.e.

$$\prod_{i=1}^2 \int_0^\infty d|\mathbf{k}_{iT}|^2 (|\mathbf{k}_{iT}|^2)^{\frac{d-4}{2}} \delta(k_{i+}k_{i-} - |\mathbf{k}_{iT}|^2) = \prod_{i=1}^2 k_{i+}^{\frac{d-4}{2}} k_{i-}^{\frac{d-4}{2}}. \quad (4.31)$$

Putting all of this together, the first master integral is

$$\begin{aligned} I_1(\alpha_1, \alpha_2, \beta_1, \beta_2, \gamma_1, \gamma_2) &= \frac{(2\pi)^{3-2d}}{2^{4-C}} \hat{s}^{-1-\frac{1}{2}C} \Omega_{d-2}^2 \int_{-i\infty}^{i\infty} \frac{d\tilde{\omega}}{2\pi i} e^{\tilde{\omega}(1-z)} \\ &\times \int_0^\infty dk_{1+} e^{\frac{-\tilde{\omega}}{\sqrt{s}} k_{1+} + k_{1+}^{\frac{d-4}{2}} - \beta_1} \int_0^\infty dk_{2+} e^{\frac{-\tilde{\omega}}{\sqrt{s}} k_{2+} + k_{2+}^{\frac{d-4}{2}} - \beta_2} \left(\frac{1}{k_{1+} + k_{2+}} \right)^{\gamma_2} \\ &\times \int_0^\infty dk_{1-} e^{\frac{-\tilde{\omega}}{\sqrt{s}} k_{1-} - k_{1-}^{\frac{d-4}{2}} - \alpha_1} \int_0^\infty dk_{2-} e^{\frac{-\tilde{\omega}}{\sqrt{s}} k_{2-} - k_{2-}^{\frac{d-4}{2}} - \alpha_2} \left(\frac{1}{k_{1-} + k_{2-}} \right)^{\gamma_1} \\ &\times \left(\underbrace{1}_A + \frac{\tilde{\omega}}{\hat{s}} \left(\underbrace{k_{1+}k_{2-}}_{B1} + \underbrace{k_{1-}k_{2+}}_{B2} \right) \right), \end{aligned} \quad (4.32)$$

where we have divided our integral into three separate integrals. We can start with the simplest integral - Integral A.

Integral A

We can immediately make the variable change $\tilde{k}_{i\pm} = \frac{\tilde{\omega}}{\sqrt{s}} k_{i\pm}$:

$$\begin{aligned} I_{1A}(\alpha_1, \alpha_2, \beta_1, \beta_2, \gamma_1, \gamma_2) &= \frac{(2\pi)^{3-2d}}{2^{4-C}} \hat{s}^{d-3-C} \Omega_{d-2}^2 \underbrace{\int_{-i\infty}^{i\infty} \frac{d\tilde{\omega}}{2\pi i} e^{\tilde{\omega}(1-z)} \left(\frac{1}{\tilde{\omega}} \right)^{2d-4-C}}_{I_{\tilde{\omega}}} \\ &\times \underbrace{\int_0^\infty d\tilde{k}_{1+} e^{-\tilde{k}_{1+} + \tilde{k}_{1+}^{\frac{d-4}{2}} - \beta_1} \int_0^\infty d\tilde{k}_{2+} e^{-\tilde{k}_{2+} + \tilde{k}_{2+}^{\frac{d-4}{2}} - \beta_2} \left(\frac{1}{\tilde{k}_{1+} + \tilde{k}_{2+}} \right)^{\gamma_2}}_{I_+} \\ &\times \underbrace{\int_0^\infty d\tilde{k}_{1-} e^{-\tilde{k}_{1-} - \tilde{k}_{1-}^{\frac{d-4}{2}} - \alpha_1} \int_0^\infty d\tilde{k}_{2-} e^{-\tilde{k}_{2-} - \tilde{k}_{2-}^{\frac{d-4}{2}} - \alpha_2} \left(\frac{1}{\tilde{k}_{1-} + \tilde{k}_{2-}} \right)^{\gamma_1}}_{I_-}. \end{aligned} \quad (4.33)$$

The integral $I_{\tilde{\omega}}$ over $\tilde{\omega}$ is an inverse Laplace transform (see appendix C.4), i.e.

$$\int_{-i\infty}^{i\infty} \frac{d\tilde{\omega}}{2\pi i} e^{\tilde{\omega}(1-z)} \left(\frac{1}{\tilde{\omega}}\right)^{2d-4-C} = \frac{(1-z)^{2d-5-C}}{\Gamma(2d-4-C)}. \quad (4.34)$$

The other integrals can be solved by the method described in appendix E. More specifically,

$$\begin{aligned} I_+ &= I(m = \frac{d-4}{2} - \beta_1, n = \frac{d-4}{2} - \beta_2, l = \gamma_2) \\ &= \frac{\Gamma(\frac{d-2}{2} - \beta_1)\Gamma(\frac{d-2}{2} - \beta_2)}{\Gamma(d-2 - \beta_1 - \beta_2)} \Gamma(d-2 - \beta_1 - \beta_2 - \gamma_2) \end{aligned} \quad (4.35)$$

$$\begin{aligned} I_- &= I(m = \frac{d-4}{2} - \alpha_1, n = \frac{d-4}{2} - \alpha_2, l = \gamma_1) \\ &= \frac{\Gamma(\frac{d-2}{2} - \alpha_1)\Gamma(\frac{d-2}{2} - \alpha_2)}{\Gamma(d-2 - \alpha_1 - \alpha_2)} \Gamma(d-2 - \alpha_1 - \alpha_2 - \gamma_1). \end{aligned} \quad (4.36)$$

This gives us

$$\begin{aligned} I_{1A}(\alpha_1, \alpha_2, \beta_1, \beta_2, \gamma_1, \gamma_2) &= \frac{(2\pi)^{3-2d}}{2^{4-C}} \Omega_{d-2}^2 s^{d-3-C} \frac{(1-z)^{2d-5-C}}{\Gamma(2d-4-C)} \\ &\quad \times \prod_{i=1}^2 \Gamma\left(\frac{d-2}{2} - \alpha_i\right) \Gamma\left(\frac{d-2}{2} - \beta_i\right) \\ &\quad \times \frac{\Gamma(d-2 - \alpha_1 - \alpha_2 - \gamma_1)\Gamma(d-2 - \beta_1 - \beta_2 - \gamma_2)}{\Gamma(d-2 - \alpha_1 - \alpha_2)\Gamma(d-2 - \beta_1 - \beta_2)}. \end{aligned} \quad (4.37)$$

Integrals B1 and B2

Now we make the variable change $\tilde{k}_{i\pm} = \frac{\tilde{\omega}}{\sqrt{s}} k_{i\pm}$ to Integral B1 of (4.32):

$$\begin{aligned} I_{1B1}(\alpha_1, \alpha_2, \beta_1, \beta_2, \gamma_1, \gamma_2) &= \frac{(2\pi)^{3-2d}}{2^{4-C}} s^{d-3-C} \Omega_{d-2}^2 \underbrace{\int_{-i\infty}^{i\infty} \frac{d\tilde{\omega}}{2\pi i} e^{\tilde{\omega}(1-z)} \left(\frac{1}{\tilde{\omega}}\right)^{2d-3-C}}_{I_{\tilde{\omega}}} \\ &\quad \times \underbrace{\int_0^\infty d\tilde{k}_{1+} e^{-\tilde{k}_{1+}} \tilde{k}_{1+}^{\frac{d-2}{2}-\beta_1} \int_0^\infty d\tilde{k}_{2+} e^{-\tilde{k}_{2+}} \tilde{k}_{2+}^{\frac{d-4}{2}-\beta_2} \left(\frac{1}{\tilde{k}_{1+} + \tilde{k}_{2+}}\right)^{\gamma_2}}_{I_+} \\ &\quad \times \underbrace{\int_0^\infty d\tilde{k}_{1-} e^{-\tilde{k}_{1-}} \tilde{k}_{1-}^{\frac{d-4}{2}-\alpha_1} \int_0^\infty d\tilde{k}_{2-} e^{-\tilde{k}_{2-}} \tilde{k}_{2-}^{\frac{d-2}{2}-\alpha_2} \left(\frac{1}{\tilde{k}_{1-} + \tilde{k}_{2-}}\right)^{\gamma_1}}_{I_-}. \end{aligned} \quad (4.38)$$

All of the integrals present are of a similar form to those of Integral A. We then have:

$$\begin{aligned}
 I_{1B1}(\alpha_1, \alpha_2, \beta_1, \beta_2, \gamma_1, \gamma_2) &= \frac{(2\pi)^{3-2d}}{2^{4-C}} \Omega_{d-2}^2 \hat{s}^{d-3-C} \frac{(1-z)^{2d-5-C}}{\Gamma(2d-4-C)} \\
 &\times \prod_{i=1}^2 \Gamma\left(\frac{d-2}{2} - \alpha_i\right) \Gamma\left(\frac{d-2}{2} - \beta_i\right) \\
 &\times \frac{\Gamma(d-2-\alpha_1-\alpha_2-\gamma_1)\Gamma(d-2-\beta_1-\beta_2-\gamma_2)}{\Gamma(d-2-\alpha_1-\alpha_2)\Gamma(d-2-\beta_1-\beta_2)} \\
 &\times \frac{1-z}{2d-4-C} \left(\frac{d-2}{2} - \beta_1\right) \left(\frac{d-2}{2} - \alpha_2\right) \\
 &\times \left(\frac{d-2-\alpha_1-\alpha_2-\gamma_1}{d-2-\alpha_1-\alpha_2}\right) \left(\frac{d-2-\beta_1-\beta_2-\gamma_2}{d-2-\beta_1-\beta_2}\right).
 \end{aligned} \tag{4.39}$$

It turns out that Integral B2 is the same as B1 under the change $\alpha_1 \leftrightarrow \alpha_2$ and $\beta_1 \leftrightarrow \beta_2$.

Finale

Putting together Integrals A, B1 and B2, we have

$$\begin{aligned}
 I_1(\alpha_1, \alpha_2, \beta_1, \beta_2, \gamma_1, \gamma_2) &= \frac{(2\pi)^{3-2d}}{2^{4-C}} \Omega_{d-2}^2 \hat{s}^{d-3-C} \frac{(1-z)^{2d-5-C}}{\Gamma(2d-4-C)} \prod_{i=1}^2 \Gamma\left(\frac{d-2}{2} - \alpha_i\right) \Gamma\left(\frac{d-2}{2} - \beta_i\right) \\
 &\times \frac{\Gamma(d-2-\alpha_1-\alpha_2-\gamma_1)\Gamma(d-2-\beta_1-\beta_2-\gamma_2)}{\Gamma(d-2-\alpha_1-\alpha_2)\Gamma(d-2-\beta_1-\beta_2)} \\
 &\times \left\{ 1 + \frac{1-z}{2d-4-C} \left[\left(\frac{d-2}{2} - \beta_1\right) \left(\frac{d-2}{2} - \alpha_2\right) + \left(\frac{d-2}{2} - \beta_2\right) \left(\frac{d-2}{2} - \alpha_1\right) \right] \right. \\
 &\times \left. \left(\frac{d-2-\alpha_1-\alpha_2-\gamma_1}{d-2-\alpha_1-\alpha_2}\right) \left(\frac{d-2-\beta_1-\beta_2-\gamma_2}{d-2-\beta_1-\beta_2}\right) \right\}.
 \end{aligned} \tag{4.40}$$

A Small Check

If the reader will permit a slight jump to the future, we can perform a small cross check with a result we will see in the next chapter. If we take $\alpha_i = \beta_i = 1, \gamma_i = 0$, (and therefore also $C = 4$), we will recover the leading soft term integrated over the full 3-body phase space for 2 real soft gluon production:

$$\begin{aligned}
 \int d\Phi^{(3)} \prod_{i=1}^2 \left(\frac{1}{p \cdot k_i}\right) \left(\frac{1}{\bar{p} \cdot k_i}\right) &= (2\pi)^{3-2d} \Omega_{d-2}^2 \hat{s}^{d-7} \frac{(1-z)^{2d-9}}{\Gamma(2d-8)} \Gamma^4\left(\frac{d-4}{2}\right) \left[1 + (1-z) \left(\frac{d-4}{4}\right) \right]
 \end{aligned} \tag{4.41}$$

which reassuringly agrees with equation (5.28) for n=2.

4.2.2 Master integral 2

Unlike Integral 1, we now have the presence of cross terms and therefore also transverse momentum in our integrand via the gluon correlation term $2k_1 \cdot k_2$. This means that we should use the phase space as per (4.25), allowing us to write Integral 2 as

$$\begin{aligned}
 I_2(\alpha_1, \alpha_2, \beta_1, \beta_2, \gamma_1, \gamma_2) &= \frac{(2\pi)^{3-2d}}{4\hat{s}} \int_{-i\infty}^{i\infty} \frac{d\tilde{\omega}}{2\pi i} e^{\tilde{\omega}(1-z)} \int_0^\infty dk_{1+} \int_0^\infty dk_{1-} \int_0^\infty d^{d-2}\mathbf{k}_{1T} \delta(k_{1+}k_{1-} - |\mathbf{k}_{1T}|^2) \\
 &\int_0^\infty dk_{2+} \int_0^\infty dk_{2-} \int_0^\infty d^{d-2}\mathbf{k}_{2T} \delta(k_{2+}k_{2-} - |\mathbf{k}_{2T}|^2) e^{\frac{-\tilde{\omega}}{\sqrt{\hat{s}}}(k_{1+}+k_{1-}+k_{2+}+k_{2-})} \\
 &\times M \times \left(1 + \frac{\tilde{\omega}}{\sqrt{\hat{s}}} 2k_1 \cdot k_2\right) 2k_1 \cdot k_2. \tag{4.42}
 \end{aligned}$$

Consider the last piece of this expression, i.e.

$$\left(1 + \frac{\tilde{\omega}}{\sqrt{\hat{s}}} 2k_1 \cdot k_2\right) 2k_1 \cdot k_2 = 2k_1 \cdot k_2 + O((k_1 \cdot k_2)^2). \tag{4.43}$$

Now, each gluon implicitly carries a factor $(1-z)$, and our area of interest is the soft limit where $z \rightarrow 1$. In this limit, $2k_1 \cdot k_2 \sim (1-z)^2$, which will act to suppress divergences. Given that we are most interested in leading divergent terms in $1-z$, we can discard:

$$O((k_1 \cdot k_2)^2) \sim O((1-z)^4). \tag{4.44}$$

Furthermore, we can express the remaining first order gluon correlation term in Sudakov coordinates, leaving us with:

$$\begin{aligned}
 I_2(\alpha_1, \alpha_2, \beta_1, \beta_2, \gamma_1, \gamma_2) &= \frac{(2\pi)^{3-2d}}{4\hat{s}} \int_{-i\infty}^{i\infty} \frac{d\tilde{\omega}}{2\pi i} e^{\tilde{\omega}(1-z)} \int_0^\infty dk_{1+} \int_0^\infty dk_{1-} \int_0^\infty d^{d-2}\mathbf{k}_{1T} \delta(k_{1+}k_{1-} - |\mathbf{k}_{1T}|^2) \\
 &\times \int_0^\infty dk_{2+} \int_0^\infty dk_{2-} \int_0^\infty d^{d-2}\mathbf{k}_{2T} \delta(k_{2+}k_{2-} - |\mathbf{k}_{2T}|^2) e^{\frac{-\tilde{\omega}}{\sqrt{\hat{s}}}(k_{1+}+k_{1-}+k_{2+}+k_{2-})} \\
 &\times M \times (k_{1+}k_{2-} + k_{1-}k_{2+} - 2\mathbf{k}_{1T} \cdot \mathbf{k}_{2T}). \tag{4.45}
 \end{aligned}$$

Now we deal with all terms containing transverse momenta in (4.45):

- The transverse momenta cross term $2\mathbf{k}_{1T} \cdot \mathbf{k}_{2T}$ will drop off using the same reasoning as we saw for the first master integral (see (4.28)).
- The integrals over transverse momenta and remaining delta functions will get the same treatment as that leading up to (4.30), i.e. a change of coordinate system to spherical polar coordinates before application of delta functions.

The resulting integral has a similar form to that of integrals 1 *B1* and *B2* (see (4.39)):

$$\begin{aligned}
 & I_2(\alpha_1, \alpha_2, \beta_1, \beta_2, \gamma_1, \gamma_2) \\
 &= \frac{(2\pi)^{3-2d}}{2^4 \hat{s}} \Omega_{d-2}^2 \int_{-i\infty}^{i\infty} \frac{d\tilde{\omega}}{2\pi i} e^{\tilde{\omega}(1-z)} \int_0^\infty dk_{1+} e^{\frac{-\tilde{\omega}}{\sqrt{\hat{s}}} k_{1+}} k_{1+}^{\frac{d-4}{2}} \int_0^\infty dk_{1-} e^{\frac{-\tilde{\omega}}{\sqrt{\hat{s}}} k_{1-}} k_{1-}^{\frac{d-4}{2}} \\
 &\times \int_0^\infty dk_{2+} e^{\frac{-\tilde{\omega}}{\sqrt{\hat{s}}} k_{2+}} k_{2+}^{\frac{d-4}{2}} \int_0^\infty dk_{2-} e^{\frac{-\tilde{\omega}}{\sqrt{\hat{s}}} k_{2-}} k_{2-}^{\frac{d-4}{2}} \\
 &\times M \times (k_{1+} k_{2-} + k_{1-} k_{2+}) \\
 &= \frac{(2\pi)^{3-2d}}{2^{4-C}} \hat{s}^{-1-\frac{1}{2}C} \Omega_{d-2}^2 \int_{-i\infty}^{i\infty} \frac{d\tilde{\omega}}{2\pi i} e^{\tilde{\omega}(1-z)} \\
 &\times \int_0^\infty dk_{1+} e^{\frac{-\tilde{\omega}}{\sqrt{\hat{s}}} k_{1+}} k_{1+}^{\frac{d-4}{2}-\beta_1} \int_0^\infty dk_{2+} e^{\frac{-\tilde{\omega}}{\sqrt{\hat{s}}} k_{2+}} k_{2+}^{\frac{d-4}{2}-\beta_2} \left(\frac{1}{k_{1+} + k_{2+}} \right)^{\gamma_2} \\
 &\times \int_0^\infty dk_{1-} e^{\frac{-\tilde{\omega}}{\sqrt{\hat{s}}} k_{1-}} k_{1-}^{\frac{d-4}{2}-\alpha_1} \int_0^\infty dk_{2-} e^{\frac{-\tilde{\omega}}{\sqrt{\hat{s}}} k_{2-}} k_{2-}^{\frac{d-4}{2}-\alpha_2} \left(\frac{1}{k_{1-} + k_{2-}} \right)^{\gamma_1} \\
 &\times (k_{1+} k_{2-} + k_{1-} k_{2+}). \tag{4.46}
 \end{aligned}$$

In the second step, we used (4.26). Using the same reasoning as for integral 1 *B1* and *B2*, we can finally arrive at an expression for master integral 2:

$$\begin{aligned}
 & I_2(\alpha_1, \alpha_2, \beta_1, \beta_2, \gamma_1, \gamma_2) \\
 &= \frac{(2\pi)^{3-2d}}{2^{4-C}} \Omega_{d-2}^2 \hat{s}^{d-2-C} \frac{(1-z)^{2d-3-C}}{\Gamma(2d-2-C)} \\
 &\prod_{i=1}^2 \Gamma\left(\frac{d-2}{2} - \alpha_i\right) \Gamma\left(\frac{d-2}{2} - \beta_i\right) \frac{\Gamma(d-2-\alpha_1-\alpha_2-\gamma_1)\Gamma(d-2-\beta_1-\beta_2-\gamma_2)}{\Gamma(d-2-\alpha_1-\alpha_2)\Gamma(d-2-\beta_1-\beta_2)} \\
 &\times \left[\left(\frac{d-2}{2} - \beta_1\right) \left(\frac{d-2}{2} - \alpha_2\right) + \left(\frac{d-2}{2} - \beta_2\right) \left(\frac{d-2}{2} - \alpha_1\right) \right] \\
 &\times \left\{ \frac{d-2-\alpha_1-\alpha_2-\gamma_1}{d-2-\alpha_1-\alpha_2} \left(\frac{d-2-\beta_1-\beta_2-\gamma_2}{d-2-\beta_1-\beta_2}\right) \right\}. \tag{4.47}
 \end{aligned}$$

The presence of the gluon correlation in this integral clearly generates a result sub-subleading in terms of soft divergence having $(1-z)^{2d-3-C}$ in comparison with master integral 1 containing a $(1-z)^{2d-5-C}$ term. However, it is really not possible to read too much into these integrals as they are not physical by themselves. Rather, they are the building blocks of various region specific components of the *K*-factor. In the next section, we will see the ensuing log terms associated with the hard and (anti)collinear regions.

4.2.3 Results for the *K*-factor from each region

For the hard and collinear regions, we have all of the necessary ingredients for assembling the Abelian-like terms ($\sim C_F$) in the 2-real, 1-virtual contribution to the

K -factor of (2.26), truncating at NLP. We arrive at these results by a combination of Laurent expansions in $z \rightarrow 1$ and $\epsilon \rightarrow 0$ (using the dimensional regularisation convention as always $d = 4 - 2\epsilon$), as well as of course reading the parameters $\alpha_i, \beta_i, \gamma_i$ given in (4.10) and (4.11). The K -factor coefficients specific to the hard region⁹ are found in table 9:

Hard Region Coefficients		$(1/\epsilon)^5$	$(1/\epsilon)^4$	$(1/\epsilon)^3$	$(1/\epsilon)^2$	$(1/\epsilon)^1$	$(1/\epsilon)^0$
LP	$\log^5(1-z)/(1-z)$						-128/15
	$\log^4(1-z)/(1-z)$					32/3	16
	$\log^3(1-z)/(1-z)$				-32/3		-128/3 + 112 ζ_2
	$\log^2(1-z)/(1-z)$			8	12	32 - 84 ζ_2	64 - 126 ζ_2 - 184 ζ_3
	$\log(1-z)/(1-z)$		-4	-6	-16 + 42 ζ_2	-32 + 63 ζ_2 + 92 ζ_3	-64 + 168 ζ_2 + 138 ζ_3 - (1017/4) ζ_4
	$1/(1-z)$	1	3/2	4 - (21/2) ζ_2	8 - (63/4) ζ_2 - 23 ζ_3	16 - 42 ζ_2 - (69/2) ζ_3 + (1017/16) ζ_4	32 - 84 ζ_2 - 92 ζ_3 + (3051/32) ζ_4 - (1053/5) ζ_5 + (483/2) ζ_6
NLP	$\log^5(1-z)$						128/15
	$\log^4(1-z)$					-32/3	-128/3
	$\log^3(1-z)$				32/3	128/3	248/3 - 112 ζ_2
	$\log^2(1-z)$			-8	-32	-62 + 84 ζ_2	-144 + 336 ζ_2 + 184 ζ_3
	$\log(1-z)$		4	16	31 - 42 ζ_2	72 - 168 ζ_2 - 92 ζ_3	144 - (651/2) ζ_2 - 368 ζ_3 + (1017/4) ζ_4
	1	-1	-4	-31/4 + (21/2) ζ_2	-18 + 42 ζ_2 + 23 ζ_3	-36 + (651/8) ζ_2 + 92 ζ_3 - (1017/16) ζ_4	-72 + 189 ζ_2 + (713/4) ζ_3 - (1017/4) ζ_4 + (1053/5) ζ_5 - (483/2) ζ_6

Figure 9: Integrated hard region coefficients at N³LO, 2R1V

The K -factor coefficients specific to the collinear region¹⁰ are found in table 10:

(Anti)collinear Region Coefficients		$(1/\epsilon)^4$	$(1/\epsilon)^3$	$(1/\epsilon)^2$	$(1/\epsilon)^1$	$(1/\epsilon)^0$
NLP	$\log^4(1-z)$					-625/24
	$\log^3(1-z)$				125/6	625/24
	$\log^2(1-z)$			-25/2	-125/8	-75/4 + (525/4) ζ_2
	$\log(1-z)$		5	25/4	15/2 - (105/2) ζ_2	10 - (525/8) ζ_2 - 205 ζ_3
	1	-1	-5/4	-3/2 + (21/2) ζ_2	-2 + (105/8) ζ_2 + 41 ζ_3	-3 + (63/4) ζ_2 + (205/4) ζ_3 + (279/16) ζ_4

Figure 10: Integrated collinear region coefficients at N³LO, 2R1V

Leading log terms have been highlighted in yellow, and subleading log terms are colour coded. The anticollinear region results are the same as those of the collinear region. The zeta functions ζ_n are defined in appendix B.4.

Although the derivation of the soft function is not part of this thesis, the soft region contributions to the K -factor are included for completeness. No table is necessary to report the coefficients, as it is quite small:

$$K^{\text{soft}} = 32 \left[\frac{1}{\epsilon} \left(\frac{2}{3} \zeta_2 + \frac{1}{3} \zeta_3 \right) - (4\zeta_2 + 2\zeta_3) \log(1-z) \right]. \quad (4.48)$$

Some observations on the above results:

- The (anti-)collinear regions are subleading log producers at NLP in comparison with the hard region, and the hard region is the only producer of LP terms, which is consistent with the findings at NNLO [59].

⁹All coefficients in the hard region need to be multiplied by a factor of 128.

¹⁰All coefficients in the collinear region need to be multiplied by a factor of 32.

- For the first time, we see a non-zero soft region contribution (albeit heavily suppressed in ϵ).
- Some structure effects are visible before phase space integration such as the (anti-)collinear region being subleading compared to the hard region, and the comparatively heavily subleading soft region, and thus are connected to the structure of the squared matrix element.

4.3 Conclusions and learnings for resummation

We have set out to learn more about NLP terms at N³LO for the purpose of resummation. We calculated a set of contributions to the 2-real 1-virtual K -factor via the method of regions, where the matrix element is organised by loop momentum modes into 4 non-overlapping regions. The region-specific squared matrix elements were integrated over the full phase space, providing data for resummation (i.e. coefficients of logs). But further to this, the method of regions approach offered some insights into the structure and sources of leading log behaviour. Our findings suggest that the collinear region is subleading compared with the hard region, which is in line with the expectations set at NNLO. This result has implications for the relevance of jet functions at higher orders in perturbation theory. Furthermore, ruling out collinear effects for LL at NLP could pave the way toward showing the exponentiation of NLP LL - an important stepping stone for resummation. Finally, we also saw that some structure effects are visible before phase space integration, and thus are connected to the structure of the squared matrix element. We could ask if the phase space also has some underlying structure such that leading and subleading contributions have distinct sources. This will be discussed in the next chapter.

Chapter 5

Next-to-Leading Power Leading Logs at $N^n\text{LO}$

In the previous chapter, we saw that certain types of logarithmic term could be connected to the structure of the squared matrix element prior to integration over the phase space. This raised the question about how the phase space contributes to the organisation of logarithmic terms. In this chapter, we will explore which parts of the phase space integrals produce leading and subleading logs at NLP.

To conduct an investigation into the role of the phase space in producing leading logs, we need to introduce some sort of structure to the phase space. We can partition the phase space and the squared matrix element of the differential cross section as a series of terms ordered in degrees of the threshold variable:

$$\hat{\sigma} = \frac{1}{2\hat{s}} \left[\int d\Phi_{\text{LP}} |M|_{\text{LP}}^2 + \int d\Phi_{\text{NLP}} |M|_{\text{LP}}^2 + \int d\Phi_{\text{LP}} |M|_{\text{NLP}}^2 + \dots \right]. \quad (5.1)$$

We expect that leading power terms must come from the first term, i.e. the combination of leading power squared matrix element integrated over the leading power part of the phase space. Highly subleading terms are associated with the ellipsis.

This classification has already been applied in studies up to NNLO. According to [18], NLP leading logs only come from the LP part of the phase space - i.e. the NLP part of the phase space only produces subleading NLP logs, even if the integrand is the LP squared matrix element. A natural question arises around the persistence of this relationship. Does the NLP part of the phase space consistently produce only subleading terms beyond NNLO? If so, this means that we would have one less calculation to worry about for the resummation of NLP LL.

In this chapter, we will investigate the Drell-Yan process with any number of real gluon emissions, i.e. a subset of NⁿLO, and find that it is indeed true: NLP leading logs can not come from the NLP part of the phase space (i.e. the second term in (5.1), so these terms must come from the third term. In order to see this, we can begin by using eikonal Feynman rules to construct $|M|_{\text{LP}}^2$.

5.1 Leading soft term for the squared matrix element

In the threshold limit, the term with leading threshold behaviour within the squared matrix element is the *Eikonal squared matrix element*, also known as the *leading soft term*. For example, at NLO, the leading soft term in the squared matrix element given by (2.19) is $\frac{-2(\bar{p}\cdot p)^2}{(p\cdot k)(\bar{p}\cdot k)}$. All other terms within (2.19) are suppressed by a power of k .

The building block of the leading soft term for any number of gluon emissions is given by the Feynman rule for a soft gluon emission with momentum k from a quark leg with momentum p , which we developed in detail for the Abelian case in section 3.1.1. For the benefit of the reader, we can re-state it here:

$$\frac{p^\mu}{p \cdot k}. \quad (5.2)$$

At NLO, the amplitude for the Drell-Yan process must take into account that the gluon emission could have emanated from the quark leg or the anti-quark leg. Furthermore, the squared matrix element must account for interference terms (see figure 5). The same principles apply for the Drell-Yan process involving n real emissions - all possible combinations of the gluons emanating from the quark and antiquark legs etc. must be accounted for. It can be shown that the leading soft term involving n real emissions (ignoring couplings, charges, and other such dressings) is (see e.g. [39, 40])

$$|M|_{\text{LP}}^2(\alpha_s^n) \sim \prod_{i=1}^n \frac{p \cdot \bar{p}}{(p \cdot k_i)(\bar{p} \cdot k_i)}. \quad (5.3)$$

Of all terms in the squared matrix element, this is the one that will produce leading terms in the threshold variable. We can now integrate this over the phase space to understand what the phase space brings to the mix in terms of threshold contributions.

5.2 Phase space integral

To begin the integration over the phase space, we use once again the Sudakov parametrisation, where each real gluon i , where $i = \{1, \dots, n\}$ is parameterized such that its

transverse momentum is distinct from the momentum (anti)collinear to the quarks:

$$k_i^\mu = \frac{k_{i+}}{\sqrt{\hat{s}}} p^\mu + \frac{k_{i-}}{\sqrt{\hat{s}}} \bar{p}^\mu + k_{iT}^\mu \quad (5.4)$$

where

$$k_{iT}^\mu = (0, \mathbf{k}_{iT}, 0) \text{ and } p \cdot k_{iT} = \bar{p} \cdot k_{iT} = 0. \quad (5.5)$$

Our Rosetta stone can now be updated (see table 3) to include the leading soft term which has a particularly convenient form in the Sudakov decomposition.

Description	Expression	Sudakov Coordinates
\hat{s}	$2p \cdot \bar{p}$	\hat{s}
$-t_i$	$2p \cdot k_i$	$\sqrt{\hat{s}} k_{i-}$
$-u_i$	$2\bar{p} \cdot k_i$	$\sqrt{\hat{s}} k_{i+}$
gluon correlation	$2k_i \cdot k_j$	$k_{i+} k_{j-} + k_{i-} k_{j+} - 2\mathbf{k}_{iT} \cdot \mathbf{k}_{jT}$
on shell condition	$k_i^2 = 0$	$k_{i+} k_{i-} - \mathbf{k}_{iT} ^2 = 0$
leading soft term	$\prod_{i=1}^n \frac{p \cdot \bar{p}}{p \cdot k_i \bar{p} \cdot k_i}$	$2^n \prod_{i=1}^n \frac{1}{k_{i+} k_{i-}}$

Table 3: Notation Key

The $n + 1$ body phase space for the Drell-Yan process 2.10 involving n real gluon emissions is given by:

$$\int d\Phi^{(n+1)} = (2\pi)^d \int \frac{d^d q}{(2\pi)^{d-1}} \left(\prod_{i=1}^n \int \frac{d^d k_i}{(2\pi)^{d-1}} \delta_+(k_i^2) \right) \delta_+(q^2 - Q^2) \delta^{(d)}(q + \sum_{j=1}^n k_j - (p + \bar{p})). \quad (5.6)$$

As for the 2-real 1-virtual case, we can choose to fix the momenta of the photon, killing off the photon integral, and allowing us to drop the “+” from the associated delta function as we are guaranteed that the centre of mass energy will never be less than the total gluon energy:

$$\int d\Phi^{(n+1)} = (2\pi)^{n+1-nd} \left(\prod_{i=1}^n \int d^d k_i \delta_+(k_i^2) \right) \delta(\left((p + \bar{p}) - \sum_{j=1}^n k_j\right)^2 - Q^2). \quad (5.7)$$

The integration measure can be expressed in Sudakov coordinates much like the 2-real, 1-virtual case - by using the Jacobian in appendix D.1, while being mindful that now we have n such Jacobians:

$$\prod_{i=1}^n \int d^d k_i = \left(\frac{1}{2}\right)^n \prod_{i=1}^n \int dk_{i+} dk_{i-} d^{d-2} \mathbf{k}_{iT}. \quad (5.8)$$

The delta function containing the on-shell condition will have the form given in (4.21). The other delta function $\delta(((p + \bar{p}) - \sum_{j=1}^n k_j)^2 - Q^2)$ requires some care due to cross terms. Following the same steps as set out around (4.22), we will be able to express this delta function as a Fourier transform in Sudakov coordinates,

$$\delta\left(\left((p + \bar{p}) - \sum_{j=1}^n k_j\right)^2 - Q^2\right) = \frac{1}{\hat{s}} \int_{-\infty}^{\infty} \frac{d\omega}{2\pi} e^{i\omega(1-z)} e^{\frac{-i\omega}{\sqrt{\hat{s}}} \sum_{j=1}^n (k_{j+} + k_{j-})} e^{\frac{2i\omega}{\hat{s}} \sum_{i=1}^{n-1} \sum_{j=i+1}^n k_i \cdot k_j}. \quad (5.9)$$

As for the 2-real 1-virtual case, we Taylor expand the exponential containing the cross term about $k_i \cdot k_j \sim 0$, i.e. the soft limit:

$$e^{\frac{2i\omega}{\hat{s}} \sum_{i=1}^{n-1} \sum_{j=i+1}^n k_i \cdot k_j} = 1 + \frac{2i\omega}{\hat{s}} \sum_{i=1}^{n-1} \sum_{j=i+1}^n k_i \cdot k_j + \dots \quad (5.10)$$

In Sudakov coordinates this is

$$1 + \frac{2i\omega}{\hat{s}} \sum_{i=1}^{n-1} \sum_{j=i+1}^n k_i \cdot k_j = 1 + \frac{2i\omega}{\hat{s}} \sum_{i=1}^{n-1} \sum_{j=i+1}^n \left(\frac{1}{2}(k_{i+} k_{j-} + k_{i-} k_{j+}) - \mathbf{k}_{iT} \cdot \mathbf{k}_{jT}\right). \quad (5.11)$$

Finally, our delta function is:

$$\begin{aligned} \delta\left(\left((p + \bar{p}) - \sum_{j=1}^n k_j\right)^2 - Q^2\right) &= \frac{1}{\hat{s}} \int_{-\infty}^{\infty} \frac{d\omega}{2\pi} e^{i\omega(1-z)} e^{\frac{-i\omega}{\sqrt{\hat{s}}} \sum_{j=1}^n (k_{j+} + k_{j-})} \\ &\quad \times \left(1 + \frac{2i\omega}{\hat{s}} \sum_{i=1}^{n-1} \sum_{j=i+1}^n \left(\frac{1}{2}(k_{i+} k_{j-} + k_{i-} k_{j+}) - \mathbf{k}_{iT} \cdot \mathbf{k}_{jT}\right)\right), \end{aligned} \quad (5.12)$$

so that our full phase space is:

$$\begin{aligned} \int d\Phi^{(n+1)} &= \frac{(2\pi)^{n+1-nd}}{2^n \hat{s}} \prod_{i=1}^n \int_0^\infty dk_{i+} \int_0^\infty dk_{i-} \int_{-\infty}^{\infty} d^{d-2} \mathbf{k}_{iT} \delta(k_{i+} k_{i-} - |\mathbf{k}_{iT}|^2) \\ &\quad \int_{-\infty}^{\infty} \frac{d\omega}{2\pi} e^{i\omega(1-z)} e^{\frac{-i\omega}{\sqrt{\hat{s}}} \sum_{j=1}^n (k_{j+} + k_{j-})} \end{aligned}$$

$$\left(1 + \frac{2i\omega}{\hat{s}} \sum_{i=1}^{n-1} \sum_{j=i+1}^n \left(\frac{1}{2}(k_{i+}k_{j-} + k_{i-}k_{j+}) - \mathbf{k}_{iT} \cdot \mathbf{k}_{jT}\right)\right). \quad (5.13)$$

The leading soft term is independent of transverse momentum. In light of this, we can evaluate the integrals of cross terms in transverse momenta. Consider the integral:

$$\int_{-\infty}^{\infty} d^{d-2} \mathbf{k}_{iT} \delta(k_{i+}k_{i-} - |\mathbf{k}_{iT}|^2) \sum_{j=i+1}^n \mathbf{k}_{iT} \cdot \mathbf{k}_{jT}. \quad (5.14)$$

The same logic as for the 2-real, 1-virtual case expressed around (4.28) applies here. The delta function is an even function in \mathbf{k}_{iT} , while the sum of cross terms is an odd function (being linear \mathbf{k}_{iT}). The integral then vanishes, leaving us with the phase space:

$$\begin{aligned} \int d\Phi^{(n+1)} &= \frac{(2\pi)^{n+1-nd}}{2^n \hat{s}} \prod_{i=1}^n \int_0^{\infty} dk_{i+} \int_0^{\infty} dk_{i-} \int_{-\infty}^{\infty} d^{d-2} \mathbf{k}_{iT} \delta(k_{i+}k_{i-} - |\mathbf{k}_{iT}|^2) \\ &\quad \int_{-\infty}^{\infty} \frac{d\omega}{2\pi} e^{i\omega(1-z)} e^{\frac{-i\omega}{\sqrt{\hat{s}}} \sum_{j=1}^n (k_{j+} + k_{j-})} \\ &\quad \times \left(1 + \frac{i\omega}{\hat{s}} \sum_{i=1}^{n-1} \sum_{j=i+1}^n (k_{i+}k_{j-} + k_{i-}k_{j+})\right). \end{aligned} \quad (5.15)$$

Switching to spherical polar coordinates as per (3.47) allows us to apply the remaining delta function, and an analytic continuation $\tilde{\omega} = i\omega$ will leave our phase space in a more readily useful form:

$$\begin{aligned} \int d\Phi^{(n+1)} &= \frac{(2\pi)^{n+1-nd}}{2^{2n} \hat{s}} \Omega_{d-2}^n \int_{-i\infty}^{i\infty} \frac{d\tilde{\omega}}{2\pi i} e^{\tilde{\omega}(1-z)} \\ &\quad \prod_{i=1}^n \int_0^{\infty} dk_{i+} e^{\frac{-\tilde{\omega}}{\sqrt{\hat{s}}} k_{i+}} k_{i+}^{\frac{d-4}{2}} \int_0^{\infty} dk_{i-} e^{\frac{-\tilde{\omega}}{\sqrt{\hat{s}}} k_{i-}} k_{i-}^{\frac{d-4}{2}} \\ &\quad \times \left(1 + \frac{\tilde{\omega}}{\hat{s}} \sum_{i=1}^{n-1} \sum_{j=i+1}^n (k_{i+}k_{j-} + k_{i-}k_{j+})\right). \end{aligned} \quad (5.16)$$

We have gone as far as we can with simplifying the phase space integral before applying it to the leading soft term. We can integrate the leading soft term by dividing up the phase space integrals into three separate terms:

$$\begin{aligned} \int d\Phi^{(n+1)} \prod_{i=1}^n \left(\frac{1}{p \cdot k_i}\right) \left(\frac{1}{\bar{p} \cdot k_i}\right) &= \frac{(2\pi)^{n+1-nd}}{\hat{s}^{n+1}} \Omega_{d-2}^n \int_{-i\infty}^{i\infty} \frac{d\tilde{\omega}}{2\pi i} e^{\tilde{\omega}(1-z)} \\ &\quad \prod_{i=1}^n \int_0^{\infty} dk_{i+} e^{\frac{-\tilde{\omega}}{\sqrt{\hat{s}}} k_{i+}} k_{i+}^{\frac{d-6}{2}} \int_0^{\infty} dk_{i-} e^{\frac{-\tilde{\omega}}{\sqrt{\hat{s}}} k_{i-}} k_{i-}^{\frac{d-6}{2}} \end{aligned}$$

$$\times \left(\underbrace{1}_A + \frac{\tilde{\omega}}{\hat{s}} \sum_{i=1}^{n-1} \sum_{j=i+1}^n \underbrace{(k_{i+} k_{j-} + k_{i-} k_{j+})}_{B1} \right) \quad (5.17)$$

where we have combined the phase space 5.16 with the Sudakov expression of the leading soft term in table 3. To solve this integral, we can start with the simplest part, integral A.

5.2.1 Integral A

$$\int d\Phi_A^{(n+1)} \prod_{i=1}^n \left(\frac{1}{p \cdot k_i} \right) \left(\frac{1}{\bar{p} \cdot k_i} \right) = \frac{(2\pi)^{n+1-nd}}{\hat{s}^{n+1}} \Omega_{d-2}^n \int_{-i\infty}^{i\infty} \frac{d\tilde{\omega}}{2\pi i} e^{\tilde{\omega}(1-z)} \prod_{i=1}^n \int_0^\infty dk_{i+} e^{\frac{-\tilde{\omega}}{\sqrt{\hat{s}}} k_{i+}} k_{i+}^{\frac{d-6}{2}} \int_0^\infty dk_{i-} e^{\frac{-\tilde{\omega}}{\sqrt{\hat{s}}} k_{i-}} k_{i-}^{\frac{d-6}{2}}. \quad (5.18)$$

Observe that the integrals over k_{i+} and k_{i-} are identical to each other and could be replaced by a dummy x . Furthermore, we can expect n integrals of each, amounting to $2n$ integrals over x . Finally, we will be able to recognize some familiar functions by making the variable change $\tilde{x} = \frac{\tilde{\omega}}{\sqrt{\hat{s}}} x$ resulting in:

$$\int d\Phi_A^{(n+1)} \prod_{i=1}^n \left(\frac{1}{p \cdot k_i} \right) \left(\frac{1}{\bar{p} \cdot k_i} \right) = (2\pi)^{n+1-nd} \hat{s}^{n(\frac{d}{2}-3)-1} \Omega_{d-2}^n \int_{-i\infty}^{i\infty} \frac{d\tilde{\omega}}{2\pi i} e^{\tilde{\omega}(1-z)} \left(\frac{1}{\tilde{\omega}} \right)^{(d-4)n} \left(\int_0^\infty d\tilde{x} e^{-\tilde{x}} \tilde{x}^{\frac{d-6}{2}} \right)^{2n}. \quad (5.19)$$

The integral over \tilde{x} is a gamma function (see appendix B.1):

$$\int_0^\infty d\tilde{x} e^{-\tilde{x}} \tilde{x}^{\frac{d-6}{2}} = \Gamma\left(\frac{d-4}{2}\right), \quad (5.20)$$

while the integral over $\tilde{\omega}$ is an inverse Laplace transform (see appendix C.4), i.e.

$$\int_{-i\infty}^{i\infty} \frac{d\tilde{\omega}}{2\pi i} e^{\tilde{\omega}(1-z)} \left(\frac{1}{\tilde{\omega}} \right)^{n(d-4)} = \frac{(1-z)^{n(d-4)-1}}{\Gamma(n(d-4))}. \quad (5.21)$$

Putting together equations 5.19 - 5.21 gives us

$$\int d\Phi_A^{(n+1)} \prod_{i=1}^n \left(\frac{1}{p \cdot k_i} \right) \left(\frac{1}{\bar{p} \cdot k_i} \right)$$

$$= (2\pi)^{n+1-nd} \hat{s}^{n(\frac{d}{2}-3)-1} \Omega_{d-2}^n \frac{(1-z)^{n(d-4)-1}}{\Gamma(n(d-4))} \Gamma^{2n} \left(\frac{d-4}{2} \right). \quad (5.22)$$

5.2.2 Integrals $B1$ and $B2$

We can start with integral $B1$:

$$\begin{aligned} \int d\Phi_{B1}^{(n+1)} \prod_{i=1}^n \left(\frac{1}{p \cdot k_i} \right) \left(\frac{1}{\bar{p} \cdot k_i} \right) &= \frac{(2\pi)^{n+1-nd}}{\hat{s}^{n+1}} \Omega_{d-2}^n \int_{-i\infty}^{i\infty} \frac{d\tilde{\omega}}{2\pi i} e^{\tilde{\omega}(1-z)} \\ &\prod_{i=1}^n \int_0^\infty dk_{i+} e^{\frac{-\tilde{\omega}}{\sqrt{\hat{s}}} k_{i+}} k_{i+}^{\frac{d-6}{2}} \int_0^\infty dk_{i-} e^{\frac{-\tilde{\omega}}{\sqrt{\hat{s}}} k_{i-}} k_{i-}^{\frac{d-6}{2}} \\ &\times \frac{\tilde{\omega}}{\hat{s}} \sum_{i=1}^{n-1} \sum_{j=i+1}^n k_{i+} k_{j-}. \end{aligned} \quad (5.23)$$

In the $k_{i+} k_{j-}$ sum, there will be $\frac{n(n-1)}{2}$ terms. Consider one of these terms. It will be evaluated by one of the n “ k_{i+} ” and one of the n “ k_{i-} ” integrals. These two integrals will both be of the form

$$\int_0^\infty dx e^{-\frac{\tilde{\omega}}{\sqrt{\hat{s}}} x} x^{\frac{d-4}{2}} = \left(\frac{\sqrt{\hat{s}}}{\tilde{\omega}} \right)^{\frac{d-2}{2}} \int_0^\infty d\tilde{x} e^{-\tilde{x}} \tilde{x}^{\frac{d-4}{2}}, \quad (5.24)$$

while the remaining $2n - 2$ integrals will have the form

$$\int_0^\infty dy e^{-\frac{\tilde{\omega}}{\sqrt{\hat{s}}} y} y^{\frac{d-6}{2}} = \left(\frac{\sqrt{\hat{s}}}{\tilde{\omega}} \right)^{\frac{d-4}{2}} \int_0^\infty d\tilde{y} e^{-\tilde{y}} \tilde{y}^{\frac{d-6}{2}}, \quad (5.25)$$

and this will happen identically $\frac{n(n-1)}{2}$ times. Thus our expression will be:

$$\begin{aligned} \int d\Phi_{B1}^{(n+1)} \prod_{i=1}^n \left(\frac{1}{p \cdot k_i} \right) \left(\frac{1}{\bar{p} \cdot k_i} \right) &= (2\pi)^{n+1-nd} \hat{s}^{n(\frac{d}{2}-3)-1} \Omega_{d-2}^n \frac{n(n-1)}{2} \\ &\times \int_{-i\infty}^{i\infty} \frac{d\tilde{\omega}}{2\pi i} e^{\tilde{\omega}(1-z)} \left(\frac{1}{\tilde{\omega}} \right)^{n(d-4)+1} \\ &\times \left(\int_0^\infty d\tilde{x} e^{-\tilde{x}} \tilde{x}^{\frac{d-4}{2}} \right)^2 \left(\int_0^\infty d\tilde{y} e^{-\tilde{y}} \tilde{y}^{\frac{d-6}{2}} \right)^{2n-2}. \end{aligned} \quad (5.26)$$

We recognize the gamma function integrals as well as the inverse Laplace transform, yielding:

$$\int d\Phi_{B1}^{(n+1)} \prod_{i=1}^n \left(\frac{1}{p \cdot k_i} \right) \left(\frac{1}{\bar{p} \cdot k_i} \right)$$

$$\begin{aligned}
 &= (2\pi)^{n+1-nd} \hat{s}^{n(\frac{d}{2}-3)-1} \Omega_{d-2}^n \frac{n(n-1)}{2} \frac{(1-z)^{n(d-4)}}{\Gamma(n(d-4)+1)} \times \\
 &\Gamma\left(\frac{d-4}{2}\right)^{2n-2} \Gamma\left(\frac{d-2}{2}\right)^2.
 \end{aligned} \tag{5.27}$$

It can easily be shown that integral $B2$ turns out to be exactly the same as $B1$.

5.2.3 Finale

Altogether, and making use of the property $\Gamma(n+1) = n\Gamma(n)$ we have

$$\begin{aligned}
 \int d\Phi^{(n+1)} \prod_{i=1}^n \left(\frac{1}{p \cdot k_i}\right) \left(\frac{1}{\bar{p} \cdot k_i}\right) &= (2\pi)^{n+1-nd} \Omega_{d-2}^n \hat{s}^{n(d-4)/2-n-1} \Gamma^{2n} \left(\frac{d-4}{2}\right) \frac{(1-z)^{n(d-4)-1}}{\Gamma(n(d-4))} \\
 &\times \left[1 + \left(\frac{(n-1)(d-4)(1-z)}{4}\right)\right].
 \end{aligned} \tag{5.28}$$

5.2.4 NLP phase space integral

Equation (5.28) represents the LP squared matrix element integrated over the entire phase space in the soft limit for n real gluons. Consider the factor of $(1-z)$ in our integral. We have arranged the expression such that the first term in square brackets $\sim (1-z)^{n(d-4)-1}$, while the second term in square brackets $\sim (1-z)^{n(d-4)}$. In 4-dimensional spacetime in the soft limit, the second term is suppressed in terms of $(1-z)$ compared with the first. Given that our squared matrix element can not be anything but eikonal, the difference in powers of $(1-z)$ between these terms must be down to the phase space. Relabelling our phase space as per (5.1), we can express (5.28) as

$$\int d\Phi^{(n+1)} \overline{|M|^2}_{\text{LP}} = \underbrace{\int d\Phi_{\text{LP}}^{(n+1)} \overline{|M|^2}_{\text{LP}}}_{\sim (1-z)^{n(d-4)-1}} + \underbrace{\int d\Phi_{\text{NLP}}^{(n+1)} \overline{|M|^2}_{\text{LP}}}_{\sim (1-z)^{n(d-4)}}. \tag{5.29}$$

To answer our original question about whether the log terms will be leading or sub-leading in our second term, we need to expand the divergent parts of our expression in $\epsilon \sim 0$ (using dimensional regularisation convention $d = 4 - 2\epsilon$). Firstly, consider the purely LP part:

$$\Gamma^{2n} \left(\frac{d-4}{2}\right) \frac{(1-z)^{n(d-4)-1}}{\Gamma(n(d-4))} = \frac{\Gamma^{2n}(-\epsilon)}{\Gamma(-2n\epsilon)} (1-z)^{-1-2n\epsilon}. \tag{5.30}$$

We know from appendix B.1 that for small ϵ , we have

$$\Gamma(\epsilon) \sim \frac{1}{\epsilon}, \tag{5.31}$$

and so we have

$$\frac{\Gamma^{2n}(-\epsilon)}{\Gamma(-2n\epsilon)} \sim \epsilon^{1-2n}. \quad (5.32)$$

Now we examine the term $(1-z)^{-1-2n\epsilon}$, and denote it by

$$f(\epsilon) \equiv (1-z)^{-1-2n\epsilon} \longrightarrow \log(f(\epsilon)) = (-1-2n\epsilon) \log(1-z). \quad (5.33)$$

Re-writing the function in this way enables a friendly expression for an expansion in ϵ close to zero

$$f(\epsilon) = f(0) + \sum_{k=1}^{\infty} \frac{f^{(k)}(0)}{k!} \epsilon^k, \quad (5.34)$$

where $f^{(k)}(\epsilon) = (-2n)^k \log^k(1-z) f(\epsilon)$ is the k^{th} derivative of $f(\epsilon)$ with respect to ϵ . Then we can evaluate (5.34) as

$$f(\epsilon) = \frac{1}{1-z} + \sum_{k=1}^{\infty} \frac{(-2n)^k \log^k(1-z)}{k!} \frac{1}{1-z} \epsilon^k. \quad (5.35)$$

Combining this expression with that of (5.32) means that our LP term (5.30) has the expansion in small ϵ

$$\frac{\Gamma^{2n}(-\epsilon)}{\Gamma(-2n\epsilon)} (1-z)^{-1-2n\epsilon} \sim \frac{1}{1-z} \epsilon^{1-2n} + \sum_{k=1}^{\infty} \frac{(-2n)^k \log^k(1-z)}{k!} \frac{1}{1-z} \epsilon^{k-(2n-1)}. \quad (5.36)$$

Consider the series of log terms on the right hand side. The terms where $k > 2n-1$ will vanish in the limit $\epsilon \rightarrow 0$, and thus can be discarded. This means that the highest power of log term will have the form

$$\left[\frac{\Gamma^{2n}(-\epsilon)}{\Gamma(-2n\epsilon)} (1-z)^{-1-2n\epsilon} \right]_{\text{largest log}} \sim \frac{\log^{2n-1}(1-z)}{1-z}. \quad (5.37)$$

Benchmarking this leading term to our general expression classifying logs in a differential cross section (2.25) tells us two things: 1) this is indeed a leading power log, and 2) the exponent $2n-1$ is the highest power possible. This is a leading LP log, produced by the LP part of the phase space combined with the LP squared matrix element.

Now we turn our attention to the NLP part of (5.29), which roughly has the form

$$\Gamma^{2n} \left(\frac{d-4}{2} \right) \frac{(1-z)^{n(d-4)-1}}{\Gamma(n(d-4))} \times (1-z)(d-4) = \frac{\Gamma^{2n}(-\epsilon)}{\Gamma(-2n\epsilon)} (1-z)^{-2n\epsilon} (-2\epsilon). \quad (5.38)$$

We give the same treatment to the NLP term as we had done for the LP term. We note that the NLP term (5.38) is essentially the LP term (5.30) suppressed by a power of ϵ

and a power of $(1 - z)$. Then it is straightforward to see that the NLP term produces NLP logs, where the highest power is:

$$\left[\frac{\Gamma^{2n}(-\epsilon)}{\Gamma(-2n\epsilon)} (1 - z)^{-2n\epsilon} (-2\epsilon) \right]_{\text{largest log}} \sim \log^{2n-2}(1 - z). \quad (5.39)$$

Because the exponent is $2n - 2$ rather than $2n - 1$, we can describe this log comparatively as subleading. And so ends the proof that for any number of real emission gluons, the leading power NLP logs can not come from the LP squared matrix element as it only produces subleading NLP logs.

5.3 Resummation of NLP leading logs

We have shown in great detail how the NLP part of the phase space does not produce NLP leading logs, and therefore can be excluded from calculations pertaining to gathering coefficients for resummation. A source for the NLP LL must be the NLP squared matrix element, i.e.

$$\int d\Phi_{\text{LP}} |M|_{\text{NLP}}^2. \quad (5.40)$$

As for the well-known LP LL resummation exercise shown in section 3.2, a similar exercise can be done for NLP LL. Although this particular calculation is not the main focus of this chapter, a few steps at bird's eye view with the final result using the same conventions as in 3.2 are included here for some sense of closure for this topic.

For the reader's convenience, we reprint here from (3.42) the LP soft function at NLO:

$$S_{\text{LP}}^{(1)}(z, Q^2, \epsilon) = \mu^{2\epsilon} g_s^2 C_F \int \frac{d^d k}{(2\pi)^{d-1}} \delta_+(k^2) \left[\delta \left(1 - z - \frac{2k \cdot (p + \bar{p})}{\hat{s}} \right) - \delta(1 - z) \right] \frac{2p \cdot \bar{p}}{p \cdot k \bar{p} \cdot k}. \quad (5.41)$$

The NLP analogue (i.e. leading terms coming from phase space integration of the NLP squared matrix element) is

$$S_{\text{NLP}}^{(1)}(z, Q^2, \epsilon) = -2\mu^{2\epsilon} g_s^2 C_F \int \frac{d^d k}{(2\pi)^{d-1}} \delta_+(k^2) \delta \left(1 - z - \frac{2k \cdot (p + \bar{p})}{\hat{s}} \right) \left[\frac{1}{p \cdot k} + \frac{1}{\bar{p} \cdot k} \right], \quad (5.42)$$

where the squared matrix element terms are recognisably the last two terms of (2.19). The soft function can then be integrated in spherical polar coordinates using the Sudakov parametrization as per (3.43), as well as the variable change as per (3.53), yielding

$$S_{\text{NLP}}^{(1)}(z, Q^2, \epsilon) = -\frac{\mu^{2\epsilon} g_s^2 C_F \Omega_{d-2}}{(2\pi)^{d-1}} \int d\tilde{z} dy \hat{s}^{\frac{d-4}{2}} (1 - \tilde{z})^{d-4} y^{\frac{d-6}{2}} (1 - y)^{\frac{d-6}{2}} \times \delta(1 - z - (1 - \tilde{z})). \quad (5.43)$$

Following the same steps as done for the LP exercise (i.e. for integral “B”, equations (3.57)-(3.62)), we arrive at

$$S_{\text{NLP}}^{(1)}(z, Q^2, \epsilon) = \frac{-\alpha_s C_F}{\pi} \left(\frac{\bar{\mu}^2}{Q^2} \right)^\epsilon \frac{e^{\epsilon\gamma_E} \Gamma^2(-\epsilon)}{\Gamma(1-\epsilon)\Gamma(-2\epsilon)} (1-z)^{-2\epsilon}. \quad (5.44)$$

Mellin transforming this yields

$$S_{\text{NLP}}^{(1)}(N, Q^2, \epsilon) = \frac{-2\alpha_s C_F}{\pi} \left(\frac{\bar{\mu}^2}{Q^2} \right)^\epsilon \frac{e^{\epsilon\gamma_E} \Gamma(-\epsilon)\Gamma(N)}{\Gamma(1-2\epsilon+N)}. \quad (5.45)$$

Now we Laurent-expand, and we can be dismissive of terms of order ϵ as they will vanish in the limit $\epsilon \rightarrow 0$. The result is

$$S_{\text{NLP}}^{(1)}(N, Q^2, \epsilon) = \frac{-2\alpha_s C_F}{\pi} \left(\frac{\bar{\mu}^2}{Q^2} \right)^\epsilon \left[\frac{1}{\epsilon N} + \frac{2}{N} \left(\psi^{(0)}(N+1) + \gamma_E \right) \right] + \mathcal{O}(\epsilon). \quad (5.46)$$

We highlight the leading log behaviour in the large N limit (see appendix B.2),

$$S_{\text{NLP}}^{(1)}(N, Q^2, \epsilon) = \frac{2\alpha_s C_F}{\pi} \left(\frac{\bar{\mu}^2}{Q^2} \right)^\epsilon \left[\frac{1}{\epsilon} \frac{1}{N} + \frac{2 \log N}{N} + \dots \right] \quad (5.47)$$

where the ellipsis indicates terms that are non-singular in ϵ , non-logarithmic in N , and terms suppressed by powers of N .

To perform the resummation, we first need to carefully combine this result with (3.66). Note that in the NLP soft function, we have a term of the form $\sim \frac{2 \log N}{N}$. This is also the case for the LP soft function of (3.65), although it is not a leading LP term and thus not present in the LP LL expression (3.66). The LP soft function (3.65) contributes a term of $\sim \frac{-\log N}{N}$. Likewise, it also contributes a subleading term of order $\frac{1}{\epsilon}$, i.e. $\frac{-1}{\epsilon 2N}$ to be combined with its NLP counterpart (and ultimately destined for absorption by PDFs). Altogether, combining leading NLP terms with leading and appropriate subleading LP terms leads to

$$S_{\text{LP+NLP}}^{(1)}(N, Q^2, \epsilon) = \frac{2\alpha_s C_F}{\pi} \left(\frac{\bar{\mu}^2}{Q^2} \right)^\epsilon \left[\frac{1}{\epsilon} \left(\log N + \frac{1}{2N} \right) + \log^2 N + \frac{\log N}{N} + \dots \right]. \quad (5.48)$$

It is now safe to exponentiate this expression. The set of terms of order $\mathcal{O}(\epsilon^{-1})$ are collinear contributions which can be absorbed in PDFs, similar to (3.69). Then the remaining terms (i.e. the logarithmic terms) can be exponentiated, resulting in the resummed K -factor

$$\Delta(N, Q^2)|_{\text{LP+NLP}} = \exp \left[\frac{2\alpha_s}{\pi} C_F \left(\log^2 N + \frac{\log N}{N} \right) \right]. \quad (5.49)$$

Now to return to z -space, we expand (5.49) in α_s and include all subleading terms. We had already performed this procedure for the LP terms, encapsulated by (3.71). Comparing the NLP terms of order ϵ^0 in (5.46) with those present in the Mellin transform for NLP terms in (C.36) allows for a very straightforward Mellin transform, i.e.,

$$\Delta(z, Q^2)|_{\text{NLP}} = \left(\frac{2\alpha_s C_F}{\pi} \right) [-2 \log(1 - z)]. \quad (5.50)$$

Combining this with the LP counterpart (3.71) yields

$$\Delta(z, Q^2)|_{\text{LP+NLP}} = \left(\frac{2\alpha_s C_F}{\pi} \right) \left[2 \left(\frac{\log(1 - z)}{1 - z} \right)_+ - 2 \log(1 - z) \right]. \quad (5.51)$$

This is in complete agreement with the result of ref. [60], and is consistent with (2.24).

5.4 Conclusions

In the interest of resumming NLP LL, we posed the question of whether the phase space could be structured such that leading and subleading logs have distinct sources. It was indeed the case for a subset of NⁿLO involving n real gluon emissions that the NLP part of the phase space only produces subleading logs and therefore lightens our load for calculating the resummation of NLP LL. Although the focus of this chapter was developing this result in great detail, we also offered a bird's eye view of the resummation exercise with the final result for completeness.

Chapter 6

Threshold Radiation Conclusion

6.1 Recap

To summarise, our study of threshold gluon radiation in QCD processes is largely motivated by improving theory predictions to match against experiment, specifically in the production of heavy particles where new physics is often found. A convenient probe for this endeavour is the Drell-Yan process, which we used throughout our research. Theory predictions such as fixed order differential cross sections are enhanced by the phenomenon of threshold radiation. However, the presence of threshold radiation gives rise to large logarithmic contributions, potentially threatening the stability of the prediction. A possible antidote to this issue is resummation, where a stable correction capturing some all-order information can be constructed. At the time of performing the research supporting this thesis, the state of the art theory prediction for the Drell-Yan process is NNLO, with resummation of next-to next-to leading logs of the LP variety. While LP log resummation is well known and firmly established, less is known about NLP logs - the focus of this thesis.

6.2 Learnings and achievements

In our research, we reviewed the resummation procedure for LP logs at NLO, and we made significant progress toward the resummation of NLP logs beyond NNLO. More specifically, we explored a subset of $N^3\text{LO}$ contributions (2-real, 1-virtual) by using a method of regions approach. We found that leading and subleading logs can be ascribed to specific regions, easing the way for exponentiation - a key stepping stone toward resummation. Some of these structure effects were visible before phase space integration, suggesting the question of how the phase space contributes to leading and subleading effects. This was studied at $N^n\text{LO}$ (real contributions only), where the phase space could be structured such that leading and subleading logs have distinct sources.

This information was helpful toward performing the resummation of leading NLP logs, of which we offered a bird's eye view.

6.3 Impact

In conjunction with our work in studying NLP logs using a diagrammatic approach, there is also a considerable effort toward NLP log resummation using Soft Collinear Effective Theory (SCET) - see e.g. [61–63]. Various methods for including leading and subleading logs at NLP are assessed and compared in ref. [64]. Studies of NLP effects have been extended to processes involving coloured final state particles - made more complex by non-negligible collinear effects associated with real radiation [65]. Furthermore, sensitivity analysis conducted for the Drell-Yan and Higgs cross sections reveals that the inclusion of NLP leading log data significantly increases the precision of predictions [66].

6.4 Further work

Building on the results presented, there are a number of directions of further work. The N^3 LO calculations in this thesis comprised only one channel - future work could center on the other contributing channels, such as 2 virtual and 1 real emissions. Furthermore, the calculations could be generalised to include all possible colour structures involving fully non-Abelian corrections. Regarding the resummation of NLP leading logs at NLO, clearly, the resummation could be extended to subleading logarithmic accuracy at NLP. This would require a more involved treatment of non-factorising phase-space effects for real emission contribution.

6.5 A bridge to gravity and other theories

While the study of threshold radiation deepens our understanding of QCD phenomenology and theory, it is also the case that infrared singularities in gauge theories such as QED and QCD can connect to those of gravity. Infrared photons and gravitons have been formalised in Weinberg's soft theorems [67], and BMS symmetries have been explored in the context of gravitational scattering with soft gravitons [68]. Infrared singularities of QCD and gravity have been shown to be related to each other via the duality of the double copy [69]. The double copy framework extends beyond this remit, to broader classical and quantum field theory amplitudes, as well as to the exact solutions of classical theories. A study of the latter forms the second half of this thesis.

Part II

The Double Copy

Chapter 7

Introduction to the Double Copy

The double copy - a novel duality relating gauge theories to gravity - is best summed up by the catch phrase “gravity is Yang-Mills squared”. This idea has its origins in the Kawai-Lewellen-Tye (KLT) relations of string theory that express closed string amplitudes in terms of sums of products of open string amplitudes [70]. In 2002, Bern found that a similar principle applies in field theory where tree level gravity amplitudes could be constructed from gauge theory amplitudes, and be subsequently promoted to loop level using the unitarity method [71]. Within a decade, Bern, Carrasco and Johansson (BCJ) proposed the double copy as a means of constructing gravity amplitudes from gauge theory amplitudes by exploiting colour-kinematics duality [72–75] (see also [76] for a comprehensive yet pedagogical introduction and overview). While this significantly reduces the complexity of quantum gravitational computations, it also suggests a relationship between seemingly disparate theories of nature.

Although still a relatively young theory, the double copy has blossomed within and beyond the study of amplitudes to classical theories. This thesis focuses largely on the classical double copy, however, we will devote this chapter to a brief tour of the older and more firmly established original BCJ double copy to fix our bearings.

Before we build double copy bridges between the amplitudes of gauge theory and gravity, we will first review what those theories are, and what their amplitudes look like.

7.1 Yang-Mills theory

Yang-Mills theories are types of gauge theory with a non-Abelian symmetry group. For example, QCD, stripped of quarks, is called *pure* Yang-Mills as it describes gluon self-interactions governed by the non-Abelian group $SU(3)$. For our discussion, we will stay general, i.e. our theory will be governed by $SU(N)$ symmetry. The Lagrangian

defining such a theory is

$$\mathcal{L}_{\text{YM}} = -\frac{1}{2}\text{Tr}(F^{\mu\nu}F_{\mu\nu}), \quad (7.1)$$

where the field strength tensor is given by

$$F_{\mu\nu} = D_\mu A_\nu - D_\nu A_\mu. \quad (7.2)$$

The gauge covariant derivative ensuring gauge invariance of our Lagrangian is defined as

$$D_\mu = \partial_\mu - igA_\mu, \quad (7.3)$$

where g is the coupling constant. This is a non-Abelian theory, and so we expect that colour generators should feature somewhere in the above. The gauge field A_μ can be expanded into a product of colour indexed fields and generators of the gauge group $\text{SU}(N)$,

$$A_\mu = A_\mu^a T^a. \quad (7.4)$$

The generators T^a obey a Lie algebra defined by the commutation relation,

$$[T^a, T^b] = if^{abc}T^c, \quad (7.5)$$

with normalisation condition

$$\text{Tr}(T^a T^b) = \frac{1}{2}\delta^{ab}. \quad (7.6)$$

The Latin indices a, b, c count out the number of generators in the adjoint representation of the group. For example, in $\text{SU}(3)$, these indices run from 1 to 8, while in $\text{SU}(2)$ they run from 1 to 3. The antisymmetric structure constants f^{abc} are at the heart of defining the theory, and are simply 0 in the case where the theory is Abelian. In double copy literature and beyond, the term *colour structure* is synonymous with factors of f^{abc} appearing in amplitudes and Feynman diagrams.

Given that the generators can be represented by matrices (e.g. in $\text{SU}(2)$, these can be related to the Pauli matrices, or the Gell-Mann matrices in $\text{SU}(3)$), they must obey the Jacobi identity

$$[T^a, [T^b, T^c]] + [T^b, [T^c, T^a]] + [T^c, [T^a, T^b]] = 0. \quad (7.7)$$

When combining this with the rules set out by the Lie algebra of (7.5), the Jacobi identity takes on an important form in terms of structure constants:

$$f^{abe}f^{cde} - f^{ace}f^{bde} + f^{ade}f^{bce} = 0. \quad (7.8)$$

This identity sets us on the road to colour-kinematics duality, a key foundation of the double copy. But before we jump ahead of ourselves, we first need to build up the quantity which will offer a playground for this duality - i.e. the amplitude. To do this, we can rewrite the Lagrangian such that we can see explicitly the interaction terms, which will determine what type of Feynman diagrams we can expect. Combining equations (7.2) to (7.5), it is possible to decompose the field strength tensor into a product of generators and colour indexed field strength tensors, i.e.,

$$F_{\mu\nu} = F_{\mu\nu}^a T^a, \quad (7.9)$$

where the colour indexed field strength tensor is

$$F_{\mu\nu}^a = \partial_\mu A_\nu^a - \partial_\nu A_\mu^a + g f^{abc} A_\mu^b A_\nu^c. \quad (7.10)$$

We use this to re-write the Lagrangian (7.1) with colour indices exposed:

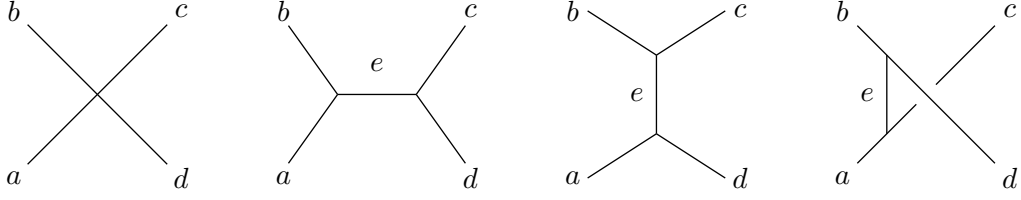
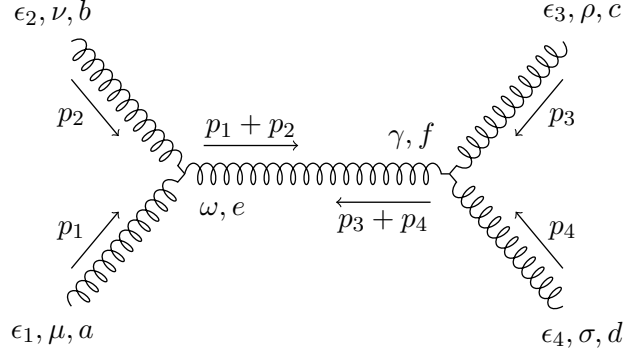
$$\mathcal{L}_{\text{YM}} = -\frac{1}{4} F_{\mu\nu}^a F^{a\mu\nu}. \quad (7.11)$$

Expanding (7.11) with definition (7.10) reveals the types of Feynman rules we can expect with this theory:

$$\begin{aligned} \mathcal{L}_{\text{YM}} = & -\frac{1}{4} \underbrace{(\partial_\mu A_\nu^a - \partial_\nu A_\mu^a)(\partial^\mu A^{a\nu} - \partial^\nu A^{a\mu})}_{\text{kinetic terms}} \\ & - \underbrace{g f^{abc} A^{a\mu} A^{b\nu} \partial_\mu A_\nu^c}_{\text{cubic interactions}} - \underbrace{\frac{g^2}{4} f^{abe} f^{ecd} A_\mu^a A_\nu^b A^{c\mu} A^{d\nu}}_{\text{quartic interactions}}. \end{aligned} \quad (7.12)$$

The first set of terms are the kinetic or “free” terms of the theory. In QCD, this is the Lagrangian for eight non-interacting, inherently colour-charged gluons, which, as far as we know, cannot be observed individually thanks to colour confinement. The remaining sets of terms indicate self-interactions - a key difference from Abelian theories where this does not happen. Of these self-interactions, we have cubic and quartic interactions. In the cubic interactions, the presence of the derivative gives a momentum factor in momentum space. The quartic interaction term is crucial in preserving gauge invariance of the Lagrangian and amplitudes.

Higher point interactions are built up from three and four-point diagrams. However, we shall soon see that actually, four-point diagrams are closely related to three-point diagrams in terms of their colour structure. In this context, the status of diagrams with three-point vertices is elevated to that of *building blocks* for higher point interac-


Figure 11: $gg \rightarrow gg$ at tree-level

Figure 12: s -channel for $gg \rightarrow gg$ at tree-level

the contact term set out by the quartic vertex, as illustrated schematically by figure 11.

Using the Feynman rules set out earlier in section 7.1.1, we can write down expressions corresponding to each diagram in 11. We start with the s -channel, which has been blown up in figure 12 and dressed with momenta, colour indices, and all the bells and whistles for the convenience of the reader. The corresponding sub-amplitude for the s -channel is:

$$\begin{aligned}
 M_s = & \underbrace{\epsilon_{1\mu}\epsilon_{2\nu}\epsilon_{3\rho}\epsilon_{4\sigma}}_{\text{incoming polarisation vectors}} \times \underbrace{gf^{abe}[g^{\mu\nu}(p_1 - p_2)^\omega + g^{\nu\omega}(p_1 + 2p_2)^\mu - g^{\omega\mu}(2p_1 + p_2)^\nu]}_{\text{cubic vertex factor}} \\
 & \times \underbrace{\frac{-ig_{\omega\gamma}\delta^{ef}}{(p_1 + p_2)^2}}_{\text{propagator}} \times \underbrace{gf^{cdf}[g^{\rho\sigma}(p_3 - p_4)^\gamma + g^{\sigma\gamma}(p_3 + 2p_4)^\rho - g^{\gamma\rho}(2p_3 + p_4)^\sigma]}_{\text{cubic vertex factor}} \quad (7.16)
 \end{aligned}$$

With on-shell conditions $\epsilon_i \cdot p_i = 0$, the above reduces to

$$\begin{aligned}
 iM_s = & \frac{g^2}{s} f^{abe} f^{cde} \times [\epsilon_1 \cdot \epsilon_2 (p_1 - p_2)^\omega + 2\epsilon_2^\omega (p_2 \cdot \epsilon_1) - 2\epsilon_1^\omega (p_1 \cdot \epsilon_2)] \\
 & \times [\epsilon_3 \cdot \epsilon_4 (p_3 - p_4)_\omega + 2\epsilon_{4\omega} (p_4 \cdot \epsilon_3) - 2\epsilon_{3\omega} (p_3 \cdot \epsilon_4)], \quad (7.17)
 \end{aligned}$$

where s is the Mandelstam invariant $s = (p_1 + p_2)^2$. Similarly, the expressions for the t and u channel diagrams are

$$iM_t = \frac{g^2}{t} f^{ade} f^{bce} \times [\epsilon_2 \cdot \epsilon_3 (p_2 - p_3)^\omega + 2\epsilon_3^\omega (p_3 \cdot \epsilon_2) - 2\epsilon_2^\omega (p_2 \cdot \epsilon_3)] \\ \times [\epsilon_1 \cdot \epsilon_4 (p_1 - p_4)_\omega + 2\epsilon_{4\omega} (p_4 \cdot \epsilon_1) - 2\epsilon_{1\omega} (p_1 \cdot \epsilon_4)], \quad (7.18)$$

$$iM_u = \frac{g^2}{u} f^{ace} f^{bde} \times [\epsilon_1 \cdot \epsilon_3 (p_1 - p_3)^\omega + 2\epsilon_3^\omega (p_3 \cdot \epsilon_1) - 2\epsilon_1^\omega (p_1 \cdot \epsilon_3)] \\ \times [\epsilon_2 \cdot \epsilon_4 (p_2 - p_4)_\omega + 2\epsilon_{4\omega} (p_4 \cdot \epsilon_2) - 2\epsilon_{2\omega} (p_2 \cdot \epsilon_4)], \quad (7.19)$$

with Mandelstam variables $t = (p_1 + p_4)^2$ and $u = (p_1 + p_3)^2$. Lastly, we have the diagram associated with the contact vertex:

$$iM_x = g^2 \times \{ f^{abe} f^{cde} [(\epsilon_1 \cdot \epsilon_3)(\epsilon_2 \cdot \epsilon_4) - (\epsilon_1 \cdot \epsilon_4)(\epsilon_2 \cdot \epsilon_3)] \\ + f^{ace} f^{bde} [(\epsilon_1 \cdot \epsilon_2)(\epsilon_3 \cdot \epsilon_4) - (\epsilon_1 \cdot \epsilon_4)(\epsilon_2 \cdot \epsilon_3)] \\ + f^{ade} f^{bce} [(\epsilon_1 \cdot \epsilon_2)(\epsilon_3 \cdot \epsilon_4) - (\epsilon_1 \cdot \epsilon_3)(\epsilon_2 \cdot \epsilon_4)] \}. \quad (7.20)$$

The full tree-level four-point scattering amplitude is the grand total of these 4 subamplitudes, i.e.,

$$\mathcal{A}_4^{(\text{tree})} = iM_s + iM_t + iM_u + iM_x. \quad (7.21)$$

This can be reorganised in a notation that clearly separates colour from kinematic factors, and highlights the cubic diagram building block notion:

$$\mathcal{A}_4^{(\text{tree})} = g^2 \times \left(\frac{c_s n_s}{s} + \frac{c_t n_t}{t} + \frac{c_u n_u}{u} \right). \quad (7.22)$$

The *colour factors* c_i correspond to the combination of structure constants distinct to each channel, i.e.,

$$c_s = f^{abe} f^{cde}; \quad c_t = -f^{ade} f^{bce}; \quad c_u = -f^{ace} f^{bde}. \quad (7.23)$$

These colour factors are also present in the contact term of (7.20), which can be rewritten to highlight the colour structure as:

$$iM_x = iM_x = g^2 \times \{ c_s [(\epsilon_1 \cdot \epsilon_3)(\epsilon_2 \cdot \epsilon_4) - (\epsilon_1 \cdot \epsilon_4)(\epsilon_2 \cdot \epsilon_3)] \\ - c_u [(\epsilon_1 \cdot \epsilon_2)(\epsilon_3 \cdot \epsilon_4) - (\epsilon_1 \cdot \epsilon_4)(\epsilon_2 \cdot \epsilon_3)] \\ - c_t [(\epsilon_1 \cdot \epsilon_2)(\epsilon_3 \cdot \epsilon_4) - (\epsilon_1 \cdot \epsilon_3)(\epsilon_2 \cdot \epsilon_4)] \}. \quad (7.24)$$

This format draws a relationship between the contact term and the three channels. Additionally, in this notation, the Jacobi identity set out in (7.8) takes on a deeper

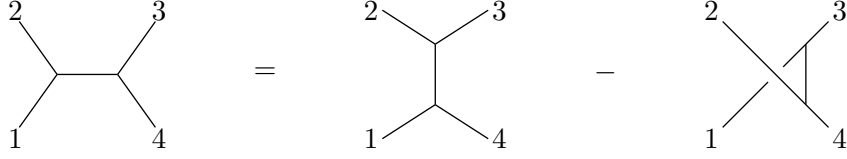


Figure 13: The Jacobi identity $c_s = c_t - c_u$ in terms of tree-level diagrams.

meaning in terms of the relationship among the colour structures of the three channels,

$$c_s - c_t + c_u = 0. \quad (7.25)$$

This relationship is depicted schematically in figure 13.

The *kinematic factors* n_i contain information about spin and momenta per channel with additional appropriate contributions of the contact term. For example, the kinematic factor n_s combines factors from the s -channel in (7.17), with the spin-related terms dressing the c_s colour factor of (7.20):

$$\begin{aligned} n_s = & [\epsilon_1 \cdot \epsilon_2 (p_1 - p_2)^\omega + 2\epsilon_2^\omega (\epsilon_1 \cdot p_2) - 2\epsilon_1^\omega (\epsilon_2 \cdot p_1)] \\ & \times [\epsilon_3 \cdot \epsilon_4 (p_3 - p_4)_\omega + 2\epsilon_{4\omega} (\epsilon_3 \cdot p_4) - 2\epsilon_{3\omega} (\epsilon_4 \cdot p_3)] \\ & + s[(\epsilon_1 \cdot \epsilon_3)(\epsilon_2 \cdot \epsilon_4) - (\epsilon_1 \cdot \epsilon_4)(\epsilon_2 \cdot \epsilon_3)]. \end{aligned} \quad (7.26)$$

Likewise, the other two kinematic factors are

$$\begin{aligned} n_t = & [\epsilon_2 \cdot \epsilon_3 (p_3 - p_2)^\omega - 2\epsilon_3^\omega (\epsilon_2 \cdot p_3) + 2\epsilon_2^\omega (\epsilon_3 \cdot p_2)] \\ & \times [\epsilon_1 \cdot \epsilon_4 (p_1 - p_4)_\omega + 2\epsilon_{4\omega} (\epsilon_1 \cdot p_4) - 2\epsilon_{1\omega} (\epsilon_4 \cdot p_1)] \\ & - t[(\epsilon_1 \cdot \epsilon_2)(\epsilon_3 \cdot \epsilon_4) - (\epsilon_1 \cdot \epsilon_3)(\epsilon_2 \cdot \epsilon_4)]; \end{aligned} \quad (7.27)$$

$$\begin{aligned} n_u = & [\epsilon_1 \cdot \epsilon_3 (p_3 - p_1)^\omega - 2\epsilon_3^\omega (\epsilon_1 \cdot p_3) + 2\epsilon_1^\omega (\epsilon_3 \cdot p_1)] \\ & \times [\epsilon_2 \cdot \epsilon_4 (p_2 - p_4)_\omega + 2\epsilon_{4\omega} (\epsilon_2 \cdot p_4) - 2\epsilon_{2\omega} (\epsilon_4 \cdot p_2)] \\ & - u[(\epsilon_1 \cdot \epsilon_2)(\epsilon_3 \cdot \epsilon_4) - (\epsilon_1 \cdot \epsilon_4)(\epsilon_2 \cdot \epsilon_3)]. \end{aligned} \quad (7.28)$$

The key observations about the four-point tree-level amplitude that advance the double copy story are:

- It is possible to factorise the amplitude such that colour factors are distinct from kinematic factors.
- The colour factors obey the Jacobi identity.
- The colour structure suggests the amplitude can be organised to resemble a sum of diagrams with cubic vertices.

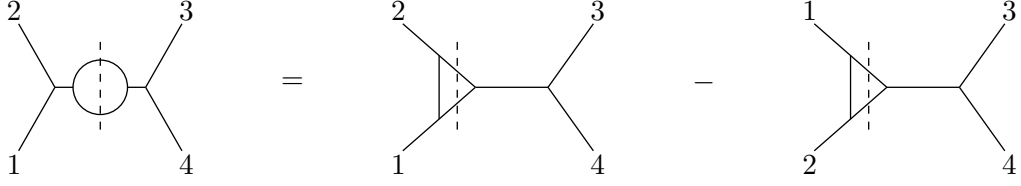


Figure 14: The Jacobi identity $c_s = c_t - c_u$ embedded in a 1-loop diagram.

These statements can be generalised beyond four-point tree-level scattering to higher-point scattering at loop level.

7.1.3 Amplitude for m -point scattering

We briefly generalise the learnings of the four-point scattering exercise in this section. Consider the general case for the scattering of m external gluons. At tree-level, the amplitude for this process can be written as (see e.g. [73])

$$\mathcal{A}_m^{(\text{tree})} = g^{m-2} \sum_{i \in \Gamma} \frac{n_i c_i}{\prod_{\alpha_i} p_{\alpha_i}^2} \quad (7.29)$$

where the sum over i refers to the sum over m -point graphs Γ with cubic vertices. Like the four-point scattering example, the amplitude is primarily organised by the colour factors c_i associated with these cubic vertices, with kinematic factors n_i dressing the colour factors. The denominator indicates a combination of propagators.

At loop level, this amplitude generalises for L loops in D spacetime dimensions to

$$\mathcal{A}_m^{(L)} = i^L g^{m-2+2L} \sum_{i \in \Gamma} \int \prod_{l=1}^L \frac{d^D k_l}{(2\pi)^D} \frac{1}{S_i} \frac{n_i c_i}{\prod_{\alpha_i} p_{\alpha_i}^2} \quad (7.30)$$

where the factor S_i accounts for symmetries typically encountered at loop level. The Jacobi identity still holds for the colour factors c_i at loop level. By making strategic unitarity cuts in which the loop momentum goes on-shell, loop diagrams effectively can be treated as tree level diagrams where the Jacobi identity is embedded (see e.g. [73,80]). Figure 14 displays an example of this idea at 1-loop.

We have an expression for a Yang-Mills amplitude, and we have organised it so that colour and kinematic factors are separate, with the colour factors obeying the Jacobi identity. The BCJ double copy relates this amplitude to that of gravity. This naturally raises the question - how does the picture we have presented for Yang-Mills theory compare with gravity?

7.2 Perturbative gravity

Our starting point for perturbative gravity (guided by [81–83]) is the same as for Yang-Mills - the Lagrangian. We can pick off the Lagrangian from the action that yields the Einstein field equations, i.e., the Einstein-Hilbert action in D spacetime dimensions for pure gravity (without matter fields),

$$S_{\text{EH}} = \frac{1}{2\kappa^2} \int d^D x \sqrt{-g} R \quad (7.31)$$

where $\kappa^2 = 8\pi G_N$ is Einstein's gravitational constant with Newton's constant G_N , the determinant of the underlying metric $g_{\mu\nu}$ is denoted by g , and R is the curvature or Ricci scalar constructed by contracting the Ricci tensor with the underlying inverse metric, i.e.

$$R = g^{\mu\nu} R_{\mu\nu}. \quad (7.32)$$

The Ricci tensor is a contraction of the Riemann tensor, i.e.

$$R_{\mu\nu} = R^\sigma{}_{\mu\sigma\nu}. \quad (7.33)$$

The Riemann tensor (also known as the curvature tensor) is defined as

$$R^\rho{}_{\mu\sigma\nu} = \partial_\sigma \Gamma^\rho_{\mu\nu} - \partial_\nu \Gamma^\rho_{\mu\sigma} + \Gamma^\lambda_{\mu\nu} \Gamma^\rho_{\lambda\sigma} - \Gamma^\lambda_{\mu\sigma} \Gamma^\rho_{\lambda\nu}. \quad (7.34)$$

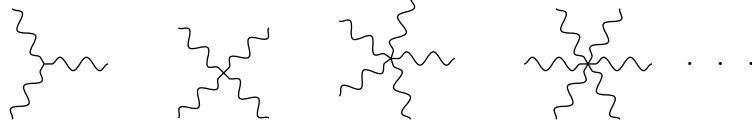
Each Christoffel symbol is composed of derivatives of the metric as per

$$\Gamma^\rho_{\mu\nu} = \frac{1}{2} g^{\rho\sigma} [\partial_\mu g_{\nu\sigma} + \partial_\nu g_{\mu\sigma} - \partial_\sigma g_{\mu\nu}]. \quad (7.35)$$

This metric is the gravitational field we wish to quantize within the context of perturbation theory. In our treatment of Yang-Mills theory, the field A_μ is quantised such that the scattering of particles is against a flat background spacetime. We can adopt this principle for our metric by modelling it as a graviton field $h_{\mu\nu}$ perturbing a Minkowski background spacetime $\eta_{\mu\nu}$, i.e.,

$$g_{\mu\nu} = \eta_{\mu\nu} + \kappa h_{\mu\nu}. \quad (7.36)$$

To be able to see what kind of Feynman diagrams could emerge in Yang-Mills theory, we expressed the Lagrangian in terms of powers of the field A_μ and its derivatives as per (7.12). To see the Feynman diagrams of gravity, we should do something similar - express (7.31) in terms of powers of the graviton field $\kappa h_{\mu\nu}$ and its derivatives. To do this, we need an expression for the inverse metric $g^{\mu\nu}$, which will be an infinite series


Figure 15: Feynman diagrams for gravity interactions

in powers of h , i.e.

$$g^{\mu\nu} = \eta^{\mu\rho}(\delta_{\rho}^{\nu} - \kappa h_{\rho}^{\nu} + \kappa^2 h_{\rho}^{\sigma} h_{\sigma}^{\nu} - \dots). \quad (7.37)$$

The term $\sqrt{-g}$, will also be an infinite series in powers of h upon Taylor-expanding the square root:

$$\sqrt{-g} = 1 + \frac{\kappa}{2} h^{\alpha}_{\alpha} - \frac{\kappa^2}{4} h^{\alpha}_{\beta} h^{\beta}_{\alpha} + \dots \quad (7.38)$$

The Ricci tensor will contain two derivatives of h in every term, but it too will be an infinite series in powers of h thanks to the inverse metric present in each Christoffel symbol. The terms of the Ricci tensor series that are lowest in order of h will be:

$$\begin{aligned} R_{\mu\nu} \approx & \frac{\kappa}{2} \eta^{\alpha\beta} \left[\partial_{\alpha} \partial_{\mu} h_{\beta\nu} - \partial_{\alpha} \partial_{\beta} h_{\mu\nu} - \partial_{\mu} \partial_{\nu} h_{\alpha\beta} + \partial_{\beta} \partial_{\nu} h_{\mu\alpha} \right] \\ & - \frac{\kappa^2}{2} h^{\alpha\beta} \left[\partial_{\alpha} \partial_{\mu} h_{\beta\nu} - \partial_{\alpha} \partial_{\beta} h_{\mu\nu} - \partial_{\mu} \partial_{\nu} h_{\alpha\beta} + \partial_{\beta} \partial_{\nu} h_{\mu\alpha} \right] \\ & + \frac{\kappa^2}{4} \eta^{\omega\alpha} \eta^{\lambda\beta} \left[\partial_{\lambda} h_{\omega\alpha} (\partial_{\mu} h_{\beta\nu} + \partial_{\nu} h_{\beta\mu} - \partial_{\beta} h_{\mu\nu}) \right. \\ & \left. - (\partial_{\mu} h_{\alpha\beta} + \partial_{\alpha} h_{\mu\beta} - \partial_{\beta} h_{\mu\alpha}) (\partial_{\lambda} h_{\omega\nu} + \partial_{\nu} h_{\lambda\omega} - \partial_{\omega} h_{\nu\lambda}) \right] + \dots \end{aligned} \quad (7.39)$$

Schematically, the types of term present in (7.39) can be expressed more clearly as

$$R_{\mu\nu} \sim \kappa \partial^2 h + \kappa^2 h \partial^2 h + \kappa^2 (\partial h)^2 + \dots \quad (7.40)$$

Altogether, this means that schematically, the action will take on a form resembling an infinite series in powers of κh ,

$$S_{\text{EH}} \sim \int d^D x \, h \partial^2 h + \kappa h^2 \partial^2 h + \kappa^2 h^3 \partial^2 h + \dots \quad (7.41)$$

where all total derivatives have vanished. This implies that gravity has Feynman diagrams for 3, 4, 5,...infinitely many point interactions, as illustrated by figure 15. This poses a stark contrast with Yang-Mills theory which presented only 3 and four-point interactions. The ensuing computations of gravitational amplitudes by Feynman rules are imaginably unwieldy, also in part because the gravitational interactions themselves are complicated in comparison with Yang-Mills theory. For example, in the de-Donder

gauge, $\partial^\mu h_{\mu\nu} = \frac{1}{2}\partial_\nu h_\mu^\mu$, the 3 graviton vertex factor has at least 100 terms (see e.g. [76]):

$$\begin{aligned}
 G^{\mu\rho,\nu\lambda,\sigma\tau}(p_1, p_2, p_3) = & i\frac{\kappa}{2} \text{Sym} \left[\right. \\
 & -\frac{1}{2}P_3(p_1 \cdot p_2 \eta^{\mu\rho} \eta^{\nu\lambda} \eta^{\sigma\tau}) - \frac{1}{2}P_6(p_1^\nu p_1^\lambda \eta^{\mu\rho} \eta^{\sigma\tau}) + \frac{1}{2}P_3(p_1 \cdot p_2 \eta^{\mu\nu} \eta^{\rho\lambda} \eta^{\sigma\tau}) \\
 & + P_6(p_1 \cdot p_2 \eta^{\mu\rho} \eta^{\nu\sigma} \eta^{\lambda\tau}) + 2P_3(p_1^\nu p_1^\tau \eta^{\mu\rho} \eta^{\lambda\sigma}) - P_3(p_1^\lambda p_2^\mu \eta^{\rho\nu} \eta^{\sigma\tau}) \\
 & + P_3(p_1^\sigma p_2^\tau \eta^{\mu\nu} \eta^{\rho\lambda}) + P_6(p_1^\sigma p_1^\tau \eta^{\mu\nu} \eta^{\rho\lambda}) + 2P_6(p_1^\nu p_2^\tau \eta^{\lambda\mu} \eta^{\rho\sigma}) \\
 & \left. + 2P_3(p_1^\nu p_2^\mu \eta^{\lambda\sigma} \eta^{\tau\rho}) - 2P_3(p_1 \cdot p_2 \eta^{\rho\nu} \eta^{\lambda\sigma} \eta^{\tau\mu}) \right] \quad (7.42)
 \end{aligned}$$

where p_i are the momenta of the three gravitons, and Sym signifies a symmetrisation of the graviton indices, i.e. $\mu \leftrightarrow \rho$, $\nu \leftrightarrow \lambda$, $\sigma \leftrightarrow \tau$. Further to this is a symmetrisation over graviton legs, indicated by P_3 and P_6 yielding three and six terms respectively. In comparison, the 3 gluon vertex presented in section 7.1.1 has only 6 terms. The two theories at this point look hopelessly different, with gravity looking painfully more complicated than Yang-Mills. However, much of the complexity of gravity arises from diffeomorphism invariance, suggesting some degree of redundancy in the Feynman rules. Under on-shell conditions for the external legs,

$$\epsilon^{\mu\rho} = \epsilon^{\rho\mu}, \quad p_\mu \epsilon^{\mu\rho} = 0, \quad p_\rho \epsilon^{\mu\rho} = 0, \quad \eta^{\mu\nu} \epsilon_{\mu\nu} = 0, \quad (7.43)$$

the three-graviton vertex reduces dramatically:

$$\begin{aligned}
 G_{\mu\rho,\nu\lambda,\sigma\tau}(p_1, p_2, p_3) = & -i\frac{\kappa}{2} \left[(p_1 - p_2)_\sigma \eta_{\mu\nu} + (p_2 - p_3)_\mu \eta_{\nu\sigma} + (p_3 - p_1)_\nu \eta_{\sigma\mu} \right] \\
 & \times \left[(p_1 - p_2)_\tau \eta_{\rho\lambda} + (p_2 - p_3)_\rho \eta_{\lambda\tau} + (p_3 - p_1)_\lambda \eta_{\tau\rho} \right]. \quad (7.44)
 \end{aligned}$$

The three-graviton vertex factor starts to resemble a striking ‘‘double copy’’ or square of the Yang-Mills cubic vertex factor. The drama heightens when we contract this vertex with graviton polarisations, and compare the expression to the gauge theory analogue. Contracting the graviton vertex (7.44) with polarisation vectors yields

$$\begin{aligned}
 \epsilon_1^{\mu\rho} \epsilon_2^{\nu\lambda} \epsilon_3^{\sigma\tau} G_{\mu\rho,\nu\lambda,\sigma\tau}(p_1, p_2, p_3) = \\
 -i\frac{\kappa}{2} [(\epsilon_1 \cdot \epsilon_2) \epsilon_3 \cdot (p_1 - p_2) + (\epsilon_2 \cdot \epsilon_3) \epsilon_1 \cdot (p_2 - p_3) + (\epsilon_3 \cdot \epsilon_1) \epsilon_2 \cdot (p_3 - p_1)]^2. \quad (7.45)
 \end{aligned}$$

Compare this expression with the cubic gluon vertex (7.14) contracted with three polarisation vectors

$$\begin{aligned}
 g f^{abc} \epsilon_1^\mu \epsilon_2^\nu \epsilon_3^\rho [g_{\mu\nu} (p_1 - p_2)_\rho + g_{\nu\rho} (p_2 - p_3)_\mu + g_{\rho\mu} (p_3 - p_1)_\nu] = \\
 g f^{abc} [(\epsilon_1 \cdot \epsilon_2) \epsilon_3 \cdot (p_1 - p_2) + (\epsilon_2 \cdot \epsilon_3) \epsilon_1 \cdot (p_2 - p_3) + (\epsilon_3 \cdot \epsilon_1) \epsilon_2 \cdot (p_3 - p_1)]. \quad (7.46)
 \end{aligned}$$

This hints that gravity may be simpler than we thought - possibly “Yang-Mills squared”. We just need to find the hidden symmetries or structures to reveal this relationship. BCJ duality is one such avenue.

7.3 Colour-kinematics duality

In section 7.2, we caught the hint of a “double copy” structure between the three-graviton vertex factor and the Yang-Mills cubic vertex factor. However, unlike gravity, the vertices and amplitudes of Yang-Mills theory are laced with colour structure. At first glance, this difference may look like an obstacle to constructing a map between the two theories. On the contrary, we will see in this section that colour factors will offer us a bridge via colour-kinematics duality, otherwise known as *BCJ* duality [72, 74] named after the founders Bern, Carrasco, and Johansson.

The foundation stone of BCJ duality rests on the Jacobi identity (7.25) we encountered in Yang-Mills theory. BCJ duality conjectures that it is possible to *choose* a representation of kinematic numerators that obeys the Jacobi identity in the same way that colour factors do, i.e.

$$c_i + c_j - c_k = 0 \implies n_i + n_j - n_k = 0. \quad (7.47)$$

This choice comes about by the freedom afforded by *generalised gauge transformations*. It is always possible to deform the kinematic numerators of (7.30) by shifts, i.e.

$$n_i \rightarrow n_i + \Delta_i, \quad (7.48)$$

where the shifts Δ_i are arbitrary functions independent of colour, satisfying the constraint

$$\sum_{i \in \Gamma} \frac{\Delta_i c_i}{\prod_{\alpha_i} p_{\alpha_i}^2} = 0. \quad (7.49)$$

We can see that under this type of transformation, the newly transformed kinematic factors n_i do not change the overall amplitude.

When the kinematic factors n_i are in a representation that obeys the Jacobi identity, we refer to them as *BCJ numerators*. Returning to the four-point example, we note that the kinematic factors are already in such a representation, i.e. the kinematic numerators (7.26), (7.27), (7.28) satisfy

$$n_s - n_t + n_u = 0. \quad (7.50)$$

Generally, at higher points, it is not as easy to find BCJ numerators! BCJ duality has been proven at tree level, and conjectured at loop level [72, 74]. However, it should be noted that there is a string of successes of finding BCJ numerators, as evidenced by just a few of many examples:

- BCJ numerators in one-loop amplitudes under certain helicity conditions in self-dual Yang-Mills [84];
- BCJ numerator extraction from one-loop ambitwistor-string correlators [85];
- Colour-kinematics duality for pure Yang-Mills and gravity at one and two loops [86], as well as for $N = 4$ supergravity at four loops [87].

The notion of colour-kinematics duality essentially places kinematic factors and colour on the same footing, paving the way for their interchangeability.

7.4 BCJ double copy

In this section, we describe how the amplitudes of Yang-Mills theory and perturbative gravity relate to each other through the double copy. The foundation of the double copy has been laid by two actions:

1. We have organised our Yang-Mills amplitude as a sum of trivalent diagrams, where kinematic factors are separate from colour factors (as per (7.29) and (7.30)).
2. We have chosen BCJ numerators, i.e. a kinematic representation that obeys the Jacobi identity, putting colour and kinematic factors on the same footing.

These two actions enable us to replace the colour factors c_i of the Yang-Mills amplitude with a set of BCJ kinematic numerators \tilde{n}_i from a second gauge-theory amplitude,

$$c_i \rightarrow \tilde{n}_i. \tag{7.51}$$

Note that these numerators *can* come from a second gauge theory amplitude, but they do not have to. They can also come from the same amplitude, and in that case, $\tilde{n}_i = n_i$.

If we also map the Yang-Mills coupling constant g to the gravitational coupling $\frac{\kappa}{2}$, then, remarkably, the resulting quantity corresponds to a gravitational amplitude [73, 75]¹¹

$$\mathcal{A}_m^{(L)} \xrightarrow{c_i \rightarrow \tilde{n}_i, g \rightarrow \frac{\kappa}{2}} \mathcal{M}_m^{(L)} = i^{L-1} \left(\frac{\kappa}{2}\right)^{m-2+2L} \sum_{i \in \Gamma} \int \prod_{l=1}^L \frac{d^D k_l}{(2\pi)^D} \frac{1}{S_i} \frac{n_i \tilde{n}_i}{\prod_{\alpha_i} p_{\alpha_i}^2}. \tag{7.52}$$

¹¹Note that the double copy of a pure Yang-Mills gauge theory will also generate a dilaton and an axion in addition to a graviton, unless polarisation vectors are chosen to be traceless and symmetric.

The “square” or “double copy” of kinematic factors in the numerator lends the name to the theory. Note that the diagrams specified by the propagators in the denominator are identical in the gravitational amplitude to those of Yang-Mills. There is no hyperbole in describing this result as anything short of astonishing, not only because it is an elegant idea, but crucially because it has been shown to work for a variety of well-understood amplitudes. One such example is the four-point scattering we have been working with throughout this chapter.

Returning back to our Yang-Mills four-point scattering, we can perform the double copy procedure immediately as we had already established that the kinematic factors are BCJ numerators. The resulting amplitude does indeed correspond to four gravitons scattering (see e.g. [76] for a pedagogical treatment),

$$M_4^{\text{tree}} = \left(\frac{\kappa}{2}\right)^2 \times \left(\frac{n_s^2}{s} + \frac{n_t^2}{t} + \frac{n_u^2}{u}\right). \quad (7.53)$$

Beyond four points, there is growing body of evidence supporting this theory, notably:

- The prefactors of the two-loop five-point $\mathcal{N} = 4$ super Yang-Mills amplitude double copy to $\mathcal{N} = 8$ supergravity [88];
- Entangled states of gluons scattering exactly like gravitons double copy at the level of the wave function [89];
- The conservative potential of a compact binary system (e.g. two-body Hamiltonian for spinless black holes) is calculated using the double copy [90];
- At tree level, the double copy encodes the KLT relations, an early precursor relating closed and open strings [70, 71];
- CHY formalism utilises the scattering equations to express field theory amplitudes as integrals, where the theory specific integrands have a manifestly double copy form. This further enables a greater generalization of the double copy to include theories beyond super Yang-Mills and supergravity, such as the non-linear sigma model (NLSM) [91–93].

It should be noted that the inverse action of replacing one set of kinematic factors in a gravitational amplitude with a set of colour factors leads to a Yang-Mills amplitude. This mapping leaves behind one single copy of kinematic factors in the numerator, and so it is aptly named *the single copy*. Figure 16 illustrates the mappings of the double copy, including an additional theory which the double copy gives us for free, *biadjoint scalar theory*.

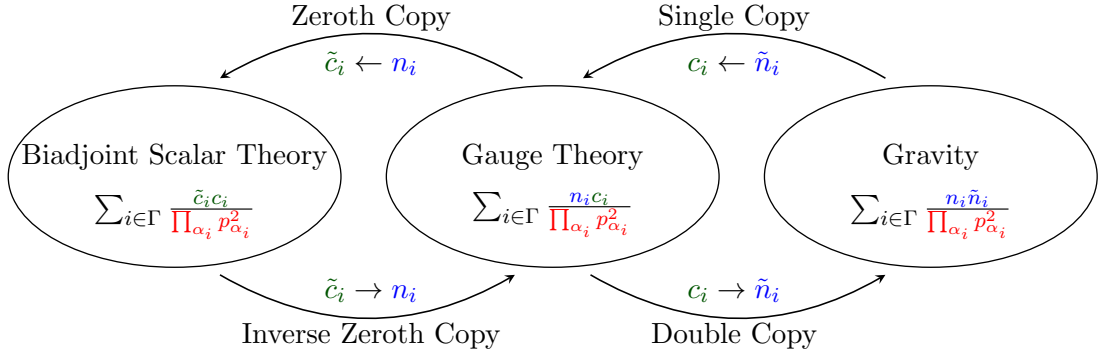


Figure 16: The double copy mappings for perturbative amplitudes

7.4.1 Biadjoint scalar theory

We have focussed on the double copy map between gauge theory and gravity, where colour in a gauge theory amplitude is replaced by kinematic factors. Likewise, the single copy replaces one set of kinematic factors in a gravity amplitude with colour. One could take this idea a step further, and perform a *zeroth copy* by replacing the kinematic factors of a gauge theory amplitude with a second set of colour factors, i.e.

$$n_i \rightarrow \tilde{c}_i. \quad (7.54)$$

These colour factors \tilde{c}_i do not need to stem from the same symmetry group as the colour factors c_i of the resident gauge group. Under the map 7.54, the gauge theory amplitude transforms into a biadjoint scalar theory amplitude [94–97]:

$$\mathcal{A}_m^{(L)} \xrightarrow{n_i \rightarrow \tilde{c}_i, g \rightarrow \lambda} \mathcal{T}_m^{(L)} = i^L \lambda^{m-2+2L} \sum_{i \in \Gamma} \int \prod_{l=1}^L \frac{d^D k_l}{(2\pi)^D} \frac{1}{S_i} \frac{c_i \tilde{c}_i}{\prod_{\alpha_i} p_{\alpha_i}^2}. \quad (7.55)$$

where λ is the coupling constant of the biadjoint scalar theory. This amplitude corresponds to a massless scalar field theory with Lagrangian

$$\mathcal{L}_{\text{BS}} = \frac{1}{2} \partial^\mu \Phi^{a\dot{a}} \partial_\mu \Phi^{a\dot{a}} + \frac{\lambda}{3} f^{abc} \tilde{f}^{\dot{a}\dot{b}\dot{c}} \Phi^{a\dot{a}} \Phi^{b\dot{b}} \Phi^{c\dot{c}}. \quad (7.56)$$

The scalar fields $\Phi^{a\dot{a}}$ transform in the adjoint representation of two Lie algebras which may be (but do not have to be) distinct.

Although this theory does not purport to be a theory of nature, it is interesting that in performing the zeroth copy, the propagators (and therefore also the structure of the diagrams) are kept intact - i.e. they are the same in biadjoint scalar theory as those of gauge theory and gravity in the double copy framework. This makes biadjoint scalar

theory a potential building block for gauge and gravity theories, but with the bonus of simplicity thanks to it being a scalar theory.

7.5 Conclusion

In this chapter, we have described how the BCJ double copy utilises the conjecture of colour-kinematics duality to relate amplitudes of seemingly disparate theories, Yang-Mills theory and perturbative gravity. We walked through an example of the double copy in action for four-point scattering in Yang-Mills and four-graviton scattering. Furthermore, we complemented this view by peppering the chapter with examples of the many successes of the double copy in more involved calculations in perturbation theory. While the double copy renders the typically unwieldy gravity amplitudes much easier to calculate, it also suggests a profound connection between theories of nature.

In addition, the double copy serves up biadjoint scalar theory, the amplitudes of which preserve or inherit some crucial structure of the amplitudes of the parent gauge theory or gravity. Being a scalar theory, it has the advantage of relatively simpler calculations than those of gauge theory or gravity. Although biadjoint scalar theory is not itself a theory of nature, a study of this theory can be a shortcut to probing those that are.

The story presented so far is in the preserve of perturbation theory, and as such, limited to quantities that are inherently approximate. It is reasonable to pose the question of whether the double copy also operates at the arguably deeper level of relating exact or non-perturbative quantities. In this domain, it would also be interesting to understand what role biadjoint scalar theory has to play. These themes will be explored in the next chapter.

Chapter 8

The Classical Double Copy

In the previous chapter, we saw how the BCJ double copy relates Yang-Mills amplitudes to gravity amplitudes. This relationship operates within perturbation theory, and is therefore inherently approximate. To formulate a more complete and potentially deeper version of the double copy, one could ask whether a non-perturbative counterpart exists.

While the focal points of interest in quantum field theory are amplitudes, classical theories on the other hand involve solving the equations of motion. A branch of the classical double copy relates well known exact classical gauge theory solutions, e.g. the solutions of Maxwell's equations, to those that solve Einstein's field equations exactly, e.g. the Schwarzschild black hole [98]. Furthermore, biadjoint scalar theory also plays an important role in this framework by encoding the information associated with the classical propagator, much like the BCJ double copy where propagators stay intact in biadjoint scalar theory amplitudes.

An argument could be made that a subset of exact solutions may still fall under the remit of perturbation theory, in that they could be viewed as tree-level or truncated perturbative expressions. Typically, this class of exact solutions is associated with *weak coupling*, i.e. where the field carries a positive power of a small coupling parameter enabling a perturbative expansion. This is in contrast to *strong coupling*, where the field carries a negative power of the coupling preventing any meaningful expansion, thus falling under the umbrella of non-perturbative phenomena.

Although classical double copy literature so far is limited to weakly coupled phenomena, this body of work inspires confidence that the pursuit of a non-perturbative version is a worthwhile endeavour. Certainly, if it were not possible to construct a classical double copy of weakly coupled exact solutions, then it would cast doubt about whether effort spent within the comparatively more complicated arena of non-perturbative phenom-

ena such as monopoles, instantons, solitons etc. could be justified. It is our view that the classical double copy canon, while interesting in its own right, is a valuable stepping stone toward finding a truly non-perturbative duality.

Despite its relatively recent inception [98], there are many examples of the classical double copy in action - perhaps too many to list in entirety. For the sake of providing some idea of this collection, we can name a few. The double copy of exact solutions extends to the self-dual sector [99–101], dimensions other than the four spacetime dimensions [102, 103], and maps based on the Weyl tensor [104–106]. Much work has also been achieved in the growing sector of gravitational and classical radiation [107–112].

In this chapter, we will review the construction of a specific type of classical double copy, namely the *Kerr-Schild double copy*, along with a few examples. We will learn about its strengths and limitations, while keeping an eye on the zeroth copy. It is our intention to use biadjoint scalar theory as a platform from which we can explore potential non-perturbative double copy maps in subsequent chapters.

Our starting point for the Kerr-Schild double copy will be an explanation of what is meant by classical gauge and gravity theories, with a focus on weak versus strong coupling.

8.1 Classical gauge theory

In section 7.1, we were introduced to non-Abelian Yang-Mills theory given by the Lagrangian (7.12). We used this to calculate amplitudes - the objects of interest in the BCJ double copy. In the classical limit of this theory, rather than calculating amplitudes, we are interested in finding solutions to its equations of motion, which in a vacuum are given by

$$\partial^\mu F_{\mu\nu}^a + g f^{abc} A^{b\mu} F_{\mu\nu}^c = 0. \tag{8.1}$$

The definition of the colour indexed field strength tensor was given in (7.10).

The non-linear term in the equations of motion (8.1) could scupper any attempt to solve this second order differential equation *exactly* for A_ν^a . Typically, the next best strategy involves finding perturbative solutions (see e.g. [113]). This relies on the assumption that the solution could be expanded into a series in the coupling g (assumed to be small), i.e.

$$A_\nu^a = A_\nu^{(0)a} + g A_\nu^{(1)a} + g^2 A_\nu^{(2)a} + \dots \tag{8.2}$$

where the coefficients $A_\nu^{(i)a}$ are functions assumed to have no dependence on the coupling g . If we were to substitute this ansatz into the equations of motion (8.1) and choose the Lorenz gauge $\partial^\mu A_\mu^a = 0$, then we would have

$$\partial^2 A_\nu^{(0)a} + g \left(\partial^2 A_\nu^{(1)a} + 2f^{abc} A_\mu^{(0)b} \partial^\mu A_\nu^{(0)c} - f^{abc} A^{(0)b\mu} \partial_\nu A_\mu^{(0)c} \right) + \mathcal{O}(g^2) = 0. \quad (8.3)$$

This power series in g is sensible only if the coupling is weak. This is why we equate weak coupling with positive powers of the g .

We could solve (8.3) order by order. At the lowest order of the coupling, we have the following set of equations:

$$\partial^2 A_\nu^{(0)a} = 0. \quad (8.4)$$

These equations are reminiscent of Abelian Yang-Mills theory, such as the Maxwell equations in covariant form,

$$\partial^\mu F_{\mu\nu}^a = j_\nu^a. \quad (8.5)$$

If the source is point-like at the origin, and vacuum elsewhere, we have $j_\nu^a \sim \delta(\vec{x})$. In an Abelian theory, the field strength tensor linearises to

$$F_{\mu\nu}^a = \partial_\mu A_\nu^a - \partial_\nu A_\mu^a. \quad (8.6)$$

We will discuss how linearity is closely linked to ‘‘Abelianisation’’ of a theory later on in the context of the Kerr-Schild double copy.

The overarching theme here which will be threaded throughout this chapter is that the solution to the leading term in a perturbative expansion can also be an exact solution to the Abelian Yang-Mills equations. Such solutions contain positive powers of the coupling, and therefore are weakly coupled and under the umbrella of perturbation theory, irrespective of whether those solutions are exact or not. A well known example which we will often refer to is the field potential of a Coulomb-like point charge,

$$A_\nu^{(0)a} = \frac{g c^a}{4\pi r} (1, \vec{0}), \quad (8.7)$$

where c^a is some arbitrary vector of colour constants (i.e. the ‘‘charge’’), and r measures the distance from the origin where the charge is located. This is a static solution of (8.4), or equivalently a static vacuum solution of (8.5). It is evident that $A_\nu^{(0)a}$ contains a charge proportional to a positive power of the coupling g , which we have stated is the hallmark of weak coupling. Furthermore, our choice of solution contains colour charge indices that are not mixed with spatial indices. This kills off the non-linear contributions of (8.3) due to the antisymmetry of the structure constants f^{abc} . So, although the

Coulomb-like point charge solution given by (8.7) is an exact solution, it can also be viewed as a perturbative expansion terminating at the leading order. For this reason, we assert that even if a solution is exact, it may not be truly non-perturbative if it contains a positive power of the coupling.

On the other hand, a strongly coupled solution - i.e. a solution containing negative powers of the coupling, is certain to be non-perturbative. A well-known example is the Dirac monopole - the solution of the Abelian equations of motion constructed on the hypothetical¹² premise of a magnetic point charge. The gauge potential of the Dirac monopole can be expressed in spherical polar coordinates (t, r, θ, ϕ) as

$$A_{\mu}^{D^a} = \frac{\tilde{g}\tilde{e}^a}{4\pi} \frac{1 - \cos\theta}{r \sin\theta} (0, 0, 0, 1), \quad (8.8)$$

where the magnetic coupling \tilde{g} is bound by the quantisation condition

$$g\tilde{g} = \frac{n}{2} \quad (8.9)$$

for some integer n . It is this quantisation condition that ensures the coupling is strong. Although \tilde{g} appears as a positive power in (8.8), it can also be understood as a negative power of g . We will elaborate further on the Dirac monopole in our discussion of shockwaves in chapter 10.

To sum up, the points about classical gauge theory which play a role in the journey toward a non-perturbative double copy are

- The solutions of weakly coupled theories contain positive powers of the coupling, while strong coupling is associated with negative powers.
- Exact solutions to the Abelian equations of motion (e.g. Maxwell's equations) could be interpreted as the leading term of a perturbative series, and as such, are not necessarily non-perturbative.
- In Abelian theories, the field strength tensor is linear in the gauge field.

On our brief tour of classical gauge theory, we highlighted the ideas which will play a central role in evolving the story of the double copy. We now turn our attention to the double copy partner of classical gauge theory - general relativity.

¹²Magnetic monopoles are hypothetical, as far as we know.

8.2 General relativity

Recall the Einstein-Hilbert Lagrangian of section 7.2. The ensuing field equations associated with this Lagrangian are

$$R_{\mu\nu} - \frac{1}{2}g_{\mu\nu}R = 8\pi G_N T_{\mu\nu}. \quad (8.10)$$

where the energy-momentum tensor $T_{\mu\nu}$ describes the distribution of matter in spacetime, and can be thought of as a source of gravitational currents. The Ricci tensor $R_{\mu\nu}$ captures information about the local curvature of spacetime, while the Ricci scalar R informs of global curvature properties. Where curvature is non-trivial, these objects can be highly non-linear in the metric. Thus, even though the field equations appear deceptively simple in this compact form, make no mistake that these second order differential equations are notoriously difficult to solve. Enter Kerr-Schild.

8.2.1 Kerr-Schild metrics

Kerr-Schild metrics form a class of solutions of the Einstein equations. Originally proposed by Kerr and Schild for the purpose of expressing the contravariant components of the metric easily in terms of the covariant components in their 1965 paper [114], a good comprehensive introduction to Kerr-Schild metrics can be found in Stephani's textbook [115]. The general Kerr-Schild metric is defined as:

$$g_{\mu\nu} = \bar{g}_{\mu\nu} + \frac{\kappa^2}{2}\phi k_\mu k_\nu, \quad (8.11)$$

where ϕ is a scalar field, $\bar{g}_{\mu\nu}$ is the background spacetime metric, and the vectors k_μ are null with respect to both the whole and background metrics,

$$g^{\mu\nu}k_\mu k_\nu = 0 = \bar{g}^{\mu\nu}k_\mu k_\nu. \quad (8.12)$$

Further to this, the null vectors k_μ must obey the *geodesic condition*

$$k^\mu \bar{\nabla}_\mu k^\nu = 0, \quad (8.13)$$

where $\bar{\nabla}_\mu k^\nu$ indicates the covariant derivative of k with respect to the background metric, i.e.,

$$\bar{\nabla}_\mu k^\nu = \partial_\mu k^\nu + \bar{\Gamma}_{\mu\rho}^\nu k^\rho. \quad (8.14)$$

The “barred” Christoffel symbol is constructed strictly from the background metric,

$$\bar{\Gamma}_{\mu\rho}^\nu = \frac{1}{2}\bar{g}^{\nu\sigma}(\partial_\mu \bar{g}_{\rho\sigma} + \partial_\rho \bar{g}_{\mu\sigma} - \partial_\sigma \bar{g}_{\mu\rho}). \quad (8.15)$$

Generally, the act of raising and lowering indices on an arbitrary tensor is carried out by the entire metric $g_{\mu\nu}$, as opposed to just the background metric $\bar{g}_{\mu\nu}$. We can relate the Kerr-Schild metric to its perturbative counterpart of (7.36) by defining the graviton field as

$$h_{\mu\nu} \equiv \frac{\kappa}{2} \phi k_\mu k_\nu. \quad (8.16)$$

The inverse of the Kerr-Schild metric is the same as that of (7.37), however the null condition $k^\mu k_\mu = 0$ effectively truncates the series at the first order. The exact form of the inverse Kerr-Schild metric is then

$$g^{\mu\nu} = \bar{g}^{\mu\nu} - \kappa h^{\mu\nu} = \bar{g}^{\mu\nu} - \frac{\kappa^2}{2} \phi k^\mu k^\nu. \quad (8.17)$$

We will often refer to the special case where the background metric is flat, i.e. Minkowski, $\bar{g}_{\mu\nu} = \eta_{\mu\nu}$, rendering the full metric as

$$g_{\mu\nu} = \eta_{\mu\nu} + \frac{\kappa^2}{2} \phi k_\mu k_\nu. \quad (8.18)$$

One of the nice properties of *this* Kerr-Schild metric is that the Einstein field equations take on a linear form. In particular, the mixed index Ricci tensor is linear in the graviton field

$$R^\mu{}_\nu = \frac{\kappa^2}{4} [\partial^\mu \partial_\alpha (\phi k^\alpha k_\nu) + \partial_\nu \partial_\alpha (\phi k^\alpha k^\mu) - \partial^\alpha \partial_\alpha (\phi k^\mu k_\nu)]. \quad (8.19)$$

The Kerr-Schild metric, by its properties of linearising the field equations, has been instrumental in revealing the classical double copy.

8.3 The Kerr-Schild double copy

Now that we have outlined our classical gauge theory and general relativity, we will see how Kerr-Schild metrics illuminate a map between the theories.

Consider the graviton field $h_{\mu\nu}$ defined in (8.16), perturbing a flat background space-time as set out in the metric (8.18). We perform the single copy by removing one null vector k_μ , in conjunction with a change of coupling constant. The result is a new gauge field A^μ :

$$h_{\mu\nu} = \frac{\kappa}{2} \phi k_\mu k_\nu \longrightarrow A_\mu = g \phi k_\mu \quad (8.20)$$

Similar to the quantum field (7.4), we can deconstruct the classical gauge field A_μ into a product of colour indexed fields and generators

$$A_\mu = T^a A_\mu^a, \quad A_\mu^a = g c^a \phi k_\mu \quad (8.21)$$

where c^a is a colour vector, not to be confused with the colour factors c_i of (7.23). For example, in $SU(3)$, as there are $a = 8$ generators in the adjoint representation, c^a would be a column vector with 8 entries.

If we repeat the mapping once more, we arrive at the zeroth copy, i.e., the biadjoint scalar field

$$A_\mu^a = g c^a \phi k_\mu \longrightarrow \Phi^{a\dot{a}} = \lambda \tilde{c}^{\dot{a}} c^a \phi \quad (8.22)$$

which should satisfy the equations of motion associated with the biadjoint scalar field theory Lagrangian defined in (7.56), i.e.,

$$\partial_\mu \partial^\mu \Phi^{a\dot{a}} - \lambda f^{abc} \tilde{f}^{\dot{a}\dot{b}\dot{c}} \Phi^{b\dot{b}} \Phi^{c\dot{c}} = 0. \quad (8.23)$$

Note that the zeroth copy fixes the choice of ϕ thereby eliminating any potential ambiguity in defining ϕ and k_μ between the double and single copies. While this alone suggests that the zeroth copy is a necessary pillar of the double copy, we will also show how biadjoint scalar theory classically preserves information about propagators - much like the amplitudes story of the previous chapter. On the other hand, it is not immediately apparent how the inverse procedure, i.e. the inverse zeroth copy, could “fix” a particular k_μ vector as this mapping appears to be one-to-many. Recent literature on the double copy in twistor space shows how the Weyl double copy procedure can be derived, and explores what kind of information the scalar function contains, potentially shedding light on how to refine the inverse zeroth copy [116, 117].

The foundation stone of the version of the double copy presented in this section is the Kerr-Schild metric, and so we refer to this mapping as the *Kerr-Schild double copy*, illustrated in figure 17.

These fields must satisfy the equations of motion of their respective theories. We show how well this works by offering a few examples.

8.3.1 Black hole and point charge examples

While the double copy in general is often relayed by the slogan “gravity is Yang-Mills squared”, the Kerr-Schild double copy can be summed up by “black hole = charge²” [118]. Of the many examples of this relationship, we will discuss two cases. The first case involves arguably the simplest solutions in gravity and gauge theory - the Schwarzschild black hole and the Coulomb point charge. This will offer an intuitive example of the Kerr-Schild double copy while highlighting the relevance of biadjoint scalar theory in this framework. The second case of the Taub-NUT metric single

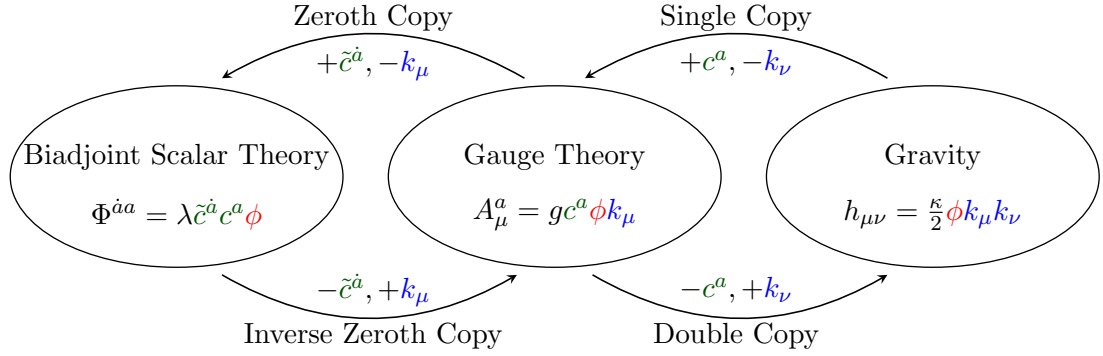


Figure 17: The double copy mappings for exact solutions

copying to dyons will lead us naturally to ponder life beyond weak-coupling and the conventional Kerr-Schild double copy - and whether biadjoint scalar theory can offer a probe therein.

Stationary solutions in general

The first written treatment of the Kerr-Schild double copy demonstrated how the double copy springs from stationary Kerr-Schild solutions [98]. Recall the mixed convention Ricci tensor of (8.19), and consider it under the following conditions:

1. stationarity - all time derivatives vanish,
2. all dynamics in the zeroth component of the metric are absorbed by ϕ , allowing us to set $k^0 = 1$.

Under such conditions, and using the mostly plus convention for the Minkowski metric $\eta^{\mu\nu} = \text{diag}(-, +, +, +)$, it is straightforward to reduce (8.19) to:

$$\begin{aligned}
 R^0_0 &= \frac{\kappa^2}{4} \nabla^2 \phi; \\
 R^i_0 &= \frac{\kappa^2}{4} \partial_j (\partial^i (\phi k^j) - \partial^j (\phi k^i)); \\
 R^i_j &= \frac{\kappa^2}{4} \partial_l (\partial^i (\phi k_j k^l) + \partial_j (\phi k^l k_i) - \partial^l (\phi k^i k_j)).
 \end{aligned} \tag{8.24}$$

In the special case of a vacuum spacetime, the Einstein field equations are

$$R^\mu_\nu = 0. \tag{8.25}$$

In light of (8.24), this implies the following relations must hold in a vacuum,

$$\nabla^2 \phi = 0; \quad \partial_j (\partial^i (\phi k^j) - \partial^j (\phi k^i)) = 0. \tag{8.26}$$

We are a step away from witnessing a double copy structure emerge from these expressions. Turning our attention to gauge theory, we construct a gauge field according to the single copy prescription (8.20), under the same stationarity conditions listed above:

$$A_\mu = g\phi k_\mu : \quad A_0 = g\phi, \quad A_i = g\phi k_i. \quad (8.27)$$

The corresponding field strength tensor $F_{\mu\nu}$ is then

$$F_{\mu\nu} = g(\partial_\mu(\phi k_\nu) - \partial_\nu(\phi k_\mu)), \quad (8.28)$$

with non-zero components being

$$F_{i0} = g\partial_i\phi; \quad F_{ij} = g(\partial_i(\phi k_j) - \partial_j(\phi k_i)). \quad (8.29)$$

The relations we found in (8.26) imply that the gauge field defined in (8.27) automatically fulfils the homogeneous Maxwell equations,

$$\partial_\mu F^{\mu\nu} = 0. \quad (8.30)$$

This theory may appear Abelian, but there is something more subtle at work here. The gauge field A_μ comprises colour factors and generators as per (8.21). The correct way to interpret A_μ is as an *Abelian-like* solution of a non-Abelian gauge theory. Pursuing this one step further, the zeroth copy defined by (8.22) inherits this Abelian-like property. In this case, the zeroth copy yields a stationary solution that satisfies the biadjoint scalar field equations (8.23) where the interaction term vanishes and the colour factors c^a, \tilde{c}^a are simply constant vectors. The biadjoint scalar field equations are then

$$\nabla^2\phi = 0. \quad (8.31)$$

A few points to note so far about the stationary solutions are

- The Kerr-Schild metric linearizes the Einstein field equations, and the single and zeroth copies inherit this linearity in that the gauge and biadjoint solutions are Abelian-like.
- It appears that the equations of motion themselves have a double copy-like structure, and that the nature of the source (i.e. vacuum) is reassuringly consistent between all three theories.
- The solution to the biadjoint scalar field equations is a Green's function,¹³ which can be interpreted as a scalar propagator. This is in line with the BCJ double

¹³The biadjoint scalar field is singular at the origin. This feature can be captured by adjusting the right-hand-side of (8.31) to be the Dirac delta function.

copy for amplitudes where the propagators are preserved in the biadjoint scalar theory.

These statements are true for any stationary solutions, such as the Schwarzschild black hole which we will explore now.

Schwarzschild black hole and the Coulomb point charge

The Schwarzschild black hole solves the vacuum Einstein equations where all spacetime can be described by a vacuum apart from one pointlike massive source. This can be captured by the energy-momentum tensor,

$$T^{\mu\nu} = M v^\mu v^\nu \delta^{(3)}(\vec{x}), \quad (8.32)$$

where M is the mass of the black hole and $v^\mu = (1, 0, 0, 0)$ is a timelike velocity vector. Note that the energy-momentum tensor has only one non-zero component T^{00} , which makes sense as the shear stress components T^{i0}, T^{ij} should vanish where the source is static.

The metric that solves the Einstein field equations for this type of source can be put in Kerr-Schild form [114],¹⁴

$$g_{\mu\nu} = \eta_{\mu\nu} + \frac{\kappa^2}{2} \phi k_\mu k_\nu = \eta_{\mu\nu} + \frac{2G_N M}{r} k_\mu k_\nu \quad (8.33)$$

where $\phi = \frac{M}{4\pi r}$, $k^\mu = (1, x^i/r)$ and we already are familiar with the gravitational constant (although here we use a slightly different convention to that of the previous chapter), $\kappa^2 = 16\pi G_N$.

Now we take the single copy of this solution [98], the details of which are captured in table 4. Among the usual prescription of dropping a k^μ vector, mapping couplings, etc. is the mapping of the gravitational mass M to a colour charge $c_a T^a$. Although there is the presence of colour, it must be trivial (i.e. c^a is a constant colour vector) as we are dealing with an intrinsically Abelian-like solution. The resulting gauge field is then

$$A^\mu = \frac{g c_a T^a}{4\pi r} (1, x^i/r) \equiv A_a^\mu T^a. \quad (8.34)$$

The Abelian-like gauge field A^μ has an immediately recognisable physical meaning in a particular gauge. Consider the gauge transformation

$$A_a^\mu \rightarrow A'^\mu = A_a^\mu + \partial^\mu \chi_a, \quad (8.35)$$

¹⁴See appendix G for details on how to transform the Schwarzschild solution in spherical polar coordinates to Kerr-Schild form.

	Gravity		Gauge Theory
Coupling Constant	$\frac{\kappa}{2}$	\longrightarrow	g
Charge	M	\longrightarrow	$c_a T^a$
Vectors	$k_\mu k_\nu$	\longrightarrow	k_μ
Scalar Field/Propagator	$\frac{1}{4\pi r}$	\longrightarrow	$\frac{1}{4\pi r}$

Table 4: Schwarzschild Black Hole parameters mapped to Coulomb point charge via the Single Copy

where the gauge is

$$\chi_a(x) = -g \frac{c_a}{4\pi} \log\left(\frac{r}{r_o}\right), \quad (8.36)$$

and r_o is some fixed radius. The transformed gauge field A'^μ becomes

$$A'^\mu = A'^\mu T^a = \left(g \frac{c_a T^a}{4\pi r}, \vec{0}\right). \quad (8.37)$$

This field can be understood as that associated with a static Coulomb colour charge located at the origin. It is the solution to the Maxwell field equations

$$\partial_\mu F^{\mu\nu} = j^\nu, \quad (8.38)$$

where the pointlike colour charge source is

$$j^\nu = -g c_a T^a v^\nu \delta^{(3)}(\vec{x}). \quad (8.39)$$

Comparing this with its gravity counterpart (8.32) could lead us to claim that the source terms appear to have a double copy-like structure. This should be viewed with caution as this example is awash with spherical symmetry. In less symmetrical examples, e.g. Kerr black hole where the source is disc-like, sources double copy only to some degree [98]. It may be more prudent instead to suggest there is consistency between the nature of the sources, i.e., they are both pointlike at the origin for the spherically symmetric cases of the Schwarzschild black hole and the Coulomb point charge (see also [119] on the double copy of sources).

Finally, we perform the zeroth copy which yields the biadjoint scalar field,

$$A_\mu^a = g c^a \phi k_\mu \longrightarrow \Phi^{a\dot{a}} = \lambda c^a \tilde{c}^{\dot{a}} \frac{1}{4\pi r}. \quad (8.40)$$

This is a Green's function as it solves the free biadjoint scalar field equations

$$\nabla^2 \Phi^{a\dot{a}} = \lambda c^a \tilde{c}^{\dot{a}} \delta^{(3)}(\vec{x}). \quad (8.41)$$

In this context, we can ascribe physical meaning to biadjoint scalar theory. The biadjoint equations of motion encapsulate how the scalar potential propagates through spacetime. This is in line with the BCJ double copy, where the amplitudes of biadjoint scalar theory contain the same propagators as those of gauge theory and gravity.

To conclude this example, we reiterate a crucial point introduced in section 8.1. Although the solutions presented in this section are exact, they could also be viewed as a perturbative expansion in the coupling that terminates at the first order. As such, these solutions are still not truly non-perturbative as they are Abelian-like, and lying in the realm of weakly coupled theories. In the next section, an element of strong coupling will present itself in the double copy of the Taub-NUT metric, however we will see that it will still be considered a perturbative map.

The Taub-NUT metric and dyons

The Taub-NUT metric is a stationary axisymmetric vacuum solution, characterised by two charges [120, 121]. Although we refer to it as a black hole, it maintains a rotational character that does not die off at infinity, and thus is not asymptotically flat (unlike the previous black hole solutions we have discussed). Of the two charges of the Taub-NUT metric, one is sourced by a pointlike mass M while the other is the so-called “NUT” charge N , named after Newman, Unti, and Tamburino. This combination of charges can be called a *gravitational dyon*. In the context of the double copy, the gravitational dyon described by the Taub-NUT metric maps to a *gauge theory dyon* consisting of an electric and a magnetic charge [122].

We will not enmesh ourselves in the calculations underpinning the Taub-NUT double copy as they are quite onerous and will not particularly add much clarity to the story of this thesis. We will instead offer a bird’s eye view sufficient enough to provide scaffolding for three main points:

1. The classical double copy of exact solutions can extend beyond the Kerr-Schild ansatz of (8.11).
2. It is possible to include strongly coupled phenomena in the double copy.
3. Although the Taub-NUT double copy may include some element of strong coupling, we can not yet claim to have found a non-perturbative double copy.

To address the first of these points, we note that in Plebanski coordinates, the Taub-NUT metric can be written in a manifestly *double Kerr-Schild* form [123],

$$g_{\mu\nu} = \bar{g}_{\mu\nu} + \kappa h_{\mu\nu} \tag{8.42}$$

where

$$h_{\mu\nu} = \frac{\kappa}{2} (M\phi k_\mu k_\nu + N\psi l_\mu l_\nu). \quad (8.43)$$

The vectors k_μ and l_μ are both null and obey the geodesic condition with respect to the background metric.

The single copy of this gravitational dyon is a gauge theory dyon,

$$A_\mu^a = c^a (g\phi k_\mu + \tilde{g}\psi l_\mu). \quad (8.44)$$

In performing the single copy, the mass and nut charges map to the electric and magnetic charges as follows,

$$M\frac{\kappa}{2} \longrightarrow c^a T^a g \quad N\frac{\kappa}{2} \longrightarrow \tilde{c}^a T^a \tilde{g}. \quad (8.45)$$

The authors of ref. [122] have verified that the gauge field (8.44) satisfies the Yang-Mills equations (which linearise).

Now we can discuss the topic of points 2 and 3 - strong coupling. The electric charge g and magnetic charge \tilde{g} are bound by the quantisation condition of (8.9). The NUT and mass charges too, are similarly bound, although the quantisation condition translates into a relation between the periodicity of the time coordinate and the NUT charge (see [124–126]). Although the inclusion of a magnetic charge does indicate the presence of strong coupling, the double copy relates dyons which are solutions composed of a weak charge and a strong charge, as opposed to monopoles which are strictly strongly coupled solutions. As we have established in section 8.1, a weakly coupled exact solution falls under the umbrella of perturbative phenomena, and so it is appropriate to classify the dyon-Taub-NUT double copy as a “perturbatively exact” relationship [122].

Last but not least, we conclude our brief Taub-NUT tour with a review of an important member of the double-copy family - the zeroth copy. The biadjoint scalar field under the zeroth copy prescription is

$$\Phi^{a\dot{a}} = c^a \tilde{c}^{\dot{a}} (\phi + \psi), \quad (8.46)$$

where the fields ϕ and ψ fulfil the linearised biadjoint equation independently of each other. They can be understood consistently with the other examples of biadjoint scalar theory so far - as scalar propagators over source charges that preserve propagator information for all the theories under the double copy. Some care must be exercised however when interpreting biadjoint scalar theory in this way where the background metric is not the Minkowski metric [127]. This will not impede our narrative as we will

not work with such metrics.

8.3.2 Beyond weak coupling and Abelian-like solutions

We have listed only a handful of examples of the classical double copy of exact solutions. However, even when taking into consideration the wider catalogue, we observe that the success of the double copy is so far limited on two fronts:

1. While we benefit from the linearity that the Kerr-Schild ansatz bestows on the Einstein field equations, its single copy appears to limit us to Abelian-like solutions. This is in contrast to the BCJ double copy narrative, where the non-Abelian nature of the gauge theory plays a central role.
2. So far, the double copy applies to weakly coupled solutions, and therefore can not be considered non-perturbative.

To break free of these bounds, we may need to leave Kerr-Schild behind. However, this makes solving the Einstein equations difficult and constructing/finding mappings between theories murky. If we are to take steps in this direction, it may be wise to begin with the “easiest” theory to solve - biadjoint scalar theory, and relate these solutions to strongly coupled gauge theory solutions such as monopoles.

But before embarking on the monopoles adventure, we should first tie up one last loose end regarding weak coupling. One may suggest that in an exact solution, there is freedom to set the coupling as one wishes - weak or strong. However, the classical double copy should have some link with the BCJ double copy, in which the couplings are already set to be small thereby removing this freedom. It may be prudent then to take a moment to anchor the Kerr-Schild double copy to the well-established BCJ double copy.

8.3.3 Comparison with the BCJ double copy

At this point, the Kerr-Schild double copy may seem to bear little resemblance to the BCJ double copy in the previous chapter. To provide some reassurance that this is not so, table 5 draws a comparison between the two dualities.

Some observations are in order to accompany this table. In both pictures,

- coupling constant mappings apply;
- moving downward from gravity to the other theories involves at each step removing a colour-free factor (e.g. kinematic n_i or null vector k_μ) and adding a colour factor, while moving upward is the inverse process of this;

	Amplitudes	Exact Solutions
Constraints	BCJ Numerators $n_i - n_j + n_k = 0$	Null Geodesic Vectors $k_\mu k^\mu = 0$; $k^\mu \bar{\nabla}_\mu k_\nu = 0$
<div style="text-align: center;"> Gravity \updownarrow Gauge Theory \updownarrow Biadjoint Scalar Theory </div>	$\sum_{i \in \Gamma} \frac{n_i \tilde{n}_i}{\prod_{\alpha_i} p_{\alpha_i}^2}$ \updownarrow $\sum_{i \in \Gamma} \frac{n_i c_i}{\prod_{\alpha_i} p_{\alpha_i}^2}$ \updownarrow $\sum_{i \in \Gamma} \frac{\tilde{c}_i c_i}{\prod_{\alpha_i} p_{\alpha_i}^2}$	$g_{\mu\nu} = \bar{g}_{\mu\nu} + \frac{\kappa^2}{2} \phi k_\mu k_\nu$ \updownarrow $A_\mu^a = g c^a \phi k_\mu$ \updownarrow $\Phi^{a\dot{a}} = \lambda c^a \tilde{c}^{\dot{a}} \phi$
Coupling Constant Mappings	$\lambda \longleftrightarrow g \longleftrightarrow \frac{\kappa}{2}$	$\lambda \longleftrightarrow g \longleftrightarrow \frac{\kappa}{2}$

Table 5: Double Copy: amplitudes vs exact solutions

- there are restrictions which must be obeyed (although admittedly, BCJ duality is not identical to the null and geodesic restrictions);
- the propagators remain unchanged and appear to be encoded in biadjoint scalar theory.

The null and geodesic restrictions apply specifically to Kerr-Schild metrics, and it must be said that not all space-times can be represented by this restrictive form. One can, however, make a sweeping statement about the broader classical double copy in general. The classical double copy can be seen as an off-shell generalization of the perturbative BCJ double copy. Since the gauge field A_μ is measured at a space-time point, the Feynman diagrams associated with this picture will include external legs that do not go off to space-time infinity.

Having bridged the classical and BCJ double copies, we can move on to hunt for the elusive non-perturbative double copy.

8.4 Conclusion

In pursuit of a non-perturbative double copy, we have reviewed how the double copy can be extended to include classical exact solutions via the Kerr-Schild metric, and we connected this back to the well-established BCJ double copy. Our review included two examples: 1) the map of the Schwarzschild black hole in general relativity to the

Coulomb point charge in classical gauge theory; 2) the Taub-NUT-dyon map to a gauge theory dyon. While the first example is the archetypal Kerr-Schild double copy, the second offers a glimpse beyond the conventional Kerr-Schild metric by the use of a double-Kerr-Schild metric. Throughout, the zeroth copy produces biadjoint scalar theory which plays a similar role to its BCJ double copy counterpart by encoding some information about the propagators of all the theories under the double copy umbrella.

Although the Kerr-Schild double copy has been fruitful, it has so far yielded maps limited to Abelian-like solutions of weakly coupled gauge theories. While these maps do connect exact solutions, we cannot yet claim we have found a non-perturbative double copy. Why not? A weakly coupled Abelian-like exact solution can also be interpreted as the first term of a perturbative expansion.

By our reasoning, a truly non-perturbative double copy is one that includes strongly coupled non-Abelian solutions. This is easier said than done. Kerr-Schild metrics linearise the Einstein field equations, and this linearity trickles its way down the single copy to effectively render Abelian-like solutions to the gauge theory. This means we may need to abandon Kerr-Schild metrics altogether in our quest.

Luckily, some groundwork toward this goal has already been achieved via (the relatively easier to solve) biadjoint scalar theory. The next chapter introduces us to a strongly coupled non-Abelian biadjoint exact solution, which we hope can equip us to springboard to other such solutions.

Chapter 9

The Biadjoint Monopole Zoo

The double copy of exact solutions presented so far has been limited to Abelian-like solutions of weakly coupled theories. As such, this duality may still fall under the umbrella of perturbation theory. A potential road toward a non-perturbative double copy could involve mapping strongly coupled gauge theory solutions to their gravitational counterparts. This is not an easy task, as such calculations can become unwieldy. This difficulty is further compounded by the lack of any precedent of a double copy prescription in this domain.

To overcome any hurdles posed by potentially onerous calculations, we can proceed instead by exploring strongly coupled exact solutions of the relatively easier biadjoint scalar theory. For the reader's ease, we write again the Lagrangian defining the theory here,

$$\mathcal{L} = \frac{1}{2} \partial^\mu \Phi^{a\dot{a}} \partial_\mu \Phi^{a\dot{a}} + \frac{\lambda}{3} f^{abc} \tilde{f}^{\dot{a}\dot{b}\dot{c}} \Phi^{a\dot{a}} \Phi^{b\dot{b}} \Phi^{c\dot{c}}. \quad (9.1)$$

This gives rise to equations of motion

$$\partial^\mu \partial_\mu \Phi^{a\dot{a}} - \lambda f^{abc} \tilde{f}^{\dot{a}\dot{b}\dot{c}} \Phi^{b\dot{b}} \Phi^{c\dot{c}} = 0. \quad (9.2)$$

Some groundwork toward solving these equations has already been paved by the spherically symmetric biadjoint monopole, as well as a solution under the common gauge group of SU(2) [128]. These solutions were then extended by the use of “form factors” [129]. The previous paper postulates a potential double copy relationship between the biadjoint monopole and the Wu-Yang monopole - but we will discuss in the next chapter why this is not so.

In this chapter, we will demonstrate that it is possible to find even more biadjoint monopoles, specifically those possessing cylindrical symmetry [1]. This choice of symmetry is partly motivated by our ultimate goal of forging a link to strongly coupled

gauge theory solutions - which tend to possess cylindrical symmetry [130]. However, as the study of biadjoint monopoles is still in its infancy, growing the zoo of such solutions is also a worthwhile task in its own right.

All of the non-perturbative solutions in this chapter are guided by the following restrictions:

- Non-perturbative solutions require that the two types of colour charge in biadjoint theory be inextricably linked, i.e., not separable functions;
- Assuming a common gauge group $f^{abc} = \tilde{f}^{abc}$ greatly simplifies the equations;
- As this is a relatively new arena, only static solutions are explored.

The last two items simplify our equations of motion,

$$\nabla^2 \Phi^{a\dot{a}} + \lambda f^{abc} f^{\dot{a}bc} \Phi^{b\dot{b}} \Phi^{c\dot{c}} = 0. \quad (9.3)$$

where we used the mostly minus convention for the Minkowski metric $\eta^{\mu\nu} = \text{diag}(+, -, -, -)$. We begin the tour of solutions to (9.3) by a brief review of the first known biadjoint monopoles - those involving spherical symmetry.

9.1 Biadjoint monopoles involving spherical symmetry

In this section, we briefly review three types of solution to the equations of motion under all of the restrictions mentioned above. The binding theme is that each one incorporates some element of spherical symmetry. We will not reproduce the supporting calculations, as they are similar to those underpinning the cylindrically symmetric solutions. Rather, we will offer a bird's eye view, highlighting key features for subsequent comparison.

i) Simple spherically symmetric solution [128]

The simplest possible spherically symmetric ansatz that can solve the equations (9.3) is

$$\Phi^{a\dot{a}} = \delta^{a\dot{a}} f(r) \quad (9.4)$$

where r is the radial coordinate. The equations (9.3) take on the form

$$\delta^{a\dot{a}} \nabla^2 f(r) + \lambda f^{abc} f^{\dot{a}bc} f^2(r) = 0. \quad (9.5)$$

The normalisation condition below makes short work of the non-linear term:

$$f^{abc} f^{\dot{a}bc} = \delta^{a\dot{a}} T_A, \quad (9.6)$$

where T_A is the normalisation constant. A power-law form for $f(r)$ solves the equations, i.e.,

$$f(r) = Kr^\alpha, \quad (9.7)$$

leading specifically to the solution

$$\Phi^{a\dot{a}} = \frac{-2\delta^{a\dot{a}}}{\lambda T_A r^2}. \quad (9.8)$$

This is a fully non-perturbative solution as it involves inverse powers of the coupling λ . Additionally, this field falls off rapidly as $r \rightarrow \infty$ and is singular at the origin $r = 0$ - much like a point-like monopole located at the origin. The profile of this monopole is further fleshed out by calculating the associated energy,

$$E = \frac{128\pi\mathcal{N}}{9\lambda^2 T_A^2 r_o^3}, \quad (9.9)$$

where \mathcal{N} is the dimension of the gauge group, and r_o is a short-distance radial cutoff imposed in order to present some type of closed form for the energy¹⁵. The energy is bounded at large distances, but divergent at small distances.

ii) SU(2) × SU(2) [128]

A further solution assumes a more involved ansatz than (9.4), while imposing a further condition that the common gauge group be SU(2) where $f^{abc} = \epsilon^{abc}$.¹⁶ This choice of gauge group allows for colour/space index mixing - a feature present in gauge theory monopoles. An ansatz incorporating this feature is

$$\Phi^{a\dot{a}} = A(r)\delta^{a\dot{a}} + B(r)x^a x^{\dot{a}} + C(r)\epsilon^{a\dot{a}d} x^d. \quad (9.10)$$

While the ansatz itself is not spherically symmetric, the coefficient functions A, B, C most certainly are, since they depend only on r . Fulfilling the equations of motion (9.3) reduces (9.10) to the following solution:

$$\Phi^{a\dot{a}} = \frac{1}{\lambda r^2} \left[-k \left(\delta^{a\dot{a}} - \frac{x^a x^{\dot{a}}}{r^2} \right) \pm \sqrt{2k - k^2} \frac{\epsilon^{a\dot{a}d} x^d}{r} \right], \quad (9.11)$$

¹⁵It is unavoidable to calculate infinite energy in such a scalar theory by Derrick's theorem [131].

¹⁶In principle, one could generalize this by considering Lie groups with embeddings of the subgroup SU(2). As far as we know, this has not yet been attempted for exact biadjoint solutions.

for $0 \leq k \leq 2$. This field has associated energy

$$E = \frac{16\pi k}{\lambda^2 r_o^3}. \quad (9.12)$$

Similar to the first example, (9.11) represents a point-like monopole located at the origin. The paper speculates that for the special value of $k = 2$, (9.11) could be rewritten to resemble a product of Wu-Yang monopoles where one traces over the space indices, i.e.,

$$\Phi^{a\dot{a}} = \frac{-2}{\lambda r^2} \epsilon^{abc} \epsilon^{\dot{a}bc} \frac{x^b x^{\dot{b}}}{r^2} \sim A_i^a A_i^{\dot{a}}, \quad (9.13)$$

where the Wu-Yang monopole could be written in a gauge in which

$$A_0^a = 0, \quad A_i^a = -\frac{\epsilon_{iak} x^k}{er^2}. \quad (9.14)$$

Note that this proposed prescription is a bit counter-intuitive in the context of the Kerr-Schild double copy procedure, i.e., it appears that a squaring of gauge theory results in biadjoint scalar theory rather than the usual vector-shedding procedure. Given that we are working outside the familiarity of the Kerr-Schild framework, we keep an open mind to this possibility. We will revisit this idea in the next chapter and discuss why this mapping turns out to be coincidental.

iii) Extended solutions [129]

In gauge theories there is an array of solutions in which a pure power-law divergence can be dressed with a non-trivial form factor, suggesting some internal structure [132]. Furthermore, such form factors can effectively screen divergent behaviour near singular regions of the field. This principle can also be applied to biadjoint monopoles. For example, the spherically symmetric ansatz of (9.4) can be dressed as follows

$$J(r) = 1 + r^2 \bar{f}(r), \quad (9.15)$$

where we rescale $f \equiv \frac{\bar{f}}{\lambda T_A}$. Dimensional analysis assures us that $J(r)$ is finite for all r . Now $f(r)$ must obey the equations of motion, and this constraint can be expressed as a differential equation in J :

$$r^2 \frac{\partial^2 J}{\partial r^2} - 2r \frac{\partial J}{\partial r} + J^2 - 1 = 0. \quad (9.16)$$

While this differential equation has no analytic solution, it can be solved numerically, and its asymptotic limits can be studied analytically. In the problematic region where there is a divergence, we can say a few words about the effect of the screening. In the

asymptotic limit $r \rightarrow 0$, the field can be approximated using

$$\bar{f}(r) \simeq \frac{c}{r}, \tag{9.17}$$

for a dimensionful constant c . The divergence near the origin is indeed softer than that of the undressed solution (9.8) which was $\sim r^{-2}$. The same can be said of the energy close to the origin. Using (9.17), the leading divergent term in the energy is

$$E \simeq \frac{\mathcal{N}}{\lambda^2 T_A^2} \frac{2\pi c^2}{r_o}. \tag{9.18}$$

In comparison with the undressed field's energy (9.9), close to the origin, the divergence is softened by the screening. The $SU(2) \times SU(2)$ solution can likewise be screened with similar softening effects.

To sum up, we have reviewed the first exact solutions to the non-Abelian biadjoint theory involving inverse powers of the coupling, implying that we have moved away from perturbation theory to the non-perturbative arena as we had desired. As for the goal of finding a non-perturbative double copy, ref. [128] does speculate on a tenuous link to monopoles in gauge theory. However, some monopoles in gauge theory are characteristic of cylindrical symmetry [130] while the biadjoint solutions presented in [128, 129] involve some element of spherical symmetry. Intent on bridging the monopoles of gauge theory and biadjoint theory, we turn now toward cylindrically symmetric biadjoint monopoles.

9.2 Biadjoint monopoles involving cylindrical symmetry

In this section, we consider exact solutions possessing cylindrical symmetry, as per reference [1]. The analysis parallels section 9.1. First, we consider a very simple static cylindrically symmetric solution to (9.3), under an unspecified common gauge group G . Secondly, we explore solutions where the common gauge group specifically is $SU(2)$ with the aim to incorporate colour/space index mixing as we see in gauge theory monopoles. Thirdly, we will dress our solutions with form factors screening the divergence close to the charge.

9.2.1 Solutions with a common gauge group

The simplest cylindrically symmetric ansatz we could write down is

$$\Phi^{a\dot{a}} = \delta^{a\dot{a}} f(\rho), \tag{9.19}$$

where the cylindrical radius is

$$\rho^2 = -x^i x_i. \quad (9.20)$$

We will use indices $i, j, k \dots \in (1, 2)$ distinct from indices $a, b, c \in (1, 2, 3)$. Throughout the remainder of this chapter we will use cylindrical coordinates (ρ, z, ϕ) . We will continue to use the normalisation condition (9.6).

Recall that the Laplacian in cylindrical polar coordinates is

$$\nabla^2 f = \frac{1}{\rho} \frac{\partial}{\partial \rho} \left(\rho \frac{\partial f}{\partial \rho} \right). \quad (9.21)$$

Plugging our static ansatz (9.19) into our equations of motion (9.3), we find

$$\delta^{a\dot{a}} \left(\frac{1}{\rho} \frac{\partial}{\partial \rho} \left(\rho \frac{\partial f}{\partial \rho} \right) + \lambda T_A f^2(\rho) \right) = 0. \quad (9.22)$$

To solve this differential equation, we try a power-law solution

$$f(\rho) = A\rho^\alpha, \quad (9.23)$$

which works for the values

$$A = \frac{-4}{\lambda T_A}, \quad \alpha = -2, \quad (9.24)$$

yielding the biadjoint solution

$$\Phi^{a\dot{a}} = \frac{-4\delta^{a\dot{a}}}{\lambda T_A \rho^2}. \quad (9.25)$$

This solution has much in common with the spherically symmetric solution of (9.8), namely:

- It has an inverse power of the coupling λ and thus is nonperturbative.
- It goes like the inverse square of the cylindrical radius ρ (r in the spherical case), which could also be deduced by conducting dimensional analysis on the Lagrangian of (9.1). More specifically, in d -dimensions, the biadjoint scalar field must have mass dimensions of $d/2 - 1$ while the coupling constant λ has mass dimensions $3 - d/2$.
- Like the spherically symmetric case, this solution has a singularity. However, where it was point-like for (9.8), the singularity here corresponds to a line defect in the field localised on the z -axis, i.e. $\rho \rightarrow 0$, which we will refer to as the “wire”.

We can offer a more concrete view of this solution and its singularity by calculating its energy, as was done for the spherically symmetric solution. The Hamiltonian density

associated with (9.1) under a common gauge group is given by

$$\mathcal{H} = \frac{1}{2} [\partial_t \Phi^{a\dot{a}} \partial_t \Phi^{a\dot{a}} + \nabla \Phi^{a\dot{a}} \cdot \nabla \Phi^{a\dot{a}}] - \frac{\lambda}{3} f^{abc} f^{\dot{a}\dot{b}\dot{c}} \Phi^{a\dot{a}} \Phi^{b\dot{b}} \Phi^{c\dot{c}}. \quad (9.26)$$

For an ansatz of the form (9.19), this is

$$\mathcal{H} = \frac{\mathcal{N}}{\lambda^2 T_A^2} \left[\frac{1}{2} \left(\frac{\partial \bar{f}(\rho)}{\partial \rho} \right)^2 - \frac{1}{3} \bar{f}^3(\rho) \right]. \quad (9.27)$$

We have rescaled $f(\rho) \equiv \frac{\bar{f}(\rho)}{\lambda T_A}$. Further, we invoked the normalisation condition (9.6), as well as the chain rule

$$\partial_i \bar{f}(\rho) = \partial_i \rho \times \frac{\partial \bar{f}}{\partial \rho} = \frac{-x_i}{\rho} \frac{\partial \bar{f}}{\partial \rho}. \quad (9.28)$$

The Hamiltonian density is then

$$\mathcal{H} = \frac{160\mathcal{N}}{3\lambda^2 T_A^2 \rho^6}. \quad (9.29)$$

To find the energy, we integrate the Hamiltonian density over space, i.e.,

$$E = \int d^3x \mathcal{H}. \quad (9.30)$$

As we are working with an expression in terms of the cylindrical radius, it makes sense to carry out the integral in cylindrical polar coordinates as per

$$\int_{-\infty}^{\infty} d^3x = \int_0^{2\pi} d\phi \int_{-\infty}^{\infty} dz \int_0^{\infty} d\rho \rho. \quad (9.31)$$

Before charging ahead, some integration bounds need to be adjusted to avoid calculating an infinite quantity that will mask the energy's distinguishing features. Firstly, integration over all of the z -axis, will incur an infinite energy, and so instead we will calculate a “unit energy” per length L of the z -axis. Secondly, the inevitable singularity around $\rho \rightarrow 0$ can be regulated by a cutoff ρ_o , comparable to r_o in the spherically symmetric energy (9.9). With these changes,

$$E = \frac{160\mathcal{N}}{3\lambda^2 T_A^2} \int_0^{2\pi} d\phi \int_0^L dz \int_{\rho_o}^{\infty} d\rho \rho^{-5}, \quad (9.32)$$

resulting in the energy per unit length

$$\frac{E}{L} = \frac{80\pi\mathcal{N}}{3\lambda^2 T_A^2 \rho_o^4}. \quad (9.33)$$

Like the spherically symmetric energy, the energy associated with the cylindrically symmetric solution falls off rapidly with distance from the wire.

9.2.2 Solutions for $SU(2) \times SU(2)$

We now consider biadjoint scalar theory, where the common gauge group is $SU(2)$ with structure constants $f^{abc} = \epsilon^{abc}$, defined by the Lagrangian:

$$\mathcal{L} = \frac{1}{2} \partial^\mu \Phi^{a\dot{a}} \partial_\mu \Phi^{a\dot{a}} + \frac{\lambda}{3} \epsilon^{abc} \epsilon^{\dot{a}\dot{b}\dot{c}} \Phi^{a\dot{a}} \Phi^{b\dot{b}} \Phi^{c\dot{c}}. \quad (9.34)$$

As mentioned prior in the example involving spherical symmetry, the $SU(2)$ group allows for gauge/space index mixing in four spacetime dimensions - a common feature of gauge theory monopoles. Another common feature of Yang-Mills solutions is cylindrical symmetry [130], which motivates an ansatz similar (but not identical) to the spherically symmetric $SU(2)$ ansatz. Consider the ansatz

$$\Phi^{33} = f_1(\rho), \quad \Phi^{ij} = f_2(\rho) \delta^{ij} + f_3(\rho) x^i x^j + f_4(\rho) \epsilon^{ij3}, \quad \Phi^{i3} = \Phi^{3i} = 0. \quad (9.35)$$

We have chosen the z direction in space (and equivalently the “3” direction in gauge space) about which we would like to impose cylindrical symmetry. Constraining the ansatz by the equations of motion of (9.3) results in differential equations in f_n , which we will show step by step. Beginning with Φ^{33} , we have

$$\partial_i \partial^i f_1(\rho) + \lambda \epsilon^{3bc} \epsilon^{3\dot{b}\dot{c}} \Phi^{b\dot{b}} \Phi^{c\dot{c}} = 0. \quad (9.36)$$

The first term is the Laplacian of a function of ρ , for which we can use the identity (9.21). As for the non-linear term, we only need to sum over non-zero terms, effectively restricting the dummy indices to $(1, 2)$, represented in this chapter by $i, j, k \dots$ etc. In this spirit, we rewrite the non-linear term as

$$\lambda \epsilon^{3ij} \epsilon^{3kl} \Phi^{ik} \Phi^{jl} = \lambda (\Phi^{ii} \Phi^{jj} - \Phi^{ij} \Phi^{ji}), \quad (9.37)$$

where we have used the identity for one contracted index in a product of Levi-Civita tensors:

$$\epsilon^{abc} \epsilon^{ade} = \delta^{bd} \delta^{ce} - \delta^{be} \delta^{cd}. \quad (9.38)$$

Given the form of the ansatz of (9.35), we have

$$\Phi^{ii} \Phi^{jj} = (f_2(\rho) \delta^{ii} + f_3(\rho) x^i x^i)^2 = (2f_2 + \rho^2 f_3)^2 = 4f_2^2 + 4\rho^2 f_2 f_3 + \rho^4 f_3^2. \quad (9.39)$$

where we de-clutter the notation of $f_k(\rho)$ to f_k . Similarly, we have

$$\begin{aligned}\Phi^{ij}\Phi^{ji} &= (f_2\delta^{ij} + f_3x^ix^j + f_4\epsilon^{ij3})(f_2\delta^{ij} + f_3x^ix^j - f_4\epsilon^{ij3}) \\ &= 2f_2^2 + 2\rho^2f_2f_3 + \rho^4f_3^2 - 2f_4^2,\end{aligned}\tag{9.40}$$

where we have used the identity for two contracted indices¹⁷ in a product of Levi-Civita tensors:

$$\epsilon^{abc}\epsilon^{abd} = 2\delta^{cd}.\tag{9.41}$$

Altogether, our equation of motion for Φ^{33} (9.36) becomes the differential equation:

$$\frac{1}{\rho}\frac{\partial f_1}{\partial\rho} + \frac{\partial^2 f_1}{\partial\rho^2} + 2\lambda(f_2^2 + \rho^2f_2f_3 + f_4^2) = 0.\tag{9.42}$$

Moving on to the equations of motion for Φ^{ij} , we have

$$\partial_k\partial^k\Phi^{ij} + \lambda\epsilon^{ibc}\epsilon^{jbc}\Phi^{bb}\Phi^{cc} = 0.\tag{9.43}$$

We tackle the first term of (9.43):

$$\begin{aligned}\partial_k\partial^k\Phi^{ij} &= \partial_k\partial^k(f_2\delta^{ij} + f_3x^ix^j + f_4\epsilon^{ij3}) \\ &= \delta^{ij}\left(\frac{1}{\rho}\frac{\partial f_2}{\partial\rho} + \frac{\partial^2 f_2}{\partial\rho^2} + 2f_3\right) + \epsilon^{ij3}\left(\frac{1}{\rho}\frac{\partial f_4}{\partial\rho} + \frac{\partial^2 f_4}{\partial\rho^2}\right) \\ &\quad + x^ix^j\left(\frac{5}{\rho}\frac{\partial f_3}{\partial\rho} + \frac{\partial^2 f_3}{\partial\rho^2}\right).\end{aligned}\tag{9.44}$$

As we did earlier, we need only sum over the non-zero terms of the non-linear term of (9.43). This simplifies to

$$\lambda\epsilon^{ibc}\epsilon^{jbc}\Phi^{bb}\Phi^{cc} = 2\lambda\epsilon^{ik3}\epsilon^{jl3}\Phi^{kl}\Phi^{33}.\tag{9.45}$$

Using our ansatz (9.35) as well as the Levi-Civita identity for one repeated index (9.38), the term (9.45) straightforwardly becomes

$$2\lambda\epsilon^{ik3}\epsilon^{jl3}\Phi^{kl}\Phi^{33} = 2\lambda f_1(\delta^{ij}(f_2 + \rho^2f_3) - x^ix^jf_3 + \epsilon^{ij3}f_4).\tag{9.46}$$

Altogether, the equation of motion for Φ^{ij} (9.43) can be written as the differential equation

$$\delta^{ij}\left(\frac{1}{\rho}\frac{\partial f_2}{\partial\rho} + \frac{\partial^2 f_2}{\partial\rho^2} + 2f_3 + 2\lambda f_1(f_2 + \rho^2f_3)\right)$$

¹⁷It would be tempting to use the identity for three contracted indices $\epsilon^{abc}\epsilon^{abc} = 6$, however, caution must be taken as we should not treat the index 3 as a dummy index to sum over in $\epsilon^{ij3}\epsilon^{ij3}$.

$$\begin{aligned}
 & +\epsilon^{ij3} \left(\frac{1}{\rho} \frac{\partial f_4}{\partial \rho} + \frac{\partial^2 f_4}{\partial \rho^2} + 2\lambda f_1 f_4 \right) \\
 & +x^i x^j \left(\frac{5}{\rho} \frac{\partial f_3}{\partial \rho} + \frac{\partial^2 f_3}{\partial \rho^2} - 2\lambda f_1 f_3 \right) = 0.
 \end{aligned} \tag{9.47}$$

Furthermore, linear independence of each line of (9.47) implies that we actually have four differential equations in total to solve (including (9.42)):

$$\frac{1}{\rho} \frac{\partial \bar{f}_1}{\partial \rho} + \frac{\partial^2 \bar{f}_1}{\partial \rho^2} + 2(\bar{f}_2^2 + \rho^2 \bar{f}_2 \bar{f}_3 + \bar{f}_4^2) = 0; \tag{9.48}$$

$$\frac{1}{\rho} \frac{\partial \bar{f}_2}{\partial \rho} + \frac{\partial^2 \bar{f}_2}{\partial \rho^2} + 2\bar{f}_3 + 2\bar{f}_1(\bar{f}_2 + \rho^2 \bar{f}_3) = 0; \tag{9.49}$$

$$\frac{1}{\rho} \frac{\partial \bar{f}_4}{\partial \rho} + \frac{\partial^2 \bar{f}_4}{\partial \rho^2} + 2\bar{f}_1 \bar{f}_4 = 0; \tag{9.50}$$

$$\frac{5}{\rho} \frac{\partial \bar{f}_3}{\partial \rho} + \frac{\partial^2 \bar{f}_3}{\partial \rho^2} - 2\bar{f}_1 \bar{f}_3 = 0. \tag{9.51}$$

In the above four equations, we have rescaled all of our functions $f_n \equiv \frac{1}{\lambda} \bar{f}_n$. To solve these equations, we assume a power law ansatz

$$\bar{f}_n = k_n \rho^{\alpha_n}. \tag{9.52}$$

On the grounds of preserving dimensionality in each of the equations (9.48)-(9.51), we can deduce that the exponents α_n are

$$\alpha_1 = \alpha_2 = \alpha_4 = -2, \quad \alpha_3 = -4. \tag{9.53}$$

Plugging this back into (9.48)-(9.51) leaves us with a set of equations in k_n :

$$2k_1 + k_2^2 + k_2 k_3 + k_4^2 = 0; \tag{9.54}$$

$$2k_2 + k_3 + k_1(k_2 + k_3) = 0; \tag{9.55}$$

$$(2 + k_1)k_4 = 0; \tag{9.56}$$

$$k_1 k_3 = 0. \tag{9.57}$$

The last equation (9.57) tells us that either $k_1 = 0$ or $k_3 = 0$. The former leads to a trivial solution, which is not particularly interesting. On the other hand, the latter leads to the general solution

$$k_1 = -2; \quad k_2 \equiv -2k; \quad k_3 = 0; \quad k_4 = \pm 2\sqrt{1 - k^2}. \tag{9.58}$$

Putting everything together, we finally have the biadjoint solution

$$\Phi^{33} = -\frac{2}{\lambda\rho^2}, \quad \Phi^{ij} = -\frac{2}{\lambda\rho^2} \left[k\delta^{ij} \mp \sqrt{1-k^2}\epsilon^{ij3} \right]. \quad (9.59)$$

The presence of the parameter k indicates that we have a continuously infinite family of solutions. The special case of $k = 1$ corresponds to our previous solution (9.25), where we invoke $T_A = 2$ for $SU(2)$. Dependence on a free parameter was also a feature of the spherically symmetric solutions of the common gauge group $SU(2)$ first presented in [128], and reviewed in section 9.1.

In keeping with the other biadjoint solutions presented in this chapter, we can calculate the energy associated with the solution (9.59), or more precisely, the energy per unit length of the z -axis. The Hamiltonian density is given by

$$\mathcal{H} = \frac{40}{\lambda^2\rho^6}. \quad (9.60)$$

Integration results in an energy per unit length,

$$\frac{E}{L} = \frac{20\pi}{\lambda^2\rho_o^4}. \quad (9.61)$$

A sense check confirms that this quantity agrees with the energy found in (9.33) for the $SU(2)$ specific values of $\mathcal{N} = 3$ and $T_A = 2$. The energy per unit length has no dependence on the parameter k , suggesting that each member of the family of solutions has identical energy associated with it. This curiosity is clarified if we re-write our solution as a matrix Φ with components $\Phi^{a\dot{a}}$, under a new parametrisation $k \equiv \cos\theta$:

$$\Phi = -\frac{2}{\lambda\rho^2} \begin{pmatrix} \cos\theta & \mp\sin\theta & 0 \\ \pm\sin\theta & \cos\theta & 0 \\ 0 & 0 & 1 \end{pmatrix}. \quad (9.62)$$

This matrix represents a rotation about the 3-axis in gauge space by the gauge parameter θ . We can further transform this field by rotation to remove the θ dependence. There is no harm in doing so, as the Lagrangian of (9.34) is invariant under such transformations. To see this explicitly, we can rewrite the Lagrangian in matrix notation. First we recall the determinant of the matrix Φ is by definition

$$\det[\Phi] = \frac{1}{3!}\epsilon^{abc}\epsilon^{\dot{a}\dot{b}\dot{c}}\Phi^{a\dot{a}}\Phi^{b\dot{b}}\Phi^{c\dot{c}}, \quad (9.63)$$

which allows us to rewrite (9.34) as

$$\mathcal{L} = \frac{1}{2} \text{Tr}[(\partial^\mu \Phi)^T (\partial_\mu \Phi)] + 2\lambda \det[\Phi]. \quad (9.64)$$

The Lagrangian written in this way is manifestly invariant under transformations of the type $\Phi \rightarrow \mathbf{R}_1^T \Phi \mathbf{R}_2$, for arbitrary rotation matrices \mathbf{R}_i . For the particular case where \mathbf{R}_1 is the identity matrix and \mathbf{R}_2 is a rotation in gauge space of an angle $-\theta$ about the 3-axis, i.e.,

$$\mathbf{R}_2 = \begin{pmatrix} \cos \theta & \pm \sin \theta & 0 \\ \mp \sin \theta & \cos \theta & 0 \\ 0 & 0 & 1 \end{pmatrix}, \quad (9.65)$$

our transformed field can be written simply as

$$\Phi = -\frac{2}{\lambda \rho^2} \begin{pmatrix} 1 & 0 & 0 \\ 0 & 1 & 0 \\ 0 & 0 & 1 \end{pmatrix}. \quad (9.66)$$

This solution brings us back home to our original solution of no specified gauge group (9.25). It clearly exhibits two properties: i) cylindrical symmetry as it is only dependent on ρ , and ii) strong coupling via the inverse power of λ . One would hope that these two properties could bring us closer to the elusive non-perturbative double copy. Although it is not clear how or if this biadjoint solution could map to a Yang-Mills solution under a double copy prescription, it is a positive step to build up the catalogue of strongly coupled exact biadjoint solutions. One could extend this solution further by the use of “form factors”.

9.2.3 Extended solutions

In this section, we will grow the catalogue of biadjoint monopole solutions by partially screening the divergence associated with the cylindrically symmetric biadjoint monopole of (9.25).

We begin by returning to the ansatz of (9.19), and define:

$$J(\rho) = 2 + \rho^2 \bar{f}(\rho). \quad (9.67)$$

Dimensional analysis fixes $\bar{f}(\rho) \sim \rho^{-2}$, assuring us that $J(\rho)$ is finite for all ρ . Under the constraint of (9.22), we have the following differential equation in $J(\rho)$:

$$\rho^2 \frac{\partial^2 J(\rho)}{\partial \rho^2} - 3\rho \frac{\partial J(\rho)}{\partial \rho} + J^2(\rho) - 4 = 0. \quad (9.68)$$

This has a cleaner form in the coordinate ξ where

$$\tilde{\rho} = e^{-\xi}, \quad (9.69)$$

and $\tilde{\rho}$ is a dimensionless variable such that the dimensionality of ρ is captured by a dimensionful quantity $\hat{\rho}$, i.e.

$$\rho = \tilde{\rho}\hat{\rho}. \quad (9.70)$$

In the ξ coordinate system, (9.68) takes the form

$$\frac{\partial^2 J(\xi)}{\partial \xi^2} + 4 \frac{\partial J(\xi)}{\partial \xi} + J^2(\xi) - 4 = 0. \quad (9.71)$$

Unfortunately, there is no analytic solution to this equation, which can be related to an Abel equation of the second kind. Our strategy then is to look for numerical solutions instead, supplemented by performing any analytical analysis wherever we can - e.g., for some critical points and asymptotic limits. This endeavour begins by defining

$$\psi \equiv \frac{dJ}{d\xi}, \quad (9.72)$$

which enables us to rewrite (9.71) as a set of coupled first order equations,

$$\left(\frac{dJ}{d\xi}, \frac{d\psi}{d\xi} \right) = (\psi, 4 - 4\psi - J^2). \quad (9.73)$$

This defines a vector field in the (J, ψ) plane, illustrated in figure 18. At each point in the plot, there is a directed curve capturing the information given by the tangent to the solution. We can observe several critical points in this plot

$$\left(\frac{dJ}{d\xi}, \frac{d\psi}{d\xi} \right) = (0, 0). \quad (9.74)$$

This occurs precisely at $(J, \psi) = (\pm 2, 0)$, as indicated in the plot. At these points, we can say a few words about what our solution looks like:

1. $J = +2$: $J = 2 + \rho^2 \bar{f} \rightarrow \bar{f} = 0 \rightarrow \phi^{a\dot{a}} = 0$, which is the trivial solution.
2. $J = -2$: $J = 2 + \rho^2 \bar{f} \rightarrow \bar{f} = \frac{-4}{\rho^2} \rightarrow \phi^{a\dot{a}} = \frac{-4\delta^{a\dot{a}}}{\lambda T_A}$, which corresponds to our original cylindrically symmetric solution (9.25).

We can also observe what happens as J approaches these critical points, holding all else fixed, i.e., we hold $\frac{\partial \psi}{\partial \xi} = 0$ but let J vary. By (9.73), this corresponds to a bounded curve given by the parabola

$$\psi_o = \frac{1}{4}(4 - J^2). \quad (9.75)$$

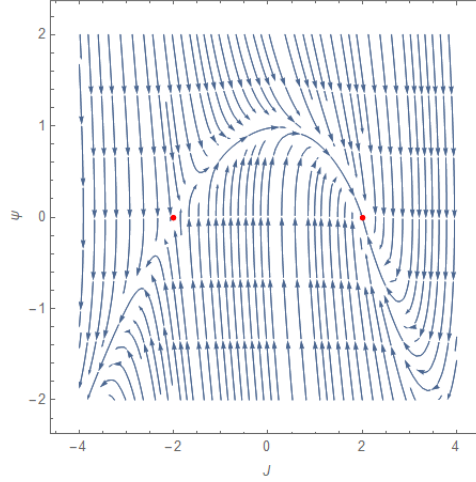


Figure 18: Integral curves of the vector field defined by (9.73), with critical points in red.

In the plot, we can see how this parabola acts as the dividing curve separating downward from upward arrows. Between the points $(J, \psi) = (-2, 0)$ and $(J, \psi) = (+2, 0)$, this parabola, i.e. ψ_o is consistently positive. Since $\psi = \frac{\partial J}{\partial \xi}$, we can deduce that in this region, J increases with ξ . This allows us to conclude

1. $J \rightarrow +2$ as $\xi \rightarrow \infty$, or equivalently by (9.69), $\rho \rightarrow 0$,
2. $J \rightarrow -2$ as $\xi \rightarrow -\infty$, or equivalently $\rho \rightarrow \infty$.

We understand J at exactly the critical points, and we have observed some behaviour close to those points. However, we can go a little further than this and analytically examine the behaviour of J in the asymptotic limits.

First we consider the case where $J \rightarrow -2$, i.e. $\xi \rightarrow -\infty$. Consider the ansatz

$$J(\xi) = -2 + \chi_-(\xi), \quad (9.76)$$

where we take $\chi_-(\xi)$ to be very small in comparison with $J(\xi)$ in the limit $\xi \rightarrow -\infty$. We plug this ansatz into our differential equation (9.71),

$$\frac{\partial^2 \chi_-(\xi)}{\partial \xi^2} + 4 \frac{\partial \chi_-(\xi)}{\partial \xi} - 4 \chi_-(\xi) = 0, \quad (9.77)$$

where we disregard any quadratic terms in $\chi_-(\xi)$. The full solution is

$$\chi_-(\xi) = c_1 e^{(-2+2\sqrt{2})\xi} + \tilde{c}_1 e^{(-2-2\sqrt{2})\xi}. \quad (9.78)$$

The second term however, blows up in the limit $\xi \rightarrow -\infty$. As such, the boundary condition requires $\tilde{c}_1 = 0$.

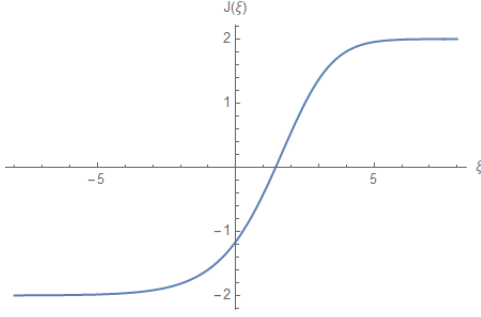


Figure 19: Numerical solution to (9.73) using a built-in Mathematica solver, with boundary conditions set by (9.82).

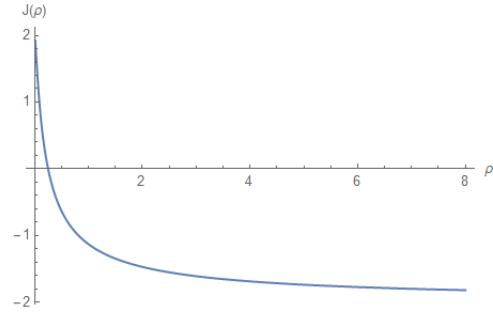


Figure 20: Numerical solution in terms of ρ .

Similarly, we can also explore the other asymptotic limit $\xi \rightarrow \infty$ or $J(\xi) \rightarrow 2$. Here we begin with a similar ansatz:

$$J(\xi) = 2 + \chi_+(\xi), \quad (9.79)$$

where the function $\chi_+(\xi)$ is small in the limit $\xi \rightarrow \infty$. Plugging this ansatz into the differential equation (9.71) gives us (disregarding quadratic terms in χ_+),

$$\frac{\partial^2 \chi_+(\xi)}{\partial \xi^2} + 4 \frac{\partial \chi_+(\xi)}{\partial \xi} + 4 \chi_+(\xi) = 0, \quad (9.80)$$

which has the solution

$$\chi_+(\xi) = c_2 e^{-2\xi} + c_3 \xi e^{-2\xi}. \quad (9.81)$$

Altogether, we have some approximate analytic solutions in the asymptotic limits

$$J(\xi) \simeq \begin{cases} -2 + c_1 e^{(-2+2\sqrt{2})\xi}, & \xi \rightarrow -\infty \\ +2 + c_2 e^{-2\xi} + c_3 \xi e^{-2\xi}, & \xi \rightarrow +\infty. \end{cases} \quad (9.82)$$

The full numerical solution is captured by plot 19, where boundary conditions have been set by the lower ξ limit, taking $c_1 = 1$. For completeness, we can also transform the extended solution of (9.82) back into terms of ρ :

$$J(\tilde{\rho}) \simeq \begin{cases} -2 + c_1 \tilde{\rho}^{-2+2\sqrt{2}}, & \rho \rightarrow \infty \\ +2 + \tilde{\rho}^2 (c_2 - c_3 \ln \tilde{\rho}), & \rho \rightarrow 0 \end{cases} \quad (9.83)$$

The numerical solution in terms of ρ is captured by plot 20. Now we can scrutinise how well the screening has worked. By reinstating the dimensions, the field in the

asymptotic limit $\rho \rightarrow 0$ is approximately

$$\Phi^{a\dot{a}} \simeq \frac{\delta^{a\dot{a}}}{\lambda T_A} \frac{1}{\hat{\rho}^2} \left[c_2 - c_3 \ln \left(\frac{\rho}{\hat{\rho}} \right) \right], \quad (9.84)$$

which is indeed less divergent than the unscreened solution given by (9.25). We can explore how the screening affects the energy in the region where there was a divergence - i.e., close to the wire. We will feed the approximation for the field in the limit $\rho \rightarrow 0$ given by (9.84) into the Hamiltonian density given by (9.27). We note that

$$\bar{f} = \frac{c_2}{\hat{\rho}^2} - \frac{c_3}{\hat{\rho}^2} \ln \left(\frac{\rho}{\hat{\rho}} \right). \quad (9.85)$$

The first term of the Hamiltonian density (stripped of the dressing factor) is then

$$\frac{1}{2} \left(\frac{\partial \bar{f}(\rho)}{\partial \rho} \right)^2 = \frac{c_3^2}{2\hat{\rho}^4} \frac{1}{\rho^2} \quad (9.86)$$

We are interested in the most divergent terms close to the wire. The non-linear term in the Hamiltonian density will be comparatively less divergent, thus we disregard it. As we are dealing with an approximation in the asymptotic limit, it is safe to claim that it is valid up to some cutoff $\rho = \Lambda$. As such, the energy can be calculated up to that point,

$$\frac{E}{L} \simeq \frac{2\pi\mathcal{N}}{\lambda^2 T_A^2} \int_{\rho_o}^{\Lambda} d\rho \rho \frac{1}{2} \left(\frac{\partial \bar{f}(\rho)}{\partial \rho} \right)^2 = \frac{\pi\mathcal{N}c_3^2}{\lambda^2 T_A^2} \frac{1}{\hat{\rho}^4} \ln \left(\frac{\Lambda}{\rho_o} \right). \quad (9.87)$$

Similar to the spherically symmetric example, this divergence is softer than the unscreened counterpart of (9.33), which has a divergence $\sim \rho_o^4$. Note that we could choose to absorb the factors of $\hat{\rho}$ into our constant c_3 , rendering c_3 dimensionful.

9.3 Conclusion

In this chapter, we populated the zoo of strongly coupled biadjoint solutions with those of cylindrical symmetry. We did so by piggybacking off the prototypical solutions - i.e., those with an element of spherical symmetry, which we also briefly reviewed and contrasted with the newer cylindrically symmetric monopoles. While the former resembled point-like monopole charges, the latter monopoles were more “wire-like”. The exercise of finding new solutions was carried out primarily in service of finding a non-perturbative double copy, which we believe necessarily involves strongly coupled solutions.

Although it is a nice addition to the catalogue of solutions, it is not clear how the

biadjoint wire could bring us any closer to a non-perturbative double copy. In this spirit, we abandon it, and return to a possible lead in ref. [128]. The paper suggests a map between a strongly coupled $SU(2)$ biadjoint solution (based on some element of spherical symmetry), and the Wu-Yang monopole. We will see in the next chapter why this is not the case, as the Wu-Yang monopole has a different role to play in the classical double copy.

Chapter 10

Making Shockwaves - the Ultraboost

We ended the previous chapter with a suitcase full of strongly coupled solutions in biadjoint theory, but without a map to any gauge theory counterparts. A double copy between strongly coupled solutions constitutes a non-perturbative double copy, which is our ultimate goal.

A speculation in [128] suggests some similarity between the strongly coupled biadjoint monopole and the Wu-Yang monopole. In this chapter, we explore this claim (as per [2]), and subsequently rule it out on account of several pieces of evidence:

1. We know that shockwaves double copy [98, 133]. We can test the strength of the potential relationship between the biadjoint and gauge theory monopoles by *ultra-boosting* (i.e. applying an infinite boost to) both to see if the ensuing shockwaves match up. Not only do they not match up, but it does not even appear possible to produce a meaningful shockwave by ultraboosting the biadjoint monopole.
2. This mismatch becomes clear when we take into account the relationship between the Wu-Yang monopole and the Dirac monopole, which we had previously overlooked. The latter is already related to the linear biadjoint solution of the Taub-NUT double copy [122]. So the Wu-Yang monopole does have a place in the Kerr-Schild double copy after all, but it is not related to the strongly coupled biadjoint monopole.

Although we still do not have a map between the biadjoint monopole and a gauge theory monopole, we do see novelty in producing shockwaves via the ultraboost procedure performed in Kerr-Schild coordinates, as well as shine a light on the interplay of Abelian-like and non-Abelian solutions in the Kerr-Schild double copy. This brings the

Kerr-Schild double copy closer in line with the BCJ double copy, where the non-Abelian nature of the gauge theory plays a leading role via BCJ duality [72–75].

We begin this chapter by laying out the steps for the ultraboost procedure, starting with the linear solutions of the Kerr-Schild double copy.

10.1 Ultraboosting the linear solutions

Shockwave solutions of field theories can be constructed by a procedure known as *the ultraboost*, first shown by Aichelburg and Sexl for a gravitational mass [134], and subsequently also successfully applied to a static electric charge [135], as well as other black hole solutions [136]. The ultraboost involves infinitely boosting a field in a particular direction, and may also involve charge or mass rescaling.

It has already been established that shockwaves double copy, shown extensively at the level of amplitude [133], and briefly touched on for exact solutions to classical theories [98]. In this section, we revisit the latter, but we will furnish the results with much more detail. More specifically, the linear Abelian solutions reviewed in section 8.3.1 will be ultraboosted to produce shockwave solutions. By recasting the ultraboost procedure explicitly in Kerr-Schild coordinates, it is possible to see how the double copy structure is manifest at various stages. Furthermore, we gain confidence in the ultraboost procedure itself before breaking new ground by ultraboosting a strongly coupled biadjoint monopole (coming up in section 10.2).

10.1.1 Linear solutions of the double copy

For the reader’s benefit, we briefly repeat here the linear Abelian-like solutions of the Kerr-Schild double copy (reviewed in more detail in section 8.3.1 and originally proposed in [98]). The example we will focus on is the Schwarzschild black hole, in Kerr-Schild form, this time where the Minkowski metric has signature $(+, -, -, -)$:¹⁸

$$g_{\mu\nu} = \eta_{\mu\nu} - \frac{\kappa^2}{2} \phi k_\mu k_\nu, \quad (10.1)$$

with

$$\phi = \frac{M}{4\pi r}, \quad k_\mu = (1, x/r, y/r, z/r). \quad (10.2)$$

¹⁸To see how the minus sign comes about in the Kerr-Schild representation, see Appendix G for details.

This single copies to a Coulomb-like point charge,

$$A_\mu^a = \frac{gc^a}{4\pi r} k_\mu, \quad (10.3)$$

and the zeroth copy is then

$$\Phi^{a\dot{a}} = \frac{\lambda c^a \tilde{c}^{\dot{a}}}{4\pi r}. \quad (10.4)$$

We will perform the ultraboost procedure on these solutions, starting with the simplest of the theories - the biadjoint scalar theory.

10.1.2 Abelian-like biadjoint scalar theory

Consider an inertial frame S' with Cartesian coordinates (t', x', y', z') moving with boost parameter v in the $+x$ direction with respect to a second frame S whose coordinates are (t, x, y, z) . The two sets of coordinates are related by the Lorentz transformation

$$x'^\mu = \Lambda^\mu{}_\nu x^\nu, \quad (10.5)$$

where the boost in the $+x$ direction takes the form of a matrix

$$\Lambda = \begin{bmatrix} \gamma & -\gamma v & 0 & 0 \\ -\gamma v & \gamma & 0 & 0 \\ 0 & 0 & 1 & 0 \\ 0 & 0 & 0 & 1 \end{bmatrix}, \quad (10.6)$$

and $\gamma = (1 - v^2)^{-1/2}$. Applying this boost to the biadjoint scalar field (10.4) is tantamount to boosting the underlying coordinates, i.e.,

$$\Phi^{a\dot{a}}(x') = \frac{\lambda c^a \tilde{c}^{\dot{a}}}{\gamma 4\pi R}, \quad (10.7)$$

where

$$R = \sqrt{(x - vt)^2 + \gamma^{-2}(y^2 + z^2)}. \quad (10.8)$$

We have boosted our biadjoint scalar field, but we would like to go further than this. Ultraboosting is akin to an infinite boost,¹⁹ i.e., $v \rightarrow 1$ or equivalently, $\gamma \rightarrow \infty$. If we were to naively take the limit of (10.7), we would find a vanishing field rather than a shockwave, which is typically characterised by the presence of a delta function in the *lightfront plane*, $x - t = 0$, i.e.,

$$\Phi_{\text{shockwave}} \sim \delta(x - t). \quad (10.9)$$

¹⁹An infinite boost entails travel at the speed of light c , where $c = 1$ in natural units.

In order to achieve this, it is necessary to rescale the charge in order to absorb any troublesome factors of γ which threaten the creation of this delta function. For the biadjoint scalar solution, it will become apparent that the following charge rescaling is required,

$$c^a \tilde{c}^{\dot{a}} \rightarrow c^a \tilde{c}^{\dot{a}} \gamma. \quad (10.10)$$

In fact, this charge rescaling is consistent with that required for a sensible ultraboosted source term. Recall that the point source is

$$p^{a\dot{a}} = c^a \tilde{c}^{\dot{a}} \delta^{(3)}(\vec{x}). \quad (10.11)$$

When boosted, the source then takes the form

$$p^{a\dot{a}} = c^a \tilde{c}^{\dot{a}} \gamma^{-1} \delta(x - vt) \delta(y) \delta(z). \quad (10.12)$$

In the ultraboost limit, it would be difficult to make sense of such a source term without rescaling the charge as per (10.10). Proceeding then with the rescaling, the boosted biadjoint field is now

$$\Phi^{a\dot{a}} = \frac{\lambda c^a \tilde{c}^{\dot{a}}}{4\pi R}. \quad (10.13)$$

In the limit $v \rightarrow 1$, the boosted field (10.13) behaves quite differently inside and outside the lightfront plane $x - t = 0$:

$$\lim_{v \rightarrow 1} \frac{1}{R} = \begin{cases} \frac{1}{|x-t|} & x - t \neq 0 \\ \infty & x - t = 0. \end{cases} \quad (10.14)$$

Some of this behaviour is reminiscent of a delta function, i.e., infinite in the lightfront plane. However, outside the plane the field is finite, as opposed to vanishing completely. We can remedy this by regularizing the field. Consider then the field redefinition:

$$\Phi^{a\dot{a}} \rightarrow \tilde{\Phi}^{a\dot{a}} = \frac{\lambda c^a \tilde{c}^{\dot{a}}}{4\pi} \left(\frac{1}{R} - \frac{1}{R_o} \right) \quad (10.15)$$

where $R_o = \sqrt{(x-t)^2 + \gamma^{-2} \rho_o^2}$ for some cylindrical radius cutoff ρ_o . This field satisfies the same equations of motion as $\Phi \sim 1/R$, and so this field redefinition belongs to the same family of solutions to the equations of motion. The proof is straightforward. Recall from section 8.3.1 that the linearized equations of motion for biadjoint scalar theory are²⁰

$$\square \Phi^{a\dot{a}} = \lambda c^a \tilde{c}^{\dot{a}} \delta^{(3)}(\vec{x}). \quad (10.16)$$

²⁰Note that the equations of motion quoted in section 8.3.1 correspond to the static case, where the d'Alembertian reduces to the Laplacian operator.

Stripping out charges and couplings, the d'Alembertian applied to the new chunk of the redefined field is

$$\square \frac{1}{R_o} = (\partial_t^2 - \partial_x^2) \frac{1}{R_o} = (\partial_t - \partial_x)(\partial_t + \partial_x) \frac{1}{R_o}. \quad (10.17)$$

Now, recall that R_o is essentially a function of $x - t$ only. If we were to switch to lightfront coordinates

$$u = x - t; \quad w = x + t, \quad (10.18)$$

then we could claim $\frac{1}{R_o} = f(u)$. Essentially this means that we can rewrite (10.17) as:

$$(\partial_t - \partial_x)(\partial_t + \partial_x) \frac{1}{R_o} = \partial_u \partial_w f(u) = 0. \quad (10.19)$$

And so we see that our redefined field still fulfils the same equations of motion as the original field, and therefore we can proceed with such a redefinition secure in the fact that we are still operating in the same theory. Returning to taking the ultraboost limit of our redefined field (10.15), we observe the following equality,

$$\frac{\partial}{\partial x} \ln \left[x - t + ((x - t)^2 + \gamma^{-2} \rho_o^2)^{1/2} \right] = \frac{1}{R_o}. \quad (10.20)$$

This allows us to rewrite our field as

$$\tilde{\Phi}^{a\dot{a}} = \frac{\lambda c^a \tilde{c}^{\dot{a}}}{4\pi} \partial_x \ln \left[\frac{x - vt + ((x - vt)^2 + \gamma^{-2} \rho^2)^{1/2}}{x - t + ((x - t)^2 + \gamma^{-2} \rho_o^2)^{1/2}} \right] \quad (10.21)$$

where we employ the cylindrical radius notation $\rho = \sqrt{y^2 + z^2}$. We can simplify (10.21) by a truncated Taylor expansion along the lines of $(1 + \alpha)^{1/2} \sim 1 + (1/2)\alpha$, i.e.,

$$((x - vt)^2 + \gamma^{-2} \rho^2)^{1/2} \approx |x - vt| + \frac{\gamma^{-2}}{2} \frac{\rho^2}{|x - vt|}. \quad (10.22)$$

Note that we are able to do this in the ultraboost limit, where the quantity $\gamma^{-2} / |x - vt|$ is small outside the lightfront plane. This simplification leads to

$$\tilde{\Phi}^{a\dot{a}} = \frac{\lambda c^a \tilde{c}^{\dot{a}}}{4\pi} \partial_x \ln \left[\frac{x - vt + |x - vt| + \frac{\gamma^{-2}}{2} \frac{\rho^2}{|x - vt|}}{x - t + |x - t| + \frac{\gamma^{-2}}{2} \frac{\rho_o^2}{|x - t|}} \right], \quad (10.23)$$

which allows us to easily take the ultraboost limit, again where the lightfront plane is a dividing line between two regions,

$$\lim_{v \rightarrow 1} \tilde{\Phi}^{a\dot{a}} = \frac{\lambda c^a \tilde{c}^{\dot{a}}}{4\pi} \partial_x \begin{cases} 0 & x - t > 0 \\ \ln \left(\frac{\rho^2}{\rho_o^2} \right) & x - t < 0. \end{cases} \quad (10.24)$$

Now we can rewrite this in terms of the Heaviside function,

$$\theta(x-t) = \begin{cases} 1 & x-t > 0 \\ 0 & x-t < 0 \end{cases} \quad (10.25)$$

and therefore our field in the ultraboost limit is,

$$\lim_{v \rightarrow 1} \tilde{\Phi}^{a\dot{a}} = \frac{\lambda c^a \tilde{c}^{\dot{a}}}{4\pi} \partial_x \left[(1 - \theta(x-t)) \ln \left(\frac{\rho^2}{\rho_0^2} \right) \right]. \quad (10.26)$$

Finally, we apply the derivative in (10.26) to arrive at

$$\Phi_{\text{sw}}^{a\dot{a}} = \lim_{v \rightarrow 1} \tilde{\Phi}^{a\dot{a}} = \frac{-\lambda c^a \tilde{c}^{\dot{a}}}{4\pi} \ln \left(\frac{\rho^2}{\rho_0^2} \right) \delta(x-t). \quad (10.27)$$

This is of course a shockwave solution to the biadjoint scalar field equations in full agreement with the solution presented in [98]. Inside the lightfront plane, the field is infinite, in contrast to all areas outside the plane where the field vanishes. The construction of this solution rests on the rescaling of the charge as per (10.10). We can have assurance of the shockwave nature of this solution by observing its effect on interacting particles. A particle interacting with a shockwave should receive a kick in the lightfront plane, in a direction transverse to the shockwave's direction of travel.

Biadjoint Impulse

The impulse of a test particle of mass m and charge $c_2^a \tilde{c}_2^{\dot{a}}$ interacting with the ultraboosted biadjoint scalar field is related to the equations of motion for the interacting particle coupled with the biadjoint scalar [108],

$$\frac{\partial p_\mu}{\partial t} = -\frac{\lambda}{m} c_2^a \tilde{c}_2^{\dot{a}} \partial_\mu \Phi_{\text{sw}}^{a\dot{a}}. \quad (10.28)$$

Here, the biadjoint field $\Phi^{a\dot{a}}$ is given by the shockwave solution given by (10.27). Stripping out charge and mass parameters for the sake of simplicity, we have

$$\frac{\partial p_\mu}{\partial t} = \partial_\mu \left(\ln \left(\frac{\rho^2}{\rho_0^2} \right) \delta(x-t) \right). \quad (10.29)$$

Switching to lightfront coordinates(10.18), the impulse experienced by the particle is

$$\delta p_\mu = \int_{-\infty}^{\infty} dt \frac{\partial p_\mu}{\partial t} = \int_{-\infty}^{\infty} du \frac{\partial p_\mu}{\partial u} = \int_{-\infty}^{\infty} du \partial_\mu \left(\ln \left(\frac{\rho^2}{\rho_0^2} \right) \delta(u) \right). \quad (10.30)$$

We will work this out for each component,

$$\delta p_u = \int_{-\infty}^{\infty} du \partial_u \left(\ln \left(\frac{\rho^2}{\rho_0^2} \right) \delta(u) \right) = \ln \left(\frac{\rho^2}{\rho_0^2} \right) \delta(u) \Big|_{u=-\infty}^{\infty} = 0$$

$$\delta p_w = 0, \quad \delta p_y = \int_{-\infty}^{\infty} du \frac{2y}{\rho^2} \delta(u) = \frac{2y}{\rho^2}, \quad \delta p_z = \int_{-\infty}^{\infty} du \frac{2z}{\rho^2} \delta(u) = \frac{2z}{\rho^2}.$$

Altogether, the interacting particle experiences an impulse with charges and couplings reinstated:

$$\delta p^\mu = -\frac{\lambda^2}{m} \frac{c \cdot c_2 \tilde{c} \cdot \tilde{c}_2}{2\pi\rho^2} (0, 0, y, z). \quad (10.31)$$

Depending on the signs of the charges of the interacting particle and the shockwave field, the particle will experience a kick toward or away from the shockwave nucleus in the $y - z$ direction, inside the lightfront plane. The further the test particle is from the nucleus on contact with the shockwave, the smaller the kick will be. This does have the hallmarks of shockwave behaviour, and so we can feel assured that the ultraboost procedure (including charge rescaling) holds for the linear biadjoint scalar theory. In the next section, we apply this procedure to gauge theory.

10.1.3 Coulomb potential in Kerr-Schild coordinates

Ultraboosting the Coulomb potential is a well-trodden path [135], however, we will perform this exercise for the field expressed in Kerr-Schild coordinates which is, as far as we know, a novelty. It is in this domain that the building block idea of Kerr-Schild coordinates will come into fruition. The gauge field $A^{a\mu}$ defined in (10.3) is boosted as follows

$$A'^{a\mu}(x') = g c^a \phi(x') k'^{\mu}(x') \quad (10.32)$$

where we define the scalar field as $\phi(x) = 1/(4\pi r)$. The classical double copy expressed in Kerr-Schild coordinates depends on the ability to add and remove copies of the null vector k^μ to the ever present scalar field ϕ . As such, we begin the ultraboost procedure by boosting these objects separately with the intention to form building blocks that will illuminate the double copy at all stages of the ultraboost. We know from the previous section how to boost the scalar field:

$$\phi(x') = \frac{1}{\gamma 4\pi R} \equiv \frac{1}{\gamma} \hat{\phi} \quad (10.33)$$

where R is defined in (10.8). The vector field k^μ picks up an extra factor of γ when boosted:

$$k'^\mu(x') = (\Lambda^{-1})^\mu{}_\nu k^\nu(x') = \begin{bmatrix} \gamma(1 - vx'/r') \\ \gamma(v - x'/r') \\ -y'/r' \\ -z'/r' \end{bmatrix} \equiv \gamma \hat{k}^\nu \quad (10.34)$$

where Λ^{-1} is the inverse of (10.6), and

$$\hat{k}^\nu = \begin{bmatrix} (1 - v(x - vt)/R) \\ (v - (x - vt)/R) \\ -y/(\gamma^2 R) \\ -z/(\gamma^2 R) \end{bmatrix}. \quad (10.35)$$

Putting together (10.32) to (10.35), the boosted gauge field $A'^{a\mu}$ is

$$A'^{a\mu} = gc^a \hat{\phi} \hat{k}^\mu. \quad (10.36)$$

Having boosted the gauge field, the behaviour of each component of \hat{k}^μ can be examined in the limit $v \rightarrow 1$ in and out of the plane $x - t = 0$. First we begin with \hat{k}^0 .

i) Inside the plane, $x = t$:

$$\lim_{v \rightarrow 1} \hat{k}^0 = 1 - \lim_{v \rightarrow 1} \frac{v(1 - v)x}{\sqrt{x^2(1 - v)^2 + \rho^2(1 - v^2)}} = 1$$

ii) Outside the plane, $x \neq t$:

$$\lim_{v \rightarrow 1} \hat{k}^0 = 1 - \frac{x - t}{\sqrt{(x - t)^2 + 0}} = \begin{cases} 0 & x - t > 0 \\ 2 & x - t < 0 \end{cases}$$

Altogether, this gives us:

$$\lim_{v \rightarrow 1} \hat{k}^0 = \begin{cases} 0 & x - t > 0 \\ 1 & x = t \\ 2 & x - t < 0 \end{cases} \quad (10.37)$$

Similarly, the x -component, i.e. \hat{k}^x has the same value as (10.37) in the ultraboost limit while the other components of \hat{k}^μ vanish. Finally, we have the ultraboosted vector \hat{k}^μ :

i) Inside the plane, $x = t$:

$$\lim_{v \rightarrow 1} \hat{k}^\mu = \begin{bmatrix} 1 \\ 1 \\ 0 \\ 0 \end{bmatrix} \equiv n^\mu, \quad (10.38)$$

ii) Outside the plane, $x \neq t$:

$$\lim_{v \rightarrow 1} \hat{k}^\mu = \begin{bmatrix} 1 \\ 1 \\ 0 \\ 0 \end{bmatrix} \times 2 \times \begin{cases} 0 & x - t > 0 \\ 1 & x - t < 0 \end{cases} = 2(1 - \theta(x - t))n^\mu. \quad (10.39)$$

We come to an important fork in the road. Outside the plane, we have two regions - one that the shockwave has already passed through, i.e. $x - t < 0$, and the region still waiting for the shockwave $x - t > 0$. In the region anticipating the shockwave, our vector \hat{k}^μ seems to be decimated in the ultraboost limit. We have to be careful about how we combine this result with $\hat{\phi}$ which we know from the biadjoint ultraboost exercise will wind up as a delta function. To be on the safe side, we can consider the limit of the combined boosted product of $\hat{\phi}\hat{k}^\mu$ in the problematic region of $x - t > 0$. Examining this for one component, we see:

$$\lim_{v \rightarrow 1} \hat{\phi}\hat{k}^0 = \frac{1}{4\pi} \lim_{v \rightarrow 1} \left(\frac{1}{R} - \frac{v(x - vt)}{R^2} \right) = 0 \text{ if } x - t > 0. \quad (10.40)$$

Similarly, the spatial components vanish as well. This signals that actually it is safe to take the product of limits. After all, in the potentially tricky case where one of those limits goes to zero, the limit of the entire product as a whole goes to zero anyhow. As for the other regions, more or less, we can say that in the ultraboost limit, $\lim_{v \rightarrow 1} \hat{k}^\mu \sim n^\mu$. To perform the remainder of the ultraboost, i.e. on $\hat{\phi}$, we should follow the same procedure as we did for the biadjoint ultraboost²¹. This will leave us with:

$$\lim_{v \rightarrow 1} \hat{\phi} = -\frac{1}{4\pi} \ln \left(\frac{\rho^2}{\rho_o^2} \right) \delta(x - t). \quad (10.41)$$

Now we are well equipped to construct the ultraboosted gauge field (that is, (10.36) in the limit $v \rightarrow 1$), as we have ultraboosted all of its ingredients. When we combine the ultraboosted $\hat{\phi}$ as per (10.41) with the ultraboosted \hat{k}^μ as per (10.38) and (10.39), we find that the δ -function kills off any activity outside the plane $x = t$ and so we are left

²¹In the biadjoint ultraboost, we justified regularizing the field by demonstrating that the redefined field belongs to the same family of solutions that solve the equations of motion. When we regularize the field in the context of gauge theory, the field redefinition turns out actually to be equivalent to a gauge transformation.

with

$$A_{\text{sw}}^{a\mu} = \lim_{v \rightarrow 1} A'^{a\mu} = \frac{-gc^a}{4\pi} \ln\left(\frac{\rho^2}{\rho_0^2}\right) \delta(x-t)n^\mu \quad (10.42)$$

which agrees with the results of [135] as expected.

When expressed in Kerr-Schild coordinates, structural elements of the double copy remain intact at key stages of the ultraboost procedure for the gauge field. By comparing the shockwave solution of gauge theory (10.42) with that of the biadjoint theory (10.27), a zeroth copy emerges by the removal of the null and geodesic vector n^μ . Furthermore, the key ingredients of the Kerr-Schild double copy, i.e., the scalar field ϕ and null and geodesic vector k^μ , can be ultraboosted *nearly* independently of each other such that the ensuing results are meaningful.²² This will facilitate ultraboosting the graviton associated with the Schwarzschild black hole, as we will see in the next section. Before moving on to gravity, we can provide further assurance that our shockwave is indeed a shockwave by allowing a test particle to interact with the shockwave field.

Gauge Theory Impulse

The impulse of a particle of charge c_2^a interacting with the ultraboosted gauge field is related to the Lorentz force, given by

$$\frac{\partial p^\mu}{\partial t} = gc_2^a F^{a\mu}{}_\nu v^\nu, \quad (10.43)$$

where v^ν is the velocity vector of the interacting particle, which we can take to be $v^\nu = (1, 0, 0, 0)$ in the rest frame of the particle. As such, we need only consider the following components of the field strength tensor:

$$F^{a\mu}{}_0 = \partial^\mu A_0^a - \partial_0 A^{a\mu} \quad (10.44)$$

where $A^{a\mu}$ is the shockwave gauge potential given by the ultraboosted field given by (10.42), and $\partial^\mu \equiv (\partial_t, -\partial_x, -\partial_y, -\partial_z)$. The components of interest of the field strength tensor are

$$\begin{aligned} F^{a1}{}_0 &= \frac{gc^a}{4\pi} \ln\left(\frac{\rho^2}{\rho_0^2}\right) (\partial_t + \partial_x)\delta(x-t) = 0 \\ F^{aj}{}_0 &= \frac{gc^a}{4\pi} \delta(x-t)\partial_j \ln\left(\frac{\rho^2}{\rho_0^2}\right) = \frac{c^a}{4\pi} \delta(x-t) \frac{2x^j}{\rho^2} \end{aligned} \quad (10.45)$$

²²We say “nearly” as opposed to completely since the overall γ -count determines the charge rescaling.

where $j = 2, 3$ or equivalently $x^j = y, z$. We can now extract the impulse,

$$\delta p^\mu = \int_{-\infty}^{\infty} dt \frac{dp^\mu}{dt} \rightarrow \delta p^j = \int_{-\infty}^{\infty} dt \frac{c_2 \cdot c}{4\pi} \delta(x-t) \frac{2x^j}{\rho^2} = \frac{c_2 \cdot c}{4\pi} \frac{2x^j}{\rho^2} \quad (10.46)$$

which leaves us finally with the impulse

$$\delta p^\mu : \frac{g^2 c_2 \cdot c}{2\pi \rho^2} (0, 0, y, z). \quad (10.47)$$

This is identical (setting aside couplings, charges etc.) to the biadjoint case. If the interacting particle were to have the same charge as that producing the shockwave, the effect of the impulse would be to send the particle away from the shockwave nucleus. Opposite charges would result in the particle being drawn in closer to the nucleus.

10.1.4 Schwarzschild black hole in Kerr-Schild coordinates

Lastly, we construct a gravitational shockwave by ultraboosting the Schwarzschild solution as per Aichelburg and Sexl ([134], and subsequently also [136]). As we have done for gauge theory, the ultraboost will be performed in Kerr-Schild coordinates. The boosted metric takes the form

$$g'_{\mu\nu}(x') = \eta_{\mu\nu} - \underbrace{\frac{\kappa^2}{2} \phi(x') k'_\mu(x') k'_\nu(x')}_{\kappa h'_{\mu\nu}(x')}. \quad (10.48)$$

The boosted graviton $h'_{\mu\nu}$ can be treated similarly to the boosted single copy gauge field A'_μ , i.e., by preserving the integrity of the scalar field and null vectors - essentially treating them as independent creatures. Employing a language similar to (10.33)²³ and (10.34), we have

$$h'_{\mu\nu} = \gamma \frac{\kappa}{2} \hat{\phi} \hat{k}_\mu \hat{k}_\nu, \quad (10.49)$$

The factor of γ will prove problematic in the ultraboost limit unless we rescale the mass as per

$$M \rightarrow M\gamma^{-1}. \quad (10.50)$$

This rescaling is justified in [134] as necessary to keep the source term finite. We employed a similar argument in biadjoint scalar theory, where we also rescaled the charge. The mass rescaling fundamentally enables us to proceed with the ultraboost (see section 10.1.3 for details on ultraboosting $\hat{\phi}$ and \hat{k}^μ). Now, in biadjoint scalar theory, we altered our field in order to produce a delta function in the ultraboost limit of $\hat{\phi}$. In gauge theory, this is akin to a gauge transformation. In gravity, our transformation of ϕ to $\hat{\phi}$ could be mediated by a diffeomorphism. The graviton associated with the

²³Of course now $\hat{\phi}$ contains a factor of mass M .

Schwarzschild black hole ultraboosts to a shockwave confined to the lightfront plane $x - t = 0$:

$$h_{\mu\nu}^{\text{sw}} = \lim_{v \rightarrow 1} h'_{\mu\nu} = -\frac{\kappa}{2} \frac{M}{4\pi} \ln\left(\frac{\rho^2}{\rho_0^2}\right) \delta(x-t) n_\mu n_\nu. \quad (10.51)$$

This shockwave agrees with the result in [134], although found by different means. For completeness, and to provide some comparison with gauge theory, we calculate the effect of this shockwave on a test particle.

Gravitational Impulse

The impulse of a particle of mass m interacting with the ultraboosted graviton field is related to the geodesic equation given by

$$\frac{\partial p^\mu}{\partial t} = -m \Gamma^\mu_{\nu\sigma} v^\nu v^\sigma, \quad (10.52)$$

where the velocity vectors can be taken to be in the rest frame of the particle, $v^\nu = (1, 0, 0, 0)$. In the rest frame, the geodesic equation simplifies greatly to

$$\frac{\partial p^\mu}{\partial t} = -m \Gamma^\mu_{00}. \quad (10.53)$$

The Christoffel symbols are based on the Kerr-Schild metric, where the flat background spacetime is perturbed by the shockwave graviton (10.51). We only need 4 of the Christoffel symbols:

$$\begin{aligned} \Gamma^0_{00} &= \frac{-1}{2} \frac{\kappa^2}{2} \frac{M}{4\pi} \ln\left(\frac{\rho^2}{\rho_0^2}\right) \partial_t \delta(x-t), & \Gamma^x_{00} &= \frac{1}{2} \frac{\kappa^2}{2} \frac{M}{4\pi} \ln\left(\frac{\rho^2}{\rho_0^2}\right) \partial_t \delta(x-t), \\ \Gamma^y_{00} &= \frac{\kappa^2}{2} \frac{M}{4\pi} \frac{y}{\rho^2} \delta(x-t), & \Gamma^z_{00} &= \frac{\kappa^2}{2} \frac{M}{4\pi} \frac{z}{\rho^2} \delta(x-t). \end{aligned}$$

The impulse δp^μ is then the time integral of these Christoffel symbols,

$$\begin{aligned} \delta p^0 &= -\delta p^x = \frac{\kappa^2}{2} \frac{Mm}{4\pi} \int_{-\infty}^{\infty} dt \frac{1}{2} \ln\left(\frac{\rho^2}{\rho_0^2}\right) \partial_t \delta(x-t) \\ &= \frac{\kappa^2}{4} \frac{Mm}{4\pi} \ln\left(\frac{\rho^2}{\rho_0^2}\right) \int_{-\infty}^{\infty} du \partial_u \delta(u) = 0, \\ \delta p^y &= \frac{-\kappa^2}{2} \frac{Mm}{4\pi} \int_{-\infty}^{\infty} dt \delta(x-t) \frac{y}{\rho^2} = \frac{-\kappa^2}{2} \frac{Mm}{4\pi} \frac{y}{\rho^2}, \\ \delta p^z &= \frac{-\kappa^2}{2} \frac{Mm}{4\pi} \int_{-\infty}^{\infty} dt \delta(x-t) \frac{z}{\rho^2} = \frac{-\kappa^2}{2} \frac{Mm}{4\pi} \frac{z}{\rho^2}. \end{aligned} \quad (10.54)$$

	Static Solution	Shockwave Solution	Charge Rescaling	Spin
Biadj. Sc. $\Phi^{a\dot{a}}$	$\lambda \frac{e^a \tilde{c}^{\dot{a}}}{4\pi r}$	$-\frac{\lambda e^a \tilde{c}^{\dot{a}}}{4\pi} \ln\left(\frac{\rho^2}{\rho_0^2}\right) \delta(x-t)$	$c^a \tilde{c}^{\dot{a}} \rightarrow \gamma^1 c^a \tilde{c}^{\dot{a}}$	0
Gauge A_μ^a	$g \frac{c^a}{4\pi r} k_\mu$	$-\frac{g c^a}{4\pi} \ln\left(\frac{\rho^2}{\rho_0^2}\right) \delta(x-t) n_\mu$	$c^a \rightarrow \gamma^0 c^a$	1
Gravity $h_{\mu\nu}$	$\frac{\kappa}{2} \frac{M}{4\pi r} k_\mu k_\nu$	$-\frac{\kappa}{2} \frac{M}{4\pi} \ln\left(\frac{\rho^2}{\rho_0^2}\right) \delta(x-t) n_\mu n_\nu$	$M \rightarrow \gamma^{-1} M$	2

Table 6: Shockwave and Rescalings Comparison

The impulse bears a resemblance to those of the biadjoint scalar and gauge theories,

$$\delta p^\mu = \frac{-\kappa^2 M m}{8\pi \rho^2} (0, 0, y, z). \quad (10.55)$$

Similar to biadjoint and gauge theories, in gravity, the particle gets a kick in the $y-z$ direction, with the magnitude of the kick diminishing the further the particle is from the nucleus of the shockwave. The impulse draws the particle toward the nucleus of the shockwave, as expected since gravity is attractive. By contrast, like charges repel in gauge theory, which results in the sign difference between (10.47) and (10.55).

10.1.5 Comparison of shockwaves across theories

By ultraboosting three linear static solutions related to each other by the double copy, we have constructed three shockwaves which also have a double copy structure, as summarised by table 6. We observe

- Our baseline is the double copy of static solutions, where copies of the null and geodesic vector k^μ are added or removed between the three theories. In the shockwave solutions, this is mediated by the null and geodesic vector n_μ .
- In all three static solutions, the scalar field $\frac{1}{4\pi r}$ is the ever-present propagator. This role is played in two spatial dimensions by the Green's function $\ln\left(\frac{\rho^2}{\rho_0^2}\right)$. Additionally, the shockwave defining factor $\delta(x-t)$ is common to all three solutions.
- While gravity and biadjoint theory require charge rescaling to produce a field with shockwave form, gauge theory does not. The nature of charge rescaling follows from the tensor structure, which is indicative of the spin associated with the theory.

Furthermore, the impulse experienced by a particle interacting with the shockwaves was consistent among the three theories. This provided further assurance that we had

performed the ultraboost correctly for the Abelian biadjoint scalar theory - an exercise that broke new ground.

Having gained confidence in the ultraboost procedure, where it proved successful for producing a shockwave for one biadjoint scalar theory solution, we can now attempt an ultraboost of strongly coupled solutions, starting with the spherically symmetric biadjoint monopole.

10.2 Ultraboosting the biadjoint monopole

Recall the spherically symmetric biadjoint monopole solution (9.8), i.e.,

$$\Phi^{a\dot{a}} = \frac{-2\delta^{a\dot{a}}}{\lambda T_A r^2}. \quad (10.56)$$

Boosting this monopole in the same manner as we had done for the linear biadjoint solution in section 10.1.2 yields,

$$\Phi^{a\dot{a}}(x') = -\frac{2\delta^{a\dot{a}}}{\lambda T_A} \frac{1}{[\gamma^2(x-vt)^2 + \rho^2]}. \quad (10.57)$$

In the ultraboost limit, we have

$$\lim_{\gamma \rightarrow \infty} \Phi^{a\dot{a}} = -\frac{2\delta^{a\dot{a}}}{\lambda T_A} \begin{cases} \frac{1}{\rho^2}, & x = t \\ 0, & x \neq t. \end{cases} \quad (10.58)$$

Due to the different dependence on the radial coordinate, this does not diverge on the transverse plane, in contrast to the boosted point charge considered in the previous section. Without this divergence, eq. (10.58) does not constitute a shockwave: it is at most a tepid ripple. That is, it imparts no finite impulse to a test particle, given that a finite field is confined to an infinitely thin plane.

In the linear solutions of gravity and biadjoint theory, the ability to form shockwaves via the ultraboost procedure depended fundamentally on rescaling the charge. Unfortunately, this is no remedy for the biadjoint monopole, as it is unclear how $\delta^{a\dot{a}}$ could be rescaled. On the other hand, a rescaling of the coupling λ in (10.57) could result in a solution that has a shockwave-like form,

$$\Phi^{a\dot{a}} \xrightarrow{\gamma \rightarrow \infty, \lambda \rightarrow \gamma^{-1}\lambda} -\frac{2\pi\delta^{a\dot{a}}}{\lambda T_A} \frac{1}{\rho} \delta(x-t). \quad (10.59)$$

However, the nature of this rescaling is very different to that of the boosted point charges considered earlier. In the latter cases, the charge parameters forming the source terms were rescaled. For the non-perturbative monopole, there is no such source, which makes it questionable that one should be able to rescale the coupling, and worse still, risk changing the theory altogether ²⁴.

Ultraboosting the spherically symmetric biadjoint monopole seems problematic, but what about the other biadjoint monopole solutions, such as those presented in chapter 9? After all, it is the SU(2) solution of (9.11) that is postulated to be related to the Wu-Yang monopole, rather than the simpler spherically symmetric solution (10.56). This too suffers the same fate. The SU(2) solution of (9.11) ultraboosts to a finite quantity rather than a shockwave, as evidenced by appendix H.

Based on the above considerations, we conservatively conclude that the non-perturbative biadjoint monopole does not survive an ultraboost. There are then two possibilities regarding the suggestion that the biadjoint monopole could be related to a Wu-Yang monopole in gauge theory. The first is that the two objects are indeed related, but that the physics of ultraboosting is potentially very different in the two theories, such that the biadjoint monopole disappears. Whether or not the Wu-Yang monopole survives an ultraboost is irrelevant for the argument. The second possibility is that the biadjoint monopole disappears because it is not related to the Wu-Yang monopole after all, and so there is no meaningful reason why the two ultraboosted solutions should match up. In the next section, we will explain why the second possibility seems the more likely of the two.

10.3 The Wu-Yang and Dirac monopoles

In this section, we will explain our reasons for asserting that a relationship between the biadjoint monopole and the Wu-Yang monopole is unlikely. The Wu-Yang monopole and the Dirac monopole are related to each other, and this relationship precludes any connection to the biadjoint monopole. The Wu-Yang monopole in SU(2) gauge theory can be related via a gauge transformation to a non-Abelian embedding of the Dirac monopole [137,138]. To see how this works, recall the gauge field of the Dirac monopole captured in (8.8), which we reiterate here:

$$A_\mu^a = c^a A_\mu^D, \tag{10.60}$$

²⁴Coupling constants are of course not constant when quantum corrections are included, leading to renormalisation. But that is not what is happening here.

where in spherical polar coordinates (t, r, θ, ϕ) ,

$$A_\mu^D = \frac{\tilde{g}}{4\pi} \left(0, 0, 0, \frac{1 - \cos \theta}{r \sin \theta} \right). \quad (10.61)$$

This solution of the Maxwell equations has a string-like singularity, which we have chosen to lie along the z -axis. Although not strictly speaking a solution of an Abelian gauge theory, we can think of this solution as *Abelian-like* as it linearises the Yang-Mills equations.

For the transformation we will perform, we may choose the constant colour vector c^a to lie in the z -direction in the internal space, such that $c^a = \delta^{a3}$. We consider an embedding of the Dirac monopole in the $SU(2)$ group with the form

$$A_\mu = -A_\mu^D \sigma_3. \quad (10.62)$$

The matrix σ_3 is one of the $SU(2)$ generators, and more generally speaking these generators can be expressed in terms of Pauli matrices,

$$\sigma_i = \frac{1}{2} \tau_i \quad (10.63)$$

where

$$\tau_1 = \begin{pmatrix} 0 & 1 \\ 1 & 0 \end{pmatrix}, \quad \tau_2 = \begin{pmatrix} 0 & -i \\ i & 0 \end{pmatrix}, \quad \tau_3 = \begin{pmatrix} 1 & 0 \\ 0 & -1 \end{pmatrix}. \quad (10.64)$$

The gauge field A_μ can be gauge transformed according to

$$A_\mu \rightarrow A'_\mu = U A_\mu U^{-1} + \frac{i}{g} U (\partial_\mu U^{-1}), \quad (10.65)$$

where the electric charge g and magnetic charge \tilde{g} are related by the quantisation condition (8.9). A special choice of transformation matrix U can transform the embedded Dirac gauge field (10.62) into that of the Wu-Yang monopole, specifically,

$$U = e^{-i\phi\sigma_3} e^{-i\theta\sigma_2} e^{i\phi\sigma_3}. \quad (10.66)$$

Applying the gauge transformation (10.66) to the embedded Dirac gauge field (10.62) according to the transformation rule (10.65) results in the gauge field in spherical polar coordinates (see appendix I for details),

$$A'_\mu = \frac{\tilde{g}}{4\pi r} (0, 0, \sigma_1 \sin \phi - \sigma_2 \cos \phi, \sigma_1 \cos \theta \cos \phi + \sigma_2 \cos \theta \sin \phi - \sigma_3 \sin \theta). \quad (10.67)$$

The gauge field can also be expressed in Cartesian coordinates, the details of which can be found in appendix I. Cartesian coordinates reveal the familiar form of the Wu-Yang monopole,

$$A_0^a = 0, \quad A_i^a = -\frac{\tilde{g}\epsilon_{iak}x^k}{4\pi r^2}. \quad (10.68)$$

Although the Wu-Yang monopole is a genuinely non-Abelian solution to the Yang-Mills equations, it can be viewed as the Dirac monopole in disguise. As such, the Wu-Yang monopole inherits the double copy relationships of the Dirac monopole - more precisely, the double copy to the NUT solution in gravity and the zeroth copy to a linear biadjoint solution (see section 8.3.1 as well as the reference [122]). The relationship between the Wu-Yang monopole and the linear biadjoint solution with a point-like source crowds out the biadjoint monopole. This exclusion is further justified by the fact that the Wu-Yang monopole can be ultraboosted to produce a shockwave, unlike the strongly coupled biadjoint monopole (see appendix J for the ultraboost of the Wu-Yang monopole).

While this chain of events marks a departure from the search for a non-perturbative double copy, it does open up new insights into the remit of the classical double copy in general.

10.3.1 New insights to the double copy

Prior to these findings, the Kerr-Schild double copy differed from the double copy of amplitudes in one important regard. While the Kerr-Schild double copy always produces an Abelian-like solution, the double copy of amplitudes crucially depends on BCJ duality, which demands that the gauge theory be non-Abelian. From the results presented in this chapter, non-Abelian solutions to gauge theories can be brought into the Kerr-Schild double copy picture. In our example, the NUT solution in gravity is the double copy of the (Abelian-like) Dirac monopole, which then can be related to the (non-Abelian) Wu-Yang monopole. The colour-stripped Wu-Yang monopole effectively can be double copied to the NUT solution. In other words, we now can see a double copy between the exact solutions of non-Abelian gauge theories and gravity, as illustrated schematically by figure 21. This is consistent with prior literature supporting the double copy of perturbative constructions of non-Abelian classical solutions [107, 108, 139].

10.4 Conclusion

Our motivation was to revisit the speculation that the strongly coupled biadjoint monopole may be related to the Wu-Yang monopole in gauge theory, signalling the first sighting of a certainly non-perturbative double copy. As we already know that shockwaves can be related under the double copy, our initial investigation involved

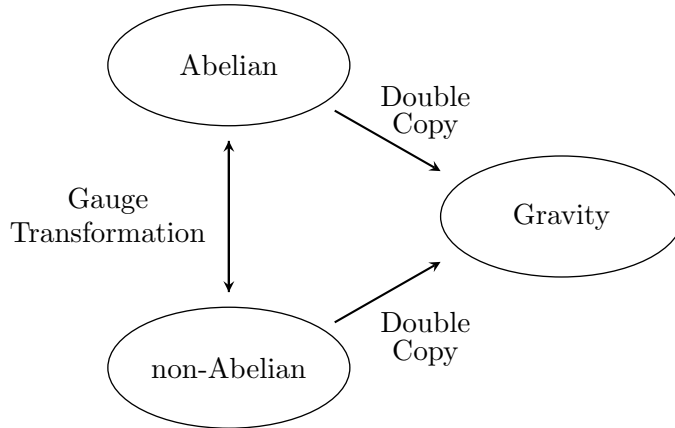


Figure 21: Generalisation of the Kerr-Schild double copy, in which one may identify Abelian or non-Abelian exact solutions of a gauge theory with the same gravity solution

creating shockwave solutions by the Aichelburg-Sexl ultraboost procedure in order to compare ensuing shockwaves of the two solutions. As a warm-up, we applied the ultraboost to linear Kerr-Schild solutions - an exercise that had not been carried out before in Kerr-Schild coordinates. We observed a double copy-like structure surviving various stages of the ultraboost, and gained the confidence to apply the ultraboost to the biadjoint monopole. While the biadjoint monopole receded to a tepid ripple under the procedure, the Wu-Yang monopole did not, potentially indicating that the relationship between the two may not be robust. This suspicion was then confirmed when exploring the relationship between the Wu-Yang and Dirac monopoles. The Wu-Yang monopole can be gauge transformed to a non-Abelian embedding of the Dirac monopole in the $SU(2)$ group. As the latter is already part of the Taub-NUT double copy, the former inherits this role, crowding out the strongly coupled biadjoint monopole from the picture.

Although we did not find an example of a truly non-perturbative double copy, we were able at least to rule out a contender, as well as learn a few interesting things along the way. Crucially, exact non-Abelian solutions can indeed double copy to a gravity theory in the Kerr-Schild double copy, bringing the Kerr-Schild double copy closer in line with the BCJ double copy of amplitudes.

The existence of a fully non-perturbative double copy remains an open question.

Chapter 11

Double Copy Conclusion

11.1 Recap

The double copy offers a promising bridge between the seemingly disparate gravity and gauge theories, where much of the propagator information can be encapsulated in a relatively simple biadjoint scalar theory. So far, this duality operates within the confines of perturbation theory - originally by linking amplitudes under the restriction of BCJ duality, but subsequently also by linking up exact classical solutions limited to weakly coupled Abelian theories.

Our research sought to address the question of whether there exists a non-perturbative double copy, such as a connection between an exact solution of a non-Abelian strongly coupled gauge theory and some appropriate counterpart in gravity. Two impediments stood in the way: 1) cumbersome calculations, and 2) the construct of the double copy involving non-Abelian strong coupling without any precedent. Help came in the form of biadjoint scalar theory, which addressed the first problem by providing a relatively simpler playing ground for calculations. Additionally, prior literature partly alleviated the second issue by proposing a potential link between a strongly coupled biadjoint monopole and the Wu-Yang monopole.

11.2 Learnings and achievements

Our research progressed on two fronts: firstly, we extended the catalogue of strongly coupled biadjoint monopole solutions to include those with cylindrical symmetry. Secondly, we tested the proposal of a link between a strongly coupled biadjoint monopole and the Wu-Yang monopole, by ultraboosting both solutions to see how well the ensuing shockwaves match up. We found that the ultraboost procedure does not produce a shockwave when applied to the strongly coupled biadjoint monopole, in contrast with

the Wu-Yang monopole. This mismatch makes sense when taking into consideration that the Wu-Yang monopole can be seen as a gauge transformed Dirac monopole embedded in colour space. The latter already has a place in the Taub-NUT dyon double copy, and so the former inherits this relationship - including the zeroth copy which is an Abelian-like biadjoint solution, not the strongly coupled biadjoint monopole. Although we did not find a non-perturbative double copy, we were able to rule out a contender, as well as gain new insight into a long-standing question about how multiple non-Abelian gauge theory solutions can map to the same gravity solution. As an additional novelty, we were also able to see how well the double copy structure holds together at various stages of the ultraboost procedure when applied to Kerr-Schild solutions.

11.3 Impact

Broadening the remit of the double copy is an ongoing project, building on and beyond the research presented in this thesis. For example, ref. [140] sets out more formally how non-Abelian and Abelian-like exact solutions in gauge theory can map to one solution in gravity, where topological information on both sides of the double copy correspondence is cast in terms of Wilson lines. Additionally, ref. [141] uses biadjoint scalar theory to formulate a version of the double copy for classical fields in curved spacetimes, affirming the importance of the role biadjoint scalar theory plays in the double copy.

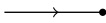
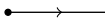
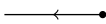
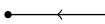





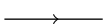
11.4 Further work

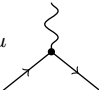
Although some double copy literature mentions biadjoint scalar theory, it is rarely the showcase subject. However, this theory is interesting in its own right, and could benefit from further study. For example, the catalogue of exact strongly coupled biadjoint solutions could be extended to include those associated with symmetries other than spherical or cylindrical, or indeed based on more general ansätze. Also, we do not have much knowledge of the features of biadjoint scalar theory in general dimensions, for example in $d = 6$ where the coupling is dimensionless (similar to Yang-Mills theory in $d = 4$). A more complete understanding of this biadjoint scalar theory may consequently have the added benefit of refining our view of its place and role in the double copy. There is scope to undertake a deeper study of the topological character biadjoint monopoles may have, as they seem to differ from gauge theory monopoles in the usual characteristics of string-like singularities, requirements for multiple coordinate patches, etc. A further line of enquiry could involve comparing the double copy to other dualities, such as the well-known and long established AdS-CFT duality [142]. Such a comparison could open up the double copy to phenomena such as confinement, and whether this feature has an analogue in biadjoint scalar theory.

Appendix A

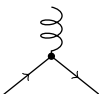
Feynman Rules

Drell-Yan cross sections are calculated by these QED and QCD Feynman rules (where p, q, k typically signify momenta, and r, s are spin indices):

incoming quark	$\bar{u}_r(p)$			$u_r(p)$	outgoing quark
incoming antiquark	$v_r(\bar{p})$			$\bar{v}_r(\bar{p})$	outgoing antiquark
incoming photon	$\epsilon_{\mu,s}(q)$			$\epsilon_{\mu,s}^*(q)$	outgoing photon
incoming gluon	$\epsilon_{\alpha,s}(k)$			$\epsilon_{\alpha,s}^*(k)$	outgoing gluon
photon propagator	$-\frac{i\eta_{\mu\nu}}{q^2+i\epsilon}$				
fermion propagator	$\frac{i(\not{p}+m)}{p^2-m^2+i\epsilon}$			where $\not{p} = p_\mu\gamma^\mu$	

QED vertex factor $-ie\delta_{ij}\gamma^\mu$ 

Note: The colour preserving δ_{ij} is for quark interactions.

QCD vertex factor $ig_s t_{ji}^a \gamma^\alpha$ 

where t_{ji}^a are elements of the Gell-Mann matrices

Further to these rules, for squared matrix elements, we also need to invoke the photon polarisation sum

$$\sum_s \epsilon_{\mu,s}^*(q) \epsilon_{\nu,s}(q) = -\eta_{\mu\nu}, \quad (\text{A.1})$$

as well as the completeness relations (where quark masses are negligible)

$$\sum_{r=1}^2 u_r(p) \bar{u}_r(p) = \not{p} \quad ; \quad \sum_{r=1}^2 v_r(\bar{p}) \bar{v}_r(\bar{p}) = \not{\bar{p}}. \quad (\text{A.2})$$

Appendix B

Special Functions

B.1 Gamma

The gamma function $\Gamma(\xi)$ is defined as

$$\Gamma(n) = (n - 1)! \tag{B.1}$$

and can also be expressed as an integral

$$\Gamma(n) = \int_0^\infty dt e^{-t} t^{n-1}. \tag{B.2}$$

The gamma function also has the recursive property,

$$\Gamma(n + 1) = n\Gamma(n - 1). \tag{B.3}$$

This property allows us to easily expand $\Gamma(\xi) = \frac{1}{\xi}\Gamma(1 + \xi)$ for small ξ ,

$$\Gamma(\xi) = \frac{1}{\xi} + \sum_{j=1}^{\infty} \frac{b_j(1)}{j!} \xi^{j-1} \tag{B.4}$$

where

$$b_j(\xi) = \frac{1}{\Gamma(\xi)} \frac{d^j}{d\xi^j} \Gamma(\xi). \tag{B.5}$$

With this definition, we can also calculate derivatives as:

$$\frac{d^k}{d\xi^k} \Gamma(\xi) = \frac{(-1)^k k!}{\xi^{(k+1)}} + \sum_{j=k+1}^{\infty} \frac{b_j(1)}{j(j - (k + 1))!} \xi^{j-(k+1)}. \tag{B.6}$$

Note that b_0 is initialised to 1.

B.2 Polygamma

The polygamma function $\psi^{(m)}(N)$ is often seen in cross sections in the threshold limit. It is defined as

$$\psi^{(m)}(N) = \frac{d^m}{dN^m} \psi(N), \quad \psi(N) = \frac{\Gamma'(N)}{\Gamma(N)} \quad (\text{B.7})$$

where the prime signifies differentiation with respect to N . Alternatively we can rewrite this definition without recursion as

$$\psi^{(m)}(N) = \frac{d^{m+1}}{dN^{m+1}} \log(\Gamma(N)). \quad (\text{B.8})$$

When exploring cross sections in the threshold limit (equivalent to $N \rightarrow \infty$), interesting leading log terms arise from $\psi^{(0)}(N) = \frac{d}{dN} \log(\Gamma(N))$. To see how this comes to be, we begin by exploring $\Gamma(N)$ as $N \rightarrow \infty$. According to Stirling's formula, in this limit,

$$\Gamma(N+1) \sim \sqrt{2\pi N} \left(\frac{N}{e}\right)^N. \quad (\text{B.9})$$

We invoke the property of gamma functions $\Gamma(N+1) = N\Gamma(N)$, which means

$$\Gamma(N) \sim \sqrt{2\pi N} N^{N-1} e^{-N}, \quad (\text{B.10})$$

and furthermore,

$$\log(\Gamma(N)) = \frac{1}{2} \log(2\pi N) - N + N \log(N) \log(N). \quad (\text{B.11})$$

Finally we have

$$\psi^{(0)}(N) = \frac{d}{dN} \log(\Gamma(N)) = \log(N) - \frac{1}{2N} \text{ for large } N. \quad (\text{B.12})$$

Further, some special values of the polygamma function which appear in differential cross sections are:

$$\psi^{(0)}(1) = -\gamma_E \quad (\text{B.13})$$

$$\psi^{(1)}(1) = \frac{\pi^2}{6}. \quad (\text{B.14})$$

B.3 The Beta Function

The Beta function has the integral form

$$B(m, n) = \int_0^1 dx x^{m-1} (1-x)^{n-1} \quad (\text{B.15})$$

which evaluates to

$$B(m, n) = \frac{\Gamma(m)\Gamma(n)}{\Gamma(m+n)} \quad (\text{B.16})$$

where m and n are real.

B.4 The Zeta Function

The Riemann Zeta function $\zeta_s \equiv \zeta(s)$ is defined as

$$\zeta(s) = \sum_{n=1}^{\infty} \frac{1}{n^s} \quad (\text{B.17})$$

for a complex variable $s = \sigma + it$, converging for $\text{Re}(s) > 1$. For those cases, the function can also be written as an integral

$$\zeta(s) = \frac{1}{\Gamma(s)} \int_0^{\infty} dx \frac{x^{s-1}}{e^x - 1} \quad (\text{B.18})$$

where the Gamma function $\Gamma(s)$ is defined in Appendix B.1. Special values of the Zeta function are

$$\zeta(2) = \frac{\pi^2}{6} \quad (\text{B.19})$$

$$\zeta(3) = 1.202056903\dots \quad (\text{B.20})$$

$$\zeta(4) = \frac{\pi^4}{90}. \quad (\text{B.21})$$

Appendix C

Distributions and Transformations

C.1 Delta Plus

The notation δ_+ should be understood as:

$$\delta_+(k^2) = \theta(k_0)\delta(k^2) \quad (\text{C.1})$$

where θ is the Heaviside function:

$$\theta(k_0) = \begin{cases} 1 & \text{if } k_0 > 0 \\ 0 & \text{if } k_0 < 0. \end{cases} \quad (\text{C.2})$$

C.2 The Plus Distribution

The plus distribution of a function $F(z)$ is defined as follows:

$$\int_0^1 dz (F(z))_+ G(z) = \int_0^1 dz F(z)[G(z) - G(1)] \quad (\text{C.3})$$

where $G(z)$ is a smooth test function. It is possible from this definition to isolate $(F(z))_+$. Consider the right-hand-side of C.3, and express $G(1)$ as $\int_{-\infty}^{\infty} dy G(y)\delta(1-y)$:

$$\int_0^1 dz F(z)[G(z) - G(1)] = \int_0^1 dz F(z)G(z) - \int_0^1 dz F(z) \int_{-\infty}^{\infty} dy G(y)\delta(1-y). \quad (\text{C.4})$$

We have definite integrals over y and z , so we should be able to relabel these. Further, we have the freedom to change the bounds of the integral with the delta function as

long as the value 1 is covered by the bounds. This means:

$$\int_0^1 dz F(z) \int_{-\infty}^{\infty} dy G(y) \delta(1-y) = \int_0^1 dz \delta(1-z) \int_0^1 dy F(y) G(z). \quad (\text{C.5})$$

Combining this with C.4 yields

$$\int_0^1 dz F(z) [G(z) - G(1)] = \int_0^1 dz \left[F(z) - \delta(1-z) \int_0^1 dy F(y) \right] G(z). \quad (\text{C.6})$$

Connecting this result back to C.3 finally offers the following identity

$$(F(z))_+ = F(z) - \delta(1-z) \int_0^1 dy F(y). \quad (\text{C.7})$$

In the context of threshold radiation, this function appears in the differential cross section as

$$F(z) = \frac{\log^m(1-z)}{1-z}. \quad (\text{C.8})$$

For the simple case of $m = 1$, identity C.7 results in

$$\left(\frac{\log(1-z)}{1-z} \right)_+ = \frac{\log(1-z)}{1-z} + c \delta(1-z) \quad (\text{C.9})$$

where c is a divergent coefficient.

C.3 The Mellin Transform

This appendix draws heavily upon the appendices of theses [143, 144] to reproduce the Mellin transform of leading power terms appearing in differential cross sections, i.e.

$$\tilde{f}(z) = \left(\frac{\log(1-z)}{1-z} \right)_+. \quad (\text{C.10})$$

The Mellin transform of $\tilde{f}(z)$ is defined as

$$M\tilde{f}(z) = \int_0^1 dz z^{N-1} \tilde{f}(z). \quad (\text{C.11})$$

Performing a Mellin transform on this type of term becomes easier if we first rewrite it as

$$\tilde{f}(z) = \left(\frac{\log(1-z)}{1-z} \right)_+ = \left(\frac{d}{d\xi} f(\xi) \Big|_{\xi=0} \right)_+ \quad (\text{C.12})$$

where

$$f(\xi) = (1-z)^{\xi-1}. \quad (\text{C.13})$$

Then we can rewrite (C.11) as

$$\begin{aligned} M\tilde{f}(z) &= M \left(\left. \frac{d}{d\xi} f(\xi) \right|_{\xi=0} \right)_+ = \int_0^1 dz z^{N-1} \left(\left. \frac{d}{d\xi} (1-z)^{\xi-1} \right|_{\xi=0} \right)_+ \\ &= \frac{d}{d\xi} \left(\int_0^1 dz z^{N-1} (1-z)^{\xi-1} - \int_0^1 dz (1-z)^{\xi-1} \right) \Big|_{\xi=0} \end{aligned} \quad (\text{C.14})$$

where we have invoked the definition of the “plus” distribution as per (C.3). The integrals evaluate to beta functions (see appendix B.3) and we have:

$$M\tilde{f}(z) = \frac{d}{d\xi} \left(\frac{\Gamma(\xi)\Gamma(N)}{\Gamma(N+\xi)} - \frac{1}{\xi} \right) \Big|_{\xi=0}. \quad (\text{C.15})$$

Taking derivatives with respect to ξ in the limit where $\xi \rightarrow 0$ will lead to terms potentially blowing up, suggesting that we need more careful treatment of the expression above. Consider an expansion of

$$g(\xi) \equiv \frac{\Gamma(N)}{\Gamma(N+\xi)} \quad (\text{C.16})$$

around $\xi \sim 0$:

$$g(\xi) = \sum_{j=0}^{\infty} \frac{g^{(j)}(0)}{j!} \xi^j \quad (\text{C.17})$$

where the notation $g^{(j)}(0)$ denotes the j^{th} derivative of g with respect to ξ evaluated at $\xi = 0$. These derivatives are functions of N and so we can denote them as

$$a_j(N) \equiv g^{(j)}(0) = \left(\frac{d^j}{d\xi^j} \frac{\Gamma(N)}{\Gamma(N+\xi)} \right) \Big|_{\xi=0} = \Gamma(N) \left(\frac{d^j}{d\xi^j} \Gamma^{-1}(N+\xi) \right) \Big|_{\xi=0} \quad (\text{C.18})$$

allowing us to neatly express

$$\frac{\Gamma(N)}{\Gamma(N+\xi)} = \sum_{j=0}^{\infty} \frac{a_j(N)}{j!} \xi^j, \quad (\text{C.19})$$

where $a_0(N) = 1$. Note that the functions $a_j(N)$ are recursive. From the definition given by (C.18) we have

$$a_{j+1}(N) = \Gamma(N) \left(\frac{d^{j+1}}{d\xi^{j+1}} \Gamma^{-1}(N+\xi) \right) \Big|_{\xi=0}. \quad (\text{C.20})$$

Now consider

$$\frac{d}{dN} a_j(N) = \Gamma'(N) \left(\frac{d^j}{d\xi^j} \Gamma^{-1}(N+\xi) \right) \Big|_{\xi=0} + \Gamma(N) \left(\frac{d}{dN} \frac{d^j}{d\xi^j} \Gamma^{-1}(N+\xi) \right) \Big|_{\xi=0} \quad (\text{C.21})$$

where the prime indicates differentiation with respect to N . In the first term, we can recognize the relation to the polygamma function as defined by (B.8), i.e.

$$\psi^{(0)}(N) = \frac{d}{dN} \log(\Gamma(N)) = \frac{\Gamma'(N)}{\Gamma(N)}. \quad (\text{C.22})$$

As for the second term, differentiation by N or ξ results in the same expression, making these interchangeable. So we can rewrite the (C.21) as

$$a_{j+1}(N) = \frac{d}{dN} a_j(N) - \psi^{(0)}(N) a_j(N) \quad (\text{C.23})$$

where the property of recursion is now evident.

We connect back to our original goal as set out by (C.15). Now that we have expansion for terms containing gamma functions, we can begin to differentiate. We use the Leibniz rule for differentiating the product of gamma functions:

$$\frac{d}{d\xi} \left(\Gamma(\xi) \frac{\Gamma(N)}{\Gamma(N+\xi)} \right) = \left(\frac{d}{d\xi} \frac{\Gamma(N)}{\Gamma(N+\xi)} \right) \Gamma(\xi) + \frac{\Gamma(N)}{\Gamma(N+\xi)} \left(\frac{d}{d\xi} \Gamma(\xi) \right). \quad (\text{C.24})$$

Consider the first term of (C.24). Using (C.19) and (B.4), we can expand this term as

$$\left(\frac{d}{d\xi} \frac{\Gamma(N)}{\Gamma(N+\xi)} \right) \Gamma(\xi) = \sum_{j'=1}^{\infty} \frac{a_{j'}(N)}{(j'-1)!} \xi^{j'-2} + \sum_{j'=1}^{\infty} \sum_{j=1}^{\infty} \frac{a_{j'}(N) b_j(1)}{j!(j-1)!} \xi^{j+j'-2}. \quad (\text{C.25})$$

In the limit $\xi \rightarrow 0$, most of the terms in these sums will vanish, which motivates a re-write of the above in orders of ξ ,

$$\left(\frac{d}{d\xi} \frac{\Gamma(N)}{\Gamma(N+\xi)} \right) \Gamma(\xi) = \frac{1}{\xi} a_1(N) + a_2(N) + a_1(N) b_1(1) + \mathcal{O}(\xi). \quad (\text{C.26})$$

Likewise, we can expand the second set of terms of (C.24) using (C.19) and (B.6):

$$\frac{\Gamma(N)}{\Gamma(N+\xi)} \left(\frac{d}{d\xi} \Gamma(\xi) \right) = - \sum_{j'=0}^{\infty} \frac{a_{j'}(N)}{j'!} \xi^{j'-2} + \sum_{j'=0}^{\infty} \sum_{j=2}^{\infty} \frac{a_{j'}(N) b_j(1)}{j'! j(j-2)!} \xi^{j+j'-2}. \quad (\text{C.27})$$

Again, we organise this expression in orders of ξ :

$$\frac{\Gamma(N)}{\Gamma(N+\xi)} \left(\frac{d}{d\xi} \Gamma(\xi) \right) = -\frac{1}{\xi^2} a_0(N) - \frac{1}{\xi} a_1(N) - \frac{1}{2} a_2(N) + \frac{1}{2} b_2(1) + \mathcal{O}(\xi). \quad (\text{C.28})$$

Altogether, we can combine (C.24), (C.26), and (C.28),

$$\frac{d}{d\xi} \left(\Gamma(\xi) \frac{\Gamma(N)}{\Gamma(N+\xi)} \right) = -\frac{1}{\xi^2} + \frac{1}{2} a_2(N) + \frac{1}{2} b_2(1) + a_1(N) b_1(1) + \mathcal{O}(\xi), \quad (\text{C.29})$$

where we have used the identity $a_0(N) = 1$. We plug this into (C.15) to finally arrive at our Mellin transform:

$$M \left(\frac{\log(1-z)}{1-z} \right)_+ = \frac{1}{2} a_2(N) + \frac{1}{2} b_2(1) + a_1(N) b_1(1). \quad (\text{C.30})$$

In terms of polygamma functions (see appendix B.2), this is

$$M \left(\frac{\log(1-z)}{1-z} \right)_+ = \frac{1}{2} \left((\psi^{(0)}(N))^2 + 2\gamma_E \psi^{(0)}(N) - \psi^{(1)}(N) + \gamma_E^2 + \frac{\pi^2}{6} \right), \quad (\text{C.31})$$

where we used identities (B.13) and (B.14) for special values of the polygamma. In the large N limit, we have $\psi^{(0)}(N) = \log(N) - \frac{1}{2N}$ (see (B.12)), and so our Mellin transform takes the form

$$M \left(\frac{\log(1-z)}{1-z} \right)_+ = \frac{1}{2} \left(\log^2(N) - \frac{\log(N)}{N} + 2\gamma_E \log(N) - (\gamma_E + 1) \frac{1}{N} \right) + \dots \quad (\text{C.32})$$

where the ellipses denote highly subleading terms and constants. We highlight the leading log of this expression,

$$M \left(\frac{\log(1-z)}{1-z} \right)_+ \Big|_{LL} = \frac{1}{2} \log^2(N). \quad (\text{C.33})$$

We can also Mellin transform NLP terms. We will only consider those appearing at NLO, i.e.,

$$\tilde{f}(z) = \log(1-z) \quad (\text{C.34})$$

The analogue of expression (C.15) for the Mellin transform of this type of term is

$$M \tilde{f}(z) = \int_0^1 dz z^{N-1} \log(1-z) = \frac{d}{d\xi} \left(\frac{\Gamma(\xi+1)\Gamma(N)}{\Gamma(N+\xi+1)} \right) \Big|_{\xi=0}. \quad (\text{C.35})$$

This simplifies to

$$M \log(1-z) = \frac{-1}{N} \left(\psi^{(1)}(N+1) + \gamma_E \right), \quad (\text{C.36})$$

which in the large N limit is

$$M \log(1-z) = \frac{-1}{N} \left(\log(N) + \gamma_E - \frac{1}{2N} \right). \quad (\text{C.37})$$

We highlight the leading log term

$$M \log(1-z) \Big|_{LL} = \frac{-\log(N)}{N}. \quad (\text{C.38})$$

C.4 The Laplace Transform

The Laplace transform of a function $f(t)$ is defined as

$$F(s) \equiv \mathcal{L}[f(t)] = \int_0^{\infty} dt e^{-st} f(t). \quad (\text{C.39})$$

The inverse Laplace transform is then

$$f(t) = \mathcal{L}^{-1}[F(s)] = \int_{\gamma-i\infty}^{\gamma+i\infty} \frac{ds}{2\pi i} e^{st} F(s), \quad (\text{C.40})$$

where γ is a real number. We will consider an example of $f(t)$ that is relevant for many calculations in this thesis,

$$f(t) = t^n \quad (\text{C.41})$$

for some positive integer n . The Laplace transform is

$$F(s) = \mathcal{L}[t^n] = \int_0^{\infty} dt e^{-st} t^n. \quad (\text{C.42})$$

Using integration by parts, we have

$$\begin{aligned} \mathcal{L}[t^n] &= \left. \frac{-1}{s} e^{-st} t^n \right|_{t=0}^{\infty} + \frac{n}{s} \int_0^{\infty} dt e^{-st} t^{n-1} \\ &= \frac{n}{s} \int_0^{\infty} dt e^{-st} t^{n-1}, \end{aligned} \quad (\text{C.43})$$

where the first term of the first line vanishes. We can repeat the integration by parts again, and will see

$$\mathcal{L}[t^n] = \frac{n(n-1)}{s^2} \int_0^{\infty} dt e^{-st} t^{n-2}. \quad (\text{C.44})$$

Repeating this step iteratively will eventually yield

$$\mathcal{L}[t^n] = \frac{n(n-1)(n-2)\dots(n-(n-1))}{s^n} \int_0^{\infty} dt e^{-st} t^0. \quad (\text{C.45})$$

Finally we have

$$F(s) = \mathcal{L}[t^n] = \int_0^{\infty} dt e^{-st} t^n = \frac{n!}{s^{n+1}} = \frac{\Gamma(n+1)}{s^{n+1}}. \quad (\text{C.46})$$

Incidentally, by (C.46) we also recover the integral identity of the gamma function (stated in equation (B.2)), where $s = 1$:

$$\Gamma(n) = \int_0^{\infty} dt e^{-t} t^{n-1}. \quad (\text{C.47})$$

Additionally, (C.46) implies that we have the inverse Laplace transform,

$$\mathcal{L}^{-1} \left[\left(\frac{1}{s} \right)^n \right] = \int_{-i\infty}^{i\infty} \frac{ds}{2\pi i} e^{st} \left(\frac{1}{s} \right)^n = \frac{t^{n-1}}{(n-1)!} = \frac{t^{n-1}}{\Gamma(n)}. \quad (\text{C.48})$$

Although this identity has been derived by considering only positive integer values of n , it also holds for any $n > 0$.

Appendix D

Sudakov Decomposition

In threshold related calculations, the Sudakov decomposition is particularly useful as it separates transverse momenta from collinear and anti-collinear momenta. In this decomposition, the emitted gluon can be parametrized as

$$k^\mu = k_+ \beta^\mu + k_- \bar{\beta}^\mu + k_T^\mu \quad (\text{D.1})$$

where k_T is a d -vector transverse to the dimensionless vectors β^μ and $\bar{\beta}^\mu$ defined in (3.18),

$$k_T \cdot \beta = k_T \cdot \bar{\beta} = 0. \quad (\text{D.2})$$

The k_+ and k_- terms can be arrived at by contracting (3.43) with \bar{p} and p respectively:

$$k_+ = \frac{2\bar{p} \cdot k}{\sqrt{\hat{s}}} \quad ; \quad k_- = \frac{2p \cdot k}{\sqrt{\hat{s}}}. \quad (\text{D.3})$$

Further to this, we can choose a parametrisation such that we can express the transverse vector as

$$k_T^\mu = (0, \mathbf{k}_T, 0) \quad (\text{D.4})$$

where \mathbf{k}_T is a $d - 2$ dimensional vector. In this case, we can also parametrize the incoming particles as:

$$p^\mu = (E_1, 0, 0, \dots, 0, E_1) \quad \text{and} \quad \bar{p}^\mu = (E_2, 0, 0, \dots, 0, -E_2) \quad (\text{D.5})$$

where the Mandelstam invariant $\hat{s} = 4E_1 E_2$.

D.1 Jacobian

The integration measure $d^d k$ can be related to the new coordinates by:

$$d^d k = |J| dk_+ dk_- d^{(d-2)} k_T \quad (\text{D.6})$$

where J is the Jacobian determinant, by definition:

$$J = \begin{vmatrix} \frac{\partial k^0}{\partial k_+} & \frac{\partial k^0}{\partial k_-} & \frac{\partial k^0}{\partial k_T^1} & \cdots & \frac{\partial k^0}{\partial k_T^{d-2}} \\ \frac{\partial k^1}{\partial k_+} & \frac{\partial k^1}{\partial k_-} & \frac{\partial k^1}{\partial k_T^1} & \cdots & \frac{\partial k^1}{\partial k_T^{d-2}} \\ \vdots & & & \ddots & \\ \frac{\partial k^{d-1}}{\partial k_+} & \frac{\partial k^{d-1}}{\partial k_-} & \frac{\partial k^{d-1}}{\partial k_T^1} & \cdots & \frac{\partial k^{d-1}}{\partial k_T^{d-2}} \end{vmatrix}. \quad (\text{D.7})$$

Now, these partial derivatives simplify to:

$$\frac{\partial k^\mu}{\partial k_+} = \begin{cases} \frac{E_1}{\sqrt{s}}, & \text{if } \mu = 0 \text{ or } d-1 \\ 0, & \text{otherwise;} \end{cases} \quad (\text{D.8})$$

$$\frac{\partial k^\mu}{\partial k_-} = \begin{cases} \frac{E_2}{\sqrt{s}}, & \text{if } \mu = 0 \\ \frac{-E_2}{\sqrt{s}}, & \text{if } \mu = d-1 \\ 0, & \text{otherwise;} \end{cases} \quad (\text{D.9})$$

$$\frac{\partial k^\mu}{\partial k_T^\nu} = \begin{cases} 0, & \text{if } \mu = 0 \text{ or } d-1 \\ \delta_\nu^\mu, & \text{otherwise.} \end{cases} \quad (\text{D.10})$$

Plugging this into D.7 gives us

$$J = \begin{vmatrix} \frac{E_1}{\sqrt{s}} & \frac{E_2}{\sqrt{s}} & 0 & 0 & 0 & \cdots & 0 \\ 0 & 0 & 1 & 0 & 0 & \cdots & 0 \\ 0 & 0 & 0 & 1 & 0 & \cdots & 0 \\ \vdots & & & & \ddots & & \vdots \\ 0 & 0 & 0 & \cdots & 0 & 1 & 0 \\ \frac{E_1}{\sqrt{s}} & -\frac{E_2}{\sqrt{s}} & 0 & 0 & 0 & \cdots & 0 \end{vmatrix} = \frac{1}{2}. \quad (\text{D.11})$$

Finally we have

$$d^d k = \frac{1}{2} dk_+ dk_- d^{(d-2)} k_T. \quad (\text{D.12})$$

D.2 Integration bounds for k_+ and k_-

The gluon respects the on-shell condition $k^2 = 0$. In Sudakov coordinates, this takes on the form:

$$\begin{aligned} 0 = k^2 &= k_0^2 - \underbrace{[(k_x^2 + \dots) + k_z^2]}_{|\mathbf{k}_T|^2} \\ &= k_0^2 - k_z^2 - |\mathbf{k}_T|^2. \end{aligned} \quad (\text{D.13})$$

This implies that the quantity $k_0^2 - k_z^2$ cannot be negative. Furthermore, we can factorize this such that:

$$k_0^2 - k_z^2 = \underbrace{(k_0 - k_z)}_{\frac{2E_2}{\sqrt{s}}k_-} \underbrace{(k_0 + k_z)}_{\frac{2E_1}{\sqrt{s}}k_+} \geq 0. \quad (\text{D.14})$$

This condition tells us that:

- the quantities $k_0 - k_z$ and $k_0 + k_z$ must either both be positive, or both negative, and
- $|k_0| \geq |k_z|$.

If we encounter a condition that forces k_0 to be non-negative (such as $\delta_+(k^2)$), then this would mean that

$$\begin{aligned} k_0 - k_z \geq 0 &\rightarrow k_- \geq 0 \\ k_0 + k_z \geq 0 &\rightarrow k_+ \geq 0. \end{aligned}$$

Finally, given that $k_0 - k_z = \frac{2E_2}{\sqrt{s}}k_-$ and $k_0 + k_z = \frac{2E_1}{\sqrt{s}}k_+$, we can write the on-shell condition as

$$k_+k_- - |\mathbf{k}_T|^2 = 0. \quad (\text{D.15})$$

Appendix E

Integrals

Integrals of the form

$$I(m, n, l) = \int_0^\infty dy e^{-y} y^n \int_0^\infty dx e^{-x} x^m \left(\frac{1}{x+y} \right)^l \quad (\text{E.1})$$

can be solved by a change of variable:

$$x = \Lambda\omega ; \quad y = \Lambda(1 - \omega)$$

Under this change of variable, we have

$$dxdy = \Lambda d\Lambda d\omega. \quad (\text{E.2})$$

Then we can rewrite integral E.1 as

$$\begin{aligned} I(m, n, l) &= \underbrace{\int_0^1 d\omega \omega^m (1 - \omega)^n}_{\text{beta function}} \underbrace{\int_0^\infty d\Lambda e^{-\Lambda} \Lambda^{m+n-l+1}}_{\text{gamma function}} \\ &= \frac{\Gamma(m+1)\Gamma(n+1)}{\Gamma(m+n+2)} \Gamma(m+n-l+2), \end{aligned} \quad (\text{E.3})$$

where we identified the integral identities of the beta function (B.15) as well as the gamma function (B.2).

Appendix F

N³LO Data

This appendix collects the coefficient functions $\{f_i^X\}$ for the squared matrix elements. The coefficients for the hard region are

$$\begin{aligned}
 f_1^H &= -\frac{2}{\epsilon^2} - \frac{3}{\epsilon} - 8 + \zeta_2 + \epsilon \left(-16 + \frac{3\zeta_2}{2} + \frac{14\zeta_3}{3} \right) + \epsilon^2 \left(-32 + 4\zeta_2 + 7\zeta_3 + \frac{47\zeta_4}{8} \right) \\
 &\quad + \epsilon^3 \left(-64 + 8\zeta_2 + \frac{56\zeta_3}{3} + \frac{141\zeta_4}{16} + \frac{62\zeta_5}{5} - \frac{7}{3}\zeta_3\zeta_2 \right) + \epsilon^4 \left(-128 + 16\zeta_2 + \frac{112\zeta_3}{3} \right. \\
 &\quad \left. + \frac{47\zeta_4}{2} + \frac{93\zeta_5}{5} - \frac{7\zeta_2\zeta_3}{2} + \frac{949\zeta_6}{64} - \frac{49\zeta_3^2}{9} \right) + \mathcal{O}(\epsilon^5); \\
 f_2^H &= (1 - \epsilon)f_1^H.
 \end{aligned} \tag{F.1}$$

The coefficients for the (anti-)collinear regions are

$$\begin{aligned}
 f_1^C &= -\frac{2}{\epsilon} - \frac{5}{2} + \epsilon(-3 + \zeta_2) + \epsilon^2 \left(-4 + \frac{5\zeta_2}{4} + \frac{14\zeta_3}{3} \right) + \epsilon^3 \left(-6 + \frac{3\zeta_2}{2} + \frac{35\zeta_3}{6} + \frac{47\zeta_4}{8} \right) \\
 &\quad + \epsilon^4 \left(-10 + 2\zeta_2 + 7\zeta_3 + \frac{235\zeta_4}{32} + \frac{62\zeta_5}{5} - \frac{7\zeta_2\zeta_3}{3} \right) + \mathcal{O}(\epsilon^5); \\
 f_2^C &= -\frac{1}{4\epsilon} + \frac{1}{8} + \epsilon \left(\frac{3}{4} + \frac{\zeta_2}{8} \right) + \epsilon^2 \left(2 - \frac{\zeta_2}{16} + \frac{7\zeta_3}{12} \right) + \epsilon^3 \left(\frac{9}{2} - \frac{3\zeta_2}{8} - \frac{7\zeta_3}{24} + \frac{47\zeta_4}{64} \right) \\
 &\quad + \epsilon^4 \left(\frac{19}{2} - \zeta_2 - \frac{7\zeta_3}{4} - \frac{47\zeta_4}{128} + \frac{31\zeta_5}{20} - \frac{7\zeta_2\zeta_3}{24} \right) + \mathcal{O}(\epsilon^5); \\
 f_3^C &= \frac{1}{4\epsilon^2} - \frac{1}{8\epsilon} - \frac{3}{4} - \frac{\zeta_2}{8} + \epsilon \left(-2 + \frac{\zeta_2}{16} - \frac{7\zeta_3}{12} \right) + \epsilon^2 \left(-\frac{9}{2} + \frac{3\zeta_2}{8} + \frac{7\zeta_3}{24} - \frac{47\zeta_4}{64} \right) \\
 &\quad + \epsilon^3 \left(-\frac{19}{2} + \zeta_2 + \frac{7\zeta_3}{4} + \frac{47\zeta_4}{128} - \frac{31\zeta_5}{20} + \frac{7}{24}\zeta_2\zeta_3 \right) + \epsilon^4 \left(-\frac{39}{2} + \frac{9\zeta_2}{4} + \frac{14\zeta_3}{3} + \frac{141\zeta_4}{64} \right. \\
 &\quad \left. + \frac{31\zeta_5}{40} - \frac{7\zeta_2\zeta_3}{48} - \frac{949\zeta_6}{512} + \frac{49\zeta_3^2}{72} \right) + \mathcal{O}(\epsilon^5).
 \end{aligned} \tag{F.2}$$

For the soft region, we have

$$\begin{aligned}
f_1^S &= \frac{1}{4\epsilon^2} + \frac{1}{4\epsilon} + \frac{1}{2} - \frac{\zeta_2}{8} + \epsilon \left(1 - \frac{\zeta_2}{8} - \frac{7\zeta_3}{12} \right) + \epsilon^2 \left(2 - \frac{\zeta_2}{4} - \frac{7\zeta_3}{12} - \frac{47\zeta_4}{64} \right) \\
&\quad + \epsilon^3 \left(4 - \frac{\zeta_2}{2} - \frac{7\zeta_3}{6} - \frac{47\zeta_4}{64} - \frac{31\zeta_5}{20} + \frac{7\zeta_2\zeta_3}{24} \right) \\
&\quad + \epsilon^4 \left(8 - \zeta_2 - \frac{7\zeta_3}{3} - \frac{47\zeta_4}{32} - \frac{31\zeta_5}{20} + \frac{7\zeta_2\zeta_3}{24} - \frac{949\zeta_6}{512} + \frac{49\zeta_3^2}{72} \right) + \mathcal{O}(\epsilon^5); \\
f_2^S &= \frac{1}{4\epsilon} + \frac{1}{2} + \epsilon \left(1 - \frac{\zeta_2}{8} \right) + \epsilon^2 \left(2 - \frac{\zeta_2}{4} - \frac{7\zeta_3}{12} \right) + \epsilon^3 \left(4 - \frac{\zeta_2}{2} - \frac{7\zeta_3}{6} - \frac{47\zeta_4}{64} \right) \\
&\quad + \epsilon^4 \left(8 - \zeta_2 - \frac{7\zeta_3}{3} - \frac{47\zeta_4}{32} - \frac{31\zeta_5}{20} + \frac{7\zeta_2\zeta_3}{24} \right) + \mathcal{O}(\epsilon^5); \\
f_3^S &= \frac{1}{4\epsilon} + \frac{1}{4} + \epsilon \left(\frac{1}{2} - \frac{\zeta_2}{8} \right) + \epsilon^2 \left(1 - \frac{\zeta_2}{8} - \frac{7\zeta_3}{12} \right) + \epsilon^3 \left(2 - \frac{\zeta_2}{4} - \frac{7\zeta_3}{12} - \frac{47\zeta_4}{64} \right) \\
&\quad + \epsilon^4 \left(4 - \frac{\zeta_2}{2} - \frac{7\zeta_3}{6} - \frac{47\zeta_4}{64} - \frac{31\zeta_5}{20} + \frac{7\zeta_2\zeta_3}{24} \right) + \mathcal{O}(\epsilon^5). \tag{F.3}
\end{aligned}$$

Appendix G

The Schwarzschild Metric in Kerr-Schild coordinates

In this appendix, we show how to move between spherical polar coordinates and Kerr-Schild coordinates for the Schwarzschild solution. We do this for both signatures of the Minkowski metric - the choice of which impacts the Kerr-Schild form.

G.0.1 Mostly + signature

For $\eta_{\mu\nu} = (-1, 1, 1, 1)$ the Schwarzschild metric in spherical polar coordinates is

$$g_{\mu\nu} dx^\mu dx^\nu = - \left(1 - \frac{2GM}{r}\right) dt^2 + \left(1 - \frac{2GM}{r}\right)^{-1} dr^2 + r^2(d\theta^2 + \sin^2 \theta d\phi^2). \quad (\text{G.1})$$

The Kerr-Schild form of this metric is given by

$$g_{\mu\nu}^{KS} = \eta_{\mu\nu} + \phi k_\mu k_\nu \quad (\text{G.2})$$

where $\phi = \frac{2GM}{r}$ and $k_\mu = (1, x^i/r)$. Here is the proof:

$$g_{\mu\nu}^{KS} dx^\mu dx^\nu = -dt_{KS}^2 + dx^2 + dy^2 + dz^2 + \frac{2GM}{r} (k_\mu dx^\mu)^2. \quad (\text{G.3})$$

We unpack $k_\mu dx^\mu$ to be

$$k_\mu dx^\mu = dt_{KS} + \frac{x^i}{r} dx^i = dt_{KS} + dr \quad (\text{G.4})$$

where we used the fact that $r^2 = x^i x_i$ to lead us to $dr = \frac{x^i}{r} dx^i$. Combining this with a change to spherical polar coordinates leaves us with

$$dS^2 = g_{\mu\nu}^{KS} dx^\mu dx^\nu = - \left(1 - \frac{2GM}{r}\right) dt_{KS}^2 + \left(1 + \frac{2GM}{r}\right) dr^2$$

$$+ \frac{4GM}{r} dt_K S dr + r^2(d\theta^2 + \sin^2 \theta d\phi^2). \quad (\text{G.5})$$

Now we consider the variable change

$$t_{KS} = t + 2GM \ln \left| \frac{r}{2GM} - 1 \right| + C \quad \rightarrow \quad dt_{KS} = dt + \frac{2GM}{r - 2GM} dr \quad (\text{G.6})$$

Plugging (G.6) into (G.5) leaves us with the Schwarzschild metric as per (G.1).

G.0.2 Mostly - signature

For $\eta_{\mu\nu} = (1, -1, -1, -1)$ the Schwarzschild metric in spherical polar coordinates is

$$g_{\mu\nu} dx^\mu dx^\nu = \left(1 - \frac{2GM}{r}\right) dt^2 - \left(1 - \frac{2GM}{r}\right)^{-1} dr^2 - r^2(d\theta^2 + \sin^2 \theta d\phi^2). \quad (\text{G.7})$$

The Kerr-Schild form of this metric is given by

$$g_{\mu\nu}^{KS} = \eta_{\mu\nu} - \phi k_\mu k_\nu \quad (\text{G.8})$$

where $\phi = \frac{2GM}{r}$ and $k_\mu = (1, x^i/r)$. Here is the proof:

$$g_{\mu\nu}^{KS} dx^\mu dx^\nu = dt_{KS}^2 - dx^2 - dy^2 - dz^2 - \frac{2GM}{r} (k_\mu dx^\mu)^2. \quad (\text{G.9})$$

We unpack $k_\mu dx^\mu$ to be

$$k_\mu dx^\mu = dt_{KS} - \frac{x^i}{r} dx^i = dt_{KS} + dr \quad (\text{G.10})$$

where we used the fact that $r^2 = -x^i x_i$ to lead us to $dr = \frac{x^i}{r} dx^i$. Combining this with a change to spherical polar coordinates leaves us with

$$\begin{aligned} dS^2 = g_{\mu\nu}^{KS} dx^\mu dx^\nu &= \left(1 - \frac{2GM}{r}\right) dt_{KS}^2 - \left(1 + \frac{2GM}{r}\right) dr^2 \\ &\quad - \frac{4GM}{r} dt_K S dr - r^2(d\theta^2 + \sin^2 \theta d\phi^2). \end{aligned} \quad (\text{G.11})$$

And now we use exactly the same variable change (G.6) as for the mostly plus case. Plugging (G.6) into (G.11) leaves us with the Schwarzschild metric as per (G.7).

Appendix H

Ultraboosting the general $SU(2) \times SU(2)$ Monopole

In section 10.2, the spherically symmetric biadjoint monopole solution of (10.56) ultraboosts to a finite quantity rather than a shockwave. In this appendix, we show that the ultraboost procedure fails to produce shockwaves when applied to the more general monopole solutions of (9.11) (derived in [128]). Recall that these solutions have the form

$$\Phi^{aa'} = \frac{1}{\lambda r^2} \left[-k \left(\delta^{aa'} - \frac{x^a x^{a'}}{r^2} \right) \pm \sqrt{2k - k^2} \frac{\epsilon^{aa'd} x^d}{r} \right], \quad 0 \leq k \leq 2. \quad (\text{H.1})$$

As in section 10.2, we boost in the x -direction, and examine the behaviour of the boosted solution inside and outside the plane $x = t$. Outside of the plane, we find that the solution vanishes completely:

$$\Phi^{aa'} \xrightarrow{\gamma \rightarrow \infty} 0 \quad \text{for } x - t \neq 0. \quad (\text{H.2})$$

Inside of the plane, just as for the ultraboost of the (10.58), the field takes finite values and displays no divergent behaviour. More specifically, in the limit $\gamma \rightarrow \infty$ we find

$$\begin{aligned} \Phi^{12} = -\Phi^{21} &\rightarrow \frac{z\sqrt{(k^2 - 2k)}}{\lambda(y^2 + z^2)^{3/2}}, \quad \Phi^{13} = -\Phi^{31} \rightarrow -\frac{y\sqrt{(k^2 - 2k)}}{\lambda(y^2 + z^2)^{3/2}}, \quad \Phi^{23} = \Phi^{32} \rightarrow \frac{yzk}{\lambda(y^2 + z^2)^2}, \\ \Phi^{11} &\rightarrow \frac{-k}{\lambda(y^2 + z^2)}, \quad \Phi^{22} \rightarrow \frac{-kz^2}{\lambda(y^2 + z^2)^2}, \quad \Phi^{33} \rightarrow \frac{-ky^2}{\lambda(y^2 + z^2)^2}. \end{aligned} \quad (\text{H.3})$$

Similarly to (10.58), the ultraboosted solutions (H.3) remain finite in the plane $x = t$, and therefore, they do not constitute shockwaves. Rescaling the coupling according to $\lambda \rightarrow \lambda/\gamma$ can remedy this, however, this entails changing the theory, than the object under the ultraboost.

Appendix I

Gauge Transforming the Dirac Monopole to the Wu-Yang Monopole

In this appendix, we transform the Dirac monopole to the Wu-Yang monopole, closely following [137, 138]. Consider the embedded Dirac monopole of (10.62), i.e.

$$A_\mu = -\frac{\tilde{g}}{4\pi} \left(0, 0, 0, \frac{1 - \cos \theta}{r \sin \theta} \right) \sigma_3. \quad (\text{I.1})$$

We apply the gauge transformation (10.66) to the above and work out what the non-zero components of the transformed gauge field will be. Note that in spherical polar coordinates, taking into account the appropriate scale factors, the four-derivative is

$$\partial_\mu = \left(\frac{\partial}{\partial t}, \frac{\partial}{\partial r}, \frac{1}{r} \frac{\partial}{\partial \theta}, \frac{1}{r \sin \theta} \frac{\partial}{\partial \phi} \right) \equiv \left(\partial_t, \partial_r, \frac{1}{r} \partial_\theta, \frac{1}{r \sin \theta} \partial_\phi \right). \quad (\text{I.2})$$

Stripping out the coupling, the ϕ component of the transformation is defined by (10.65) as

$$A'_{(\phi)} = U A_{(\phi)} U^{(-1)} + \frac{i}{r \sin \theta} U \partial_\phi U^{-1}. \quad (\text{I.3})$$

In the first term, we utilise the fact that σ_3 commutes with itself:

$$U A_{(\phi)} U^{(-1)} = -\frac{1 - \cos \theta}{r \sin \theta} \left[e^{-i\phi\sigma_3} e^{-i\theta\sigma_2} \sigma_3 e^{i\theta\sigma_2} e^{i\phi\sigma_3} \right]. \quad (\text{I.4})$$

This is likewise the case in the second term

$$\begin{aligned} \frac{i}{r \sin \theta} U \partial_\phi U^{-1} &= \frac{i}{r \sin \theta} \left[U (-i\sigma_3) U^{-1} + U U^{-1} (i\sigma_3) \right] \\ &= \frac{1}{r \sin \theta} \left[e^{-i\phi\sigma_3} e^{-i\theta\sigma_2} \sigma_3 e^{i\theta\sigma_2} e^{i\phi\sigma_3} - \sigma_3 \right]. \end{aligned} \quad (\text{I.5})$$

Altogether, we have

$$A'_{(\phi)} = \frac{1}{r \sin \theta} \left[\cos \theta (e^{-i\phi\sigma_3} e^{-i\theta\sigma_2} \sigma_3 e^{i\theta\sigma_2} e^{i\phi\sigma_3}) - \sigma_3 \right]. \quad (\text{I.6})$$

We can simplify the above by expressing each exponential as a Taylor series, e.g.

$$e^{i\theta\sigma_2} = \sum_{k=0}^{\infty} \frac{(i\theta\sigma_2)^k}{k!}. \quad (\text{I.7})$$

Note that for any σ_m (defined in (10.63)) we have

$$\sigma_m^k = \begin{cases} \left(\frac{1}{2}\right)^k I, & k \text{ is even} \\ \left(\frac{1}{2}\right)^{k-1} \sigma_m, & k \text{ is odd.} \end{cases} \quad (\text{I.8})$$

With these two identities, it is straightforward to show that

$$e^{i\theta\sigma_2} = I \cos\left(\frac{\theta}{2}\right) + 2i\sigma_2 \sin\left(\frac{\theta}{2}\right). \quad (\text{I.9})$$

This simplifies (I.6) considerably. For example,

$$e^{-i\theta\sigma_2} \sigma_3 e^{i\theta\sigma_2} = \left[I \cos\left(\frac{\theta}{2}\right) + 2i\sigma_2 \sin\left(\frac{\theta}{2}\right) \right] \sigma_3 \left[I \cos\left(\frac{\theta}{2}\right) - 2i\sigma_2 \sin\left(\frac{\theta}{2}\right) \right], \quad (\text{I.10})$$

which, when expanded, reduces to

$$e^{-i\theta\sigma_2} \sigma_3 e^{i\theta\sigma_2} = \sigma_3 \cos \theta + \sigma_1 \sin \theta. \quad (\text{I.11})$$

The same process applies for the remaining exponentials, ultimately resulting in

$$A'_{(\phi)} = \frac{1}{r} [\sigma_1 \cos \theta \cos \phi + \sigma_2 \cos \theta \sin \phi - \sigma_3 \sin \theta], \quad (\text{I.12})$$

which is still stripped of the coupling. The other non-zero component $A'_{(\theta)}$ (stripped of the coupling) is much simpler,

$$A'_{(\theta)} = \frac{i}{r} U \partial_{\theta} U^{-1} = \frac{-1}{r} e^{-i\phi\sigma_3} \sigma_2 e^{i\phi\sigma_3}. \quad (\text{I.13})$$

Using the same technology described above, this reduces to

$$A'_{(\theta)} = \frac{1}{r} [\sigma_1 \sin \phi - \sigma_2 \cos \phi]. \quad (\text{I.14})$$

To transform the field into Cartesian coordinates, we use the tensor transformation law

$$A_\mu = \frac{\partial x'^\nu}{\partial x^\mu} A'_{(\nu)} h_{(\nu)} \quad (\text{I.15})$$

where $h_{(\nu)}$ is a scale factor, and $A'_{(\nu)}$ has the same units as the field. Their product forms the covariant tensor components

$$A'_\nu = A'_{(\nu)} h_{(\nu)}. \quad (\text{I.16})$$

For a deeper discussion on tensor transformations of this type, see [145]. In our case, the scale factors we need are

$$h_{(\theta)} = r, \quad h_{(\phi)} = r \sin \theta. \quad (\text{I.17})$$

The non-zero partial derivatives in a convenient form are

$$\begin{aligned} \frac{\partial \theta}{\partial x} &= \frac{z}{r^2} \cos \phi, & \frac{\partial \theta}{\partial y} &= \frac{z}{r^2} \sin \phi, & \frac{\partial \theta}{\partial z} &= \frac{-\sin \theta}{r}, \\ \frac{\partial \phi}{\partial x} &= \frac{-y}{r^2 \sin^2 \theta}, & \frac{\partial \phi}{\partial y} &= \frac{x}{r^2 \sin^2 \theta}. \end{aligned} \quad (\text{I.18})$$

When combining the partial derivatives (I.18), scale factors (I.17), and physical components (I.12),(I.14) according to the tensor transformation law (I.15), we have

$$\begin{aligned} A_x &= \frac{1}{r^2} [y\sigma_3 - z\sigma_2] \\ A_y &= \frac{1}{r^2} [z\sigma_1 - x\sigma_3] \\ A_z &= \frac{1}{r^2} [x\sigma_2 - y\sigma_1]. \end{aligned} \quad (\text{I.19})$$

Reinstating the coupling, and expressing this in index notation, we have

$$A_0^a = 0; \quad A_i^a = \frac{-\tilde{g}\epsilon_{iak}x^k}{4\pi r^2}, \quad (\text{I.20})$$

where

$$A_\mu = A_\mu^a \sigma_a. \quad (\text{I.21})$$

Appendix J

Ultraboosting the Wu-Yang Monopole

Consider a boost to the Wu-Yang monopole²⁵ in the x -direction,

$$A'^{\mu} = (\Lambda^{-1})^{\mu}_{\nu} A^{\nu}(\Lambda x) = \frac{1}{\gamma^2(x-vt)^2 + \rho^2} \begin{pmatrix} \gamma v(y\sigma_3 - z\sigma_2) \\ \gamma(y\sigma_3 - z\sigma_2) \\ -\gamma(x-vt)\sigma_3 + z\sigma_1 \\ \gamma(x-vt)\sigma_2 - y\sigma_1 \end{pmatrix}, \quad (\text{J.1})$$

where Λ is the Lorentz boost matrix defined in (10.6). To understand how (J.1) behaves in the ultraboost limit $v \rightarrow 1$, we will examine each component inside and outside the lightfront plane $x - t = 0$. The y and z components are the most straightforward,

$$\lim_{v \rightarrow 1} A'^y = \begin{cases} \frac{z\sigma_1}{\rho^2}, & x = t \\ 0, & x \neq t \end{cases} ; \quad \lim_{v \rightarrow 1} A'^z = \begin{cases} \frac{-y\sigma_1}{\rho^2}, & x = t \\ 0, & x \neq t. \end{cases} \quad (\text{J.2})$$

Now onto the A'^x component:

$$\lim_{v \rightarrow 1} A'^x = \lim_{v \rightarrow 1} \frac{\gamma(y\sigma_3 - z\sigma_2)}{\gamma^2(x-vt)^2 + \rho^2} = \begin{cases} \infty, & x = t \\ 0, & x \neq t. \end{cases} \quad (\text{J.3})$$

This has the profile of a delta function. If we postulate that

$$\lim_{v \rightarrow 1} \frac{\gamma(y\sigma_3 - z\sigma_2)}{\gamma^2(x-vt)^2 + \rho^2} = a \delta(x-t), \quad (\text{J.4})$$

²⁵It is easiest to use the form in (I.19), stripped of coupling. The A^0 component is zero.

then integration of both sides over x should recover the normalisation a . In this vein, we have

$$\lim_{v \rightarrow 1} \int_{-\infty}^{\infty} dx \frac{\gamma(y\sigma_3 - z\sigma_2)}{\gamma^2(x - vt)^2 + \rho^2} = (y\sigma_3 - z\sigma_2) \int_{-\infty}^{\infty} \frac{d\tilde{x}}{\tilde{x}^2 + \rho^2}, \quad (\text{J.5})$$

where we made the variable change $\tilde{x} = \gamma(x - vt)$ thereby removing all dependence of v from the integral. A further variable change $\tilde{x} = \rho \tan \theta$ simplifies the above considerably, since

$$\int_{-\infty}^{\infty} \frac{d\tilde{x}}{\tilde{x}^2 + \rho^2} = \int_{-\frac{\pi}{2}}^{\frac{\pi}{2}} \frac{d\theta}{\rho} = \frac{\pi}{\rho}. \quad (\text{J.6})$$

As A'^t has the same profile as A'^x then we have the succinct form for the ultraboosted Wu-Yang monopole (with coupling stripped),

$$A'^{\mu} = (y\sigma_3 - z\sigma_2) \frac{\pi}{\rho} \delta(x - t) n^{\mu} + w^{\mu}, \quad (\text{J.7})$$

where n^{μ} is defined in (10.38), and w^{μ} is a vector representing a finite quantity inside the lightfront plane

$$w^{\mu} = \frac{\sigma_1}{\rho^2} \begin{cases} (0, 0, z, -y), & x = t \\ (0, 0, 0, 0), & x \neq t. \end{cases} \quad (\text{J.8})$$

This finite quantity could be gauged away, but its presence does not affect our conclusion. Clearly the delta function in (J.7) indicates that the Wu-Yang monopole has been ultraboosted to a shockwave.

Bibliography

- [1] N. Bahjat-Abbas, R. Stark-Muchão, and C. D. White, *Biadjoint wires*, *Physics Letters B* **788** (Jan, 2019) 274–279.
- [2] N. Bahjat-Abbas, R. Stark-Muchão, and C. D. White, *Monopoles, shockwaves and the classical double copy*, *JHEP* **04** (2020) 102, [[arXiv:2001.0991](https://arxiv.org/abs/2001.0991)].
- [3] N. Bahjat-Abbas, J. Sinninghe Damsté, L. Vernazza, and C. D. White, *On next-to-leading power threshold corrections in Drell-Yan production at N^3LO* , *Journal of High Energy Physics* **2018** (Oct., 2018) 144, [[arXiv:1807.0924](https://arxiv.org/abs/1807.0924)].
- [4] N. Bahjat-Abbas, D. Bonocore, J. Sinninghe Damsté, E. Laenen, L. Magnea, L. Vernazza, and C. D. White, *Diagrammatic resummation of leading-logarithmic threshold effects at next-to-leading power*, *Journal of High Energy Physics* **2019** (Nov., 2019) 2, [[arXiv:1905.1371](https://arxiv.org/abs/1905.1371)].
- [5] G. Luisoni and S. Marzani, *QCD resummation for hadronic final states*, *Journal of Physics G Nuclear Physics* **42** (Oct., 2015) 103101, [[arXiv:1505.0408](https://arxiv.org/abs/1505.0408)].
- [6] J. Campbell, J. Huston, and F. Krauss, *The Black Book of Quantum Chromodynamics*. 2017.
- [7] T. Kinoshita, *Mass singularities of Feynman amplitudes*, *J. Math. Phys.* **3** (1962) 650–677.
- [8] T. D. Lee and M. Nauenberg, *Degenerate Systems and Mass Singularities*, *Phys. Rev.* **133** (1964) B1549–B1562. [[25\(1964\)](https://arxiv.org/abs/25(1964))].
- [9] N. Nakanishi, *General Theory of Infrared Divergence*, *Progress of Theoretical Physics* **19** (02, 1958) 159–168, [<https://academic.oup.com/ptp/article-pdf/19/2/159/5387237/19-2-159.pdf>].
- [10] M. Dittmar, S. Forte, A. Glazov, S. Moch, S. Alekhin, G. Altarelli, J. Andersen, R. D. Ball, J. Blumlein, H. Bottcher, T. Carli, M. Ciafaloni, D. Colferai, A. Cooper-Sarkar, G. Corcella, L. Del Debbio, G. Dissertori, J. Feltesse, A. Guffanti, C. Gwenlan, J. Huston, G. Ingelman, M. Klein, J. I. Latorre,

- T. Lastovicka, G. Lastovicka-Medin, L. Magnea, A. Piccione, J. Pumplin, V. Ravindran, B. Reisert, J. Rojo, A. Sabio Vera, G. P. Salam, F. Siegert, A. Stasto, H. Stenzel, C. Targett-Adams, R. S. Thorne, A. Tricoli, J. A. M. Vermaseren, and A. Vogt, *Parton Distributions: Summary Report*, *arXiv e-prints* (Nov., 2005) hep-ph/0511119, [hep-ph/0511119].
- [11] V. Bertone, M. Botje, D. Britzger, S. Camarda, A. Cooper-Sarkar, F. Giuli, A. Glazov, A. Luszczak, F. I. Olness, R. Placakyte, V. Radescu, W. Slominski, and O. Zenaiev, *xFitter 2.0.0: An Open Source QCD Fit Framework*, in *Proceedings of the XXV International Workshop on Deep-Inelastic Scattering and Related Subjects. 3-7 April 2017. University of Birmingham*, p. 203, Jan., 2017. arXiv:1709.0115.
- [12] J. Gao, L. Harland-Lang, and J. Rojo, *The Structure of the Proton in the LHC Precision Era*, *Phys. Rept.* **742** (2018) 1–121, [arXiv:1709.0492].
- [13] S. Forte and G. Ridolfi, *Renormalization group approach to soft gluon resummation*, *Nuclear Physics B* **650** (Feb., 2003) 229–270, [hep-ph/0209154].
- [14] S. D. Drell and T.-M. Yan, *Massive Lepton Pair Production in Hadron-Hadron Collisions at High-Energies*, *Phys. Rev. Lett.* **25** (1970) 316–320. [Erratum: *Phys. Rev. Lett.* 25,902(1970)].
- [15] G. Altarelli, R. K. Ellis, and G. Martinelli, *Large Perturbative Corrections to the Drell-Yan Process in QCD*, *Nucl. Phys.* **B157** (1979) 461–497.
- [16] T. Matsuura, R. Hamberg, and W. L. Van Neerven, *The contribution of the gluon-gluon subprocess to the Drell-Yan K-factor*, *Nuclear Physics B Proceedings Supplements* **23** (Aug., 1991) 3–8.
- [17] R. Hamberg, W. L. van Neerven, and T. Matsuura, *A complete calculation of the order α_s^2 correction to the Drell-Yan K-factor*, *Nuclear Physics B* **359** (Aug., 1991) 343–405.
- [18] T. Matsuura, S. C. van der Marck, and W. L. van Neerven, *The calculation of the second order soft and virtual contributions to the Drell-Yan cross section*, *Nuclear Physics B* **319** (June, 1989) 570–622.
- [19] T. Matsuura, S. C. van der Marck, and W. L. van Neerven, *The order α_s^2 contribution to the K-factor of the Drell-Yan process*, *Physics Letters B* **211** (Aug., 1988) 171–178.
- [20] T. Matsuura and W. L. van Neerven, *Second order logarithmic corrections to the Drell-Yan cross-section*, *Zeitschrift fur Physik C Particles and Fields* **38** (Dec., 1988) 623–642.

-
- [21] D. Bonocore, E. Laenen, L. Magnea, S. Melville, L. Vernazza, and C. D. White, *A factorization approach to next-to-leading-power threshold logarithms*, *Journal of High Energy Physics* **6** (June, 2015) 8, [[arXiv:1503.0515](#)].
- [22] G. Sterman, *Summation of large corrections to short-distance hadronic cross sections*, *Nuclear Physics B* **281** (Jan., 1987) 310–364.
- [23] S. Catani and L. Trentadue, *Resummation of the QCD perturbative series for hard processes*, *Nuclear Physics B* **327** (Nov., 1989) 323–352.
- [24] G. P. Korchemsky and G. Marchesini, *Partonic distributions for large x and renormalization of Wilson loop*, *Nuclear Physics B* **406** (Sept., 1993) 225–258, [[hep-ph/9210281](#)].
- [25] H. Contopanagos, E. Laenen, and G. Sterman, *Sudakov factorization and resummation*, *Nuclear Physics B* **484** (Feb., 1997) 303–327, [[hep-ph/9604313](#)].
- [26] T. Becher and M. Neubert, *Threshold Resummation in Momentum Space from Effective Field Theory*, *Physical Review Letters* **97** (Aug., 2006) 082001, [[hep-ph/0605050](#)].
- [27] G. Parisi, *Summing large perturbative corrections in qcd*, *Physics Letters B* **90** (1980), no. 3 295 – 296.
- [28] G. Curci and M. Greco, *Large Infrared Corrections in QCD Processes*, *Phys. Lett. B* **92** (1980) 175–178.
- [29] S. Catani and L. Trentadue, *Comment on QCD exponentiation at large x* , *Nucl. Phys. B* **353** (1991) 183–186.
- [30] D. Bonocore, E. Laenen, L. Magnea, L. Vernazza, and C. D. White, *Non-abelian factorisation for next-to-leading-power threshold logarithms*, *Journal of High Energy Physics* **2016** (Dec., 2016) 121, [[arXiv:1610.0684](#)].
- [31] H. Gervais, *Soft photon theorem for high energy amplitudes in Yukawa and scalar theories*, *Phys. Rev. D* **95** (June, 2017) 125009, [[arXiv:1704.0080](#)].
- [32] H. Gervais, *Soft graviton emission at high and low energies in Yukawa and scalar theories*, *Phys. Rev. D* **96** (Sept., 2017) 065007, [[arXiv:1706.0345](#)].
- [33] D. W. Kolodrubetz, I. Moutl, and I. W. Stewart, *Building blocks for subleading helicity operators*, *Journal of High Energy Physics* **2016** (May, 2016) 139, [[arXiv:1601.0260](#)].

-
- [34] A. J. Larkoski, D. Neill, and I. W. Stewart, *Soft theorems from effective field theory*, *Journal of High Energy Physics* **2015** (June, 2015) 77, [arXiv:1412.3108].
- [35] I. Moulton, L. Rothen, I. W. Stewart, F. J. Tackmann, and H. X. Zhu, *Subleading power corrections for N -jettiness subtractions*, *Phys. Rev. D* **95** (Apr., 2017) 074023, [arXiv:1612.0045].
- [36] I. Moulton, I. W. Stewart, and G. Vita, *A subleading operator basis and matching for $gg \rightarrow H$* , *Journal of High Energy Physics* **2017** (July, 2017) 67, [arXiv:1703.0340].
- [37] C.-H. Chang, I. W. Stewart, and G. Vita, *A subleading power operator basis for the scalar quark current*, *Journal of High Energy Physics* **2018** (Apr., 2018) 41, [arXiv:1712.0434].
- [38] I. Feige, D. W. Kolodrubetz, I. Moulton, and I. W. Stewart, *A complete basis of helicity operators for subleading factorization*, *Journal of High Energy Physics* **2017** (Nov., 2017) 142, [arXiv:1703.0341].
- [39] C. D. White, *An introduction to webs*, *Journal of Physics G Nuclear Physics* **43** (Apr., 2016) 033002, [arXiv:1507.0216].
- [40] E. Laenen, L. Magnea, G. Stavenga, and C. D. White, *Next-to-eikonal corrections to soft gluon radiation: a diagrammatic approach*, *Journal of High Energy Physics* **1** (Jan., 2011) 141, [arXiv:1010.1860].
- [41] R. Akhouri, R. Saotome, and G. Sterman, *High energy scattering in perturbative quantum gravity at next-to-leading power*, *Phys. Rev. D* **103** (Mar, 2021) 064036.
- [42] E. Laenen, G. Stavenga, and C. D. White, *Path integral approach to eikonal and next-to-eikonal exponentiation*, *JHEP* **03** (2009) 054, [arXiv:0811.2067].
- [43] J. Gatheral, *Exponentiation of Eikonal Cross-sections in Nonabelian Gauge Theories*, *Phys. Lett. B* **133** (1983) 90–94.
- [44] J. Frenkel and J. Taylor, *NONABELIAN EIKONAL EXPONENTIATION*, *Nucl. Phys. B* **246** (1984) 231–245.
- [45] G. F. Sterman, *Infrared divergences in perturbative QCD*, *AIP Conf. Proc.* **74** (1981) 22–40.
- [46] L. J. Dixon, L. Magnea, and G. F. Sterman, *Universal structure of subleading infrared poles in gauge theory amplitudes*, *JHEP* **08** (2008) 022, [arXiv:0805.3515].

-
- [47] E. Gardi and L. Magnea, *Infrared singularities in QCD amplitudes, Frascati Phys. Ser.* **50** (2010) 137–157, [[arXiv:0908.3273](#)].
- [48] A. M. Polyakov, *Gauge Fields as Rings of Glue*, *Nucl. Phys. B* **164** (1980) 171–188.
- [49] I. Arefeva, *QUANTUM CONTOUR FIELD EQUATIONS*, *Phys. Lett. B* **93** (1980) 347–353.
- [50] V. Dotsenko and S. Vergeles, *Renormalizability of Phase Factors in the Nonabelian Gauge Theory*, *Nucl. Phys. B* **169** (1980) 527–546.
- [51] R. A. Brandt, F. Neri, and M.-a. Sato, *Renormalization of loop functions for all loops*, *Phys. Rev. D* **24** (Aug, 1981) 879–902.
- [52] G. Korchemsky and A. Radyushkin, *Loop Space Formalism and Renormalization Group for the Infrared Asymptotics of QCD*, *Phys. Lett. B* **171** (1986) 459–467.
- [53] G. Korchemsky and A. Radyushkin, *Renormalization of the Wilson Loops Beyond the Leading Order*, *Nucl. Phys. B* **283** (1987) 342–364.
- [54] R. Hamberg, W. van Neerven, and T. Matsuura, *A Complete calculation of the order α_s^2 correction to the Drell-Yan K factor*, *Nucl.Phys.* **B359** (1991) 343–405.
- [55] R. Hamberg, W. van Neerven, and T. Matsuura, *Erratum to: A complete calculation of the order α_s^2 correction to the Drell-Yan K-factor: [Nucl. Phys. B 359 (1991) 343]*, *Nuclear Physics B* **644** (2002), no. 1-2 403 – 404.
- [56] M. Beneke and V. A. Smirnov, *Asymptotic expansion of Feynman integrals near threshold*, *Nucl.Phys.* **B522** (1998) 321–344, [[hep-ph/9711391](#)].
- [57] A. Pak and A. Smirnov, *Geometric approach to asymptotic expansion of Feynman integrals*, *Eur.Phys.J.* **C71** (2011) 1626, [[arXiv:1011.4863](#)].
- [58] B. Jantzen, *Foundation and generalization of the expansion by regions*, *JHEP* **1112** (2011) 076, [[arXiv:1111.2589](#)].
- [59] D. Bonocore, E. Laenen, L. Magnea, L. Vernazza, and C. D. White, *The method of regions and next-to-soft corrections in Drell-Yan production*, *Physics Letters B* **742** (Mar., 2015) 375–382, [[arXiv:1410.6406](#)].
- [60] S. Moch and A. Vogt, *On non-singlet physical evolution kernels and large- x coefficient functions in perturbative QCD*, *JHEP* **11** (2009) 099, [[arXiv:0909.2124](#)].

-
- [61] M. Beneke, A. Broggio, M. Garny, S. Jaskiewicz, R. Szafron, L. Vernazza, and J. Wang, *Leading-logarithmic threshold resummation of the Drell-Yan process at next-to-leading power*, *JHEP* **03** (2019) 043, [arXiv:1809.1063].
- [62] M. Beneke, A. Broggio, S. Jaskiewicz, and L. Vernazza, *Threshold factorization of the Drell-Yan process at next-to-leading power*, *JHEP* **07** (2020) 078, [arXiv:1912.0158].
- [63] M. A. Ebert, I. Moulton, I. W. Stewart, F. J. Tackmann, G. Vita, and H. X. Zhu, *Power Corrections for N-Jettiness Subtractions at $\mathcal{O}(\alpha_s)$* , *JHEP* **12** (2018) 084, [arXiv:1807.1076].
- [64] M. van Beekveld, W. Beenakker, R. Basu, E. Laenen, A. Misra, and P. Motylinski, *Next-to-leading power threshold effects for resummed prompt photon production*, *Phys. Rev.* **D100** (2019), no. 5 056009, [arXiv:1905.1177].
- [65] M. van Beekveld, W. Beenakker, E. Laenen, and C. D. White, *Next-to-leading power threshold effects for inclusive and exclusive processes with final state jets*, *JHEP* **03** (2020) 106, [arXiv:1905.0874].
- [66] M. van Beekveld, E. Laenen, J. S. Damsté, and L. Vernazza, *Next-to-leading power threshold corrections for finite order and resummed colour-singlet cross sections*, 2021.
- [67] S. Weinberg, *Infrared photons and gravitons*, *Phys. Rev.* **140** (Oct, 1965) B516–B524.
- [68] A. Strominger, *On bms invariance of gravitational scattering*, *Journal of High Energy Physics* **2014** (Jul, 2014).
- [69] S. Oxburgh and C. D. White, *BcJ duality and the double copy in the soft limit*, *Journal of High Energy Physics* **2013** (Feb, 2013).
- [70] H. Kawai, D. Lewellen, and S.-H. Tye, *A relation between tree amplitudes of closed and open strings*, *Nuclear Physics B* **269** (1986), no. 1 1 – 23.
- [71] Z. Bern, *Perturbative quantum gravity and its relation to gauge theory*, *Living Rev. Rel.* **5** (2002) 5, [gr-qc/0206071].
- [72] Z. Bern, J. Carrasco, and H. Johansson, *New Relations for Gauge-Theory Amplitudes*, *Phys. Rev. D* **78** (2008) 085011, [arXiv:0805.3993].
- [73] Z. Bern, J. J. M. Carrasco, and H. Johansson, *Perturbative Quantum Gravity as a Double Copy of Gauge Theory*, *Phys. Rev. Lett.* **105** (2010) 061602, [arXiv:1004.0476].

-
- [74] Z. Bern, T. Dennen, Y.-t. Huang, and M. Kiermaier, *Gravity as the Square of Gauge Theory*, *Phys. Rev. D* **82** (2010) 065003, [[arXiv:1004.0693](#)].
- [75] Z. Bern and H. Ita, *Harmony of scattering amplitudes: From qcd to gravity*, *Nuclear Physics B - Proceedings Supplements* **216** (2011), no. 1 2 – 22. String Theory: Formal Developments and Applications.
- [76] Z. Bern, J. J. Carrasco, M. Chiodaroli, H. Johansson, and R. Roiban, *The Duality Between Color and Kinematics and its Applications*, [arXiv:1909.0135](#).
- [77] J. Gervais and A. Neveu, *Feynman rules for massive gauge fields with dual diagram topology*, *Nuclear Physics B* **46** (1972), no. 2 381 – 401.
- [78] Z. Bern and A. K. Grant, *Perturbative gravity from QCD amplitudes*, *Physics Letters B* **457** (June, 1999) 23–32, [[hep-th/9904026](#)].
- [79] A. Luna Godoy, *The double copy and classical solutions*. PhD thesis, University of Glasgow, 2017.
- [80] Z. Bern, S. Davies, and J. Nohle, *Double-copy constructions and unitarity cuts*, *Physical Review D* **93** (May, 2016).
- [81] H. Elvang and Y.-t. Huang, *Scattering Amplitudes*, [arXiv:1308.1697](#).
- [82] M. J. G. Veltman, *Quantum Theory of Gravitation*, in *Methods in Field Theory: Les Houches Session XXVIII. Edited by BALIAN ROGER & ZINN-JUSTIN JEAN. Published by World Scientific Publishing Co. Pte. Ltd*, pp. 265–328, Jan., 1981.
- [83] S. M. Carroll, *Spacetime and geometry. An introduction to general relativity*. 2004.
- [84] R. H. Boels, R. S. Isermann, R. Monteiro, and D. O’Connell, *Colour-Kinematics duality for one-loop rational amplitudes*, *Journal of High Energy Physics* **2013** (Apr., 2013) 107, [[arXiv:1301.4165](#)].
- [85] A. Edison, S. He, O. Schlotterer, and F. Teng, *One-loop Correlators and BCJ Numerators from Forward Limits*, *arXiv e-prints* (May, 2020) [arXiv:2005.03639](#), [[arXiv:2005.0363](#)].
- [86] Z. Bern, S. Davies, T. Dennen, Y.-t. Huang, and J. Nohle, *Color-Kinematics Duality for Pure Yang-Mills and Gravity at One and Two Loops*, *arXiv e-prints* (Mar., 2013) [arXiv:1303.6605](#), [[arXiv:1303.6605](#)].

- [87] Z. Bern, S. Davies, T. Dennen, A. V. Smirnov, and V. A. Smirnov, *Ultraviolet properties of $n=4$ supergravity at four loops*, *Physical Review Letters* **111** (Dec, 2013).
- [88] S. Abreu, L. J. Dixon, E. Herrmann, B. Page, and M. Zeng, *The two-loop five-point amplitude in $N = 8$ supergravity*, *Journal of High Energy Physics* **2019** (Mar., 2019) 123, [arXiv:1901.0856].
- [89] C. Cheung and G. N. Remmen, *Entanglement and the double copy*, *Journal of High Energy Physics* **2020** (May, 2020) 100, [arXiv:2002.1047].
- [90] Z. Bern, C. Cheung, R. Roiban, C.-H. Shen, M. P. Solon, and M. Zeng, *Black hole binary dynamics from the double copy and effective theory*, *Journal of High Energy Physics* **2019** (Oct., 2019) 206, [arXiv:1908.0149].
- [91] F. Cachazo, S. He, and E. Y. Yuan, *Scattering of massless particles in arbitrary dimensions*, *Physical Review Letters* **113** (Oct, 2014).
- [92] F. Cachazo, S. He, and E. Y. Yuan, *Scattering equations and matrices: from einstein to yang-mills, dbi and nlsm*, *Journal of High Energy Physics* **2015** (Jul, 2015).
- [93] E. Casali, Y. Geyer, L. Mason, R. Monteiro, and K. A. Roehrig, *New ambitwistor string theories*, 2015.
- [94] N. E. J. Bjerrum-Bohr, P. H. Damgaard, R. Monteiro, and D. O’Connell, *Algebras for amplitudes*, *Journal of High Energy Physics* **2012** (June, 2012) 61, [arXiv:1203.0944].
- [95] F. Cachazo, S. He, and E. Y. Yuan, *Scattering of massless particles: scalars, gluons and gravitons*, *Journal of High Energy Physics* **2014** (July, 2014) 33, [arXiv:1309.0885].
- [96] Z. Bern, A. de Freitas, and H. L. Wong, *Coupling Gravitons to Matter*, *Phys. Rev. Lett.* **84** (Apr., 2000) 3531–3534, [hep-th/9912033].
- [97] Y.-J. Du, B. Feng, and C.-H. Fu, *BCJ relation of color scalar theory and KLT relation of gauge theory*, *Journal of High Energy Physics* **2011** (Aug., 2011) 129, [arXiv:1105.3503].
- [98] R. Monteiro, D. O’Connell, and C. D. White, *Black holes and the double copy*, *Journal of High Energy Physics* **2014** (2014) 1–23.
- [99] D. S. Berman, E. Chacón, A. Luna, and C. D. White, *The self-dual classical double copy, and the Eguchi-Hanson instanton*, *Journal of High Energy Physics* **2019** (Jan., 2019) 107, [arXiv:1809.0406].

-
- [100] E. Chacón, H. García-Compeán, A. Luna, R. Monteiro, and C. D. White, *New heavenly double copies*, *arXiv e-prints* (Aug., 2020) arXiv:2008.09603, [arXiv:2008.0960].
- [101] G. Elor, K. Farnsworth, M. L. Graesser, and G. Herczeg, *The Newman-Penrose Map and the Classical Double Copy*, *arXiv e-prints* (June, 2020) arXiv:2006.08630, [arXiv:2006.0863].
- [102] M. Carrillo González, B. Melcher, K. Ratliff, S. Watson, and C. D. White, *The classical double copy in three spacetime dimensions*, *arXiv e-prints* (Apr., 2019) arXiv:1904.11001, [arXiv:1904.1100].
- [103] M. Kemal Gumus and G. Alkac, *More on the Classical Double Copy in Three Spacetime Dimensions*, *arXiv e-prints* (May, 2020) arXiv:2006.00552, [arXiv:2006.0055].
- [104] A. Luna, R. Monteiro, I. Nicholson, and D. O’Connell, *Type D spacetimes and the Weyl double copy*, *Classical and Quantum Gravity* **36** (Mar., 2019) 065003, [arXiv:1810.0818].
- [105] R. Alawadhi, D. S. Berman, and B. Spence, *Weyl doubling*, *arXiv e-prints* (July, 2020) arXiv:2007.03264, [arXiv:2007.0326].
- [106] C. Keeler, T. Manton, and N. Monga, *From Navier-Stokes to Maxwell via Einstein*, *arXiv e-prints* (May, 2020) arXiv:2005.04242, [arXiv:2005.0424].
- [107] W. D. Goldberger and A. K. Ridgway, *Radiation and the classical double copy for color charges*, *Phys. Review D* **95** (June, 2017) 125010, [arXiv:1611.0349].
- [108] W. D. Goldberger, S. G. Prabhu, and J. O. Thompson, *Classical gluon and graviton radiation from the bi-adjoint scalar double copy*, *Phys. Rev. D* **96** (2017), no. 6 065009, [arXiv:1705.0926].
- [109] B. Maybee, D. O’Connell, and J. Vines, *Observables and amplitudes for spinning particles and black holes*, *Journal of High Energy Physics* **2019** (Dec., 2019) 156, [arXiv:1906.0926].
- [110] G. L. Almeida, S. Foffa, and R. Sturani, *Classical gravitational self-energy from double copy*, arXiv:2008.0619.
- [111] T. Adamo and A. Ilderton, *Classical and quantum double copy of back-reaction*, *arXiv e-prints* (May, 2020) arXiv:2005.05807, [arXiv:2005.0580].
- [112] C.-H. Shen, *Gravitational Radiation from Color-Kinematics Duality*, *JHEP* **11** (2018) 162, [arXiv:1806.0738].

-
- [113] D. O’Connell, A. Luna, R. Monteiro, I. Nicholson, A. Ochirov, N. Westerberg, and C. D. White, *Perturbative spacetimes from yang-mills theory*, *Journal of High Energy Physics* (Apr., 2017).
- [114] R. Kerr and A. Schild, *Republication of: A new class of vacuum solutions of the einstein field equations (reprinted)*, *General Relativity and Gravitation* **41** (10, 2009) 2485–2499.
- [115] H. Stephani, D. Kramer, M. MacCallum, C. Hoenselaers, and E. Herlt, *Exact Solutions of Einstein’s Field Equations*, pp. i–vi. Cambridge Monographs on Mathematical Physics. Cambridge University Press, 2 ed., 2003.
- [116] C. D. White, *Twistorial foundation for the classical double copy*, *Physical Review Letters* **126** (Feb, 2021).
- [117] E. Chacón, S. Nagy, and C. D. White, *The weyl double copy from twistor space*, 2021.
- [118] C. Cheung, *TASI Lectures on Scattering Amplitudes*, pp. 571–623. 2018. [arXiv:1708.0387](https://arxiv.org/abs/1708.0387).
- [119] A. K. Ridgway and M. B. Wise, *Static spherically symmetric kerr-schild metrics and implications for the classical double copy*, *Physical Review D* **94** (Aug, 2016).
- [120] A. Taub, *Empty space-times admitting a three parameter group of motions*, *Annals Math.* **53** (1951) 472–490.
- [121] E. Newman, L. Tamburino, and T. Unti, *Empty space generalization of the Schwarzschild metric*, *J. Math. Phys.* **4** (1963) 915.
- [122] A. Luna, R. Monteiro, D. O’Connell, and C. D. White, *The classical double copy for Taub–NUT spacetime*, *Phys. Lett. B* **750** (2015) 272–277, [[arXiv:1507.0186](https://arxiv.org/abs/1507.0186)].
- [123] J. F. Plebański, *A class of solutions of einstein-maxwell equations with the cosmological constant*, *Symposium - International Astronomical Union* **64** (1974) 188–190.
- [124] C. W. Misner, *The Flatter regions of Newman, Unti and Tamburino’s generalized Schwarzschild space*, *J. Math. Phys.* **4** (1963) 924–938.
- [125] J. S. Dowker, *The nut solution as a gravitational dyon*, *General Relativity and Gravitation* **5** (1974) 603–613.

-
- [126] T. Ortin, *Gravity and Strings*. Cambridge Monographs on Mathematical Physics. Cambridge University Press, 2nd ed. ed., 7, 2015.
- [127] N. Bahjat-Abbas, A. Luna, and C. D. White, *The Kerr-Schild double copy in curved spacetime*, *Journal of High Energy Physics* **2017** (Dec., 2017) 4, [[arXiv:1710.0195](#)].
- [128] C. D. White, *Exact solutions for the biadjoint scalar field*, *Phys. Lett. B* **763** (2016) 365–369, [[arXiv:1606.0472](#)].
- [129] P.-J. De Smet and C. D. White, *Extended solutions for the biadjoint scalar field*, *Phys. Lett. B* **775** (2017) 163–167, [[arXiv:1708.0110](#)].
- [130] P. Sikivie and N. Weiss, *Classical yang-mills theory in the presence of external sources*, *Phys. Rev. D* **18** (Nov, 1978) 3809–3821.
- [131] G. Derrick, *Comments on nonlinear wave equations as models for elementary particles*, *J. Math. Phys.* **5** (1964) 1252–1254.
- [132] E. J. Weinberg, *Classical solutions in quantum field theory: Solitons and Instantons in High Energy Physics*. Cambridge Monographs on Mathematical Physics. Cambridge University Press, 9, 2012.
- [133] R. Saotome and R. Akhoury, *Relationship Between Gravity and Gauge Scattering in the High Energy Limit*, *JHEP* **01** (2013) 123, [[arXiv:1210.8111](#)].
- [134] P. Aichelburg and R. Sexl, *On the Gravitational field of a massless particle*, *Gen. Rel. Grav.* **2** (1971) 303–312.
- [135] M. Kozyulin and Z. Silagadze, *Light bending by a Coulomb field and the Aichelburg-Sexl ultraboost*, *Eur. J. Phys.* **32** (2011) 1357–1365, [[arXiv:1104.2557](#)].
- [136] C. Lousto and N. G. Sanchez, *The Curved Shock Wave Space-time of Ultrarelativistic Charged Particles and Their Scattering*, *Int. J. Mod. Phys. A* **5** (1990) 915.
- [137] R. A. Brandt and F. Neri, *Stability analysis for singular non-abelian magnetic monopoles*, *Nuclear Physics B* **161** (1979), no. 2 253 – 282.
- [138] R. A. Brandt and F. Neri, *Magnetic monopoles in $su(n)$ gauge theories*, *Nuclear Physics B* **186** (1981), no. 1 84 – 108.
- [139] W. D. Goldberger, J. Li, and S. G. Prabhu, *Spinning particles, axion radiation, and the classical double copy*, *Physical Review D* **97** (May, 2018).

- [140] L. Alfonsi, C. D. White, and S. Wikeley, *Topology and Wilson lines: global aspects of the double copy*, *JHEP* **07** (2020) 091, [[arXiv:2004.0718](#)].
- [141] S. G. Prabhu, *The classical double copy in curved spacetimes: Perturbative Yang-Mills from the bi-adjoint scalar*, [arXiv:2011.0658](#).
- [142] E. Witten, *Anti-de Sitter Space, Thermal Phase Transition, And Confinement In Gauge Theories*, *arXiv e-prints* (Mar., 1998) hep-th/9803131, [[hep-th/9803131](#)].
- [143] M. Bonvini, *Resummation of soft and hard gluon radiation in perturbative QCD*. PhD thesis, Genoa U., 2012. [arXiv:1212.0480](#).
- [144] D. Westmark, *Threshold Resummation and the Determination of Parton Distribution Functions*. PhD thesis, Florida State University, 2015.
- [145] D. A. Clarke, *A primer on Tensor Calculus*, 2011.